Investigation of the Toxicity of Cyanobacterial Peptides by Chemical Biology Approaches

Inauguraldissertation

zur
Erlangung der Würde eines Doktors der Philosophie
vorgelegt der
Philosophisch-Naturwissenschaftlichen Fakultät
der Universität Basel

von

Verena Grundler

aus Würzburg, Deutschland

Basel, 2014

Genehmigt von der Philosophisch-Naturwissenschaftlichen Fakultät

auf Antrag von

Prof. Dr. K.Gademann
Prof. Dr. M. Arand
Prof. Dr. R. Eggen

Basel, den 24. Juni 2014

Prof. Dr. Jörg Schibler
Dekan

Für meine Familie

"Schau tief in die Natur, und dann wirst du alles besser verstehen."

Albert Einstein (1879-1955)

This PhD-Thesis is based on the following manuscripts:

The Toxicity and Enzyme Activity of a Chlorine and Sulfate Containing Aeruginosin Isolated from a Non-Microcystin-Producing Planktothrix Strain, E. Kohler, V. Grundler, D. Häussinger, R. Kurmayer, K. Gademann, J. Pernthaler, J. F. Blom

Direct Arginine Modification in Native Peptides and Application to Fluorescent Drug Monitoring, V. Grundler, K. Gademann

Following the Fate of Modified MC-LR, V. Grundler, S. Faltermann, K. Fent, K. Gademann

Abstract

Global warming together with the extensive agriculture favours the uncontrolled growth of cyanobacteria, also called blue-green algae. Being one of the oldest life forms on our planet, they have reached evolutionary perfection over time. They are distributed at a variety of habitats, primarily in water. Cyanobacterial blooms present immediate danger to animals and humans, as cyanobacteria are known to produce various toxic compounds. This thesis addresses some of the open questions regarding cyanobacterial toxins. The current project involves the isolation, characterization, derivatization and biological and toxicological evaluation of various toxic compounds derived from cyanobacteria.

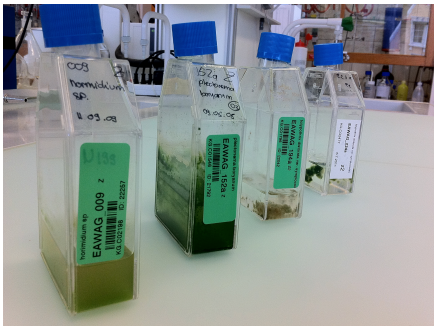

Figure 1. Cyanobacterial culture

Our attempts for labelling cyanobacterial toxins led to the development of an optimized protocol for arginine derivatization in complex peptides. This straightforward procedure allows modifying the arginine moiety in peptides containing with other functional groups, such as fluorophores or biotin under mild conditions in an operatively simple procedure. This method was applied for labelling leuprolide, a clinical drug, for *in vivo* studies in *Daphnia*.

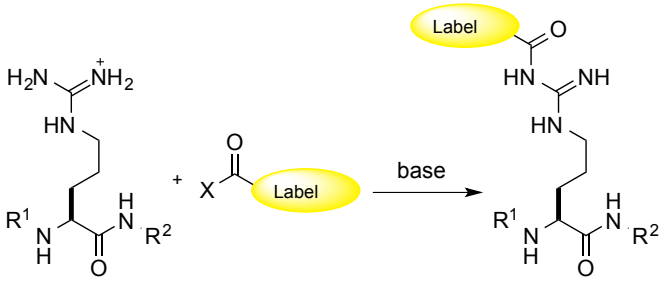

Scheme 1. Arginine derivatization strategy

Microcystins are one of the most common and widely distributed cyanobacterial toxins. Their hepatotoxicity in humans makes them an important compound class. Microcystin-LR is the most toxic and common representative of the microcystin family (LD_{50} = 50 μgkg^{-1}), yet the precise mechanism of its action is still under debate. To gain an insight into the uptake, distribution, accumulation and excretion of MC-LR, biological studies are necessary. One way to investigate the molecular mechanism of interaction of microcystin-LR is fluorescence labelling. An efficient synthesis route for the modification of the toxin's arginine-residue was established, which allowed the preparation of microcystin derivatives with a variety of markers attached (fluorescent tags, biotin, diazirine). These derivatives preserved the parent toxicity as judged by phosphatase inhibition assays, cell viability assays, and acute toxicity assays against *Thamnocephalus platyurus*.

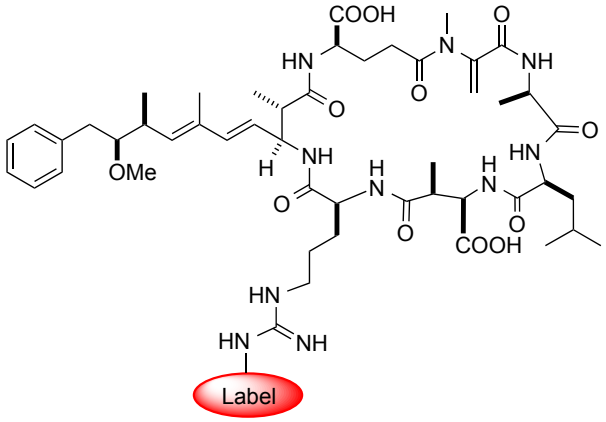

Figure 2. Microcystin derivative

Structure elucidation of a newly isolated toxic peptide,aeruginosin 828A, from *Planktothrix* strains was conducted. 2D-NMR studies and MS-characterization of the toxin revealed the presence of phenyllactic acid (Pla), chloroleucine (Cleu), 2-carboxy-6-(4'-sulfo-xylosyl)-octahydroindole (Choi), and 3-aminoethyl-1-*N*-amidino-Δ^3-pyrroline (Aeap) residues. This peptide showed inhibitory activity against thrombin and trypsin. Furthermore, for the first time within this compound class, toxicity against *Thamnocephalus platyurus* was observed. This toxic peptide could only be found in microcystin-deficient *Planktothrix* strains.

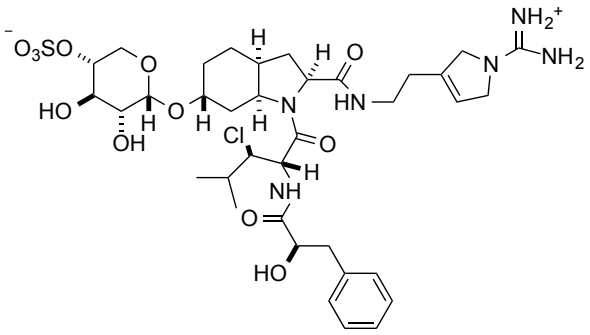

Figure 3. Aeruginosin 828A

Another group of toxins, produced along with the microcystins *via* the nonribosomal pathway, are the cyanopeptolins. A member of this group, cyanopeptolin 1020, is a potent inhibitor of trypsin, human kallikrein and factor Xia. Unlike the microcystins, cyanopeptolins and cyanopeptolin 1020 in particular have not been investigated in detail so far. One way to get a better understanding of the toxicity of this compound class are biological test with fluorescently-labelled cyanopeptolins. A method for labelling the glutamate residue in cyanopeptolin 1020 was established. The protocol allows fast coupling on the carboxylic function of the toxin. As the products are highly sensitive, an improvement for product stability is under investigation.

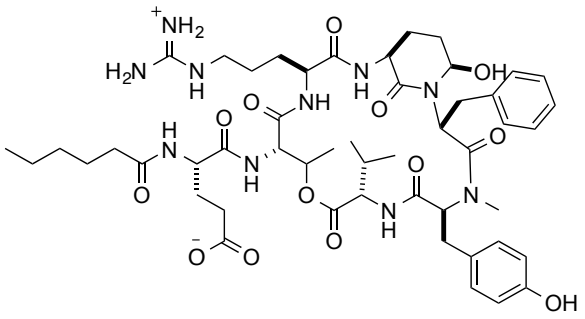

Figure 4. Cyanopeptolin 1020

Zusammenfassung

Steigende globale Durchschnittstemperaturen in Verbindung mit extensiver Landwirtschaft begünstigen das unkontrollierte Wachstum von Cyanobakterien, früher bekannt als Blaualgen. Da diese zu den ältesten Lebensformen auf der Erde zählen, sind sie in ihrer Lebensweise perfektioniert. Sie besiedeln viele verschiedene Ökosysteme, hauptsächlich jedoch Wasser. Unglücklicherweise produzieren diese Organismen eine Reihe verschiedener Toxine, weswegen von einer Algenblüte unter Umständen große Gefahren für Mensch und Tier ausgehen können. Diese Arbeit behandelt offene Fragestellungen zu cyanobakteriellen Toxinen. Die Projekte umfassen die Isolation, die Charakterisierung, die Derivatisierung und die biologische sowie toxikologische Analyse von verschiedenen Verbindungen aus Cyanobakterien.

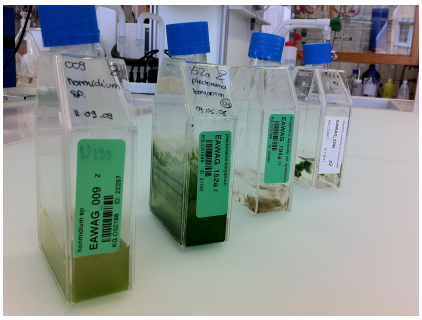

Abbildung 1. Cyanobakterien-Kultur

In Hinblick auf die Markierung von Cyanotoxinen wurde eine effektive Derivatisierungsmethode für Arginin in komplexen Peptiden etabliert. Dieses unkomplizierte Verfahren erlaubt eine unter milden Bedingungen durchführbare Modifizierung der Arginin-Funktion in Peptiden mit verschiedenen funktionellen Gruppen, wie zum Beispiel Fluorophoren und Biotin. Diese Methode wurde auch für die Markierung des Medikaments Leuprorelin angewandt, um anschließend *in vivo* Studien in *Daphnien* durchzuführen.

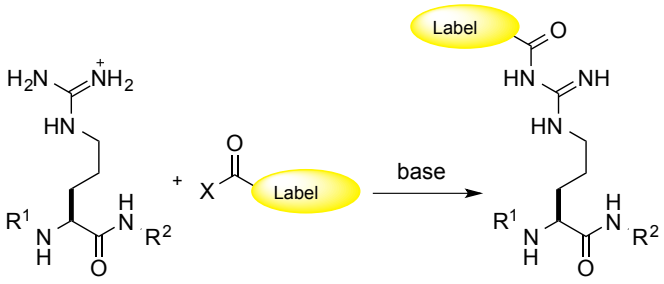

Schema 1. Strategie zur Arginin Derivatisierung

Microcystine gehören zu den häufigsten und verbreitetsten cyanobakteriellen Toxinen. Durch ihre Hepatotoxizität gehören sie zu einer bedeuteten Stoffklasse. Der häufigste und am stärksten toxisch wirkende Vertreter aus der Klasse der Microcystine ist Microcystin-LR mit einem LD_{50}-Wert von 50 µg kg^{-1}. Jedoch ist die genaue Ursache für diese starke Toxizität noch völlig unbekannt. Um die Aufnahme, die Verteilung, die Akkumulation und die Ausscheidung von Microcystin-LR im Organismus zu verstehen, sind biologische Studien unerlässlich. Eine zentrale Methode um die molekularen und zellulären Mechanismen zu untersuchen, ist die Verwendung fluoreszenzmarkierter Derivate. Aus diesem Grund wurde im Rahmen dieser Doktorarbeit eine effiziente Synthese entwickelt, welche es erlaubt, verschiedene funktionelle Gruppen an die Arginin-Funktion von Microcystin-LR zu koppeln (Fluorophore, Biotin, Diazirin). Es wurde zudem gezeigt, dass diese Verbindungen in Inhibierungsassays, Zellviabilitätsassays und Toxizitätsassays mit *Thamnocephalus platyurus* vergleichbare Aktivitäten wie Microcystin-LR aufwiesen.

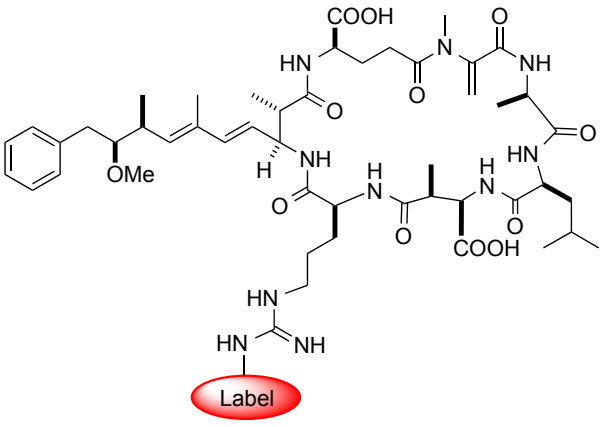

Abbildung 2. Markiertes Microcystin

Es wurde eine Strukturaufklärung eines neu-isolierten toxischen Peptids, Aeruginosin 828A, aus sechs verschiedenen *Planktothrix*-Stämmen durchgeführt. Durch 2D-NMR Studien und massenspektrometrische Methoden konnten wir dessen Struktur

aufgeklären. Folgende Fragmente wurden identifiziert: Phenylessigsäure (Pla), Chloroleucin (Cleu), 2-Carboxy-6-(4'-sulfo-xylosyl)-octahydroindol (Choi), und 3-Aminoethyl-1-*N*-amidino-Δ^3-pyrrolin (Aeap). Dieses Peptid inhibierte die Enzyme Thrombin und Trypsin. Zusätzlich wurde zum ersten Mal in dieser Verbindungsklasse Toxizität für *Thamnocephalus platyurus* beobachtet. Dieses Toxin wurde nur in Stämmen gefunden, welche nicht in der Lage waren Microcystin zu produzieren.

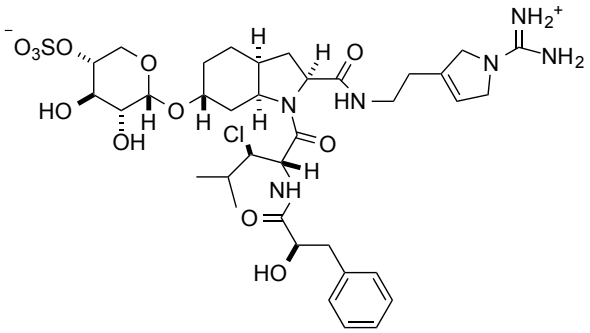

Abbildung 3. Aeruginosin 828A

Eine andere Gruppe von Toxinen, welche zusammen mit den Microcystinen durch nichtribosomale Peptidsynthese hergestellt werden, sind die Cyanopeptoline. Ein Vertreter dieser Klasse ist das Cyanopeptolin 1020, welches ein starker Inhibitor von Trypsin, Kallikrein und Faktor Xia ist. Im Gegensatz zu den Microcystinen wurden die Cyanopeptoline und das Cyanopeptolin 1020 bisher nicht ausführlich untersucht. Um die Toxizität dieser Verbindungen zu verstehen, ist es wichtig biologische Tests mit fluoreszenzmarkierten Cyanopeptolinen durchzuführen. Aus diesem Grund haben wir eine Derivatisierungsmethode für Cyanopeptolin 1020 am Glutamat-Rest entwickelt. Diese Methode ermöglicht eine schnelle Kupplung verschiedener funktioneller Gruppen an die Carbonsäurefunktion. Auf Grund hoher Sensitivität der Kupplungsprodukte, wird eine Verbesserung der Produktstabilität untersucht.

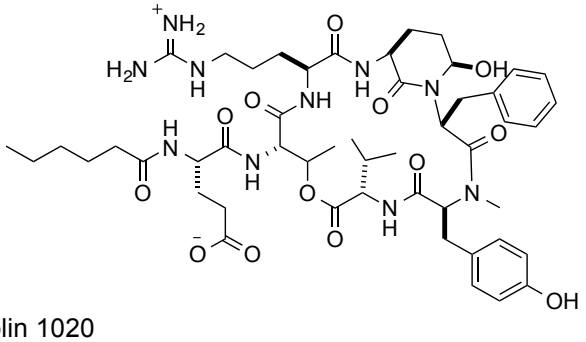

Abbildung 4. Cyanopeptolin 1020

Table of content

Abbreviations

ACE inhibitor	Angiotensin-converting-enzyme inhibitor
AcOH	Actid acid
Adda	3-Amino-9-methoxy-2,6,8-trimenthyl-10-phenyl-4,6-decadienoic acid
Aeap	3-Aminoethyl-1-*N*-amidino-Δ^3-pyrroline
Ahp	3-Amino-6-hydroxy-2-piperidone
Arg	Arginine
Asx	Asparagine or aspartic acid
BC	Before Christ
BiP	Binding immunoglobulin protein
Boc	Di-*t*-butyl dicarbonate
BSA	Bis(trimethylsilyl)acetamide
SPE	Solid-phase extraction
Choi	2-Carboxy-6-hydroxyoctahydroindole
CIE	International commission on illumination
Cleu	Chloroleucine
CP	Cyanopeptolin
CP1020	Cyanopeptolin 1020
CYP450	Cytochrome P450
Cys	Cysteine
D -Glu	D-Glutamate
D-MeAsp	D-3-Methylaspartic acid
DBU	1,8-Diazabicyclo[5.4.0]undec-7-ene
DCC	*N*,*N*'-Dicyclohexylcarbodiimide
Dha	Dehydroalanine
DiFMUP	6,8-Difluoro-4-methylumbelliferyl phosphate
DMAP	4-Dimethylaminopyridine
DMEM	Dulbecco's Modified Eagle's medium
DMF	Dimethylformamide
DMSO	Dimethyl sulfoxide
DNA	Deoxyribonucleic acid

DTT	Dithiothreitol
EDC	1-Ethyl-3-(3-dimethylaminopropyl)carbodiimide
EGTA	Ethylene glycol-bis(2-aminoethylether)-*N*,*N*,*N*′,*N*′-tetraacetic acid
ER-stress	Endoplasmic reticulum stress
ESI	Electrospray ionization
Et_2O	Diethyl ether
5(6)-FAM	5(6)-Carboxyfluorescein
FBS	Fetal bovine sera
Fmoc	Fluorenylmethyloxycarbonyl chloride
GAPDH	Glyceraldehyde 3-phosphate dehydrogenase
Glu	Glutamate
Glx	Glutamic acid or glutamine
HATU	1-[Bis(dimethylamino)methylene]-1H-1,2,3-triazolo[4,5-b] pyridinium 3-oxid hexafluorophosphate
His	Histidine
HIV	Human immunodeficiency virus
Hpla	Hydroxyphenyl-lactic acid
HPLC	High-performance liquid chromatography
HRMS	High-resolution mass spectrometry
Huh 7 cells	Hepato cellular carcinoma cells
Ile	Isoleucine
L-Arg	L-Arginine
LC-MS	Liquid chromatography–mass spectrometry
LD_{50}	Median lethal dose
Leu	Leucine
Lys	Lysine
MC	Microcystin
MC-LR	Microcystin-(Leucine-Arginine)
Mdha	*N*-Methyldehydroalanine
MeAsp	3-Methylaspartic acid
MeCN	Acetonitrile
MeDhb	Methyldehydrobutyrine
MS	Mass spectrometry

MTT	3-(4,5-Dimethylthiazol-2-Yl)-2,5-diphenyltetrazolium bromide
N-Me-Tyr	*N*-Methyl-L-tyrosine
NCS	*N*-Chlorosuccinimide
NEt_3	Triethylamine
NHS-diazirine	Succinimidyl 4,4-azipentanoate
NMM	4-Methylmorpholine
NRPS	Nonribosomal peptide synthetases
OATP	Organic anion polypeptide transporter
pGlu	Pyrrolidone carboxylic acid
Phe	Phenylalanine
pK_a	Ionisation constant
Pla	Lactic acid
PP2A	Protein phosphatase 2A
qPCR	Quantitative polymerase chain reaction
RNA	Ribonucleic acid
RP-HPLC	Reversed phase high-performance liquid chromatography
Ser	Serine
TBTU	O-(Benzotriazol-1-yl)-*N*,*N*,*N*',*N*'-tetramethyluronium tetrafluoroborate
TFA	Trifluoroacetic acid
THF	Tetrahydrofuran
Thr	Threonine
TLC	Thin-layer chromatography
Tris-HCl	Tris-(hydroxymethyl)-aminomethane-hydrochloric acid
Trp	Tryptophan
Tyr	Tyrosine
UV	Ultraviolet
Val	Valine
WHO	World health organization

1

Introduction

1.1 Natural products

Natural products are compounds that originate from natural sources such as plants, microorganisms or animals. Among them, substances which have no primary role in the metabolism of the respective organism are referred to as secondary metabolites.[1] Because of evolutionary reasons, for example to give a species an advantage over another, many naturally produced compounds have an unique structure and thereby might act in various modes and to several different species.[2] Therefore these molecules also quite often interact with human proteins (e.g. teprotide a ACE inhibitor or muscarine a agonist of the muscarinic acetylcholine receptor), causing diverse positive or negative effects.[3,4] As a consequence, numerous compounds derived from plants, animals, marine- or microorganisms have been a source and inspiration for molecules with different purposes for human health.[5]

The use of natural material as treatment for human diseases is very old, whereby even the Neanderthals might have utilized plants as origin for medical applications.[6] Furthermore, ancient civilisations, such as the Chinese, Indian, African and Greeks, used natural compounds to heal various sicknesses.[7] For example in India the medical curcumin was administered against eye infections and various skin diseases; *Guggul* from *Commiphor wightii* was used to treat different afflictions including internal tumors.[8,9] Nowadays herbal medicines are still in use in developing countries even serious diseases like malaria or tuberculosis are mainly treated by traditional medicine (**Figure 1.1**).[10]

Figure 1.1. Bags of herbal medicine at a market in the town of Maradi
Used with permission by © UNICEF/NYHQ2007-2652/Pirozzi

Until the nineteenth century, standardization of the herbal medicines was problematic due to varying concentration of the active compound and either the presence of toxic or harmful components in the plant material. This dangerous circumstance dramatically changed when Friedrich Wilhelm Sertüner isolated the pure, active compound morphine 1806 from *Papaver somniferum*.[11] With this academic achievement, it was possible to apply accurate doses of the pharmacological active substance to minimize side effects and intoxication. Since then numerous natural sources have been screened for relevant molecules to treat various diseases and is today a main source of new medicines, whereas an estimation indicates that 60 % of all available drugs come directly or in a derivatized form from natural products.[12,13] Besides morphine, aspirin from salicyclic acid in the willow bark (*Salix*), penicillin from mold (*Penicillium*) and the potent anticancer reagent taxol from the bark of the pacific yew tree (*Taxus brevifolia*) are very well known examples of powerful drugs having their origin in nature.[14-16] Furthermore, natural products may have the potential to cure yet undefeated diseases, which are a dominant issue in our society, such as cancer, HIV and neurodegenerative diseases.[17-19] Additionally they can be a powerful tool against the significantly growing problem of multidrug resistant strains of bacteria, for example in *M. tuberculosis*.[20]

The positive health effect aside, the natural products can also act as toxins and cause serious poisonings. Many plants and animals contain potent toxic compounds mainly used as defence against predators or to hunt a prey. Some of the most potent toxins on our planet are derived from natural sources for example the deadliest plant poison ricin, originated from the castor bean (*Ricinus communis*), or the most potent toxin existing on earth, produced by the bacterium *Clostridium botulinum*.[21,22] In the past, poisonous substances obtained from natural sources were often used for intentional intoxication. As an example the alkaloid atropine from *Atropa belladonna* has been used by women for dilating the pupils but also for homicide.[23] Another example is the alkaloid strychnine from *Strychnos nux vomica*, which was the prevailing toxic compound to kill people with poisoned chocolate.[24,25] One of the most prominent cases of death through poisoning with natural products is the execution of Socrates in 399 BC with hemlock.[26] More often, though, intoxication happens as an accident by unwilling consumption or accidental contamination with toxic compounds from natural sources.[27-29] To protect humans from these naturally

occurring toxins, to find antidotes or treatments for acute intoxication, it is crucial to study certain toxins in more detail to understand their origin and mechanism of action.

1.2 Cyanobacteria

Cyanobacteria (formerly called blue-green algae) are one of the oldest species on our planet, as indicated by fossils findings from western Australia, which postulate an existence on Earth for 3.5 billion years.[30] For this reason, cyanobacteria can be found almost everywhere, whereby the majority lives in water (freshwater, brackish water as well as saline water).[31]
Furthermore, they can grow on terrestrial habitats and in soil, where they manage to survive on surfaces of buildings, on rocks, in mountains and on tree bark.[32] In addition, cyanobacteria can adapt and survive environmental stress, such as dry periods, very high and low temperatures, as well as large temperature amplitudes. They can inhabit Polar Regions, Antarctic terrestrial environment or hot springs (e.g., at the Yellowstone National park at 74 °C).[33-37] Even extreme hostile environments like volcanic ash and desert sand are occupied by cyanobacteria.[38,39] Some species like *Synechococcus/Synechocytsis spp.* can live in symbiosis with dinoflagellates, whereby others associate with fungi and plants.[40-42]

This synergy is mainly due to the ability of cyanobacteria to fix nitrogen from the atmosphere, which is then further enzymatically converted into ammonia.[43,44] Responsible for this process are specialised cells, the so-called heterocysts, which are large and round shaped and possess thick cell walls with oxygen-binding glycolipids, necessary for nitrogen fixation under anaerobic conditions.[45] As energy source, these photoautotrophic organisms use photosynthesis.[46] This circumstance and likewise the age of cyanobacteria are assumed to have played a key role in the evolution of life on Earth as this species may actually have generated the first oxygen in the atmosphere.[47]

Cyanobacteria are unicellular or multicellular prokaryotes, which belong to the *Bacteria* domain, whereby the multicellular bacteria can be further categorized in filamentous, undifferentiated and differentiated species.[48,49] The multicellular bacteria are able to communicate intercellularly, differentiate and form colonies (cell-cell adhesion).[50] An example for an unicellular bacteria is *Microcystis aeruginosa*. An example of multicellular filamentous and undifferentiated bacteria is *Planktothrix*. *Anabaena sp.* belongs to the group of multicellular differentiated cyanobacteria (**Figure 1.2**).[51]

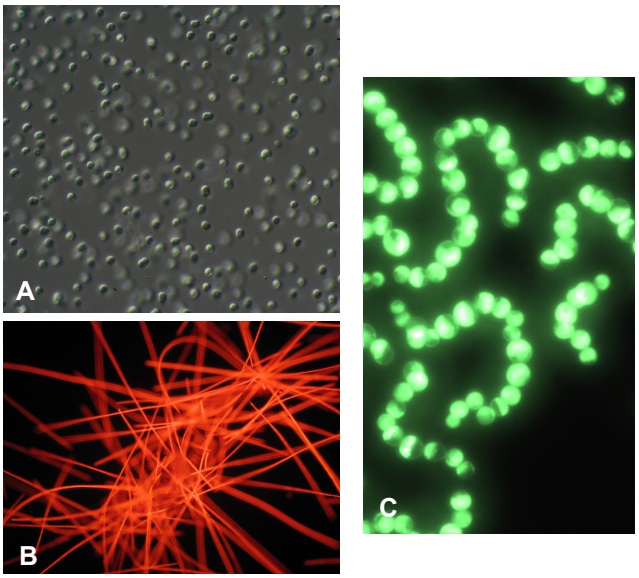

Figure 1.2. A: *Microcystis aeruginosa*; Used with permission by Bettina Eugster & Esther Kohler **B:** *Planktothrix rubescens*; Used with permission by Thomas Posch **C:** *Nostoc sp.*

Cyanobacteria produce a great variety of secondary metabolites, such as carotenoids, fatty acids, lipopetides, polysaccharides, as well as different bioactive molecules.[52] A large number of the cyanobacterial compounds are peptides or contain a peptide-like substructure. So far more than 600 representatives have been characterized.[53] These compounds are not only structurally diverse, but they also contain a number of unusual or modified amino acids.

As cyanobacteria have populated the Earth for a long time, it is not surprising that many of the above-mentioned molecules show significant bioactivity. It has been reported that some secondary metabolites of cyanobacteria show anticancer, cytotoxic, antibiotic, antifungal and antiviral activity, as well as have antimycotic, immunosuppressive and anti-malarial features; additionally, they even show activity against multi-drug resistant bacteria.[54] As the compounds, produced by cyanobacteria, are chemically stable and with good water solubility, they can be considered as promising candidates for medical applications, such as the anticancer agent dolastatin, whereby its synthetic analogue soblidotin has entered phase III of clinical trials.[55,56]

In addition to these compounds that may have a positive impact by being potentially used as drugs, cyanobacteria produce several highly toxic molecules, the

cyanotoxins, which pose a danger to humans, animals and the ecosystems as a whole.[57] These toxins are also characterized by a high chemical stability and water solubility and thereby have the potential to cause severe intoxication in humans and animals.[57] In fact, due to eutrophication, cyanobacteria often grow uncontrollably in aquatic environment and cause dangerous blooms all over the world. In addition, climate changes and the rising temperatures on our planet could further facilitate the growth of toxic cyanobacteria so that they become an even greater problem.[45,58] Toxic blooms mainly affect warm regions as Africa or South America, where every year many people are affected and the fresh-water supplies are endangered.[59] Europe is also struggling with those problems, for example the Baltic Sea, where the occurrence of blooms increased over the past years. Furthermore, the lakes in Europe are also affected by increasing density of toxic cyanobacteria.[60-62] These phenomena of widespread cyanobacteria blooms are even visible from space, as a satellite picture clearly demonstrates (**Figure 1.3**).

Figure 1.3. Phytoplankton bloom in the Baltic Sea
Used with permission by European Space Agency, ESA

Over the past years, many cases of poisoning by cyanobacteria were reported, whereby the regular intoxication occurs via oral intake, although other uptake mechanisms, such as inhalation or skin contact are also possible.[63] The majority of the cases of intoxication occur in animals, for example at a lake in Canada where approximately 1000 bats died after ingesting contaminated water.[64] Humans also suffer from cyanobacterial poisoning. A tragic accident of acute intoxication with cyanobacteria containing water occurred in Brazil in 1996, where dialysis patients

were treated with contaminated water and this conjuncture lead to the death of 52 people.[65] A more recent case of intoxication is reported in Argentina, where of a young person dived in a lake with a cyanobacteria bloom and afterwards suffered of clear intoxication symptoms (nausea and respiratory distress).[66]

1. 3 Cyanobacterial toxins

Cyanobacteria produce a wide range of potent toxins, which structural variety comes from peptides, linear or heterocyclic, and lipid compounds (**Figure 1.4**).[67]

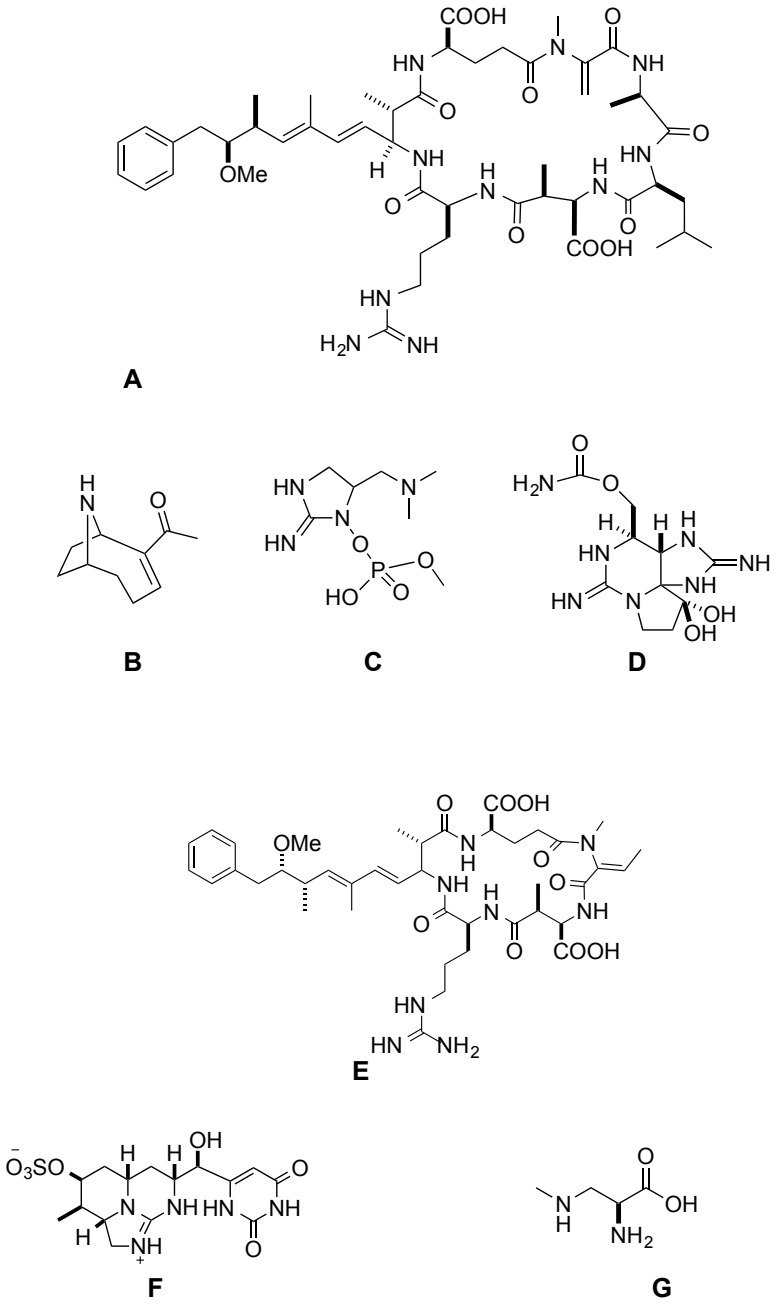

Figure 1.4. A: Microcystin-LR; **B:** Anatoxin-a; **C:** Anatoxin-a(s); **D:** Saxitoxin; **E:** Nodularin; **F:** Cylindrospermopsin*;* **G:** β-*N*-methylamino-L-alanine

Based on their toxicity effect and their mode of action and uptake, the cyanobacterial toxins can be categorized into different groups; neurotoxins, cytotoxins, dermatotoxins, irritants and hepatotoxins.[68]

For example, the neurotoxic compounds anatoxin-a, anatoxin-a(s) and saxitoxin are among the cyanobacterial toxins the most toxic compounds produced mainly by *Anabaena*, but display, due to their rare occurrence and therefore reduced exposure, a minor danger to humans when compared to the hepatotoxins, such as the microcystins (MCs) and nodularins.[69] Anatoxin-a is a bicyclic, secondary amine, which is a strong agonist of the nicotinic acetylcholine receptors.[70] Toxicity symptoms appear quickly after ingestion of contaminated water: paralysis, tremors, convulsions and death.[71]

Anatoxin-a(s) constitutes an organophosphate, structurally not related to anatoxin-a, which irreversibly blocks acetylcholinesterase and enhances salivation.[72,73] Furthermore, the administration of pure toxin to mice leads to fast death and respiratory failure within a few hours.[74] Saxitoxin, produced by a freshwater cyanobacteria as well as marine dinoflagellates, is a strong neurotoxin, which accumulates in the food chain and causes paralytic shellfish poisoning.[75] Symptoms occur rapidly after intake of poisoned food and are manifested as preliminary numbness around the lips, which later affects the whole body and can lead to respiratory paralysis.[76] Its chemical core structure is a trialkyl tetrahydropurine and 30 derivatives are known.[77]

Another example is cylindrospermopsin, which can be found in *Cylindrospermopsis raciborskii*. It is a cytotoxic and genotoxic alkaloid, which covalently binds to DNA and affects the liver, the kidneys and the lungs.[78] In addition, it is carcinogenic and inhibits protein synthesis.[79] The strong liver toxicity effect is explained by the oxidation by CYP450, which leads to a more potent metabolite.[80]

Additional toxins, primarily produced by tropical and subtropical marine cyanobacteria like *Oscillatoria*, are, for example, lyngbyatoxin-a, debromoaplysiatoxin and aplysiatoxin, representing common dermatotoxins.[69] The typical common clinical symptom of these toxins is dermatitis, complemented by tumor promoter activity and protein kinase C activation in the case of debromoaplysiatoxin and aplysiatoxin, as well as gastrointestinal inflammation for lyngbyatoxin-a.[81,82]

Another class of toxins are the irritants. Some compounds with lipopolysaccharide core also fall in this category, as they represent a crucial component of the cell wall of all bacteria.[67] The toxicity effect occurs after a contact with these toxins and is manifested as an allergic response, gastroenteritis and inflammation.[83] These less serious toxic effects, in comparison to the above mentioned compounds, gives them less importance in research.[84]

The last and best-studied compound class are the hepatotoxins. As mentioned above, cyanobacteria are known to be hepatotoxic and exposure to blooms cause typical clinical symptoms for liver damage, such as increased liver size, haemorrhage and blood pooling and deep-red coloration of the liver. Furthermore, enhanced activity of glutamate pyruvate transaminase/alanine aminotransferase, lactate dehydrogenase and alkaline phosphatase is observed.[85]

The two common hepatotoxins are represented by the microcystins, whereby the main producers are *Anabaena*, *Microcystis*, *Nostoc* and *Planktothrix*, and by nodularin, produced by *Nodularia spumigena*, whereas this toxin shows a similar toxicity effect as microcystin.[86]

A characteristic feature of both compounds is the strong inhibition effect of protein phosphatase 1 and 2A, as well as promotion of liver cancer.[87,88] The microcystins show a great variety of structures (80 derivatives known to date).[89] Beside a general core structure, two variable amino acids (Xaa, Yaa) lead to this great structural diversity.[90] Within this compound class, MC-LR (Xaa = Leu, Yaa = Arg) has an exceptional position as the most precisely studied microcystin, due to its high LD_{50} value (50 $\mu g kg^{-1}$).[91] In fact, it is one of most potent and toxic compound produced by cyanobacteria and on this account the WHO set a guideline value of MC-LR in drinking water of 1 $\mu g L^{-1}$.[92,93]

Nodularin has a similar structure as microcystin, containing the Adda function (3-amino-9-methoxy-2,6,8-trimenthyl-10-phenyl-4,6-decadienoic acid), D-Glu, D-MeAsp, L-Arg and MeDhb. In contrast, to the microcystins a much smaller number of different structures has been described so far: only seven isoforms of this toxin have been reported.[75]

In addition to the above-mentioned categorized toxins, cyanobacteria produce other classes of natural products, which share structural similarity and biological effects. These compounds can be further classified regarding their general core structure into aeruginosins, microginins, anabaenopeptins, cyanopeptolins,

microcystins, microviridins and cyclamides.[53] A large group of these toxins are the aeruginosins, which are trypsin-type serine protease inhibitors produced by *Microcystis* and *Oscillatoria*.[94,95] More than 40 variants are known up to date, and the characteristic core structure of this peptide class contains the unusual amino acid 2-carboxy-6-hydroxyoctahydroindole (Choi) and hydroxyphenyl-lactic acid (Hpla) or lactic acid (Pla), further a variable amino acid (Leu, Ile, Phe, or Tyr) and an arginine or arginine derivative (agmatine, ariginol or 3-aminoethyl-1-*N*-amidino-Δ^3-pyrroline).[96] Another group of serine protease inhibitors are the cyclic peptides belonging to the group of cyanopeptolins, which have the amino acid 3-amino-6-hydroxy-2-piperidone (Ahp).[97] These toxins show a great structural diversity based on the variation of several amino acids as well as derivatization, like sulfonation and chlorination.[98,99]

The synthesis of these biomolecules is mostly performed by large enzyme complexes, the nonribosomal peptide synthetases (NRPS) or a combination of polyketide synthases and NRPSs systems.[100] The gene clusters of those synthetases contain highly conserved NRPS operons, comprising of, for example the *mcyABC* gene cluster for microcystin production within the different strains and thus suggest a horizontal gene transfer as an explanation for the similarity of the produced compounds.[90,101] The compounds produced by the NRPS pathway are further characterized by a remarkable structural variety within one class, which is not only resulting from variations in the amino acid sequence but also from modifications like methylation, glycosylation, chlorination or sulfation.[53] Nevertheless, ribosomal peptide synthesis and posttranslational modification is also suggested for some cyanobacterial peptides, as it is the case for microcyclamides, and microviridins.[102]

Recently, β-*N*-methylamino-L-alanine, a neurotoxic amino acid produced by cyanobacteria, received attention as it is considered to be a trigger for human neurological diseases, such as Amyotrophic Lateral Sclerosis, Parkinson's and Alzheimer's disease.[103,104] These diseases seem to be initiated by an overactivation of neuroexcitatory glutamate receptors, which leads to damage of the neurons.[105]

Despite all the research done on cyanobacterial toxins, the ecological and biological role of these compounds is still under investigation. Today the purpose of toxin production is mainly linked to the protection against grazers, e.g. against the waterflea *Daphnia*.[106-108] In contrast to this theory, phylogenetic analyses suggests that the synthetase genes developed simultaneously with the housekeeping genes

and thus are older than grazers.[109] They are also thought to act as allelochemicals to repel other photosynthetic competitors or for cell signalling or iron scavenging, since the long existence of these compounds and the effort for their production hypothesize a fundamental biological role.[110,111] In both cases, the existence of mutants of cyanobacteria, which have lost the ability to produce microcystin by inactivation of the mycrocystin synthetase through mutations in the gene cluster, could exclude the toxic function of microcystin.[112] This circumstance is even more complex, as non-toxic cyanobacteria exist and form blooms.[113,114] Therefore, the missing "final explanation" for the purpose of the toxin production renders toxic cyanobacteria still a mysterious species. Many things regarding their toxicity are known but nevertheless the challenge is to answer more open questions and resolve the last riddles, which this mysterious organisms preserves.

1.4 Overview

In this thesis, open questions regarding cyanobacterial toxins are addressed. The projects involve the isolation, characterization, derivatization and biological evaluation of various toxic compounds derived from cyanobacteria. It is divided into **4** chapters, each representing a separated research topic.

Chapter 2 is addressing the general chemical behaviour of an arginine moiety in a peptide. It involves the development of a standardized method for efficient modification of the guanidinium group in native peptides.

Chapter 3 describes the successful derivatization of the cyanobacterial toxin microcystin-LR. Furthermore, it contains biological tests to examine its possibly changed behaviour towards biological targets. First applications in zebrafish (*Danio rerio*) were tested by our cooperation partner Susanne Faltermann (University of Applied Sciences and Arts Northwestern Switzerland).

Chapter 4 includes the structure elucidation of an unknown peptide isolated from cyanobacteria. It is estimated to be a replacement of microcystin in non-microcystin producing strains. The isolation was performed by our cooperation partner Esther Kohler (University of Zurich).

Chapter 5 focuses on the chemical modification of the cyanobacterial toxin Cyanopeptolin 1020.

1.5 References

[1] D. H. Williams, M. J. Stone, P. R. Hauck, S. K. Rahman, *J. Nat. Prod.* **1989**, *52*, 1189–1208.

[2] M. J. Stone, D. H. Williams, *Mol. Microbiol.* **1992**, *6*, 29–34.

[3] M. J. Stone, D. H. Williams, *Pharm. Unserer Zeit* **2003**, *32*, 11–16.

[4] C. Collin, F. Hauser, E. Gonzalez de Valdivia, S. Li, J. Reisenberger, E. M. Carlsen, Z. Khan, N. O. Hansen, F. Puhm, L. Søndergaard, J. Niemiec, M. Heninger, G. R. Ren, C. J. Grimmelikhuijzen, *Cell. Mol. Life Sci.* **2013**, 70, 3231–3242.

[5] M. Lahlou, *Pharmacology & Pharmacy* **2013**, *4*, 17–31.

[6] R. S. Solecki, *Science* **1975**, *190*, 880–881.

[7] J. D. Phillipson, *Phytochemistry* **2001**, *56*, 237–243.

[8] S. Shishodia, K. B. Harikumar, S. Dass, K. G. Ramawat, B. B. Aggarwal, *Anticancer Res.* **2008**, *28*, 3647–3664.

[9] H. Hatcher, R. Planalp, J. Cho, F. M. Torti, S. V. Torti, *Cell. Mol. Life Sci.* **2008**, *65*, 1631–1652.

[10] G. A. Cordell, M. D. Colvard, *J. Nat. Prod.* **2012**, *75*, 514–525.

[11] G. Lockemann, *J. Chem. Educ.* **1951**, 277–279.

[12] D. J. Newman, *J. Med. Chem.* 2008, *51*, *2589*–2599.

[13] D. J. Newman, G. M. Cragg, *J. Nat. Prod.* **2007**, *70*, 461–477.

[14] B. L. Ligon, *Semin. Pediatr. Infect. Dis.* **2004**, *15*, 52–57.

[15] A. J. J. Wood, E. K. Rowinsky, R. C. Donehower, *N. Engl. J. Med.* **1995**, *332*, 1004–1014.

[16] J. R. Vane, R. M. Botting, *Thrombosis Research* **2003**, *110*, 255–258.

[17] J. Singh, A. Kumar, V. Kumar, J. S. Sethi, *Int. J. Nat. Prod. Sci.* **2011**, 1–8.

[18] G. M. Cragg, P. G. Grothaus, D. J. Newman, *Chem. Rev.* **2009**, *109*, 3012–3043.

[19] H. R. González, M. A. Tututi, *CNS Neurosci. Ther.* **2008**, *14*, 234–247.

[20] A. García, V. Bocanegra-García, J. P. Palma-Nicolás, G. Rivera, *Eur. J. Med.* **2012**, *49*, 1–23.

[21] J. M. Lord, L. M. Roberts, J. D. Robertus, *FASEB J.* **1994**, *8*, 201–208.

[22] H. Sugiyama, *Microbiol. Rev.***1980**, *44*, 419–448.

[23] M. R. Lee, *J. R. Coll. Physicians. Edinb.* **2007**, *37*, 77–84.

[24] W. Vycudilik, G. Gmeiner, *Drug Test Anal.* **2009**, *1*, 177–183.

[25] Editorials, *Jour. A. M. A.* **1932**, *98*, 1992–1994.

[26] T. Reynolds, *Phytochemistry* **2005**, *66*, 1399–1406.

[27] S. Vichi, P. Lavorini, E. Funari, S. Scardala, E. Testai, *Food Chem. Toxicol.* **2012**, *50*, 4493–4499.

[28] C. M. Placinta, J. P. F. D'Mello, A. M. C. Macdonald, *Anim. Feed Sci. Tech.* **1999**, *78*, 21–37.

[29] E. Despott, M. J. Cachia, *Malta Med. J.* **2004**, *16*, 39–41.

[30] J. W. Schopf, B. M. Packer, *Science* **1987**, *237*, 70–73.

[31] W. W. Carmichael, R. Li, *Saline System* **2006,** 19;2:5.

[32] S. N. Tripathi, I. K. Chung, J. A. Lee, *J. Plant. Biol.* **2007**, *50*, 50–59.

[33] J. F. Briand, C. Leboulanger, J. F. Humbert, *J. Phycol.* **2004**, *40*, 231–238.

[34] E. Tang, R. Tremblay, W. F. Vincent, *J. Phycol.* **1997**, *33*, 171–181.

[35] A. D. Jungblut, C. Lovejoy, W. F. Vincent, *ISME J.* **2009**, *4*, 191–202.

[36] D. M. Ward, M. J. Ferris, S. C. Nold, M. M. Bateson, *Microbiol. Mol. Biol. Rev.* **1998**, *62*, 1353–1370.

[37] E. S. Reichwaldt, A. Ghadouani, *Water Res.* **2012**, *46*, 1372–1393.

[38] I. Dor, A. Danin, *Algological Studies* **1996**, *83*, 197–206.

[39] L. M. Gerasimenko, V. K. Orleanskii, G. A. Karpov, G. T. Ushatinskaya, *Microbiology* **2013**, *82*, 111–118.

[40] N. Gordon, D. L. Angel, A. Neori, N. Kress, B. Kimor, *Msr. Ecol. Prog. Ser.* **1994**, *107*, 83–88.

[41] J. C. Meeks, *BioScience* **1998**, *48*, 266–276.

[42] M. Hyvarinen, R. Hardling, J. Tuomi, *Oikos* **2002**, *98*, 498–504.

[43] N. Latysheva, V. L. Junker, W. J. Palmer, G. A. Codd, D. Barker, *Bioinformatics* **2012**, *28*, 603–606.

[44] A. Herrero, A. M. Muro-Pastor, E. Flores, *J. Bacteriol.* **2001**, *183*, 411–425.

[45] S. Pitois, M. H. Jackson, B. J. B. Wood, *Int.J. Environ. Health Res.* **2000**, *10*, 203–218.

[46] R. Y. Stanier, G. C. Bazine, *Annu. Rev. Microbiol.* **1977**, *31*, 225–274.

[47] G. C. Dismukes, V. V. Klimov, S. V. Baranov, Y. N. Kozlov, J. DasGupta, A. Tyryshkin, *Proc. Natl. Acad. Sci. U.S.A.* **2001**, *98*, 2170–2175.

[48] A. Rokas, *Annu. Rev. Genet.* **2008**, *42*, 235–251.

[49] E. Flores, A. Herrero, C. P. Wolk, I. Maldener, *Trends Microbiol.* **2006**, *14*, 439–443.

[50] E. Flores, A. Herrero, *Nat. Rev. Microbiol.* **2010**, *8*, 39–50.

[51] B. E. Schirrmeister, A. Antonelli, H. C. Bagheri, *BMC Evol. Biol.* **2011**, *11*: 45.

[52] R. B. Dixit, M. R. Suseela, *Antonie Van Leeuwenhoek* **2013**, *103*, 947–961.

[53] M. Welker, H. von Döhren, *FEMS Microbiol. Rev.* **2006**, *30*, 530–563.

[54] A. M. Burja, B. Banaigs, E. Abou-Mansour, *Tetrahedron* **2001**, *57*, 9347–9377.

[55] H. Luesch, R. E. Moore, V. J. Paul, S. L. Mooberry, T. H. Corbett, *J. Nat. Prod.* **2001**, *64*, 907–910.

[56] Y Wang, Z. Miao, *Mar. Drugs* **2013**, *11*, 903–933.

[57] W. W. Carmichael, *J. Appl. Microbiol.* **1992**, *72*, 445–459.

[58] H. W. Paerl, J. Huisman, *Science* **2008**, *320*, 57–58.

[59] N. Lagos, H. Onodera, P. A. Zagatto, D. Andrinolo, S. M. F. Q. Azevedo, Y. Oshima, *Toxicon* **1999**, *37*, 1359–1373.

[60] M. Kahru, O. P. Savchuk, R. Elmgren, *Mar. Ecol. Prog. Ser.* **2007**, *343*, 15–23.

[61] A. Eiler, S. Drakare, S. Bertilsson, J. Pernthaler, S. Peura, C. Rofner, K. Simek, Y. Yang, P. Znachor, E. S. Lindström, *PLoS ONE* **2013**, *8*, e53516.

[62] R. Kurmayer, M. Gumpenberger, *Mol. Ecol.* **2006**, *15*, 3849–3861.

[63] I. Stewart, P. M. Webb, P. J. Schluter, G. R. Shaw, *Environ. Health* **2006**, *5*: 6.

[64] M. J. Pybus, D. P. Hobson, D. K. Onderka, *J. Wildl. Dis.* **1986**, *22*, 449–450.

[65] S. M. F. O. Azevedo, W. W. Carmichael, E. M. Jochimsen, K. L. Rinehart, S. Lau, G. R. Shaw, G. K. Eaglesham, *Toxicology* **2002**, *181*, 441–446.

[66] L. Giannuzzi, D. Sedan, R. Echenique, D. Andrinolo, *Mar. Drugs* **2011**, *9*, 2164–2175.

[67] L. Bláha, P. Babica, B. Maršálek, *Interdiscip. Toxicol.* **2009**, *2*, 36–41.

[68] C. Wiegand, S. Pflugmacher, *Toxicol. Appl. Pharmacol.* **2005**, *203*, 201–218.

[69] J. Mankiewicz, M. Tarczynska, Z. Walter, *Acta Biol. Cracov. Ser. Bot.* **2003**, *45*, 9–20.

[70] J. P. Devlin, O. E. Edwards, P. R. Gorham, *Can. J. Chem.* **1977**, *55*, 1367–1371.

[71] E. H. Rogers, E. S. Hunter, V. C. Moser, P. M. Phillips, J. Herkovits, L. Muñoz, L. L. Hall, N. Chernoff, *J. Appl. Toxicol.* **2005**, *25*, 527–534.

[72] S. Matsunaga, R. E. Moore, W. P. Niemczura, *J. Am. Chem. Soc.* **1989**, *111*, 8021–8023.

[73] E. Dittmann, D. P. Fewer, B. A. Neilan, *FEMS Microbiol. Rev.***2013**, *37*, 23–43.

[74] H. Onodera, Y. Oshima, P. Henriksen, T. Yasumoto, *Toxicon* **1997**, *35*, 1645–1648.

[75] L. Pearson, T. Mihali, M. Moffitt, R. Kellmann, B. Neilan, *Mar. Drugs* **2010**, *8*, 1650–1680.

[76] K. D. Cusick, G. S. Sayler, *Mar. Drugs* **2013**, *11*, 991–1018.

[77] L. E. Llewellyn, *Nat. Prod. Rep.* **2006**, *23*, 200–222.

[78] C. Moreira, J. Azevedo, A. Antunes, V. Vasconcelos, *J. Appl. Microbiol.* **2013**, *114*, 605–620.

[79] I. R. Falconer, A. R. Humpage, *Environ. Toxicol.* **2006**, *21*, 299–304.

[80] M. T. Runnegar, S. M. Kong, Y. Z. Zhong, S. C. Lu, *Biochem. Pharmacol.* **1995**, *49*, 219–225.

[81] J. S. Mynderse, R. E. Moore, M. Kashiwagi, T. R. Norton, *Science* **1977**, *196*, 538–540.

[82] J. H. Cardellina, F. J. Marner, R. E. Moore, *Science* **1979**, *204*, 193–195.

[83] R. Mur, O. M. Skulberg, H. Utkilen, *Appl. Environ. Microbiol.* **1982**, *43*, 104–109.

[84] G. Keleti, J. L. Sykora, *Appl. Environ. Microbiol.* **1982**, *43*, 104–109.

[85] A. Kumar, D. P. Singh, R. P. Sinha, M. B. Tyagi, *EXCLI J.* **2006**, *5*, 66–78.

[86] R. W. Zurawell, H. Chen, J. M. Burke, E. E. Prepas, *J. Toxicol. Environ. Health B.* **2005**, *8*, 1–37.

[87] C. MacKintosh, K. A. Beattie, S. Klumpp, P. Cohen, G. A. Codd, *FEBS Lett.* **1990**, *264*, 187–192.

[88] H. Fujiki, M. Suganuma, *Anticancer Agents Med. Chem.* **2011**, *11*, 4–18.

[89] P. Zeller, M. Clément, V. Fessard, *Toxicology* **2011**, *290*, 7–13.

[90] B. Mikalsen, G. Boison, O. M. Skulberg, J. Fastner, W. Davies, T. M. Gabrielsen, K. Rudi, K. S. Jakobsen, *J. Bacteriol* **2003**, *185*, 2774–2785.

[91] E. M. Rodríguez, J. L. Acero, L. Spoof, J. Meriluoto, *Water Res.* **2008**, *42*, 1744–1752.

[92] N. Gupta, S. C. Pant, R. Vijayaraghavan, P. V. L. Rao, *Toxicology* **2003**, *188*, 285–296.

[93] WHO Cyanobacterial toxins: Microcystin-LR in drinking water **2003**, 1–18.

[94] M. Murakami, K. Ishida, T. Okino, Y. Okita, H. Matsuda, *Tetrahedron Lett.* **1995**, *36*, 2785–2788.

[95] H. J. Shin, H. Matsuda, M. Murakami, K. Yamaguchi, *J. Org. Chem.* **1997**, *62*, 1810–1813.

[96] S. Elkobi-Peer, R. K. Singh, T. M. Mohapatra, S. P. Tiwari, S. Carmeli, *J. Nat. Prod.* **2013**, *76*, 1187–1190.

[97] C. Martin, L. Oberer, T. Ino, W. A. König, M. Busch, J. Weckesser, *J. Antibiot.* **1993**, *46*, 1550–1556.

[98] J. Weckesser, C. Martin, C. Jakobi, *Syst. Appl. Microbiol.* **1996**, *19*, 133–138.

[99] U. Matern, L. Oberer, R. A. Falchetto, M. Erhard, W. A. König, *Phytochemistry* **2001**, *58*, 1087–1095.

[100] D. Schwarzer, R. Finking, M. A. Marahiel, *Nat. Prod. Rep.* **2003**, *20*, 275–287.

[101] T. B. Rounge, T. Rohrlack, T. Kristensen, K. S. Jakobsen, *BMC Microbiol.* **2008**, *8*, 141.

[102] N. Ziemert, K. Ishida, A. Liaimer, C. Hertweck, E. Dittmann, *Angew. Chem. Int. Ed. Engl.* **2008**, *47*, 7756–7759.

[103] S. A. Banack, T. A. Caller, E. W. Stommel, *Toxins* **2010**, *2*, 2837–2850.

[104] J. Pablo, S. A. Banack, P. A. Cox, T. E. Johnson, S. Papapetropoulos, W. G. Bradley, A. Buck, D. C. Mash, *Acta Neurol. Scand.* **2009**, *120*, 216–225.

[105] K. J. Vyas, J. H. Weiss, *Amyotroph. Lateral. Scler.* **2009**, *10*, 50–55.

[106] A. E. Wilson, O. Sarnelle, A. R. Tillmanns, *Limnol. Oceanogr.* **2006**, *51*, 1915–1924.

[107] J. F. Blom, J. A. Robinson, F. Jüttner, *Toxicon* **2001**, *39*, 1923–1932.

[108] M. Lürling, *Limnology and Oceanography* **2003**, *48*, 2214–2220.

[109] A. Rantala, D. P. Fewer, M. Hisbergues, L. Rouhiainen, J. Vaitomaa, T. Börner, K. Sivonen, *Proc. Natl. Acad. Sci. U.S.A.* **2004**, *101*, 568–573.

[110] A. Holland, S. Kinnear, *Mar. Drugs* **2013**, *11*, 2239–2258.

[111] J. P. Berry, M. Gantar, M. H. Perez, G. Berry, F. G. Noriega, *Mar. Drugs* **2008**, *6*, 117–146.

[112] G. Christiansen, C. Molitor, B. Philmus, R. Kurmayer, *Mol. Biol. Evol.* **2008**, *25*, 1695–1704.

[113] S. Merel, D. Walker, R. Chicana, S. Snyder, E. Baurès, O. Thomas, *Environ. Int.* **2013**, *59*, 303–327.

[114] V. Ostermaier, R. Kurmayer, *Microb. Ecol.* **2009**, *58*, 323–333.

2

Method Development for Arginine Modification in Peptides

2.1 Introduction

Countless peptides are produced by various species through all domains of life. In fact, they are one of the main compound classes of natural products. A great diversity of structure and function is reached mainly by only 20 natural amino acids, and expanded by the nonribosomal synthesis in posttranslational modification or incorporation of unnatural amino acids.[1,2] The common feature peptides share is the backbone structure consisting of amide bonds, nevertheless a great variety can be achieved by sequence variation and length of the amino acid chain as well as the folding. Since these unique compounds are an integral part of many biological processes, they are one of the building blocks of life, and their different functions ranges from transport to signalling and defence.[3] Being involved in many biochemical processes in the body, peptides play an important role as inherent part as key compounds in a variety of research fields such as drug discovery, chemical biology, and medicinal applications.[4,5] The birth of peptide chemistry started in 1901 with the coupling reaction of two amino acids to a dipeptide done by Emil Fischer, the father of Biochemistry.[6] The improvement of the method by the development of coupling reagents, protecting groups and auxiliaries to prevent racemisation, helped developing strategies for the synthesis of more complex peptides The field grew rapidly with the work of Merrifield, who introduced the solid-phase peptide synthesis in 1963. That not only allowed a faster and cleaner synthesis of peptides but also made automation of this reaction possible (**Scheme 2.1**).[7] For this break-through in synthetic chemistry, Robert Bruce Merrifield received the Nobel price in 1984. Using this methodology it was possible to synthesize peptides of around 70 amino acids within few hours.

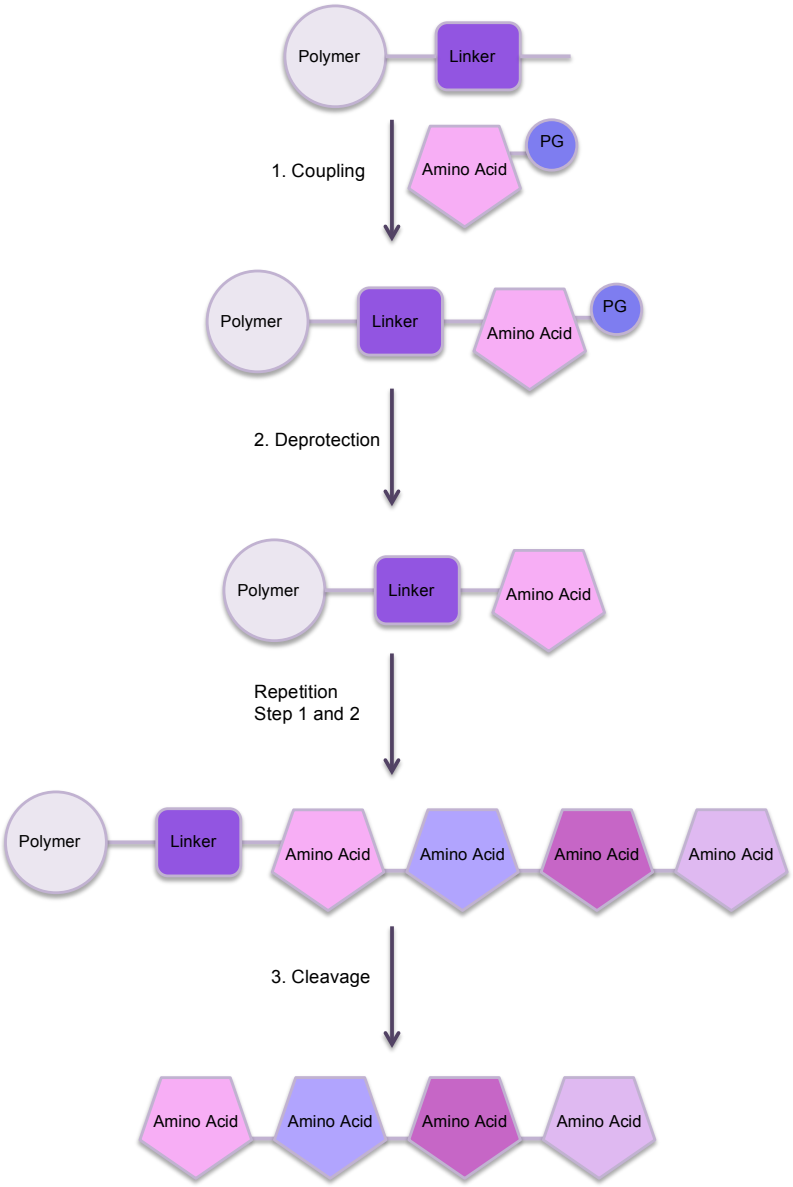

Scheme 2.1. Solid-phase peptide synthesis (PG: Protecting group)

The chain length limitation of this methodology was later circumvented by discovering the chemical ligation method, which allowed the coupling of two medium-size peptide fragments in a larger biopolymer (**Scheme 2.2**). This procedure was first reported by Wieland and later used, refined and modified by Kemp, Schnölzer and Kent.[8,9]

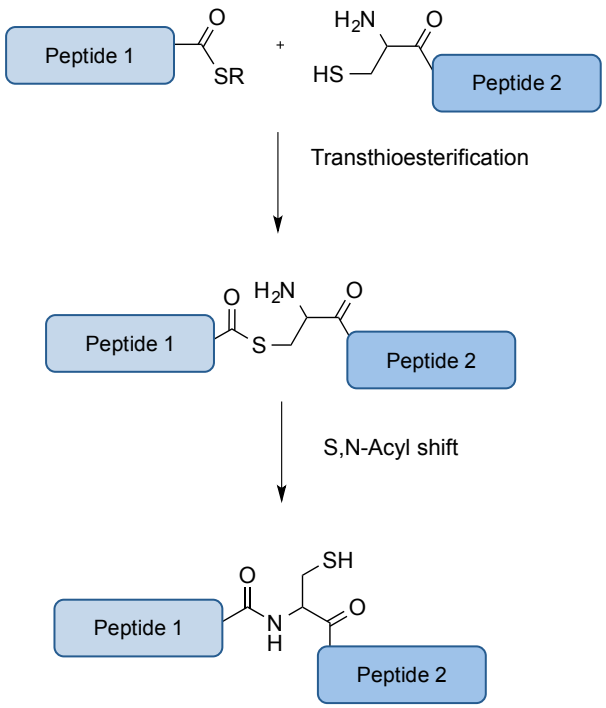

Scheme 2.2. Chemical ligation of two peptide fragments

Nowadays, peptide chemistry grew to a large scientific field, and methods for improving the synthesis are still explored and discovered.[10-14] In addition, the chemical modification of peptides has developed as a complementary area of research with a great significance. Molecules bearing different tags (fluorophore, biotin, polyethylene glycol) are crucial for various applications, such as mechanistic studies or tracing the compound in a living organism. Also the derivatization of biologically active substances to improve, for example the activity, remains to be a great challenge, particularly in medicinal chemistry.[15] The modification in peptides is frequently carried out on nucleophilic side-chains, such as NH_2, SH or OH in Lys, Cys, Ser, Thr, Glx or Asx residues.[16-21] The arginine moiety is rarely used as a modification site, due to its high pK_a value of the protonated base (pK_a ≈ 12.5) and the reduced reactivity towards electrophiles. The known procedures in literature mainly focus on modification of the arginine alone rather than functionalization of arginine-containing peptides.[22-31] An example of a direct procedure for arginine side-chain modification is the glyoxal approach.[26,27,30] Unfortunately, this strategy involves rather sensitive intermediates and results in low yields. Another widely used method employs sodium or potassium hydroxide to deprotonate the guanidinium

group, thereby increasing its nucleophilicity.[28,32] Such highly basic conditions are, however, not compatible with many base-sensitive functions and result in complications such as isomerization and degradation. NEt_3, DBU or Hünig's base (*N,N*-diisopropylethylamine) are alternatives to the hydroxide bases, however, for some more complex systems, especially on a small scale, those methods often result in low reactivity and therefore compromised yields.[22-31]

In this context, and with regards to our research project to modifying MC-LR on the arginine function, a facile and straightforward method label arginines in peptides would allow modification of peptides that cannot be labelled with current methods. For the development of such a procedure, we first focused on protected arginine to screen different conditions. Afterwards, we investigated the scope and limitations of the method by examining the compatibility of functional groups and restrictions in the size of the peptides with various penta- to hepta-peptides. All promising modification routes and the final method were then used for the side-chain modification of MC-LR (**Chapter 3**).

2.2 Results and discussion

2.2.1 Strategy

The strategy for the method development was to study compatibility by incrementally increasing the substrate complexity. We hence set out to investigate the reaction behaviour of the guanidinium moiety in protected arginine. Labelling of the Arg guanidinium group via, for example acylation, is challenging because of the high pK_a value of the protonated base (pK_a ≈ 12.5). To ensure fast deprotonation of the guanidinium group, it was crucial to find a base sufficiently strong to deprotonate the guanidinium group, but mild enough to prevent degradation of the sensitive peptides. For studying the reactivity of the arginine group towards electrophiles and diketones, we started with protected arginine.

Sulfonyl chlorides were first attempted on Boc-Arg-OH (**Scheme 2.3**).

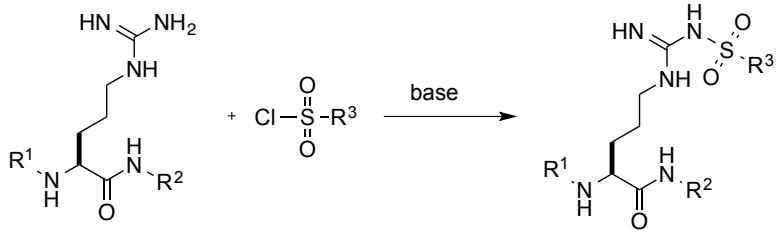

Scheme 2.3. General procedure for arginine labelling with sulfonyl chlorides

A reaction with dansyl chloride (2 eq.) with 4 molL^{-1} KOH at room temperature in acetone showed that the strong basic conditions led to deprotection of the amide and thus to undesired side reactions (**Entry 1**, **Table 2.1**). Even a change to a milder base, such as a $NaHCO_3$/Na_2CO_3 (pH = 10.8) buffer system, formed also the free amine (**Entry 1**). One of the main problems was the instability of the Boc-group with strong aqueous bases. Furthermore, the fluorophore used to hydrolyse rather quickly under these conditions.

Because of these drawbacks, we decided to use a more stable protecting group for the amine function such as a Bz-group (Bz-Arg-OMe). We first focused on diketones and tried the reaction with glyoxal (40 %) and a $NaHCO_3$/Na_2CO_3 (pH = 9) buffer system in acetone at 40 °C (**Scheme 2.4, Entry 3**).

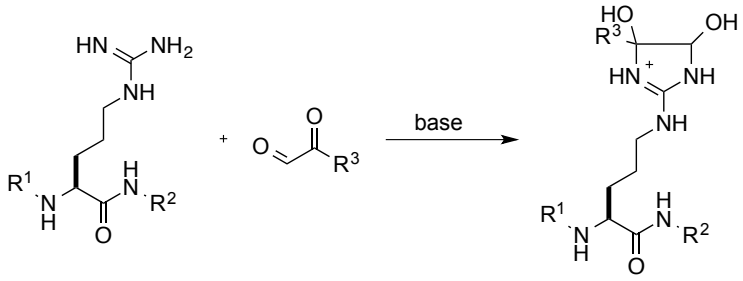

Scheme 2.4. General procedure for arginine labelling with diketones

This condition showed no conversion of the starting material. The change from glyoxal to acetylacetone (10 eq.), in attempt to obtain a more stabilized six-membered ring, led also to no conversion (**Entry 4**). A last approach was made with phenylglyoxal (1.5 eq.) at room temperature (**Entry 5**). A product formed after 15 minutes but it decomposed rather quickly (followed by TLC). Unfortunately no pure compound could be isolated due to its instability.

Our next step was changing from diketones to electrophiles, which can form an sulfonamide bond with the guanidinium group, such as dansyl chloride (2 eq.) in a $NaHCO_3/Na_2CO_3$ (pH = 9) buffer system in dry acetone at room temperature and 40 °C (**Entry 6**). No conversion of the starting material was observed under these conditions. An attempt to carry out the reaction in different solvents (THF, CH_2Cl_2, EtOAc and DMF) was also unsuccessful (**Entry 7-10**). Another set of strong basic conditions, 4 $molL^{-1}$ KOH in acetone at room temperature, caused deprotection of the methylester, which then reacted with dansyl chloride (**Entry 6**). In addition, a partial degradation of dansyl chloride was observed. Using the $NaHCO_3/Na_2CO_3$ (pH = 10.8) buffer system in acetone or Na_2CO_3 (pH = 12) at room temperature to obtain milder conditions led to **2.1** in a small yield (< 10 %, **Entry 6**).

One reason for that could be the fast hydrolysis of dansyl chloride. To verify this hypothesis, we used NEt_3 (4 eq.) in DMF or pyridine, to prevent the competing hydrolysis of the sulfonyl chloride group (**Entry 9**). While using pyridine as base resulted in no conversion, the use of NEt_3 showed similar yields as with the buffer system. The use of different solvents, such as THF, EtOAc or CH_2Cl_2 showed no improve of yield or even to formation of desired product (**Entry 7-10**). Likewise, the increase of the reaction temperature to 40 °C or to reflux could not significantly raise the yield.

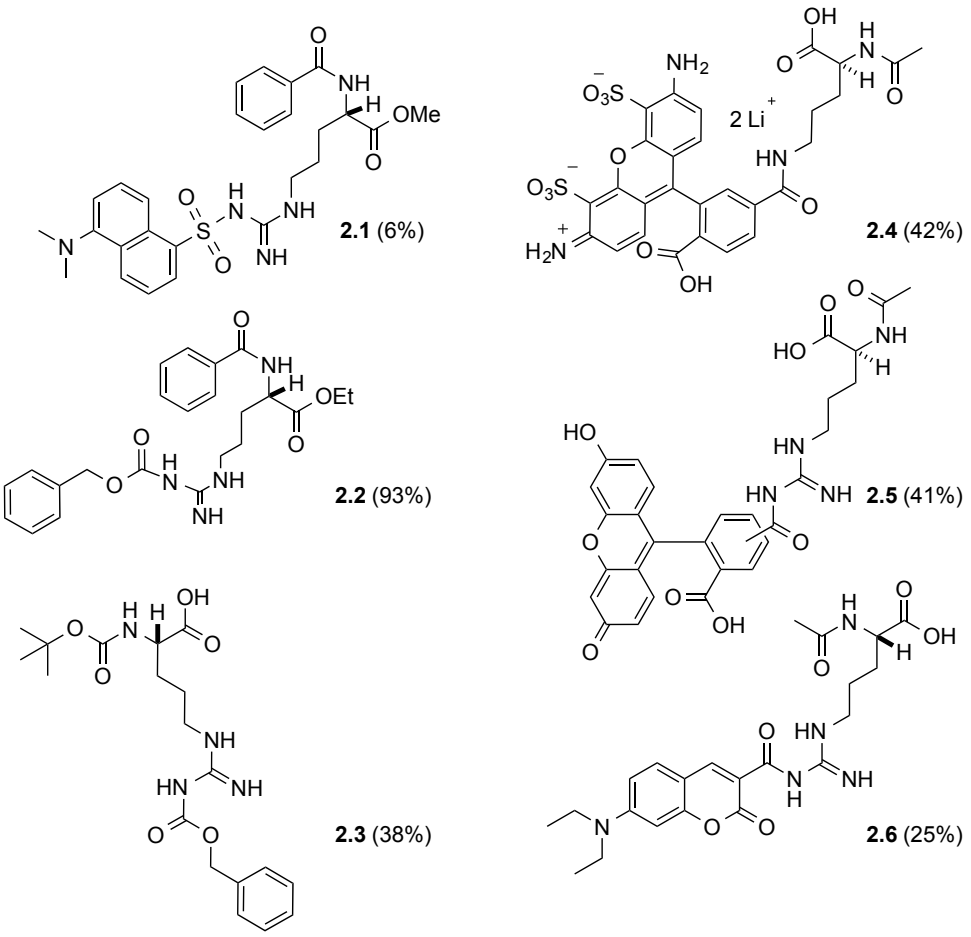

Figure 2.1. Synthesized test substrates

Next, we subjected the Bz-Arg-OMe to a less reactive sulfonyl chloride in order to improve the yield. In a first attempt, we used the $NaHCO_3/Na_2CO_3$ (pH = 10.8) buffer system in acetone with lissamine rhodamin B (2 eq.). However, no reaction was observed in this experiment (**Entry 12**). A change to DMF and NEt_3 (4 eq.) led to some conversion of the starting material, but due to the high polarity of the newly formed product, the isolation of the latter was unsuccessful (**Entry 13**).
In addition, we also tested regular peptide coupling conditions (**Scheme 2.5**).

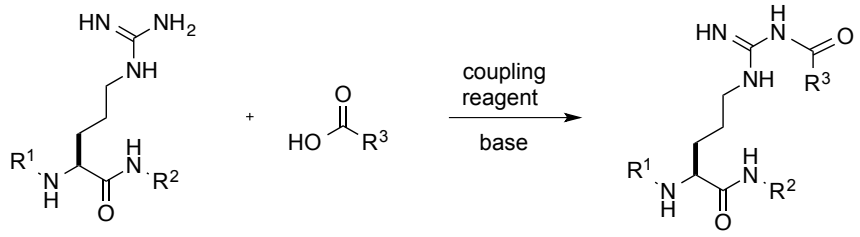

Scheme 2.5. General procedure for arginine labelling with peptide coupling conditions

Bz-Arg-OMe was treated with rhodamine B (1 eq.) in DMF and PYBOP (1 eq.) in NMM at room temperature, but also with these conditions no product was observed (**Entry 14**). Rhodamine B (1 eq.) in MeCN, *N*-hydroxysuccinimide (1.5 eq.) and EDC (1.5 eq.) led also to no product formation (**Entry 15**). In summary, only the reaction with dansyl chloride led to a promising result. Unfortunately, this method showed very low yields, maybe due to side reactions of dansyl chloride, and the poor solubility of the Bz-Arg-OMe.

With this in mind, we changed the model substrate once more. We chose Bz-Arg-OEt, as this derivative has better solubility and stability. First, the diketones, as described above, were tested. We started with phenylglyoxal (1 eq.) and the $NaHCO_3/Na_2CO_3$ (pH = 10.8) buffer system in acetone at room temperature (**Entry 16**). Only traces of product could be observed in this attempt. The same observation was made when using acetylacetone (15eq) (**Entry 17**). A peptide coupling approach, using rhodamine B (1 eq.), *N*-hydroxysuccinimide (2.5 eq.), EDC (2.5 eq.) and NEt_3 (4 eq.) in MeCN, led to a small conversion (**Entry 18**). Also the use of DMAP did not improve the reaction.

As the reaction with sulfonyl chlorides showed product formation with Bz-Arg-OMe, we investigated the reaction with Bz-Arg-OEt, dansyl chloride (3 eq.), DBU (12 eq.) and DMAP (catalytic) in DMF, which led to no improvement of the yield (**Entry 19**). Other bases, such as the $NaHCO_3/Na_2CO_3$ (pH = 10.8) buffer system, NEt_3 (4 eq.) and pyridine (excess), were tested, but none showed an improvement (**Entry 20**). Furthermore, a change of the sulfonyl chloride compound to lissamine rhodamin B (1 eq.) using NEt_3 (4 eq.) in DMF at room temperature showed no conversion (**Entry 21**). The use of DBU (12 eq.) showed only traces of the desired product (**Entry 21**). The electrophilic nature of the label was changed by using isothiocyanates (**Scheme 2.6**).

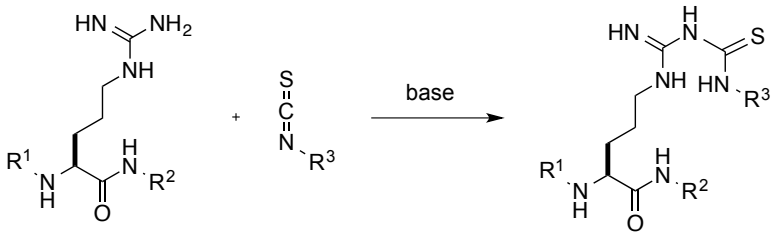

Scheme 2.6. General procedure for arginine labelling with isothiocyanates

Rhodamine B, NCS (1 eq.) was used in combination with DBU (6 eq.) or 2-(*tert*-butyl)-1,1,3,3-tetramethylguanidine base (*Barton's base*) (6 eq.) in DMF at room temperature: in the last setup traces of product were observed (**Entry 21**). Next, the succinimidyl group was used as activated ester, as they are known to have excellent reactivity towards nucleophiles under mild conditions (**Scheme 2.7**).[33]

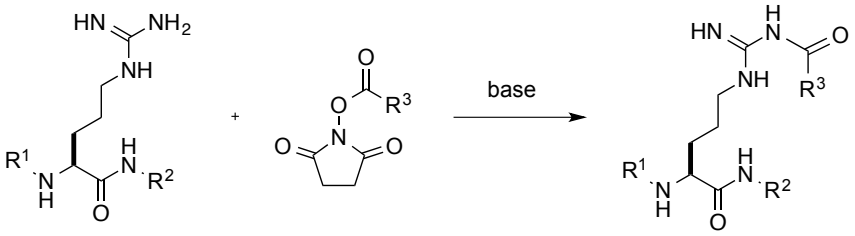

Scheme 2.7. General procedure for arginine labelling with succinimidyl esters

First we subjected Bz-Arg-OEt to 2,5-dioxopyrrolidin-1yl *N*-methylcarbamate (2.5 eq.) and DBU (6 eq.) in DMF at 40 °C, no product could be observed (**Entry 22**). We then performed the reaction with *N*-(benzylcarbonyloxy)succinimide in DMF and DBU (10 eq.) at 40 °C (**Entry 23**). Monitoring by LC-MS confirmed the desired product formation. However, the change to NEt_3 (10 eq.) in MeCN or DMAP (catalytic) as additive in DMF showed no improvement (**Entry 24,25**). Intriguingly, the use of the Barton's base (10 eq.) in DMF showed full conversion of the starting material to the desired product **2.2** (**Entry 26**). This commercially available base proved to act as an ideal proton acceptor. The advantage of the Barton's base, which is characterized by its poor nucleophilicity and a pK_a value of 14, is its structural similarity with the guanidinium group. That assures complete and fast deprotonation of the Arg guanidinium group and enables the nucleophilic attack on the activated esters.

With this efficient base identified, we tested different solvents, such as MeCN, EtOAc, THF, CH_2Cl_2, DMSO and DMF, whereby DMSO and DMF appeared to be the best (**Entry 27-31**). One disadvantage of DMSO it behaves as penetration enhancer, which is especially problematic while working with potent toxins. For this reason the use of DMF was preferred. Additionally various reaction temperatures were investigated: room temperature, 40 °C and 80 °C, whereby 80 °C showed full conversion of the starting material (**Entry 26,32,33**). A temperature of 40 °C turned out to be the compromise between reaction rate and stability of the reactants.

With our optimized conditions, we were curious if Barton's base is mild enough to acylate sensitive peptides. Additionally, we wanted to explore if a free carboxylic function is compatible with the developed method. Therefore, Boc-Arg-OH was treated with *N*-(benzylcarbonyloxy)succinimide (2 eq.) and Barton's base (10 eq.) in DMF at 40 °C (**Entry 2**). We were pleased, that these conditions led to no deprotection of the Boc-group and yielded the desired product **2.3**.

We next investigated the scope and limitations of this method, especially to explore the range of compatible functional groups. A number of penta- to hepta-peptides, containing various functionalized amino acids (Ser, Glu, Lys, Cys, His, etc; **2.7**-**2.15**), were synthesized by the standard solid-phase methodology (**Figure 2.2**). For synthetic reasons, an acetyl protecting group for primary amines was used. Furthermore, we wanted study if the size of the electrophile poses a limitation to the developed method, as we planned to attach mainly large fluorophores to the peptides.

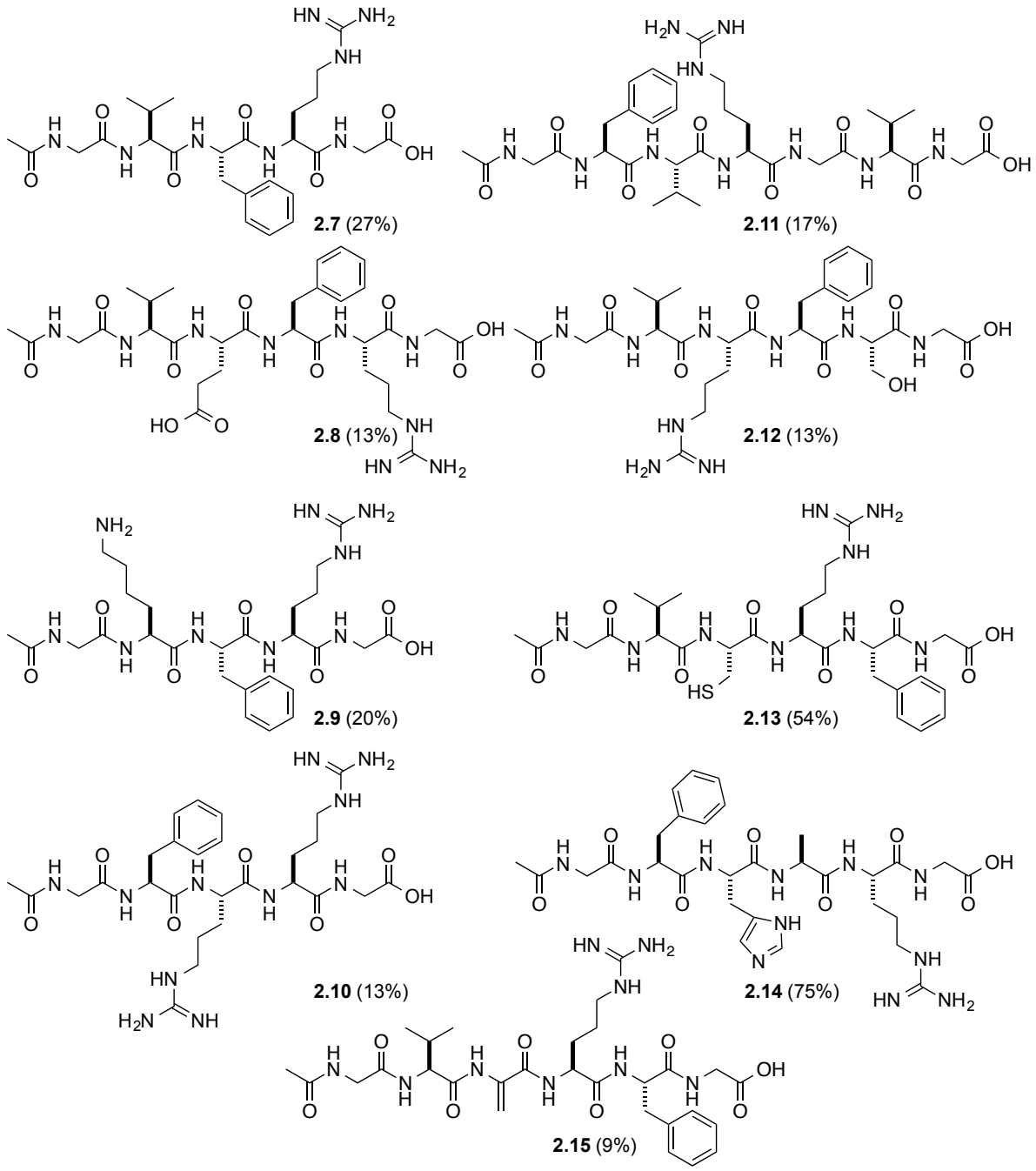

Figure 2.2. Synthesized peptide substrates

For this purpose, we subjected *N*-Ac-Arg-OH to the fluorophore Alexa 488 (1 eq.) with Barton's base (10 eq.) in DMSO (due to the low solubility of the fluorophore) (**Entry 34**). We were pleased to see that the product **2.4** was formed in 42 % yield. The change to carboxyfluorescein (2 eq.) or 7-(diethylamino)coumarin-3-carboxylic acid *N*-succinimidyl ester and Barton's base in DMF led to the formation of the product **2.5** or **2.6** in 41 % and 25 % yield, respectively (**Entry 35,36**).

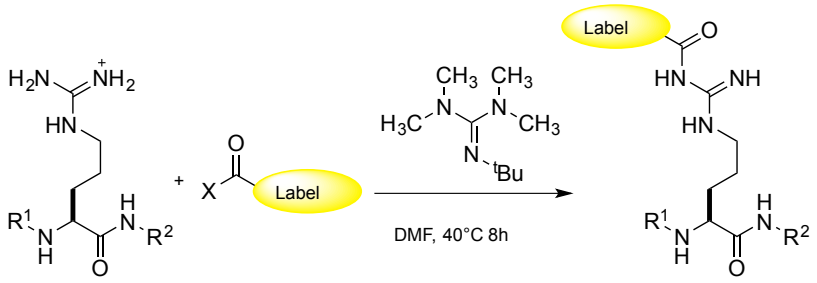

Scheme 2.8. General procedure for arginine labelling

In summary we developed an efficient and practically facile derivatization method for the guanidinium moiety in arginine. This method allows modification of arginine containing peptides with a variety of biologically relevant labels, such as fluorescent moieties, diazirine and biotin (**Scheme 2.8**).

Table 2.1. Different conditions tested with protected arginine

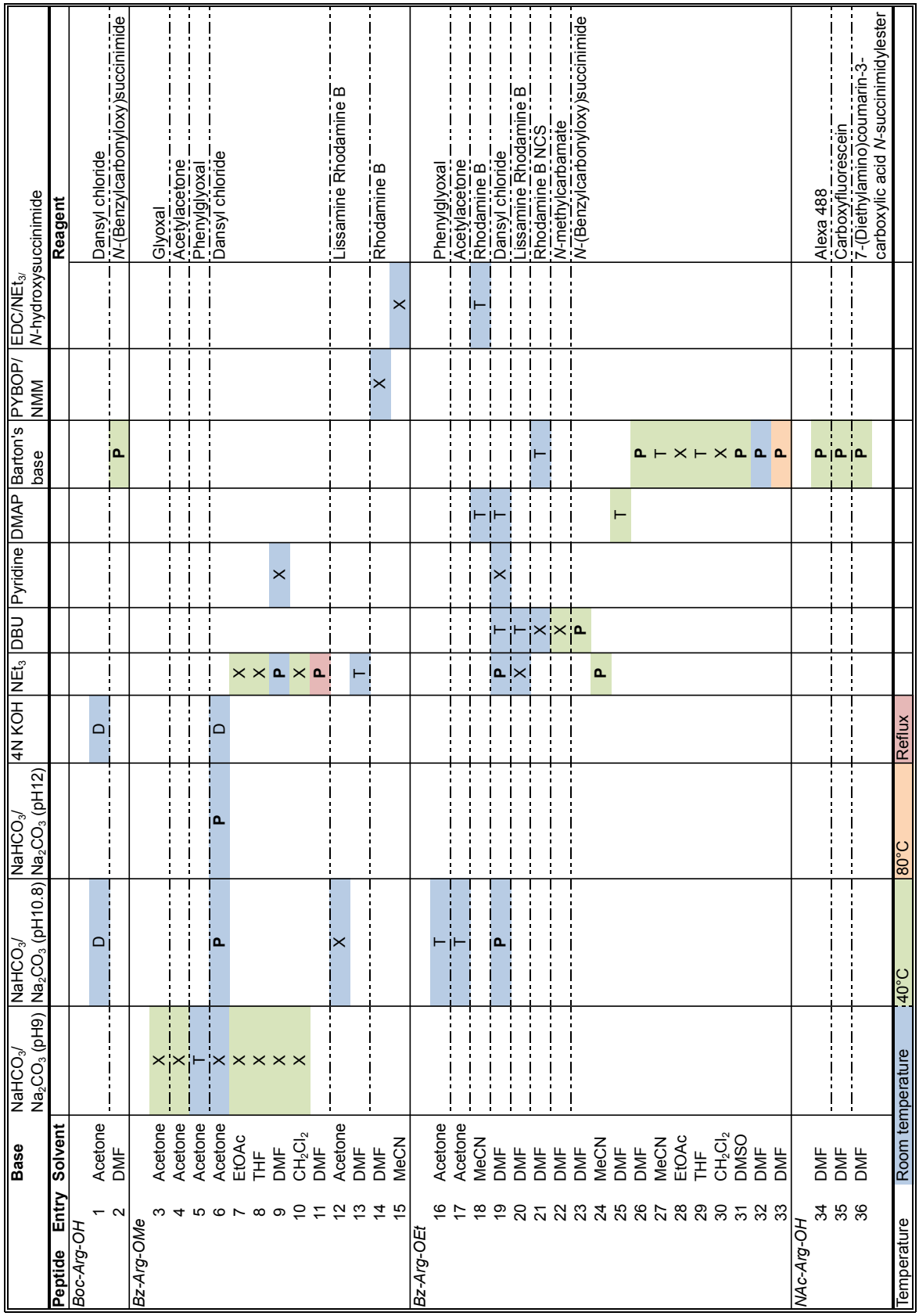

D: Deprotection, T: Traces of product, X: No reaction

2.2.2 Synthesis of the peptide substrates

With optimized conditions for arginine modification in hand, we wanted to investigate the scope and limitations of the method with focus on functional groups compatibility. The synthesis of Arg-containing peptides was done following the standard solid-phase methodology. The synthesis of a number of penta- to hepta-peptides was in adequate yields. All peptides contained a phenylalanyl residue to allow UV detection and an acytylated glycin at the *N*-terminal position to prevent side reactions. The majority of the peptides contained one arginine in the sequence (compound **2.7**-**2.9, 2.11**-**2.15**), whereas one peptide featured two arginine side chains (**2.10**, **Figure 2.2**). Purification in all cases was done by preparative HPLC.

2.2.3 Synthesis of the modified peptides

The synthesized peptides were first subjected to acylating conditions with the mixed isomer 5(6)-carboxyfluorescein succinimide. The reaction was performed by dissolving the peptides in dry DMF followed by addition of Barton's base. Subsequently, the mixture was stirred for 15 minutes to ensure complete deprotonation of the guanidinium group followed by dropwise addition of the activated ester. The reaction was stirred for one (**2.16**, **2.17**, **2.18**, **2.20**, **2.21** and **2.29**) or eight hours at 40 °C. We observed, that the reaction vial played a crucial role for the reaction time. The change of the reaction vessel from a small cylindrical insert (300µl volume) to a 1.5 mL HPLC vial led to an acceleration of the reaction time from eight to one hour. The volatiles were removed under reduced pressure and the remaining residue was dissolved in water and directly purified by RP-HPLC to give labelled peptides in moderate to good yield (> 95% purity). The use of a semi-preparative column with one injection of crude product led to 80 % yield. The pentapeptide **2.6** was successfully modified to give acylated peptide **2.16** in good yields (81 %).

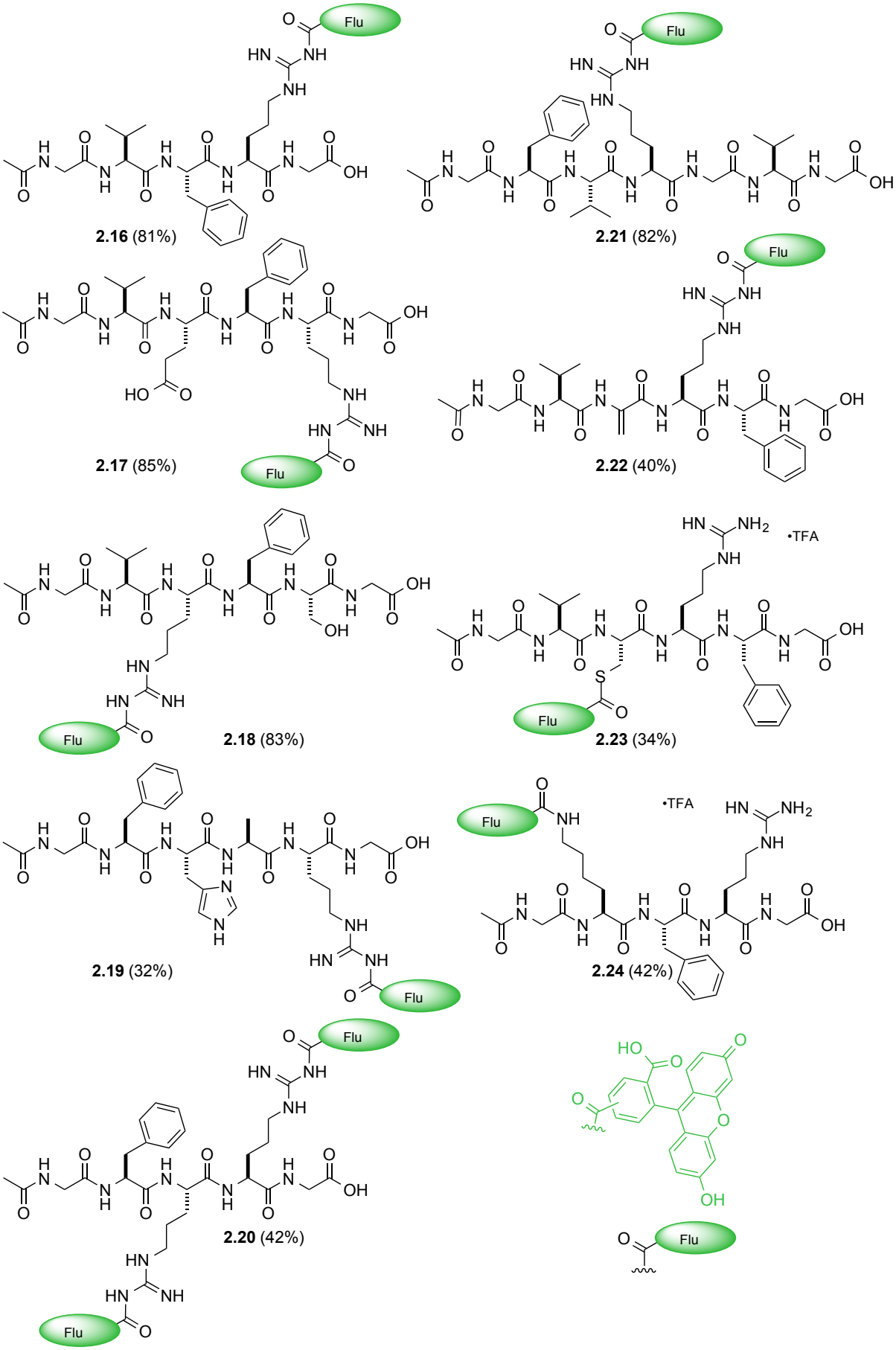

Figure 2.3. Peptides modified with carboxyfluorescein (green)

The presence of either a Glu residue (to give compound **2.17**) or a Ser residue (as in **2.18**) did not affect the acylation of the Arg, as the guanidinium group was preferred over both CO_2H and OH groups.

It should be pointed out that all peptides were obtained with free *C*-termini, *i.e.* carboxylate groups, and modification of the C-terminus was never observed. Additionally the presence of a His residue in peptide **2.19** was well tolerated, and the nucleophilic imidazole ring did not result in side reactions to the desired Arg modification.

Peptides containing two Arg residues also did not affect the method, and increasing the corresponding equivalents of base allowed for a smooth conversion to a bis-labelled peptide **2.20**. In addition, longer peptides such as heptapeptide **2.21** were obtained, as well as the peptide **2.22** carrying the non-proteinogenic Dha amino acid (dehydroalanine). This is important, as the presence of the α,β-unsaturated acceptor could interfere with various nucleophiles in the reaction.[34] All of these amino acids are frequently found in peptides of biological interest. The limitations of the method were observed in the presence of Lys or Cys residues, as their side chains react with the acylating agent. However, we are confident that these limitations could be overcome by a protection, *i.e.* as an imine for Lys and a disulfide for Cys, which would then be removed *in situ* after derivatization of Arg.

We next evaluated the scope of the acylating agents, both with regard to the nature of the activated carboxylate derivative and its suitability for conjugation. While the studies for peptides **2.16**-**2.24** have been carried out with *N*-hydroxysuccinimide esters, we have also evaluated the use of *p*-nitrophenylesters. The corresponding biotin derivatives were prepared and subjected to the same reaction conditions as described before. The corresponding peptides **2.25** and **2.26** biotinylated at the Arg residue were obtained in similar yields as for the fluorescent derivatives.

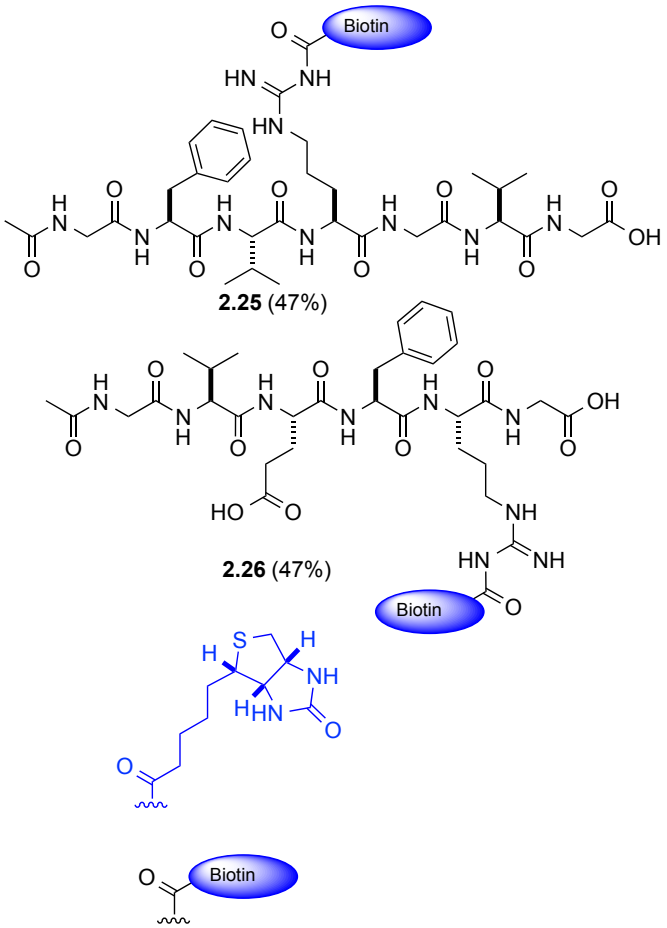

Figure 2.4. Peptides modified with a biotin (blue)

A third class of molecular probes, the sensitive diazirin-tag was also successfully introduced using this method, and the peptides **2.27** and **2.28** bearing a photoaffinity label at the Arg position were prepared.

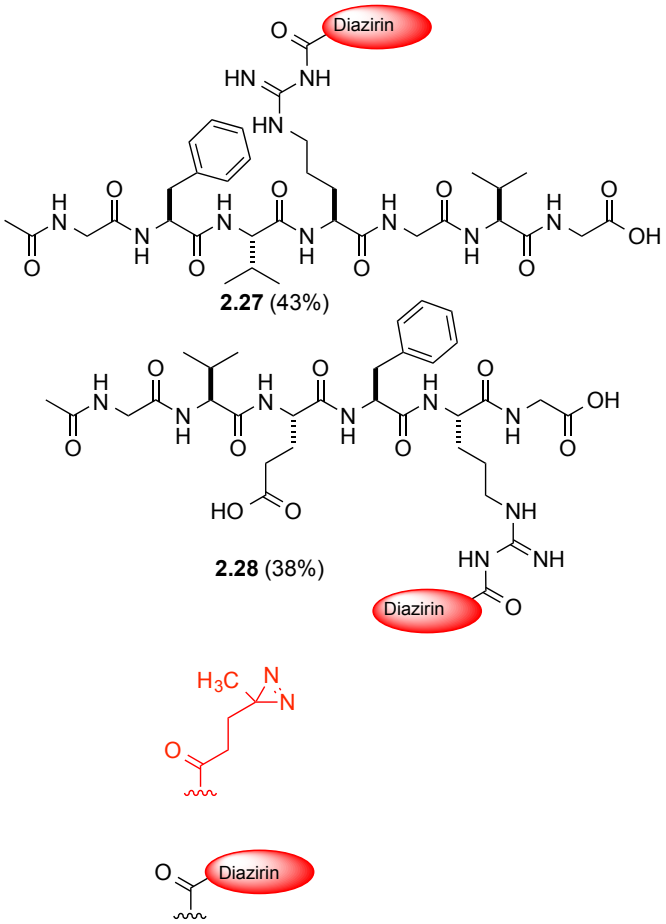

Figure 2.5. Peptides modified with a diazirin (red)

We then sought to apply this method for the fluorescent labelling of a bioactive peptides of clinical importance. Labelling of such widely used peptides could allow to monitor their distribution, both in a patient or in the environment. For this purpose, we selected the commercially available nonapeptide leuprolide acetate (**2.29**).[35] This biologically active peptide is an agonist of the luteinizing hormone-releasing receptor and is in clinical use for a variety of indications related to the suppression of luteinizing hormone, in particular prostate cancer, endometriosis, central precocious puberty and *in vitro* fertilization techniques.[35] Recent experiments suggest that leuprolide possesses neurotrophic properties, which is of interest in the context of our research program on small-molecule neurotrophin mimics.[36,37] From a chemical point of view, leuprolide (**2.29**) contains a variety of functionalized amino acids that could interfere with our acylation protocol.

Using this method, we were able to selectively acylate leuprolide (**2.29**) at the guanidium side chain of arginine; the fluorescently labelled leuprolide analogue **2.30** was obtained after HPLC purification in high purity (>95 %) (**Figure 2.6**).

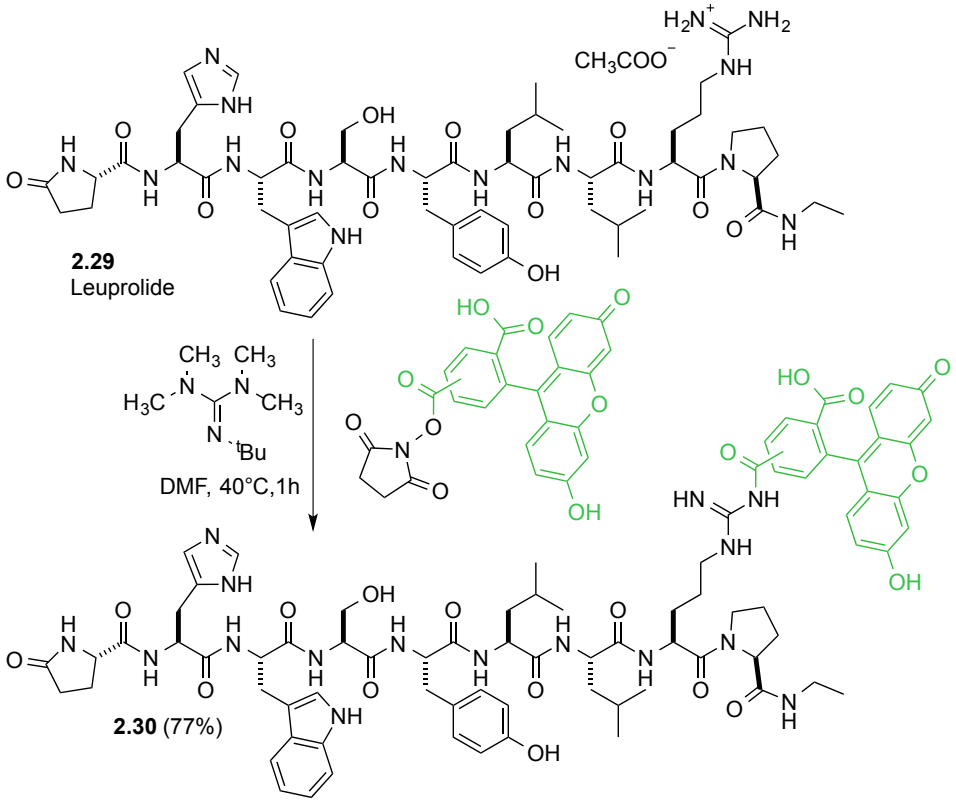

Figure 2.6. Direct and selective labelling of leuprolide (**2.29**) with a fluorescent derivative to give derivative **2.30**

The presence of pGlu, His, Trp, Ser and Tyr residues did not interfere with Arg labelling, which underlines the power and the selectivity of the presented method. MS-MS data (**chapter 7.4**.) further supports our assignment of the product.

2.2.4 Expanding the scope of the method

As pointed out before, the developed method is not suitable for peptides containing strong nucleophilic groups such as primary amines (Lys). We envisioned an orthogonal protecting group like Boc would help us overcome this limitation. We first installed the Boc protecting group under basic conditions with before applying our method. We were pleased to see, that the guanidinium group of arginine got

efficiently labelled over the protected primary amine. MS-MS experiments supported the formation of the desired product (**7.4**).

After deprotection under acidic conditions, we obtained the arginine labelled peptide **2.33** in 33 % overall yield (**Figure 2.7**).

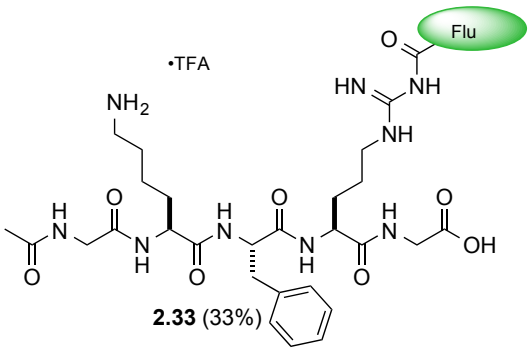

Figure 2.7. Modified peptide with carboxyfluorescein (green) on the arginine moiety

2.2.5 Photochemical properties of leuprolide with carboxyfluorescein

After successfully labelling the nonapeptide leuprolide with carboxyfluorescein, we investigated the photochemical properties of compound **2.30**, as we needed it later for uptake studies in *Daphnia magna*. The fluorescent spectrum is shown in **Figure 2.8**. The maximum absorption of the derivative was found at 502 nm and the maximum emission is located at 535 nm.

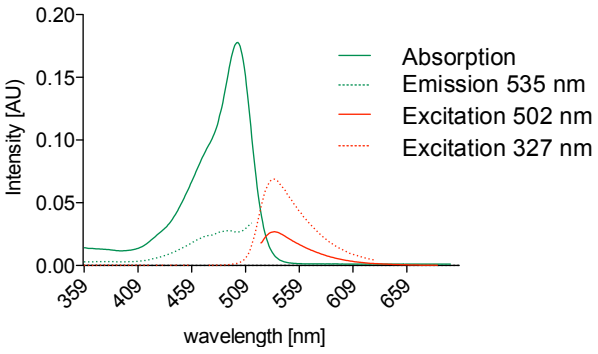

Figure 2.8. Spectral profile of compound **2.30**

The colour space chromaticity diagram is shown in **Figure 2.9**. The fluorescence of the peptide is located at the yellowish-green range (x = 0.35, y = 0.63).

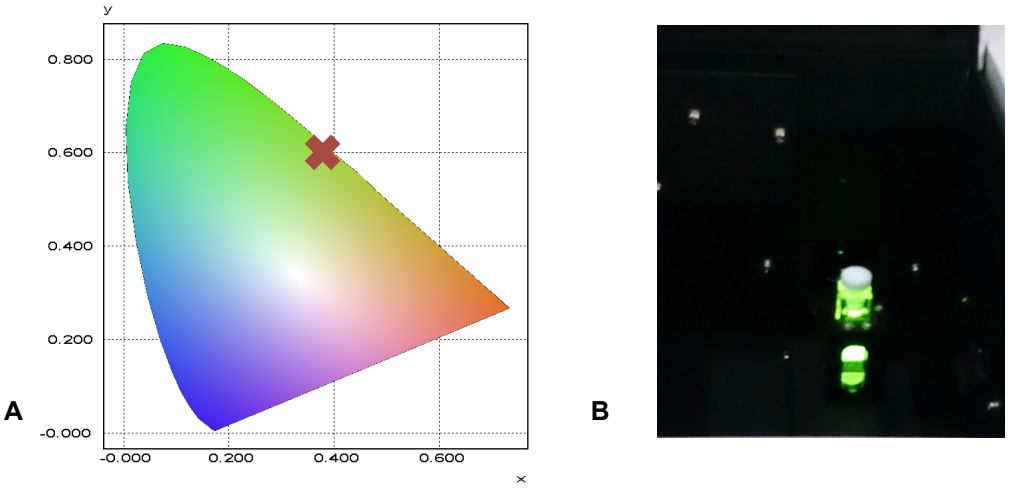

Figure 2.9. A: CIE colour space chromaticity diagram of Leuprolide-(6-FAM) **2.30** **B:** Fluorescent picture of Leuprolide-(6-FAM) **2.30**

In addition, the quantum yield of compound **2.30** was determined as it is an important parameter of the fluorescence intensity at the minimum concentration for biological experiments. Leuprolide-(6-FAM) had a quantum yield of Φ = 0.28 (Ex: 493 nm), which allows no large dilutions for high enough sensitivity of the measurements.

2.2.6 Uptake studies in Daphnia magna

In order to study the environmental fate of the leuprolide derivative **2.30**, we chose *Daphnia magna* as a test organism. *Daphnia magna* is a small grazing crustacean, which is standardly used as a model in ecotoxicology studies.[38] The labelled peptide **2.30** was dissolved in the medium, and the 48 h old animals were subsequently exposed to this dilution for three and six hours. The living animals were washed and immobilized in 1 % agarose gel for microscopic analysis using confocal microscopy. As seen in images **A** and **B**, the labelled compound **2.30** had entered the digestive tract of the animal (**Figure 2.10**). Furthermore, uptake into the cells of the ventral ceca (hepatopancreas) has occurred, which requires passing of the peritrophic membrane (**C** in **Figure 2.10**).[39] More interestingly, the hormone is first distributed in the entire gastrointestinal tract, whereas after six hours, the compound mainly accumulates in the cecum.

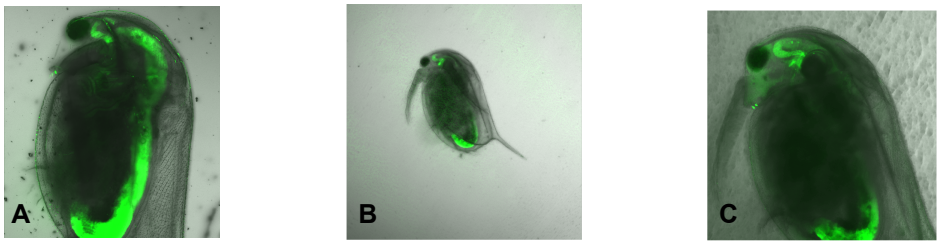

Figure 2.10. Exposure of *D. magna* to fluorescently labelled leuprolide derivative **2.30**
A: Distribution after 3h **B:** Distribution after 6h **C:** Optical magnification of **B**

2.3 Conclusion

In conclusion, we have developed a facile and straightforward method for the direct labelling of the guanidinium side-chain of arginine moieties in native peptides. This method relies on the use of Barton's base, which matches the reactivity of the guanidinium group in the substrate due to the similar chemical structure and higher basicity.

Furthermore, we were able to introduce various biologically interesting tags (fluorophores, diazirine and biotin) in yields compared to current methods. Additionally, a series of peptides containing Glu, Ser, His, Trp, Tyr or Dha residues carrying sensitive side-chains has been selectively acylated at the Arg residue using both *N*-hydroxysuccinimide and *p*-nitrophenyl esters. As a direct application, the clinically used nonapeptide leuprolide, a representative of a more complex peptide, was selectively acylated at the Arg residue.

The method is affected by the presence of other strong nucleophiles (Cys, Lys). This could be overcome by initially protecting these functions using orthogonal protecting groups such as Boc-group.

We are convinced the method will find various applications in biochemical, toxicological, pharmacological and environmental studies of Arg-labelled peptides and would open the door to many exciting new discoveries.

2.4 Methods

2.4.1 General

The following reagents were purchased and used as received: Amino acids (Bachem), Pyr-His-Trp-Ser-Tyr-D-Leu-Leu-Arg-Pro-NHEt (Bachem), 2-chlorotrityl chloride resin (Bachem), NHS-diazirine (Thermo Scientific), seaplaque agarose (Lonza), all other chemicals were purchased from Sigma-Aldrich Co. and were of analytical grade. Biotin *p*-nitrophenylester and 2,5-dibromohexanediamide was prepared according to the literature.[40,41] Peptides **2.7-2.14** were synthesized by the standard Fmoc solid-phase procedure using a Syro I Peptide Synthesizer (Biotage). All reactions were carried out in oven-dried glassware under an atmosphere of argon. HPLC purifications of the peptides were carried out by preparative reverse phase HPLC using a Varian PrepStar HPLC with a Phenomenex Gemini NX-C18 10 µ (250 mm x 21.2 mm) column and a linear gradient: 5 % to 100 % CH_3CN in H_2O over 30 min at a flow rate of 25 mL/min. HPLC purifications of the functionalized peptides were obtained on a Dionex P-680 HPLC System with a Phenomenex Gemini C18 5 µ (150 mm x 4.6 mm) column or a Phenomenex Gemini-NX C18 5 µ (75 mm x 21.2 mm) using a linear gradient: 5 % to 100 % CH_3CN in 0.1 % TFA/H_2O over 30 min or 20 min at a flow rate of 1 or 5 mL/min.

^{1}H-NMR spectra were recorded on a Bruker Avance 400 MHz or a Bruker Avance DRX 500MHz spectrometers at room temperature. Chemical shifts (δ-values) are reported in ppm, spectra were calibrated related to solvent's residual proton chemical shift (DMSO, δ = 2.50). Multiplicity is reported as follows: s = singlet, bs = broad singlet, d = doublet, dd = doublet of doublet, t = triplet, m = multiplet. The coupling constant *J* is specified in Herz (Hz). UV-Vis Data was recorded on an Agilent 8453 spectrophotometer, the fluorescence was measured on a Fluorimeter: Shimadzu 5301PC spectrofluorophotometer and the quantum yield was determined on a Hamamatsu absolute PL quantum yield spectrometer C11347 Quantaurus_QY. HRMS spectra were recorded on a Bruker maXis 4G instrument or measured by the mass spectrometric service of the University of Bern on a *Sciex QSTAR Pulsar mass spectrometer*. HRMS spectra were obtained on a Bruker maXis 4G with ESI in positive or negative mode. MS-MS experiments were obtained on a Bruker Esquire 3000 with ESI in positive mode.

2.4.2 Synthesis of the test-substrates

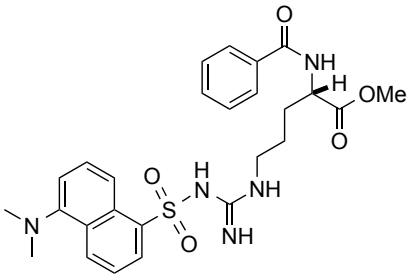

Bz-Arg(Dansyl)-OMe, (2.1):

Bz-Arg-OMe (2.0 mg, 6.8 µmol), $NaHCO_3/Na_2CO_3$ (pH = 10.8) and dansyl chloride (3.7 mg, 13.7 µmol) were dissolved in acetone and stirred for 3 h at room temperature. Direct purification by HPLC afforded **2.1** (0.20 mg, 0.38 µmol, 6 %) as a yellow solid. HPLC: t_R = 12.5 min; HRMS-ESI: calcd. for $C_{26}H_{32}N_5O_5S^+$ $[M+H]^+$: 526.2119; found: 526.2121.

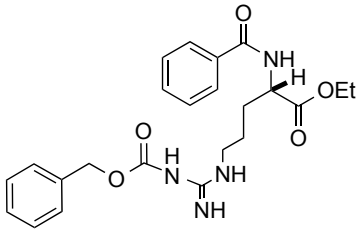

Bz-Arg(*N*-succinimid)-OEt, (2.2):

Bz-Arg-OEt (2.0 mg, 5.8 µmol), Barton's base (9.9 mg, 0.058 mmol) and *N*-(benzyloxycarbonyloxy)succinimid (1.5 mg, 5.8 µmol) were dissolved in 0.5 mL of dry DMF. The resulting reaction mixture was stirred for 2 h at 40 ° C. Direct purification by HPLC afforded **2.2** (2.4 mg, 5.4 µmol, 93 %) as a white solid. HPLC: t_R = 9.1 min; HRMS-ESI: calcd. for $C_{23}H_{29}N_4O_5^+$ $[M+H]^+$: 441.2132; found: 441.2138.

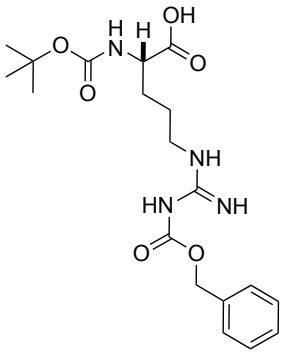

Boc-Arg(*N*-succinimid)-OH, (2.3):

Boc-Arg-OH (2.0 mg, 7.3 µmol), Barton's base (12.4 mg, 73 µmol) and *N*-(benzyloxycarbonyloxy)succinimid (3.6 mg, 14.6 µmol) were dissolved in 0.5 mL of dry DMF. The resulting reaction mixture was stirred for 2 h at 40 °C. Direct purification by HPLC afforded **2.3** (1.1 mg, 2.8 µmol, 38 %) as a white solid. HPLC: t_R = 8.9 min; HRMS-ESI: calcd. for $C_{19}H_{29}N_4O_6^+$ $[M+H]^+$: 409.2082; found: 409.2082.

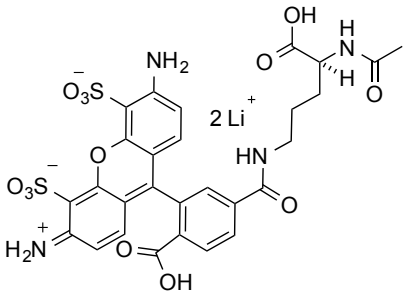

N-Ac-Arg(Alexa488)-OH, (2.4):

N-Ac-Arg-OH (0.50 mg, 2.3 µmol), Barton's base (4.0 mg, 0.023 mmol) and Alexa488 *N*-succinimidyl ester (3.5 mg, 2.3 µmol) were dissolved in 0.5 mL of dry DMF. Direct purification by HPLC afforded **2.4** (0.70 mg, 1.0 µmol, 42 %) as a red solid. HPLC: t_R = 7.5 min; HRMS-ESI: calcd. for $C_{29}H_{26}N_6O_{13}S_2^{2-}$ $[M-H]^{2-}$: 365.0505; found: 365.0501.

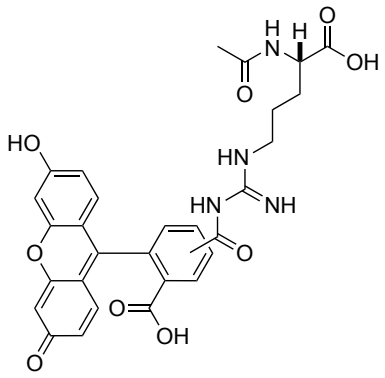

N-Ac-Arg(6-FAM)-OH, (2.5):

N-Ac-Arg-OH (0.5 mg, 2.3 µmol), Barton's base (4.0 mg, 0.023 mmol) and 5(6)-carboxyfluorescein *N*-succinimidyl ester (1.1 mg, 2.3 µmol) were dissolved in 0.5 mL of dry DMF. The resulting reaction mixture was stirred for 2 h at 40 °C. Direct purification by HPLC afforded **2.5** (0.54 mg, 0.94 µmol, 41 %) as a red solid. HPLC: t_R = 8.3 min; HRMS-ESI: calcd. for $C_{29}H_{27}N_4O_9^+$ $[M+H]^+$: 575.1773; found: 575.1772.

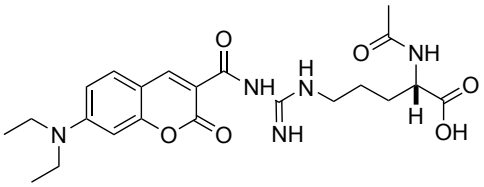

N-Ac-Arg(coumarin)-OH, (2.6):

N-Ac-Arg-OH (1.0 mg, 2.5 µmol), Barton's base (4.2 mg, 0.025 mmol) and 7-(diethylamino)coumarin-3-carboxylic acid (0.28 mg, 1.3 µmol) were dissolved in 0.5 mL of dry DMSO. The resulting reaction mixture was stirred for 2 h at 40 °C. Direct purification by HPLC afforded **2.6** (0.14 mg, 1.3 µmol, 25 %) as a yellow solid. HPLC: t_R = 8.9 min; HRMS-ESI: calcd. for $C_{22}H_{30}N_5O_6^+$ $[M+H]^+$: 460.2191; found: 460.2193.

2.4.3 Synthesis of the peptide substrates

2.4.3.1 General procedure 1 for the functionalization of 2-chlorotrityl chloride resin with carboxylic acids (GP1)

The *N*-Fmoc-protected amino acid Fmoc-Gly-OH (3 eq.) and $^{i}Pr_2NEt$ (3 eq.) were added to the suspension of 2-chlorotrityl chloride resin (20 mg for Peptide **2.12**, **2.13**, **2.14** or 200 mg for Peptide **2.7**, **2.8**, **2.9**, **2.10**, **2.11**; loading: 2.5 mmol/g) in dry CH_2Cl_2 (2/20 mL). The reaction mixture was stirred for 2 h, the solvent was removed and the resin was washed with DMF (3x) and CH_2Cl_2 (5x). After drying in high vacuum, a functionalization of the resin over 95 % was indicated by mass analysis.

2.4.3.2 General procedure 2 for peptide synthesis (GP2)

The peptides **2.7-2.14** were synthesized on the 2-chlorotrityl resin on a 50 mmol scale. For the coupling reaction, Fmoc-Xxx-OH (3 eq.) and HCTU (3 eq.) were dissolved in DMF. $^{i}Pr_2NEt$ (16 eq.) was dissolved in NMP and the resulting solution was added with the activated amino acid to the amino-functionalized resin. The mixture was stirred for 1 h and washed with DMF (3x). Fmoc deprotections were carried out with a solution of 20 % piperidine in DMF that was added to the resin and the reaction mixture was stirred for 3 min, the solvents were removed and the residue was treated again for 10 min with 20 % piperidine in DMF. Finally, the resin was washed with DMF (5x). Capping of the synthesized peptide was performed with Ac-Gly-OH. The peptide was cleaved from the solid support by stirring the resin in a 1:1:8 mixture of AcOH, TFA and CH_2Cl_2 for 20 min. The solvents were then removed under high vacuum. Final overall deprotection of the free peptide was achieved by dissolving the residue in a mixture of 95 % aqueous TFA and Et_3SiH. The resulting mixture was then stirred for 2 h. All volatiles were removed under reduced pressure. The residue was precipitated with Et_2O and the isolated peptide was purified by HPLC.

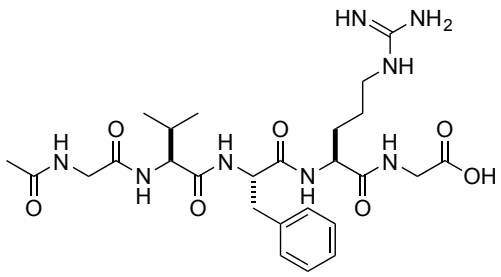

***N*-Ac-Gly-Val-Phe-Arg-Gly-OH (2.7):**

The peptide **2.7** was synthesized according to GP2. HPLC purification gave the target peptide **2.7** (78 mg, 140 µmol, 27 %) as a white solid. HPLC: t_R = 6.8 min; ^{1}H-NMR (400 MHZ, d_6-DMSO 25 °C): 8.26 – 8.23 (m, 2H), 8.11 (d, *J* = 8.0 Hz, 1H), 8.03 (t, *J* = 5.8 Hz, 1H), 7.95 (s, 1H, Arg-NH), 7.87 (d, *J* = 8.7 Hz, 1H), 7.27 – 7.15 (m, 7H, Phe, Arg-NH), 4.54 – 4.48 (m, 1H, Phe-α), 4.32 – 4.26 (m, 1H, Arg-α), 4.06 – 4.04 (m, 1H, Val-α), 3.77 – 3.66 (m, 4H; Gly-α), = 3.08 – 3.00 (m, 3H, Arg-δ, Phe-β), 2.90 – 2.84 (m, 1H; Phe-β), 1.93 – 1.86 (m, 4H; Ac, Val-β), 1.76 – 1.49 (m, 4H; Arg-βγ), 0.71 – 0.68 (m, 6H; Val-γ); HRMS-ESI: calcd. for $C_{26}H_{41}N_8O_7^+$ $[M+H]^+$: 577.3093; found: 577.3103.

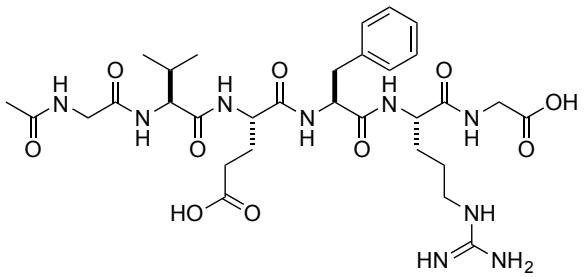

***N*-Ac-Gly-Val-Glu-Phe-Arg-Gly-OH (2.8):**

The peptide **2.8** was synthesized according to GP2. HPLC purification gave the target peptide **2.8** (52 mg, 70 µmol, 13 %) as a white solid. HPLC: t_R = 6.5 min; ^{1}H-NMR 400 MHZ, d_6-DMSO 25 °C): δ = 11.60 (bs, 1H, OH), 8.22 (d, *J* = 8.3 Hz, 1H), 8.14 – 8.00 (m, 2H), 8.07 (s, 1H), 7.86 (d, *J* = 8.5 Hz, 1H), 7.69 (bs, 1H, Arg-NH), 7.22 – 7.14 (m, 5H, Phe), 4.54 – 4.49 (m, 1H, Phe-α), 4.31 – 4.26 (m, 1H, Arg-α), 4.22 – 4.13 (m, 2H, Val-α, Glu-α), 3.76 – 3.68 (m, 4H, Gly-α), 3.10 – 2.99 (m, 3H, Arg-δ, Phe-β), 2.87 – 2.80 (m, 1H, Phe-β), 2.19 – 2.13 (m, 2H, Glu-β), 1.94 – 1.89 (m, 1H, Val-β), 1.84 (s, 3H, Ac), 1.71 – 1.48 (m, 6H, Arg-βγ, Glu-β), 0.78 (t, *J* = 7.1 Hz, 6H, Val-γ); HRMS-ESI: calcd. for $C_{31}H_{48}N_9O_{10}^+$ $[M+H]^+$: 706.3519; found: 706.3528.

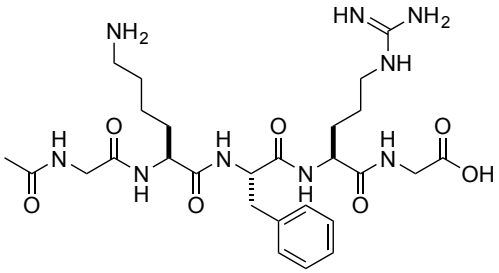

***N*-Ac-Gly-Lys-Phe-Arg-Gly-OH, (2.9):**

The peptide **2.9** was synthesized according to GP2. HPLC purification gave the target peptide **2.9** (60 mg, 100 µmol, 20 %) as a white solid. HPLC: t_R = 2.6 min; ^{1}H-NMR (400 MHZ, d_6-DMSO 25 °C): δ = 8.41 (d, *J* = 6.9 Hz, 1H), 8.24 (t, *J* = 5.7 Hz, 1H), 8.18 (d, *J* = 8.0 Hz, 1H), 8.10 – 8.06 (m, 2H), 8.02 (s, 1H, Arg-NH), 7.79 (s, 2H, Lys-NH), 7.29 – 7.15 (m, 7H, Phe, Arg-NH), 4.47 – 4.41 (m, 1H, Phe-α), 4.31 – 4.26 (m, 1H, Arg-α), 4.19 – 4.14 (m, 1H, Lys-α), 3.75 – 3.68 (m, 4H, Gly-α), 3.13 – 3.02 (m, 3H, Arg-δ, Phe-β), 2.95 – 2.93 (m, 1H, Phe-β), 3.13 – 3.02 (m, 2H, Lys-δ), 1.86 (s, 3H, Ac), 1.73 – 1.40 (m, 8H, Arg-βγ, Lys-βγ), 1.23 – 1.15 (m, 2H, Arg-βγ, Lys-βγ); HRMS-ESI: calcd. for $C_{27}H_{44}N_9O_7^+$ $[M+H]^+$: 606.3358; found: 606.3350.

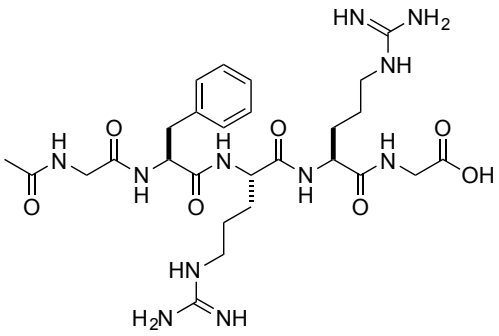

***N*-Ac-Gly-Phe-Arg-Arg-Gly-OH, (2.10)**:

The peptide **2.10** was synthesized according to GP2. HPLC purification gave the target peptide **2.10** (43 mg, 70 µmol, 13 %) as a white solid. HPLC: t_R = 2.3 min; ^{1}H-NMR (400 MHZ, d_6-DMSO 25 °C): δ = 8.26 (t, *J* = 5.8 Hz, 1H), 8.20 (d, *J* = 7.9 Hz, 1H), 8.10 (t, *J* = 5.8 Hz, 1H), 8.06 (d, *J* = 8.1 Hz, 1H), 7.99 (d, *J* = 7.9 Hz, 1H), 7.54 – 7.51 (m, 2H, Arg-NH), 7.27 – 7.17 (m, 6H, Phe, Arg-NH), 4.55 – 4.49 (m, 1H, Phe-α), 4.33 – 4.26 (m, 2H, Arg-α), 3.79 – 3.68 (m, 3H, Gly-α), 3.55 – 3.49 (dd, *J* = 5.6 Hz, 16.5 Hz, 1H, Gly-α), 3.10 – 3.09 (m, 4H, Arg-δ), 3.04 - 2.99 (s, 1H, Phe-β), 2.81 – 2.77 (d, *J* = 5.5 Hz, 1H, Phe-β), 1.82 (s, 6H, Ac), 1.75 – 1.43 (m, 8H, Arg-βγ); HRMS-ESI: calcd. for $C_{27}H_{45}N_{11}O_7^{2+}$ $[M+H+H]^{2+}$: 317.6746; found: 317.6754.

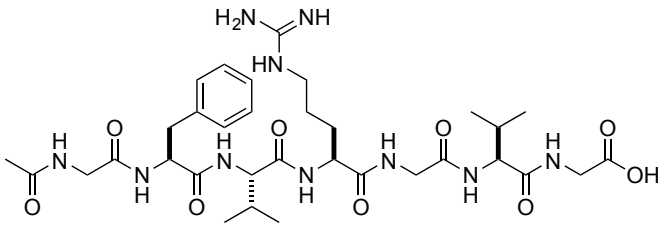

***N*-Ac-Gly-Phe-Val-Arg-Gly-Val-Gly-OH, (2.11):**

The peptide **2.11** was synthesized according to GP2. HPLC purification gave the target peptide **2.11** (63 mg, 90 µmol, 17 %) as a white solid. HPLC: t_R = 2.82 min; ^{1}H-NMR (400 MHZ, d_6-DMSO 25 °C): δ = 8.14 (t, *J* = 5.7 Hz, 1H), 8.07 (t, *J* = 6.0 Hz, 2H), 8.02 (d, *J* = 8.2 Hz, 1H), 7.96 – 7.94 (m, 2H), 7.84 (d, *J* = 8.9 Hz, 1H), 7.51 (t, *J* = 5.7 Hz, 1H, Arg-NH), 7.27 – 7.17 (m, 6H, Phe, Arg-NH), 4.62 – 4.58 (m, 1H, Phe-α), 4.33 – 4.27 (m, 1H, Arg-α), 4.22 – 4.15 (m, 2H, Val-α), 3.82 – 3.66 (m, 5H, Gly-α), 3.59 – 3.53 (m, 1H, Gly-α), 3.13 – 3.08 (m, 2H, Arg-δ), 3.01 (dd, *J* = 4.53 Hz, 13.9 Hz, 1H, Phe-β), 2.81 – 2.77 (m, 1H, Phe-β), 2.02 – 1.96 (m, 2H, Val-β), 1.82 (s, 3H, Ac), 1.73 – 1.66 (m, 1H, Arg-βγ), 1.60 – 1.45 (m, 3H, Arg-βγ), 0.88 – 0.83 (m, 12H, Val-γ); HRMS-ESI: calcd. for $C_{33}H_{53}N_{10}O_9^+$ $[M+H]^+$: 733.3991; found: 733.3989.

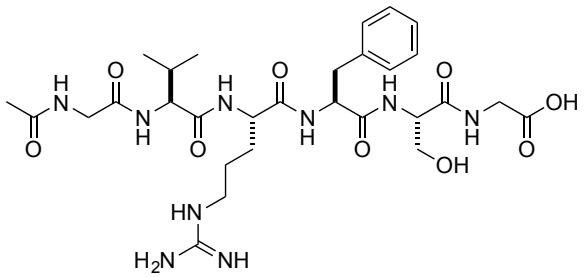

***N*-Ac-Gly-Val-Arg-Phe-Ser-Gly-OH, (2.12):**

The peptide **2.12** was synthesized according to GP2. HPLC purification gave the target peptide **2.12** (43 mg, 100 µmol, 13 %) as a white solid. HPLC: t_R = 8.2 min; ^{1}H-NMR (400 MHZ, d_6-DMSO 25 °C): δ = 9.88 (s, 1H, OH), 8.38 – 8.34 (m, 2H), 8.14 – 8.08 (m, 3H), 7.79 (d, *J* = 8.8 Hz, 1H), 7.26 – 7.16 (m, 7H, Phe, Arg-NH), 7.04 (bs, 2H, Arg-NH), 4.54 – 4.48 (m, 1H, Phe-α), 4.36 – 4.30 (m, 1H, Arg-α), 4.23 – 4.15 (m, 2H, Val-α, Ser-α), 3.79 – 3.69 (m, 3H, Gly-α), 3.55 – 3.44 (m, 3H, Gly-α, Ser-β), 3.06 – 3.02 (m, 2H, Arg-δ), 2.96 (dd, *J* = 13.6, 5.6 Hz, 1H, Phe-β), 2.86 (dd, *J* = 13.6, 8.3 Hz, 1H, Phe-β), 1.93 – 1.88 (m, 1H, Val-β), 1.86 (s, 3H, Ac), 1.56 – 1.35 (m, 4H, Arg-βγ), 0.78 (d, *J* = 6.8 Hz, 6H, Val-γ); HRMS-ESI: calcd. for $C_{29}H_{45}N_9NaO_9^+$ $[M+Na]^+$: 686.3232; found: 686.3233.

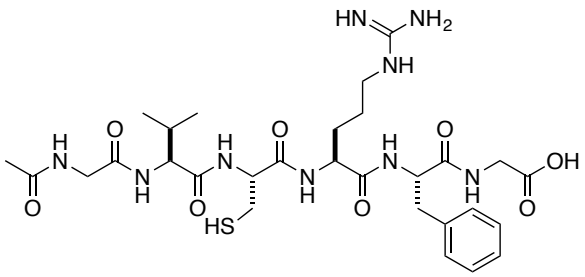

***N*-Ac-Gly-Val-Cys-Arg-Phe-Gly-OH, (2.13):**

The peptide **2.13** was synthesized according to GP2. HPLC purification gave the target peptide **2.13** (18 mg, 30 µmol, 54 %) as a white solid. HPLC: t_R = 7.2 min; ^{1}H-NMR (400 MHZ, d_6-DMSO 25 °C): δ = 8.83 (s, 1H, Cys-SH), 8.43 (d, *J* = 8.7 Hz, 1H), 8.18 – 8.11 (m, 2H), 7.91 – 7.85 (m, 2H), 7.68 (bs, 1H), 7.25 – 7.11 (m, 9H, Phe, Arg-NH), 4.50 – 4.18 (m, 4H, Phe-α, Arg-α, Ser-α, Val-α), 3.75 – 3.72 (m, 2H, Gly-α), 3.49 (d, *J* = 4.8 Hz, 2H, Gly-α), 3.08 – 2.95 (m, 4H, Arg-δ, Ser-β, Phe-β), 2.80 – 2.64 (m, 2H, Ser-β, Phe-β), 2.0 – 1.93 (m, 1H, Val-β), 1.84 (s, 3H, Ac), 1.57 – 1.41 (m, 3H, Arg-βγ), 1.23 – 1.16 (m, 1H, Arg-βγ), 0.83 – 0.75 (m, 6H, Val-γ); HRMS-ESI: calcd. for $C_{29}H_{46}N_9O_8S^+$ $[M+H]^+$: 680.3185; found: 680.3193.

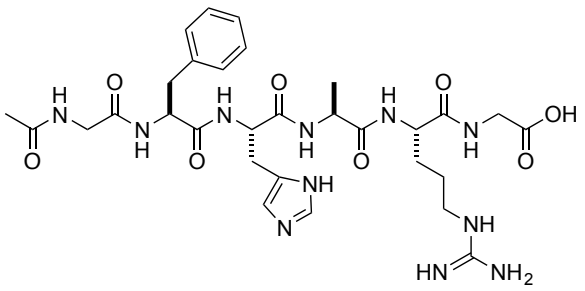

***N*-Ac-Gly-Phe-His-Ala-Arg-Gly-OH, (2.14):**

The peptide **2.14** was synthesized according to GP2. HPLC purification gave the target peptide **2.14** (25 mg, 40 µmol, 75 %) as a white solid. HPLC: t_R = 3.2 min; ^{1}H-NMR (400 MHZ, d_6-DMSO 25 °C): δ = 8.69 (s, 1H, His-NH), 8.32 (d, *J* = 8.0 Hz, 1H), 8.26 – 8.19 (m, 2H), 8.16 – 8.06 (m, 3H), 7.65 (t, *J* = 5.6 Hz, 1H, Arg-NH), 7.27 – 7.17 (m, 7H, Phe, His), 4.57 – 4.53 (m, 1H, His-α), 4.49 – 4.44 (m, 1H, Phe-α), 4.34 – 4.24 (m, 2H, Ala-α, Arg-α), 3.84 – 3.68 (m, 3H, Gly-α), 3.57 – 3.52 (m, 1H, Gly-α), 3.10 – 3.06 (m, 3H, Arg-δ, His-β), 3.00 – 2.92 (m, 2H, His-β, Phe-β), 2.78 – 2.71 (m, 1H, Phe-β), 1.83 (s, 3H, Ac), 1.77 – 1.71 (m, 1H, Arg-βγ), 1.60 – 1.47 (m, 3H, Arg-βγ), 1.24 (d, *J* = 7.0 Hz, 3H, Ala-β); HRMS-ESI: calcd. for $C_{30}H_{44}N_{11}O_8^+$ $[M+H]^+$: 686.3369; found: 686.3362.

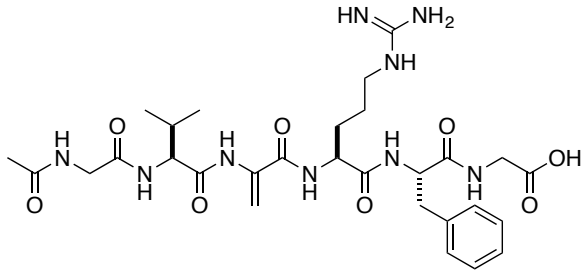

***N*-Ac-Gly-Val-Dha-Arg-Phe-Gly-OH, (2.15):**

Compound **2.13** (39 mg, 57 µmol) and 2,5-dibromohexanediamide (17 mg, 57 µmol) were dissolved in 1:1 MeCN:phosphate buffer pH = 8. The reaction was stirred at room temperature for 1 h. After 1 h the reaction mixture was heated up to 40 °C and stirred additional 1 h. HPLC purification gave the target peptide **2.15** (3.5 mg, 5.0 µmol, 9 %) as a white solid. HPLC: t_R = 7.4 min; ^{1}H-NMR (500 MHZ, d_6-DMSO 25°C): δ = 9.28 (bs, 1H, OH), 8.62 – 8.22 (m, 6H), 7.31 (t, *J* = 9.05 Hz, 1H, Arg-NH), 7.26 – 7.15 (m, 6H, Phe, Arg-NH), 6.08 (s, 1H, Dha-β), 5.55 (s, 1H, Dha-β), 4.40 – 4.36 (m, 2H, Phe-α, Arg-α), 4.23 – 4.21 (m, 2H, Gly-α, Val-α), 3.81 – 3.71 (m, 3H, Gly-α), 3.11 – 3.07 (m, 2H, Phe-β, Arg-δ), 2.98 – 2.93 (m, 1H, Arg-δ), 2.81(dd, *J* = 3.91, 10.25 Hz, 1H, Phe-β), 2.09 – 2.02 (m, 1H, Val-β), 1.84 (s, 3H, Ac), 1.62 – 1.39 (m, 4H, Arg-βγ), 0.87 – 0.84 (m, 6H, Val-γ); HRMS-ESI: calcd. for $C_{29}H_{44}N_9O_8^+$ $[M+H]^+$: 646.3307; found: 646.3304.

2.4.4 Synthesis of the functionalized peptides

2.4.4.1 General procedure 3 for the functionalization of the arginine residue of the peptides (GP3)

To a solution of the peptide (1 eq.) in DMF (300 µL) were added Barton's base (10 eq.) followed by a solution of the activated ester (1.5 eq.) in DMF (100 µL). The resulting mixture was stirred at 40 °C for 1h (**2.16**, **2.17**, **2.18**, **2.20**, **2.21** and **2.29**) or 8h. All volatiles were removed under reduced pressure and the residue was subsequently purified by HPLC.

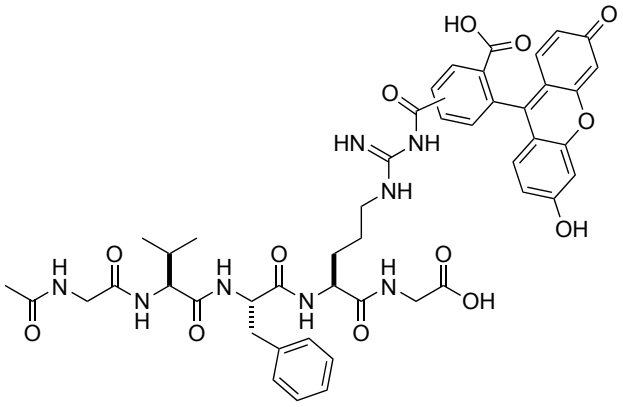

***N*-Ac-Gly-Val-Phe-Arg(6-FAM)-Gly-OH, (2.16):**

According to the general procedure GP3 compound **2.16** was synthesized starting from compound **2.7** (1.0 mg, 1.7 µmol), Barton's base (2.9 mg, 17 µmol) and 5(6)-carboxyfluorescein *N*-succinimidyl ester (1.2 mg, 2.6 µmol) were used. Direct purification by HPLC afforded **2.16** (1.3 mg, 1.4 µmol, 81 %) as a red solid. HPLC: t_R = 9.5 min; HRMS-ESI: calcd. for $C_{47}H_{52}N_8O_{13}^{2+}$ $[M+H+H]^{2+}$: 468.1821; found: 468.1829.

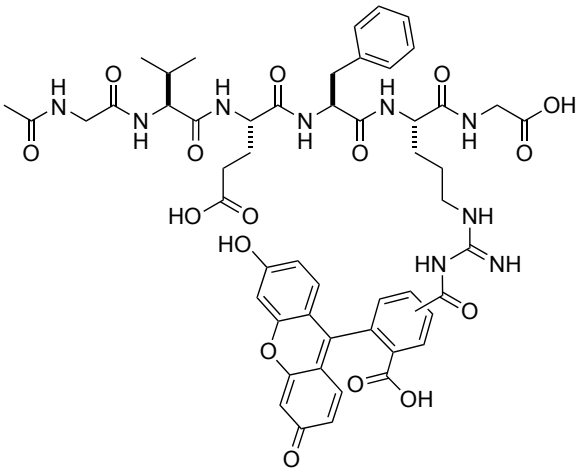

***N*-Ac-Gly-Val-Glu-Phe-Arg(6-FAM)-Gly-OH, (2.17):**

According to the general procedure GP3 compound **2.17** was synthesized starting from compound **2.8** (1.0 mg, 1.4 µmol), Barton's base (2.4 mg, 14 µmol) and 5(6)-carboxyfluorescein *N*-succinimidyl ester (0.99 mg, 2.1 µmol) were used. Direct purification by HPLC afforded **2.17** (1.3 mg, 1.6 µmol, 85 %) as a red solid. HPLC: t_R = 11.3 min; HRMS-ESI: calcd. for $C_{52}H_{56}N_9O_{16}^-$ [M-H]$^-$: 1062.3851; found: 1062.3847.

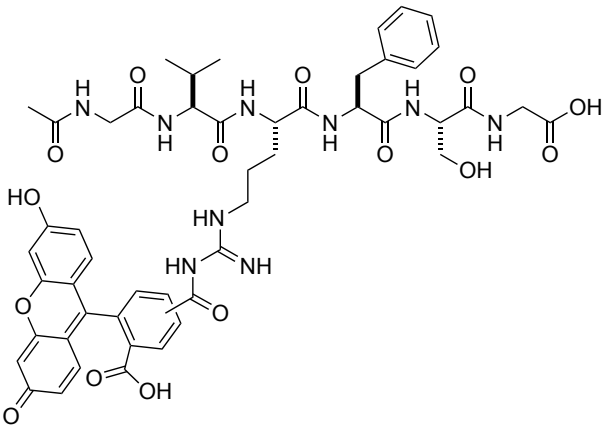

***N*-Ac-Gly-Val-Arg(6-FAM)-Phe-Ser-Gly-OH, (2.18):**

According to the general procedure GP3 compound **2.18** was synthesized starting from compound **2.12** (1.0 mg, 1.5 µmol), Barton's base (2.5 mg, 15 µmol) and 5(6)-carboxyfluorescein *N*-succinimidyl ester (1.1 mg, 2.3 µmol) were used. Direct purification by HPLC afforded **2.18** (1.2 mg, 1.2 µmol, 83 %) as a red solid. HPLC: t_R = 8.2 min; HRMS-ESI: calcd. for $C_{50}H_{54}N_9O_{15}^-$ [M-H]$^-$: 1020.3745; found: 1020.3729.

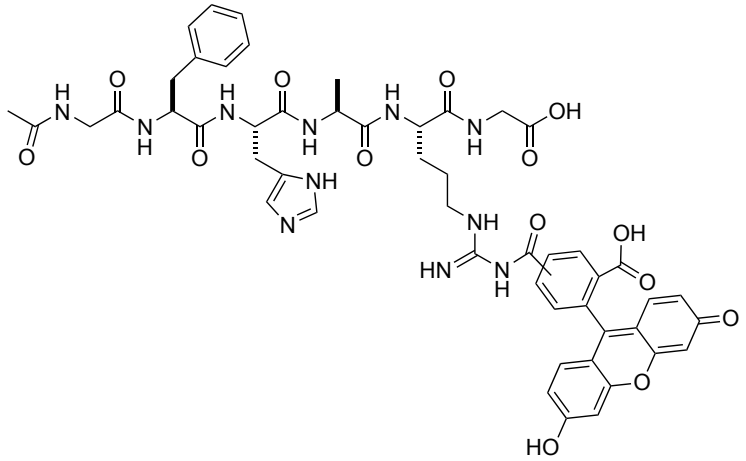

***N*-Ac-Gly-Phe-His-Ala-Arg(6-FAM)-Gly-OH, (2.19):**

According to the general procedure GP3 compound **2.19** was synthesized starting from compound **2.14** (2.0 mg, 2.9 µmol), Barton's Base (5.0 mg, 29 µmol) and 5(6)-Carboxyfluorescein *N*-succinimidyl ester (2.1 mg, 4.4 µmol) were used. Direct purification by HPLC afforded **2.19** (0.98 mg, 0.94 µmol, 32 %) as a red solid. HPLC: t_R = 7.6 min; HRMS-ESI: calcd. for $C_{51}H_{54}N_{11}O_{14}^+$ $[M+H]^+$: 1044.3846; found: 1044.3839.

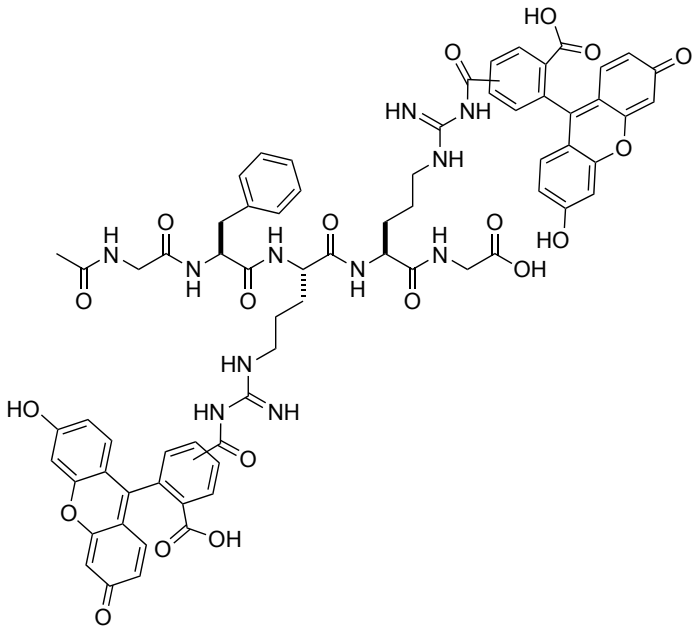

***N*-Ac-Gly-Phe-Arg(6-FAM)-Arg(6-FAM)-Gly-OH, (2.20):**

According to the general procedure GP3 compound **2.20** was synthesized starting from compound **2.10** (1.0 mg, 1.6 µmol), Barton's base (5.4 mg, 32 µmol) and 5(6)-carboxyfluorescein *N*-succinimidyl ester (2.2 mg, 4.7 µmol) were used. Direct purification by HPLC afforded **2.20** (1.1 mg, 0.81 µmol, 42 %) as a red solid. HPLC: t_R = 8.2 min; HRMS-ESI: calcd. for $C_{69}H_{64}N_{11}O_{19}^{+}$ $[M+H]^+$: 1350.4374; found: 1350.4386.

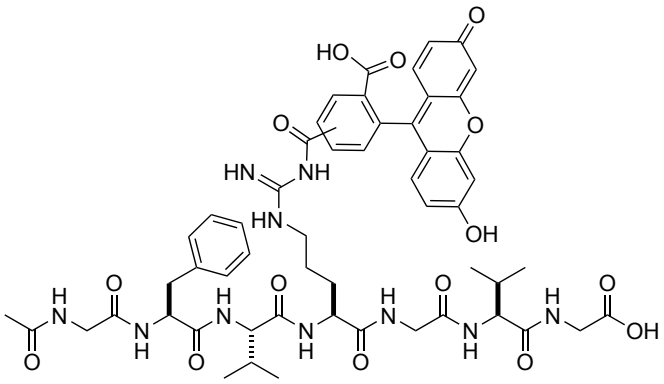

***N*-Ac-Gly-Phe-Val-Arg(6-FAM)-Gly-Val-Gly-OH, (2.21):**

According to the general procedure GP3 compound **2.21** was synthesized starting from compound **2.11** (1.0 mg, 1.4 µmol), Barton's base (2.4 mg, 14 µmol) and 5(6)-carboxyfluorescein *N*-succinimidyl ester (0.99 mg, 2.1 µmol) were used. Direct purification by HPLC afforded **2.21** (1.2 mg, 1.1 µmol, 82 %) as a red solid. HPLC: t_R = 10.9 min; HRMS-ESI: calcd. for $C_{54}H_{64}N_{10}O_{15}^{2+}$ $[M+H+H]^{2+}$: 546.2271; found: 546.2273.

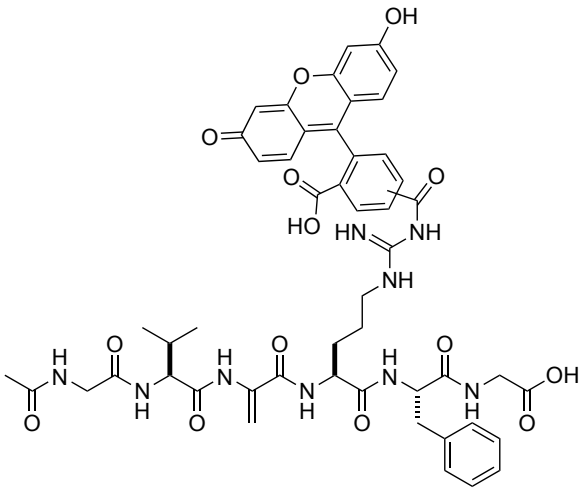

***N*-Ac-Gly-Val-Dha-Arg(6-FAM)-Phe-Gly-OH, (2.22):**

According to the general procedure GP3 compound **2.22** was synthesized starting from compound **2.15** (0.99 mg, 1.4 µmol), Barton's base (2.4 mg, 14 µmol) and 5(6)-carboxyfluorescein *N*-succinimidyl ester (0.99 mg, 2.1 µmol) were used. Direct purification by HPLC afforded **2.22** (0.56 mg, 0.56 µmol, 40 %) as a red solid. HPLC: t_R = 8.7 min; HRMS-ESI: calcd. for $C_{50}H_{54}N_9O_{14}^+$ $[M+H]^+$: 1004.3785; found: 1004.3772.

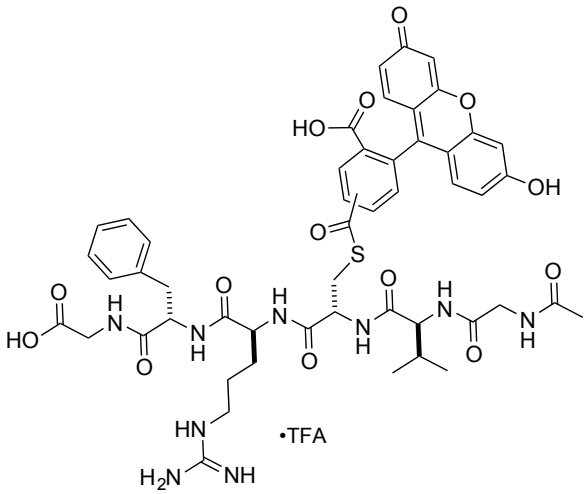

***N*-Ac-Gly-Val-Cys(6-FAM)-Arg-Phe-Gly-OH, (2.23):**

According to the general procedure GP3 compound **2.23** was synthesized starting from compound **2.13** (2.0 mg, 2.9 µmol), Barton's base (5.0 mg, 29 µmol) and 5(6)-carboxyfluorescein *N*-succinimidyl ester (2.1 mg, 4.4 µmol) were used. Direct purification by HPLC afforded **2.23** (1.0 mg, 0.98 µmol, 34 %) as a red solid. HPLC: t_R = 9.82 min; HRMS-ESI: calcd. for $C_{50}H_{56}N_9O_{14}S^+$ $[M+H]^+$: 1038.3662; found: 1038.3663.

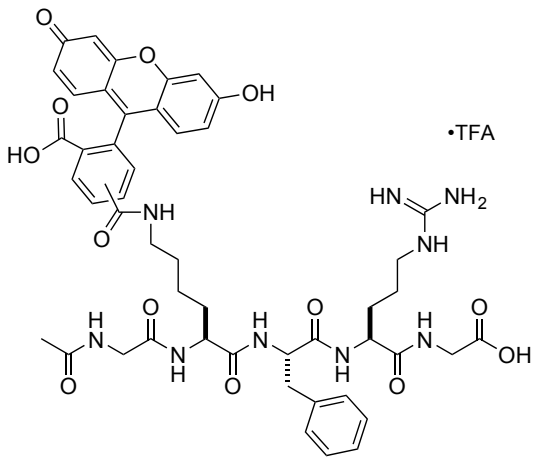

***N*-Ac-Gly-Lys(6-FAM)-Phe-Arg-Gly-OH, (2.24):**

According to the general procedure GP3 compound **2.24** was synthesized starting from compound **2.9** (1.0 mg, 1.7 µmol), Barton's base (2.9 mg, 17 µmol) and 5(6)-carboxyfluorescein *N*-succinimidyl ester (1.2 mg, 2.6 µmol) were used. Direct purification by HPLC afforded **2.24** (0.67 mg, 0.66 µmol, 42 %) as a red solid. HPLC: t_R = 9.8 min; HRMS-ESI: calcd. for $C_{48}H_{54}N_9O_{13}^+$ $[M+H]^+$: 964.3836; found: 964.3845.

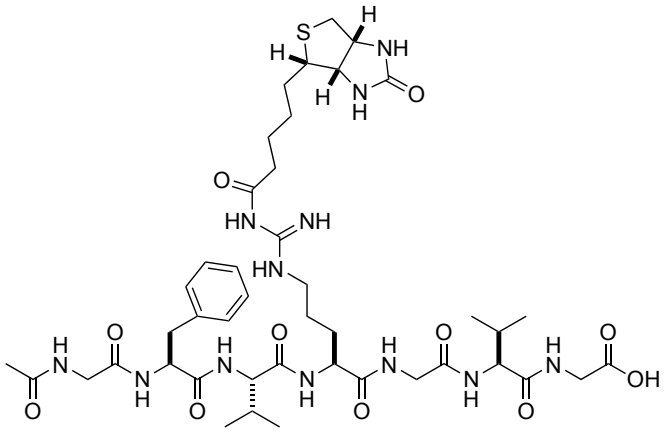

***N*-Ac-Gly-Phe-Val-Arg(Biotin)-Gly-Val-Gly-OH, (2.25):**

According to the general procedure GP3 compound **2.25** was synthesized starting from compound **2.11** (1.0 mg, 1.4 µmol), Barton's base (2.4 mg, 14 µmol) and *p*-nitrophenylester (0.77 mg, 2.1 µmol) were used. Direct purification by HPLC afforded **2.25** (0.60 mg, 0.63 µmol, 47 %) as a red solid. HPLC: t_R = 9.5 min; HRMS-ESI: calcd. for $C_{43}H_{67}N_{12}NaO_{11}S^{2+}$ $[M+H+Na]^{2+}$: 491.2330; found: 491.2331.

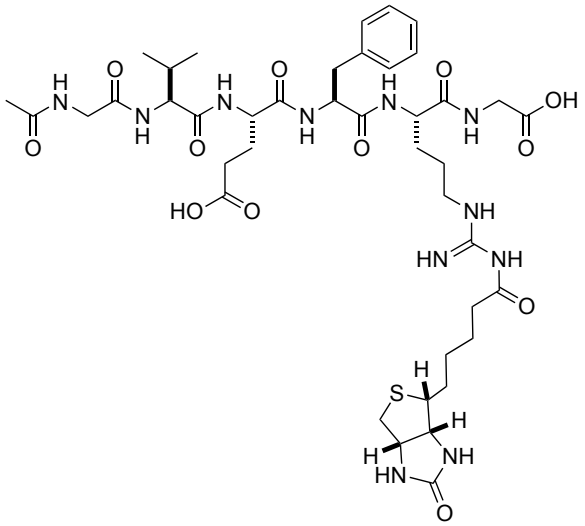

***N*-Ac-Gly-Val-Glu-Phe-Arg(Biotin)-Gly-OH, (2.26):**

According to the general procedure GP3 compound **2.26** was synthesized starting from compound **2.8** (1.0 mg, 1.4 µmol), Barton's base (2.4 mg, 14 µmol) and *p*-nitrophenylester (0.77 mg, 2.1 µmol) were used. Direct purification by HPLC afforded **2.26** (0.61 mg, 0.86 µmol, 47 %) as a red solid. HPLC: t_R = 9.3 min; HRMS-ESI: calcd. for $C_{41}H_{62}N_{11}O_{12}S^{+}$ $[M+H]^{+}$: 932.4295; found: 932.4285.

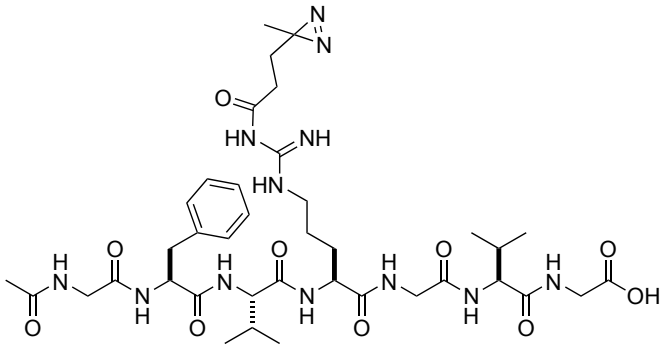

***N*-Ac-Gly-Phe-Val-Arg(DA)-Gly-Val-Gly-OH, (2.27):**

According to the general procedure GP3 compound **2.27** was synthesized starting from compound **2.11** (1.0 mg, 1.4 µmol), Barton's base (2.4 mg, 14 µmol) and succinimidyl-diazirine (0.77 mg, 2.1 µmol) were used. Direct purification by HPLC afforded **2.27** (0.49 mg, 0.58 µmol, 43 %) as a red solid. HPLC: t_R = 8.6 min; HRMS-ESI: calcd. for $C_{38}H_{59}N_{12}O_{10}^+$ $[M+H]^+$: 843.4472; found: 843.4482.

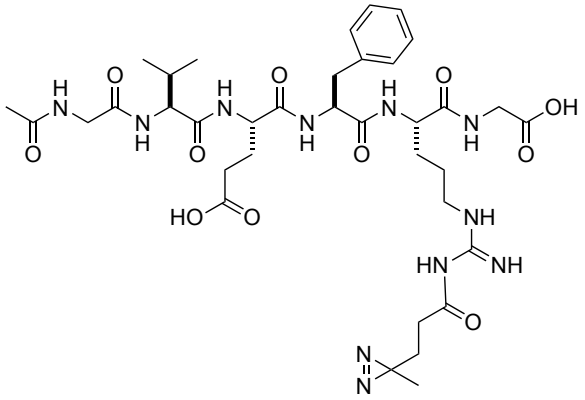

***N*-Ac-Gly-Val-Glu-Phe-Arg(DA)-Gly-OH, (2.28):**

According to the general procedure GP3 compound **2.28** was synthesized starting from compound **2.8** (1.0 mg, 1.4 µmol), Barton's base (2.4 mg, 14 µmol) and succinimidyl-diazirine (0.49 mg, 2.1 µmol) were used. Purification by HPLC afforded **2.28** (0.43 mg, 0.53 µmol, 38%) as a red solid. HPLC: t_R = 8.2 min; HRMS-ESI: calcd. for $C_{36}H_{54}N_{11}O_{11}^+$ $[M+H]^+$: 816.3999; found: 816.4004.

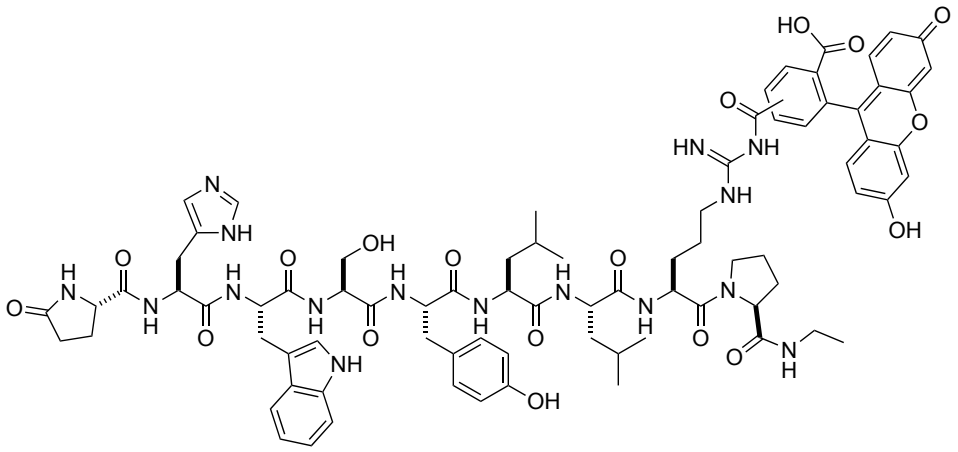

Pyr-His-Trp-Ser-Tyr-D-Leu-Leu-Arg(6-FAM)-Pro-NHEt, (2.30):

According to the GP3 compound **2.30** was synthesized starting from commercially available leuprolide **2.29** (1.0 mg, 0.83 µmol), Barton's base (1.4 mg, 8.3 µmol) and 5(6)-carboxyfluorescein *N*-succinimidyl ester (0.56 mg, 1.2 µmol) were used. Direct purification by HPLC afforded **2.30** (1.01 mg, 0.64 µmol, 77 %) as a red solid. HPLC: t_R = 10.4 min; HRMS-ESI: calcd. for $C_{80}H_{96}N_{16}O_{18}^{2+}$ $[M+H+H]^{2+}$: 784.3539; found: 784.3548.

2.4.5 Prevention of limitation of method

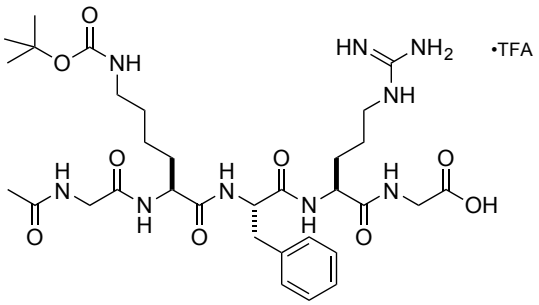

***N*-Ac-Gly-Lys(Boc)-Phe-Arg-Gly-OH, (2.31):**

Compound **2.9** (1.0 mg, 1.7 µmol) was dissolved in water and Na_2CO_3 (0.30 mg, 2.8 µmol). The solution was cooled down to 5 °C and BOC anhydride in dioxane (0.50 mg, 2.3 µmol) was added slowly. After the mixture was stirred for 1 h, the cooling bath was removed and the reaction was warmed to room temperature over night. Purification by HPLC afforded **2.31 (**0.70 mg, 0.99 µmol, 64 %) as a white solid. HPLC: t_R = 14.1 min; HRMS-ESI: calcd. for $C_{32}H_{52}N_9O_9^+$ $[M+H]^+$: 706.3883; found: 706.3890.

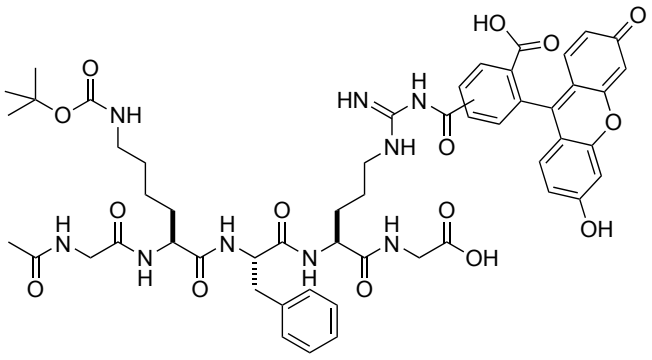

***N*-Ac-Gly-Lys(Boc)-Phe-Arg(6-FAM)-Gly-OH, (2.32):**

According to the general procedure GP3 compound **2.32** was synthesized starting from compound **2.31** (0.50 mg, 0.71 µmol). Barton's base (1.2 mg, 7.07 µmol) and 5(6)-carboxyfluorescein *N*-succinimidyl ester (0.40 mg, 0.84 µmol) were used. Direct purification by HPLC afforded **2.32** (0.40 mg, 0.38 µmol, 53 %) as a red solid. HPLC: t_R = 17.4 min; HRMS-ESI: calcd. for $C_{53}H_{62}N_9O_{15}^+$ $[M+H]^+$: 1064.4360; found: 1064.4375.

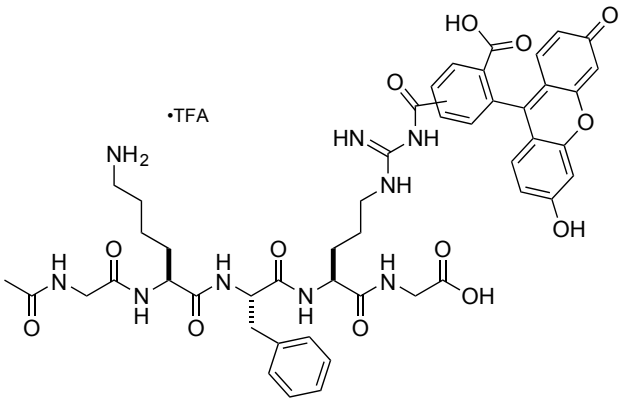

***N*-Ac-Gly-Lys-Phe-Arg(6-FAM)-Gly-OH, (2.33):**

Final deprotection of compound **2.32** (0.20 mg, 0.19 µmol) was carried out in 50 % TFA over 2 h. Direct purification by HPLC afforded **2.33** (0.061 mg, 0.062 µmol, 33 %) as a red solid. HPLC: t_R = 12.2 min; HRMS-ESI: calcd. for $C_{48}H_{54}N_9O_{13}^+$ $[M+H]^+$: 964.3836; found: 964.3843.

2.4.6 Uptake studies in Daphnia magna

The uptake studies were carried out by using 48 h old *Daphnia magna,* that were exposed to an aqueous solution of compound **2.29** (6.9 µM). For each experiment, 10 animals were placed in a 50 mL beaker in 15 mL M4 media with the labelled compound without food and incubated at 20 °C over 6 h. Samples were taken after 3 h and 6 h, whereby the Daphnia were rinsed with fresh M4 media and immobilized afterwards on 1 % agarose gel. Imaging of the samples was performed on an Olympus Fluoview FV1000 confocal laser-scanning microscope with a 4x and 10x magnification. The excitation wavelength of the samples was 488 nm with 15 % laser transmission. Analyses of the pictures were carried out with FV 10-ASW Version 03.00.02.00.

2.5 References

[1] C. T. Walsh, S. G. Tsodikova, G. J. Gatto, *Angew. Chem. Int. Ed.* **2005**, *44*, 7342–7372.

[2] S. A. Sieber, M. A. Marahiel, *J. Bacteriol.* **2003**, *185*, 7036–7043.

[3] T. Kimmerlin, D. Seebach, *J. Peptide Res.* **2008**, *65*, 229–260.

[4] P. Vlieghe, V. Lisowski, J. Martinez, M. Khrestchatisky, *Drug Discov. Today* **2010**, *15*, 40–56.

[5] A. W. Purcell, J. McCluskey, J. Rossjohn, *Nat. Rev. Drug Discov.* **2007**, *6*, 404–414.

[6] M. O. Forster, *J. Chem.Soc.,Trans* **1920**, *117*, 1157–1201.

[7] R. B. Merrifield, *J. Am. Chem. Soc.* **1963**, *85*, 2149–2154.

[8] D. S. Kemp, S. L. Leung, D. J. Kerkman, *Tetrahedron Lett.* **1981**, *22*, 181–184.

[9] M. Schnolzer, S. B. Kent, *Science* **1992**, *256*, 221–225.

[10] J. Xie, P. G. Schultz, *Curr. Opin. Chem. Biol.* **2005**, *9*, 548–554.

[11] T. Passioura, H. Suga, *Chem. Eur. J.* **2013**, *19*, 6530–6536.

[12] A. Angelini, C. Heinis, *Curr. Opin. Chem. Biol.* **2011**, *15*, 355–361.

[13] S. B. H. Kent, *Chem. Soc. Rev*. **2009**, *38*, 338–351.

[14] V. R. Pattabiraman, J. W. Bode, *Nature* **2011**, *480*, 471–479.

[15] L. J. Kricka, P. Fortina, *Clin. Chem.* **2009**, *55*, 670–683.

[16] E. Baslé, N. Joubert, M. Pucheault, *Chemistry & Biology* **2010**, *17*, 213–227.

[17] G. DeSantis, J. B. Jones, *Curr. Opin. Biotechnol.* **1999**, *10*, 324–330.

[18] X. Yang, W. A. van der Donk, *Chemistry: A European Journal* **2013**, *19*, 7662–7677.

[19] J. M. Chalker, G. J. L. Bernardes, Y. A. Lin, B. G. Davis, *Chem. Asian J.* **2009**, *4*, 630–640.

[20] P. M. S. D. Cal, J. B. Vicente, E. Pires, A. V. Coelho, L. F. Veiros, C. Cordeiro, P. M. P. Gois, *J. Am. Chem. Soc.* **2012**, *134*, 10299–10305.

[21] F. T. Hofmann, J. W. Szostak, F. P. Seebeck, *J. Am. Chem. Soc.* **2012**, *134*, 8038–8041.

[22] A. Späth, B. König, *Tetrahedron* **2010**, *66*, 1859–1873.

[23] M. Keller, N. Pop, C. Hutzler, A. G. Beck-Sickinger, G. Bernhardt, A. Buschauer, *J. Med. Chem.* **2008**, *51*, 8168–8172.

[24] M. J. Dixon, O. A. Andersen, D. M. F. van Aalten, I. M. Eggleston, *Bioorg. Med. Chem. Lett.* **2005**, *15*, 4717–4721.

[25] K. R. Shreder, Y. Liu, T. Nomanhboy, S. R. Fuller, M. S. Wong, W. Z. Gai, J. Wu, P. S. Leventhal, J. R. Lill, S. Corral, *Bioconjug. Chem.* **2004**, *15*, 790–798.

[26] M. A. Glomb, G. Lang, *J. Agric. Food Chem.* **2001**, *49*, 1493–1501.

[27] M. O. Lederer, R. G. Klaiber, *Bioorg. Med. Chem.* **1999**, *7*, 2499–2507.

[28] D. R. Kent, W. L. Cody, A. M. Doherty, *Tetrahedron Lett.* **1996**, *37*, 8711–8714.

[29] H. F. Gilbert, M. H. O'Leary, *Biochemistry* **1975**, *14*, 5194–5199.

[30] K. Takahashi, *J. Biol. Chem.* **1968**, *243*, 6171–6179.

[31] A. Isidro, D. Latassa, M. Giraud, M. Álvarez, F. Albericio, *Org. Biomol. Chem.* **2009**, *7*, 2565–2569.

[32] W. F. Veldhuyzen, Q. Nguyen, G. McMaster, D. S. Lawrence, *J. Am. Chem. Soc.* **2003**, *125*, 13358–13359.

[33] C. A. G. N. Montalbetti, V. Falque, *Tetrahedron* **2005**, *61*, 10827–10852.

[34] F. P. Seebeck, A. Ricardo, J. W. Szostak, *Chem. Commun.* **2011**, *47*, 6141–6143.

[35] A. C. Wilson, S. V. Meethal, R. L. Bowen, C. S. Atwood, *Expert. Opin. Investig. Drugs* **2007**, *16*, 1851–1863.

[36] I. Guzmán-Soto, E. Salinas, I. Hernández-Jasso, J. L. Quintanar, *Neurochem. Res.* **2012**, *37*, 2190–2197.

[37] H. J. Jessen, A. Schumacher, T. Shaw, A. Pfaltz, K. Gademann, *Angew. Chem. Int. Ed.* **2011**, *50*, 4222–4226.

[38] J. Martins, L. Oliva Teles, V. Vasconcelos, *Eniviron. Int.* **2007**, *33*, 414–425.

[39] D. Ebert 2005. Ecology, Epidemiology, and Evolution of Parasitism in *Daphnia* [Internet]. Bethesda (MD): National Library of Medicine (US), National Center for Biotechnology Information.

[40] M. Bodanszky, D. T. Fagan, *J. Am. Chem. Soc.* **1977**, *99*, 235–239.

[41] J. M. Chalker, L. Lercher, N. R. Rose, J. Schofield, B. G. Davis, *Angew. Chem. Int. Ed.* **2012**, *51*, 1835–1839.

3

Following the Fate of MC-LR

3.1 Introduction

In 1996, 52 dialysis patients died in Brazil because of treatment with cyanobacteria contaminated water.[1] In Argentina, a man suffered of intoxication symptoms after diving in a lake with a cyanobacteria bloom.[2,3] Such incidents are occurring more often due to global warming and eutrophication. Dangerous cyanobacterial growth begins to threaten safety and viability of the aquatic resources all over the world (**Figure 3.1**).

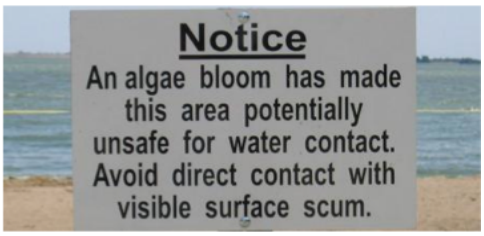

Figure 3.1. Marion Reservoir, Kansas (*Photo Credit: Jennifer L. Graham, USGS)*

Responsible for these blooms are certain types of microorganisms, the cyanobacteria, formerly called blue-green algae. After the death of the cyanobacterial colonies, a number of highly toxic molecules are released and thereby pollute fresh and marine waters, which creates a serious threat to the water supply, public health, livestock and wildlife.[4] This poses a great danger to humans, animals, and the ecosystem as a whole, as these toxins are highly chemically stable and water-soluble.[5] In humans, the toxic effects result in symptoms like nausea, dizziness, respiratory distress and skin itching and they can even cause severe diseases like liver damage or cancer.[4,6,7]

Besides this, another problem arises from these toxins being able to enter the food chain via accumulation in fish, mussels or shellfish, eventually finding their way into the human body.[8] Over the past years, cases of cyanobacterial poisoning have been more and more frequently reported, whereby the regular intoxication occurs via oral intake, although other uptake mechanisms such as inhalation or skin contact are also possible.[9]

The main toxin class thought to be responsible for a large number of these poisonings belongs to the microcystin family of cyclic peptides, a diverse compound class of more than 80 different derivatives known to date.[10] These molecules contain

the general structure *cyclo*(-D-Ala-Xaa-D-MeAsp-Yaa-Adda-D-Glu-Mdha-), whereby the two amino acid residues in position 2 and 4 (Xaa and Yaa) are of varied structure and therefore responsible for this great diversity, while the other positions are more conserved (**Figure 3.2**).[11]

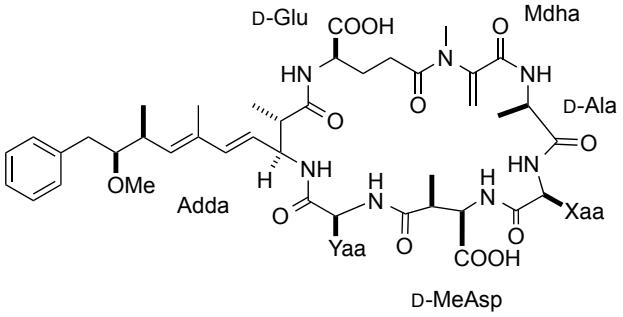

Figure 3.2. General structure of microcystin (Yaa and Xaa represent variable amino acids)

Adda is the unusual amino acid 3-amino-9-methoxy-2,6,8-trimenthyl-10-phenyl-4,6-decadienoic acid, D-MeAsp represent the 3-methylaspartic acid and Mdha is *N*-methyldehydroalanine. Other variable groups in microcystins are the Dha, which is sometimes methylated (Mdha) like in microcystin-LR (MC-LR) or substituted by a threonine derivative (2-amino-2-butenoic acid, Dhb) or replaced by a native serine.[12] Furthermore, variations in the Adda side chain are possible, like acetylation or removal of the *O*-methyl group.[13]

The name of this toxin class is derived from first poisonous compound isolated from *Microcystis aeruginosa*.[14] Additionally, the precise name of the microcystin isoforms are determined by the two highly variable amino acids Xaa and Yaa, e.g. microcystin-LR (MC-LR) where Xaa = Leu at position 2, and Yaa = Arg at position 4 (**Figure 3.3**).

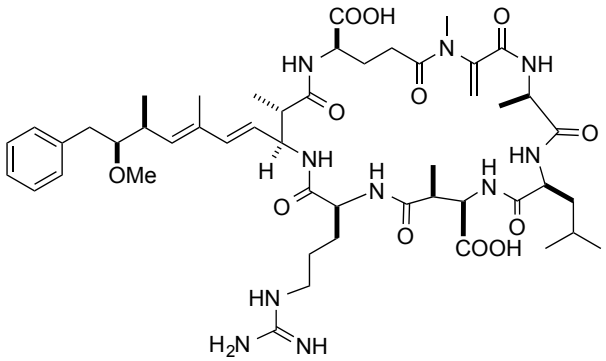

Figure 3.3. Structure of MC-LR

The synthesis of the different toxins takes place outside the ribosome (non-ribosomally) in an enzyme complex that includes peptide synthetases, polyketide synthases and other enzymes.[15,16] A 55 kb gene cluster, possessing two putative operons (*mcyA-C* and *mcyD-J*) is responsible for the MC-production, whereas for the activation and incorporation of Mdha, D-Ala, L-Xaa, D-MeAsp and L-Yaa the genes *mcyA*, *mcyB*, and *McyC* are reported to be in charge.[17,18] In this way, it is possible for different cyanobacteria strains to produce several diverse microcystins in parallel.[8] Within this toxin class, MC-LR is the most extensively studied microcystin due to its high LD_{50} value (50 $\mu g kg^{-1}$ in rats).[19] The fact that the World Health Organization (WHO) has set a maximal guideline value of 1 $\mu g L^{-1}$ MC-LR in drinking water further emphasize its potency and toxicity.[20,21] In humans, this substances shows a hepatotoxic effect through inhibition of protein phosphatases 1 (PP1) and 2A (PP2A) and the chronic exposure can cause liver cancer.[6,7,23] It also causes a disruption of the cytoskeletal components accompanied by cell deformation initiated by cytokeratin hyperphosphorylation, which ends in a collapse of the whole liver architecture.[24] Moreover, MC-LR seems to cause DNA-damage, apoptosis, disruption in the cell-signalling and endoplasmic reticulum stress.[25-27] The known transport of MCs in the cell is the organic anion polypeptide transporter (OATP), e.g. in human hepatocytes.[28,29] In aquatic organisms, which are particularly vulnerable to cyanobacterial microcystins due to the increased levels of exposure, such toxic effects are also displayed. For example, in *Daphnia magna*, which is an important grazer of algae as a food source, disturbance in the reproduction together with higher mortality rates and deteriorated development are observed.[1,10,30-32] In fish and invertebrates, the toxin accumulates in the tissues and leads to a number of toxic effects.[11,33]

Even though microcystins have been known for decades, the reasons for the strong toxicity in animals are not yet fully understood. To gain an insight into the uptake, distribution, accumulation and excretion of MC-LR, biological studies are necessary. The main goal of this project was the synthesis of fluorescently labelled MC-LR in order to monitor its behaviour as mode of action, uptake and excretion in aquatic animals. It was crucial to synthetically modify the molecule for these studies without inactivating its toxicity effect. That necessitated an investigation of the structural elements involved in the enzyme binding.

It has beed reported that the reactive Mdha groups binds in a Michael-type addition covalently to Cys 273 of the phosphate 1 and the Adda side chain interacts with the hydrophobic cage of the active pocket.[34] Furthermore, the crystal structure of the MC-LR/PP1 complex shows that leucine and the carboxylate groups are also involved in enzyme binding.[22] But interestingly, it also reveals, as the arginine function sticks out of the binding pocket (see arrow), that this residue is not participating in the inhibition of the phosphatase 1 and, thus, presents a promising site for modification (**Figure 3.4**).[22]

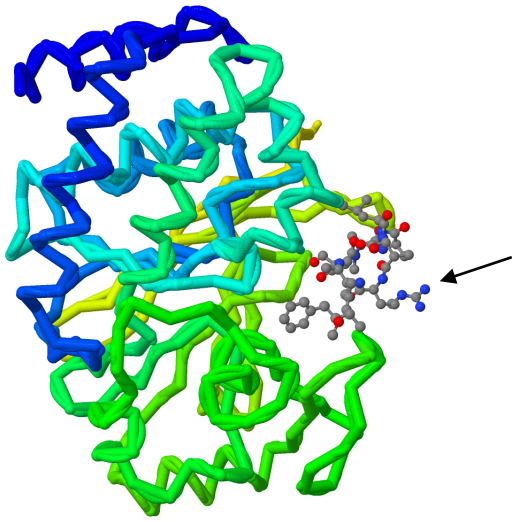

Figure 3.4. Structure of the catalytic domain of phosphatase 1α with MC-LR[22]

Nevertheless, efficient acetylation of the arginine guanidine group had proved to be difficult due to the high pK_a value of this protonated side chain (pK_a = 12.5). Shreder and co-workers have successfully introduced a fluorophore at this moiety in MC-LR with a compromised yield by using a two-step procedure.[35] Similar yields were obtained by a comparable reaction to a MC-LR-DNA conjugate.[36] In consideration of the limited availability of the toxin, further methods are needed to modify MC-LR. In this work, we describe the development of a facile labelling procedure of MC-LR. In addition, we test our derivatives with regard to remaining toxicity compared to the parent compound.

3.2 Results and discussion

3.2.1 Synthesis of the modified MC-LR

As already discussed, modification of the arginine residue should not affect the enzyme binding as suggested by the crystal structure.[22] Furthermore, hypervariations in the amino acid sequence at this position in natural occurring microcystins support the assumption that this residue is not important for the inhibitory effect.

To find an effective labelling method for MC-LR, we had to consider several difficulties: (a) The poor reactivity of the guanidinium group, (b) MC-LR contains other reactive groups like the reactive unsaturated Mdha residue, (c) MC-LR gets degraded under strong basic or acidic conditions, and (d) the availability of the toxin, which can only be isolated on a microgram scale.[37]

Thus, different strategies for labelling this moiety has to be investigated. Different promising conditions described in **chapter 2** were tested with MC-LR in parallel, to identify the best labelling strategy. Furthermore, to examine the behaviour of the sensitive groups and to monitor possible side reactions in MC-LR, the optimized conditions were first tested with Boc-Asp and *Z*-dehydro-Ala-OH together with Bz-Arg-OEt.

The first modification on MC-LR was carried out with dansyl chloride (1.5 eq.) with NEt_3 in DMF. The high reactivity of dansyl chloride was presumed to be problematic due to the small size of the compound. We then moved to a more bulky sulfonyl chloride reagent. To this extent, lissamine rhodamine B (1.5 eq.) was used. This reaction was not showing conversion to the desired product, but gave a complex mixture. A solvent change to dioxane was also not leading to success. We then decided to apply a method known to label amines in an efficient manner.[38]

For this matter we performed the coupling with *N*-hydroxysucinimide (2 eq.), EDC (2 eq.), rhodamine B (2 eq.) and NEt_3 (10 eq.) in MeCN. The use of NEt_3 did not led to the desired compound. We next sought to simplify the setup. Subsequently, Alexa fluor555 succinimide (2 eq.), DBU (12 eq.) in DMF was used. Unfortunately, this also did not leading to the desired conversion. Similarly, the use of NEt_3 showed no product formation. Another drawback of the above-mentioned conditions was that MC-LR degraded and could not be recovered. For this reason we focused on mild

reaction conditions to identify a base strong enough to deprotonate the guanidinium group, without degrading the MC-LR.

We therefore studied the use of Barton`s base (see also **chapter2**). The coupling of MC-LR was performed according to the standardized protocol at 40 °C dissolving the toxin in DMF and adding Barton's base. After initial stirring and subsequent addition of the dissolved activated ester, the reaction was stirred for eight hours. To our delight, the desired coupled product was obtained in moderate to good yields (35 % to 84 %). Interestingly, an "one shot" purification by HPLC could double the yield, compared to the multistep purification. The reason for that is probably the loss of material on the needlepoint of the HPLC. Utilizing this method, we synthesized four fluorescently labelled derivatives, as well as a biotin and a diazirine conjugates (**Figure 3.5, 3.6 and 3.7**). A proton NMR of **3.1** could be measured, however, an assignment of the signals was difficult due to the complexity of the molecule. MS-MS studies were performed to confirm the formation of the correct product. We identified the labelled Arg moiety of the MC-LR-(6-FAM) and the MC-LR-(Texas-Red) conjugate, however for MC-LR-(Alexa-430), we could not entirely exclude modification of the Glu or MeAsp side chains.

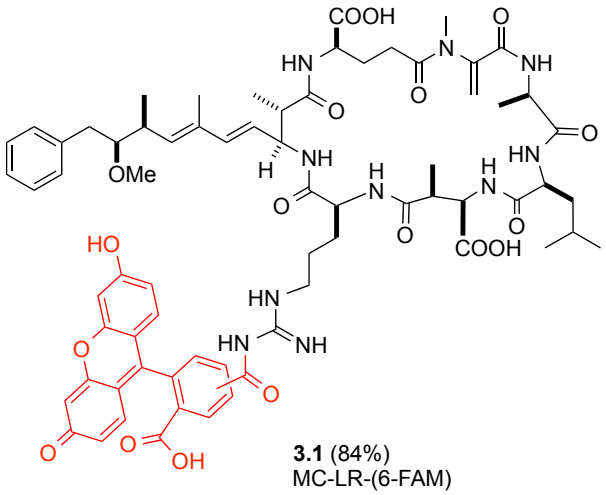

3.1 (84%)
MC-LR-(6-FAM)

Figure 3.5. Synthesized derivatives of MC-LR
MC-LR coupled with carboxyfluorescein (**3.1**)

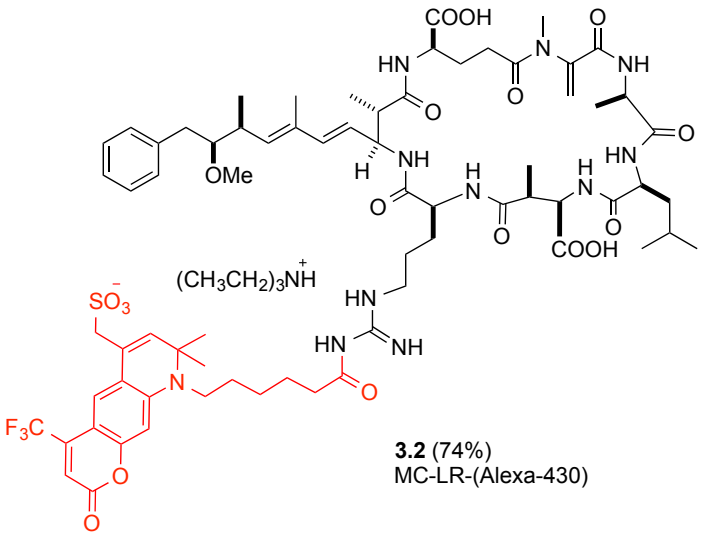

3.2 (74%)
MC-LR-(Alexa-430)

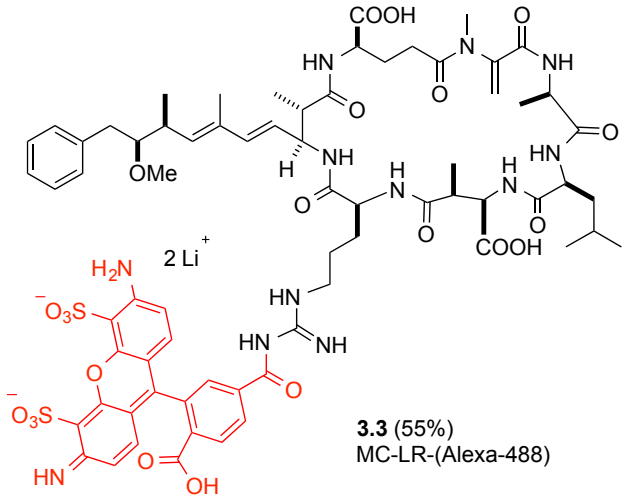

3.3 (55%)
MC-LR-(Alexa-488)

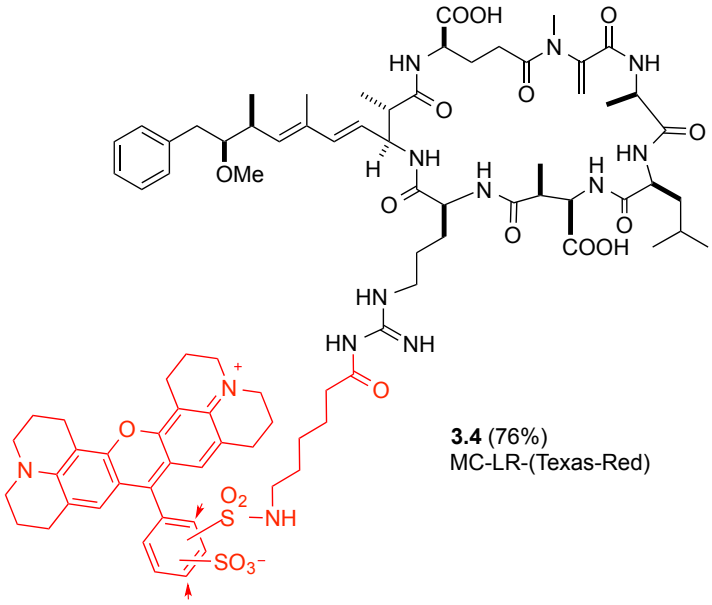

3.4 (76%)
MC-LR-(Texas-Red)

Figure 3.6. Synthesized derivatives of MC-LR

MC-LR coupled with Alexa-430 (**3.2**), Alexa-488 (**3.3**) and Texas Red (**3.3**)

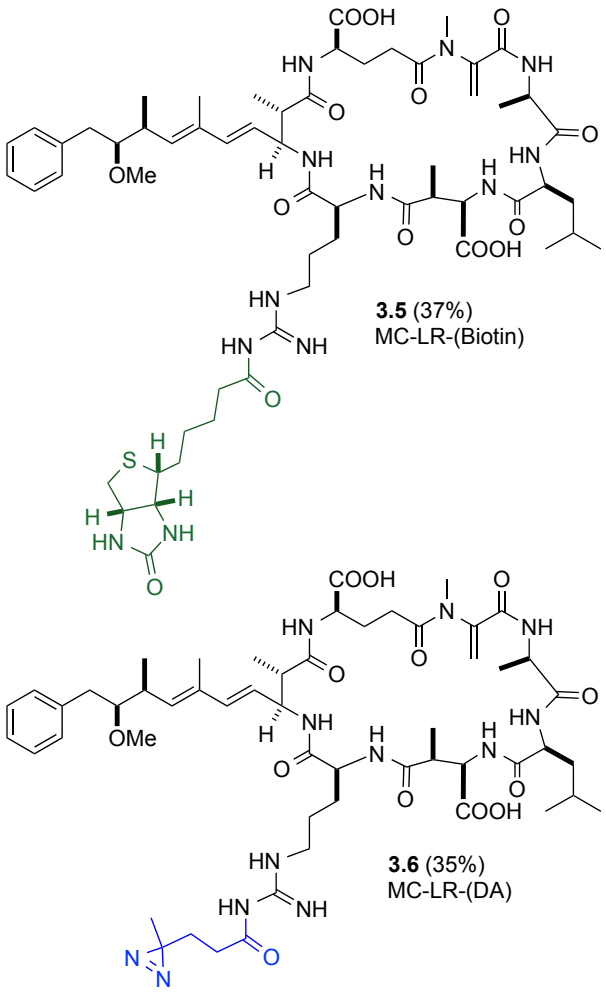

Figure 3.7. Synthesized derivatives of MC-LR
MC-LR coupled with biotin (**3.5**) or diazirine (**3.6**)

3.2.2 Photochemical properties of MC-LR-(6-FAM), MC-LR-(Alexa-430) and MC-LR-(Texas-Red)

After successfully labelling of MC-LR with different fluorophores, we investigated the photochemical properties of compounds **3.1**, **3.2** or **3.4**. We anticipated that these derivatives could be used in further biological tests. The fluorescent spectrum of **3.1**, **3.2**, or **3.4** is shown in **Figure 3.8** The maximum absorption of the derivatives was at 499 nm for MC-LR-(6-FAM), at 425 nm for MC-LR-(Alexa-430) and at 586 for MC-LR-(Texas-Red). Furthermore, the maximum emission is located at 525 nm for MC-LR-(6-FAM), at 434 nm for MC-LR-(Alexa-430) and at 605 nm for MC-LR-(Texas-Red). With this data, we were able to choose the right compounds for

the various uptake studies, with regards to overlapping with intrinsic fluorescence of the used chemicals and test systems.

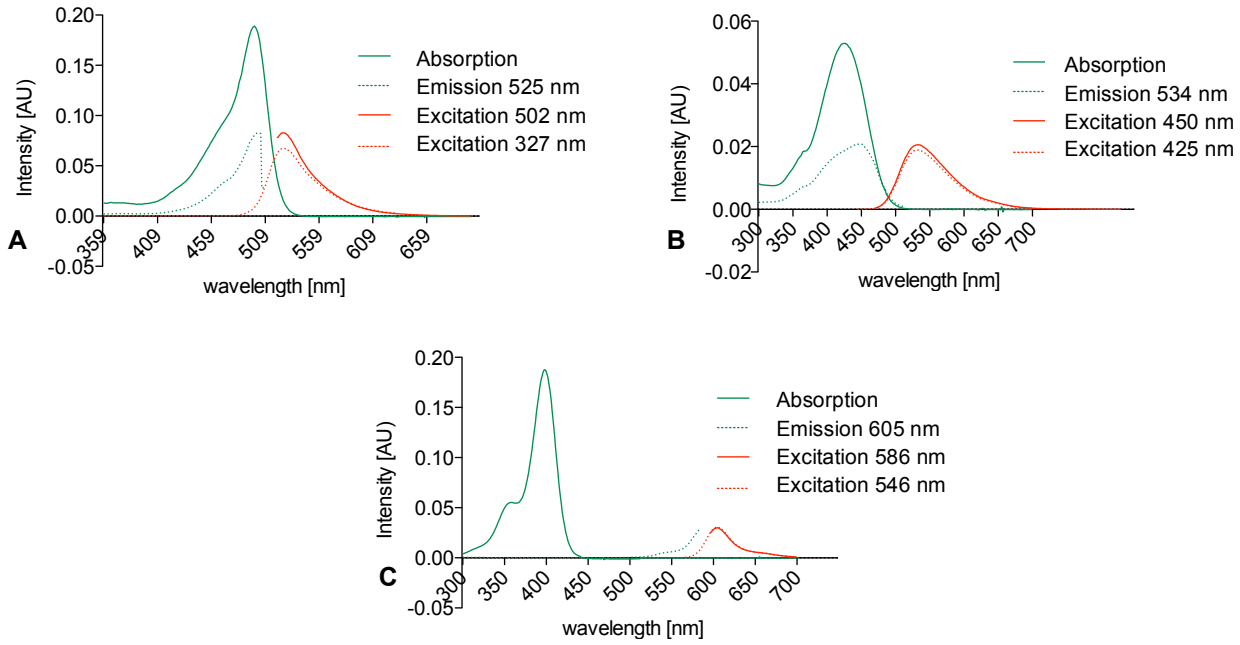

Figure 3.8. Spectral profile

A: MC-LR-(6-FAM) **B:** MC-LR-(Alexa-430) **C:** MC-LR-(Texas-Red)

To visualize the spectral colour of the different compounds, the colour space chromaticity diagrams are shown in **Figure 3.9**. MC-LR-(6-FAM) is located more in the yellowish-green range (x: 0.32 y: 0.66), whereas MC-LR-(Alexa-430) is already in the yellow-green area (x: 0.38 y: 0.58) and MC-LR-(Texas-Red) is situated in the orange-yellow section (x: 0.65 y: 0.36).

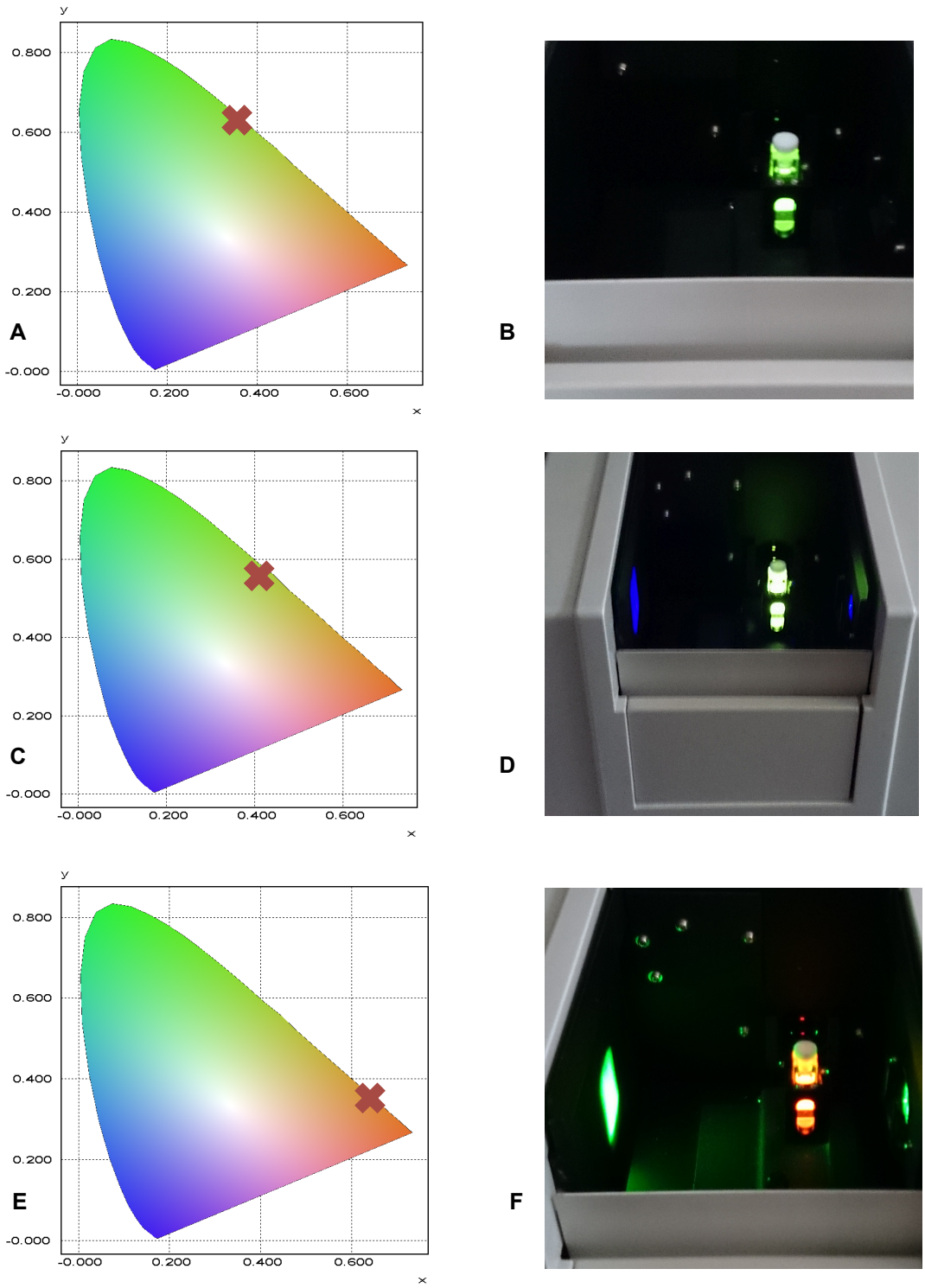

Figure 3.9. CIE colour space chromaticity diagram and fluorescent picture

A: CIE colour space chromaticity diagram of MC-LR-(6-FAM) **B:** Fluorescent picture of MC-LR-(6-FAM)

C: CIE colour space chromaticity diagram of MC-LR-(Alexa-430) **D:** Fluorescent picture of MC-LR-(Alexa-430)

E: CIE colour space chromaticity diagram of MC-LR-(Texas-Red) **F:** Fluorescent picture of MC-LR-(Texas-Red)

In addition, the quantum yield of compounds **3.1**, **3.2** or **3.4** was determined as an important parameter for the fluorescence intensity at the minimum concentration for biological experiments. The following values were obtained: MC-LR-(6-FAM) Φ = 0.66 (Ex: 503 nm); MC-LR-(Alexa-430) Φ = 0.57 (Ex: 450 nm); MC-LR-(Texas-Red) Φ = 0.88 (Ex: 546). The Texas-Red derivative is the best choice for large dilutions as its quantum yield of 0.88 allowing high enough sensitivity for the following measurements.

3.2.3 Comparison of biological activities of native MC-LR and modified MC-LR

With the derivatives in hand, we were ready to investigate whether the prepared compounds had retained biological activity for the parent species. We performed selected bioassays with the MC-LR derivatives. Afterwards, we compared the results to known literature values of MC-LR to identify if the derivatives retained their toxicity. First, we used phosphatase inhibition assays to examine the differences in inhibition activity of the derivatized MC-LR in comparison to the native MC-LR towards the phosphatase 2A, one of its primary targets. In addition, we tested the ability of the derivatives to induce ER-stress. We then examined the cellular uptake of the MC-LR derivatives and performed cell viability assays in Huh 7 liver cells. Next, we analysed the toxicity of the modified compounds toward aquatic organisms to verify that the toxin remains toxic in the living organism. The uptake of the labelled MC-LR derivatives was imaged in uptake studies with adult *Daphnia galeata* and *Daphnia magna*.

3.2.3.1 Phosphatase inhibition assays

The inhibitory effect of labelled MC-LR in comparison to unlabelled MC-LR was tested against PP2A. The primary tests showed that the fluorophores themselves were not interfering with the absorbance and the emission of the substrate, which allowed the use of compound **3.1** and **3.2** in the inhibition assays as test substrates. These derivatives were chosen to investigate, if a negative charge in the compounds has a different influence on the inhibitory activity. For this the PP2A was incubated

with the toxin in different concentrations (0.004 nM up to 40 nM) and 6,8-difluoro-4-methylumbelliferyl phosphate (DiFMUP). The activity of the non-inhibited PP2A enzyme reaction is associated with the measured fluorescence of released 6,8-difluoro-4-methylumbelliferone.

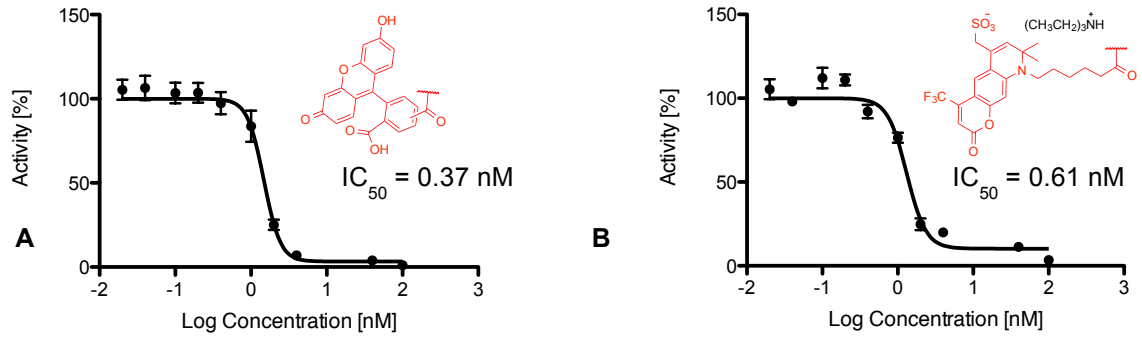

Figure 3.10. Phosphatase inhibition assay
A: with MC-LR-(6-FAM) IC_{50} = 0.37 nM **B:** with MC-LR-(Alexa-430) IC_{50} = 0.61 nM

The data showed that MC-LR-(6-FAM) with an IC_{50} value of 0.37 nM inhibits PP2A much stronger than MC-LR-(Alexa-430) with an IC_{50} value of 0.61 nM respectively (**Figure 3.10**). In comparison with MC-LR itself, having an IC_{50} value of 0.05 nM, both compounds inhibit the enzyme to a lesser extent.[39] Although the inhibition is seven to twelve times weaker than the inhibition of MC-LR itself, the compounds have not completely lost their toxicity. Possibly, the size (1.5 times more than that of MC-LR) of the molecules and the proximity of the fluorophore to the Adda side chain might have an influence on their binding and inhibition activity.[40] The difference in the inhibition ability of the two compounds could be explained by the negative charge of the MC-LR-(Alexa-430) derivative. The sulphate moiety of the fluorophore could interact with the metal site of the enzyme and thus competes with the binding of the glutamate to the latter.[22] In this way the positioning of the toxin in the binding pocket would be altered, therefore hindering the efficient binding or significantly slowing down the process of covalently attaching of the Mdha residue.[41]

3.2.3.2 RNA isolation, reverse transcription and quantitative (q)PCR for ER-stress response

To investigate the ability of the derivatives to induce ER-stress response, we performed quantitative (q)PCR measurements with the key ER-stress marker *BiP* and an internal control (GAPDH). In order to do that, we incubated Huh7 cells with 5 µM and 50 µM of MC-LR-(Alexa-430) over 24 h. DNA was obtained from isolated RNA using reverse transcription. The qPCR showed an upregulation of *BiP* (**Figure 3.11**).

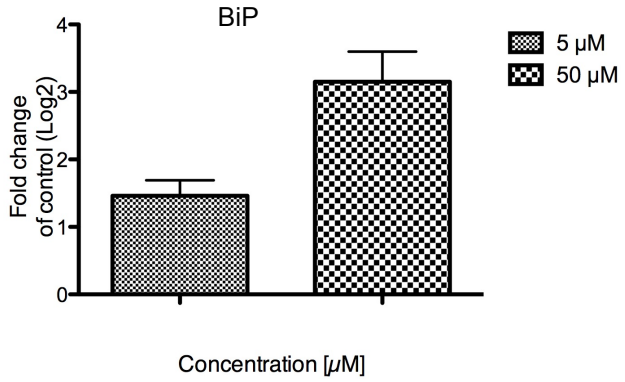

Figure 3.11. Induction of ER-stress
Huh7 cells after exposure of MC-LR-(Alexa-430), expression of BiP after 24 h

This induction of the chaperon *BiP* suggests that the derivative is still causing ER-stress. However, we did not observe this tendency in follow up studies. An explanation for that could be that the toxicity of the compound is higher than the parent compound and the cells were already dead after a short incubation time. The RNA started to degrade before measurements of the ER-induction could be obtained.

3.2.3.3 MTT assay for cytotoxicity

To examine the cellular uptake and the toxicity of the MC-LR derivatives, MTT cytotoxicity assays for cell viability were performed. Huh 7 cells were incubated with different concentrations of compound **3.2** for 24 h. Additionally fluorescent imaging of the cells was performed after 4 h to visualize the uptake of the labelled toxin. Cytotoxicity was validated with MTT assays. In comparison to MC-LR (4.3 µM[25]) an EC_{50} value of 16.3 µM for compound **3.2** was measured (**Figure 3.12**). The EC_{50} value of MC-LR-(Alexa-430) is four times higher than the parent compound. This is maybe due to the negative charge of the derivative as described before.

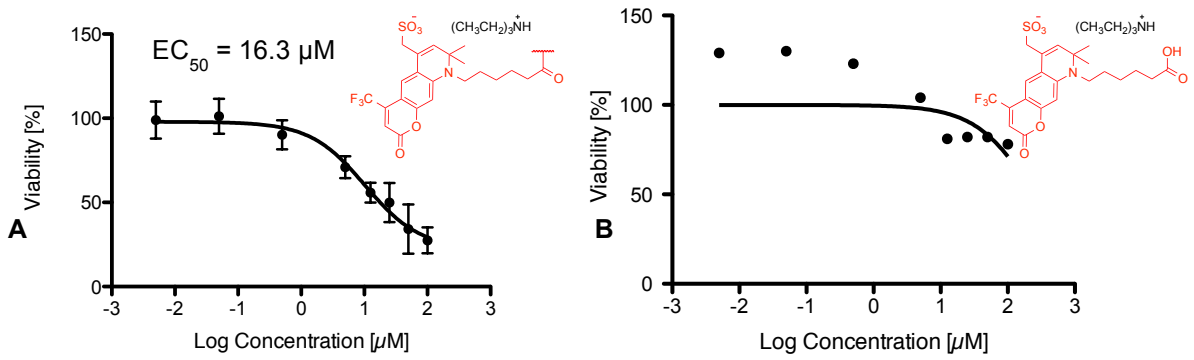

Figure 3.12. Cell viability assay
A: with MC-LR-(Alexa-430), EC_{50} = 16.3 µM **B:** with hydrolysed Alexa-430

Interestingly, the inhibition behaviour of the phosphatase 2A seemed to be more affected by the derivatization than the cell uptake. This can either be due to the longer time of the experiment as well as the longer incubation time, whereas eventual binding problems can be overcome. This result could also be explained with the assumption, that the transporters responsible for MC-LR uptake, the OATPs, are suited for negatively charged compounds.[42]

Furthermore, visualization of the treated cells revealed that the toxin is present in the cells (**Figure 3.13**). Additionally, the control picture of the hydrolysed fluorophores showed that the fluorophore itself couldn't be taken up into the cells. This also revealed that the fluorescent MC-LR derivative is not hydrolysed under the conditions of the assay. Therefore, compound **3.2** demonstrated efficient cell uptake with retained cytotoxicity.

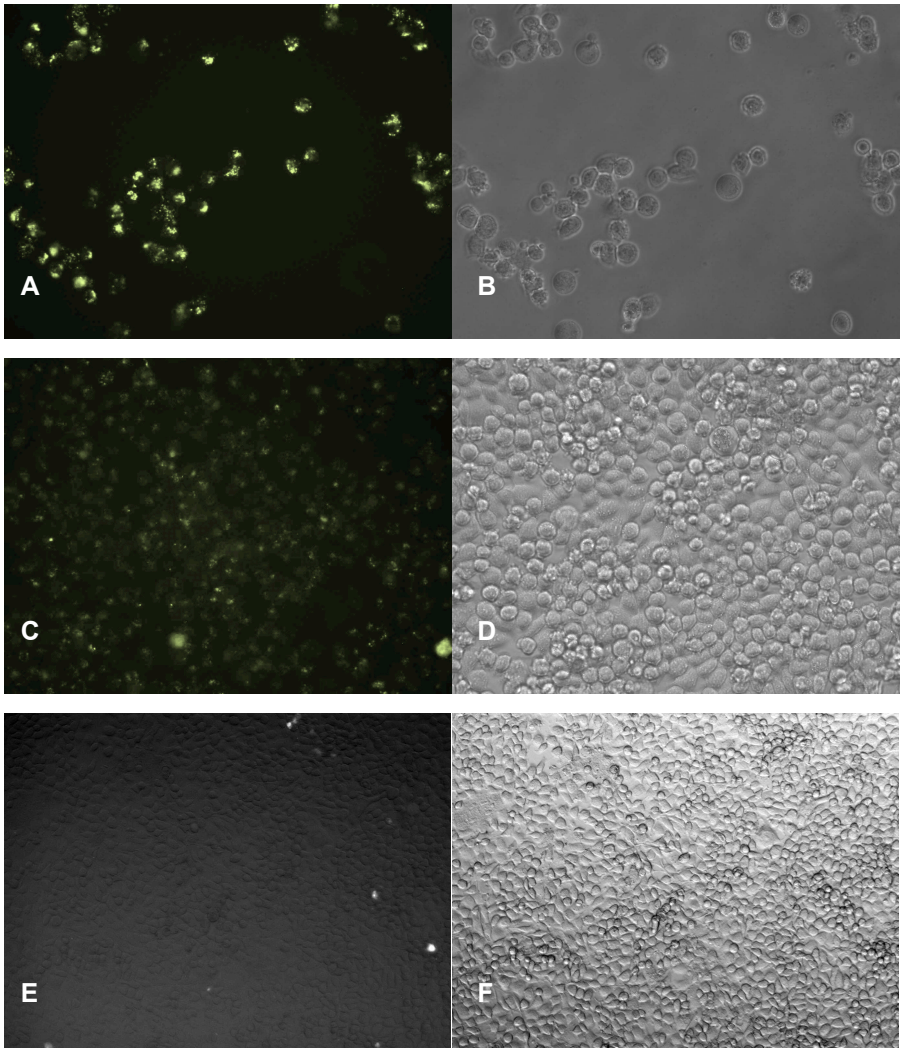

Figure 3.13. Fluorescent imaging of Huh 7 liver cells
A: Fluorescent image at 100 µM with MC-LR-(Alexa-430) **B:** Phase Contrast at 100 µM with MC-LR-(Alexa-430) **C:** Fluorescent image at 12.5 µM with MC-LR-(Alexa-430) **D:** Phase Contrast at 12.5 µM with MC-LR-(Alexa-430) **E:** Fluorescent image at 100 µM with hydrolysed Alexa-430 **D:** Phase Contrast at 100 µM hydrolysed Alexa-430

3.2.3.4 Acute toxicity assay

We analysed the toxicity of the modified compounds towards aquatic organisms. The freshwater crustacean *Thamnocephalus platyurus* was chosen for the acute toxicity test, as it is a widely used system for such cyanotoxin toxicity assessment.[43] As test substrates we took derivatives **3.1** and **3.2**. We administered these compounds over

24 h, to determine the LC_{50} value compared to unlabelled MC-LR. With an LC_{50} value of 5.7 µM for **3.1** and 15.7 µM for **3.2**, the test revealed toxicity towards aquatic organisms comparable to MC-LR (10.8 µM)[39] (**Figure 3.14**). This implied that the functional tag is not interfering with the mode of action of the toxin.

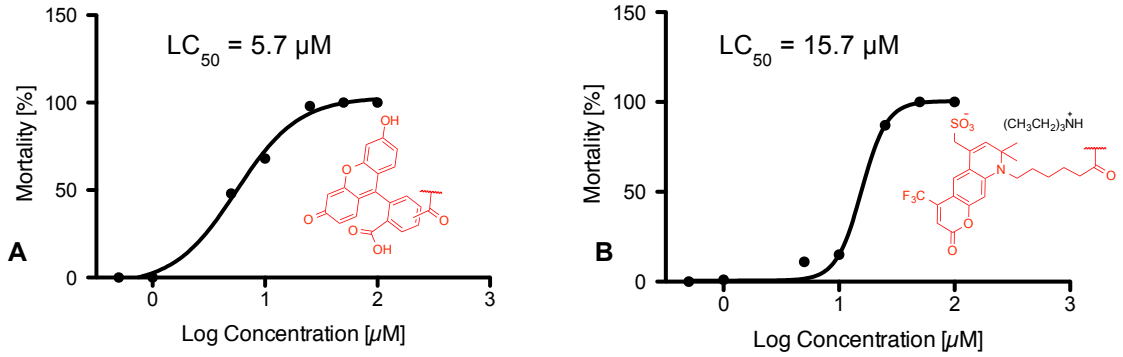

Figure 3.14. Acute toxicity assay
A: with MC-LR-(6-FAM), LC_{50} = 5.7 µM **B:** with MC-LR-(Alexa-430), LC_{50} = 15.7 µM

Fluorescent imaging of animals treated with MC-LR-(Alexa-430) was revealed that the compound was only accumulated in the digestive track (**Figure 3.15**).[44]

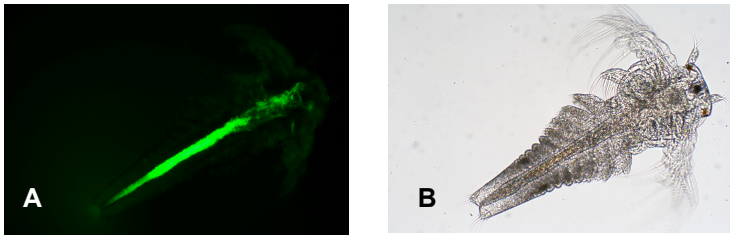

Figure 3.15. Fluorescent imaging of MC-LR-(Alexa-430) treated *Thamnocephalus platyurus*
A: Fluorescent image at 100 µM with MC-LR-(Alexa-430) **B:** Phase Contrast at 100 µM with MC-LR-(Alexa-430)

Interestingly, the MC-LR-(6-FAM) derivative has a better inhibition behaviour than MC-LR-(Alexa-430). It suggests that the negative charge indeed hinders the activity of the toxin. Another difference is, that the toxicity is not as much decreases as the inhibitory effect. This can be explained with the time difference of the experiments. It is possible, that the process of inactivation of important enzymes by the modified MC-LR is completed after 24 h, whereas the inhibition of the phosphatase 2A is still continuing after 10 min.

3.2.3.5 Uptake studies in Daphnia galeata and Daphnia magna

The uptake of the labelled MC-LR derivatives was traced in studies with adult *Daphnia galeata* and *Daphnia magna*. The microscopic investigation of *Daphnia galeata* showed compound **3.2** not only distributed in the gastrointestinal tract, but also in another area which is not accessible to food, in this case the cecum, which is separated from the gut by a membrane (**Figure 3.16**).

Figure 3.16. Fluorescent imaging of *Daphnia galeata*
Exposure of *Daphnia galeata* to **3.1** after 3 h; Compound **3.1** accumulates in the cecum (arrow)

To examine the uptake behaviour in an extended time range, uptake studies with *Daphnia magna* were performed over 72 h. Different points in time were taken to monitor the distribution of the toxin. The toxin was also accumulating in the gastrointestinal tract and the cecum after a short time period. The same distribution is observed over time, whereas after 72 h an accumulation in the cecum could only be observed in smaller concentrations of compound **3.1**.

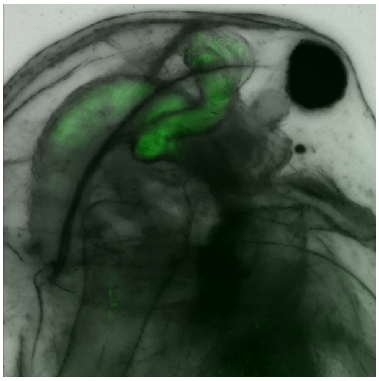

Figure 3.17. Fluorescent imaging of *Daphnia magna*
Exposure of *Daphnia magna* to **3.1** after 72 h; Compound **3.1** accumulates in the cecum

3.3 Conclusion

In conclusion, we have successfully developed a mild and operatively simple derivatization method for MC-LR in moderate to good yield. This method allows the modification of the toxin with a variety of biologically important tags, such as fluorescent labels, diazirine and biotin tags. Furthermore, we demonstrated that the MC-LR derivative remains active towards one of the primary target, the enzyme phosphatase 2A (IC_{50} value of 0.37 nM) and is active towards aquatic organisms (LC_{50} value of 5.7 µM). In addition, the tagged MC-LR successfully undergoes cellular uptake by Huh 7 cells and retains toxicity (EC_{50} value of 4.3 µM). The compound uptake in an *in vivo* system was also performed with *Daphnia galeata* and *Daphnia magna*, where it remains not only in the digestive tract, but also penetrates the membrane barrier into the cecum. Additional ongoing studies aim to investigate the uptake of the labelled MC-LR derivatives in parental *Daphnia magna*, as MC-LR is known to affect reproduction.

3.4 Methods

3.4.1 General

The following reagents were purchased and used as received: NHS-diazirine (Thermo Scientific), all reactive succinimidyl ester fluorophores (Invitrogen), Seaplaque agarose (Lonza), all further chemicals were purchased from Sigma-Aldrich Co. and were of analytical grade. Biotin *p*-nitrophenylester was kindly provided by K. Tishinov (Universit of Basel); Microcystin-LR was isolated or provided by E. Kohler or purchased from Enzo Life Sciences. *Thamnocephalus platyurus* for the acute toxicity assay were purchased from MicroBioTests Inc., Belgium. The PP2A enzyme was purchases from Promega, USA. 6,8-difluoro-4-methylumbelliferyl phosphate was received from Molecular Probes, Leiden, The Netherlands. HuH7 cells were provided by Susanne Faltermann (University of Applied Sciences and Arts Northwestern Switzerland).

For measuring the fluorescence in the protease inhibition assays a fluorescence microplate reader (Spectra MAX gemini XS; Molecular Devices Cooperation, Sunnyvale, California, USA) was used set at l_{em} = 365 nm, l_{ex} = 444 nm. All reactions were carried out in oven-dried glassware under an atmosphere of argon. HPLC purifications of the functionalized MC-LR was obtained on a Dionex P-680 HPLC System with a Phenomenex Gemini C18 5 µ (250 mm x 4.6 mm) column or a Phenomenex Gemini C18 5 µ (150 mm x 4.6 mm) column using a linear gradient: 5 % to 100 % CH_3CN in 0.1 % Formic acid/H_2O over 40 minutes at a flow rate of 1 mL/min. For removal of the formic acid a final purification step was performed on a C_{18} SPE cartridge (500 mg, Supelco) starting with a first washing step with water to remove the acid and a final elution step with 80 % acetonitrile.

The yield of modified MC-LR was determined using a NanoDrop 2000 Spectrophotometer (Thermo scientific). UV-Vis data was recorded on an Agilent 8453 spectrophotometer, the fluorescence was measured on a Fluorimeter: Shimadzu 5301PC spectrofluorophotometer and the quantum yield was determined on a Hamamatsu absolute PL quantum yield spectrometer C11347 Quantaurus_QY. ^{1}H-NMR spectrum was recorded on a Bruker Avance III Ultrashield 600MHz with a 5mm BBFO+ plus SP probe or a Bruker Avance III Ascend 700MHz with a 5mm TCI (H-C/N-D) cryo probe spectrometers at room temperature. HRMS spectra were recorded on a Bruker maXis 4G instrument or measured by the mass spectrometric

service of University of Bern on a *Sciex QSTAR Pulsar mass spectrometer*. HRMS spectra were obtained on a Bruker maXis 4G with ESI in positive or negative mode. MS-MS experiments were obtained on a Bruker Esquire 3000 with ESI in positive mode.

3.4.2 Cell culturing, extraction and isolation

M. aeruginosa UV-006 was cultivated in 500 mL Falcon tubes in 200 mL mineral medium at 25 °C with 12h light and night cycle.[45] The resulting biomass was harvested every three months with a 6K15 centrifuge (Sigma), freezed and stored at -20 °C. To obtain pure MC-LR the cyanobacteria were suspended in 20 mL of 60 % acetonitrile per 1 g biomass and sonicated for 10 min (Branson 2510). The resulting homogenous mixture was centrifuged for 15 min at 25000 x g and the supernatants were combined and evaporated in a rotarory evaporator (Büchi, Switzerland). The residue was dissolved in 60 % acetonitrile and prepurified on a C_{18} SPE cartridge (10 g, Supelco). The crude mixture was eluted with 80 % acetonitrile (500 mg biomass afforded 15 mg crude extract), concentrated and applied on a Dionex P-680 HPLC System with a Phenomenex Gemini-NX C18 5µ (75 mm x 21.2 mm) column using a linear gradient: 5 % to 100 % CH_3CN in 0.1 % Formic acid/H_2O over 40 minutes at a flow rate of 5 mL/min for further purification. For removal of the formic acid a final purification step was performed on a C_{18} SPE cartridge (500 mg, Supelco) starting with a first washing step with water to remove the acid and a final elution step with 80 % acetonitrile. After removal of all volatiles and lyophilisation pure MC-LR (600 µg from 15 mg crude extract) was afforded as a white solid. HPLC: t_R = 18.1 min; MS (ESI): *m/z* = 995.9 $[M+H]^+$

3.4.3 Synthesis of the modified MC-LR

3.4.3.1 General procedure for the functionalization MC-LR

To a solution of MC-LR (1 eq.) in DMF (50 µl) were added Barton's base (10 eq.) and the activated ester (1.5,1.1 or 4 eq.) in DMF (20 µl). The resulting mixture was stirred at 40 °C for 8h. All volatiles were removed under reduced pressure and the residue was purified by HPLC.

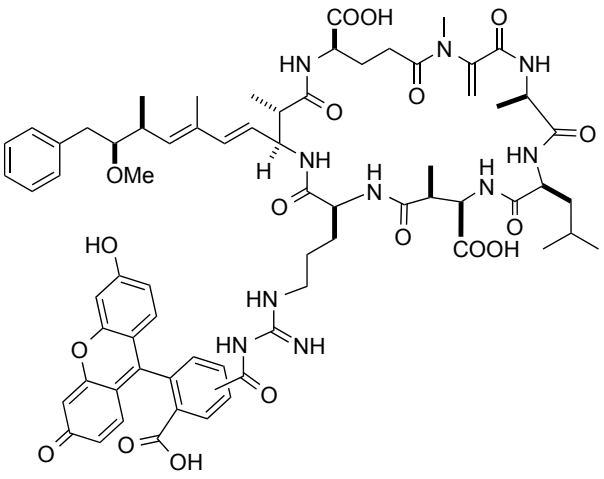

MC-LR-(6-FAM), (3.1):

According to the general procedure compound **3.1** was synthesized starting from MC-LR (0.40 mg, 0.40 µmol). Barton's base (0.70 mg, 4.09 µmol) and 5(6)-carboxyfluorescein *N*-succinimidyl ester (0.22 mg, 0.46 µmol) were used. Direct purification by HPLC afforded **3.1** (423 µg, 0.31 µmol, 84 %) as a red solid. HPLC: t_R = 23.6 min; HRMS-ESI: calcd. for $C_{70}H_{85}N_{10}O_{18}^+$ $[M+H]^+$: 1353.6038; found: 1353.6087.

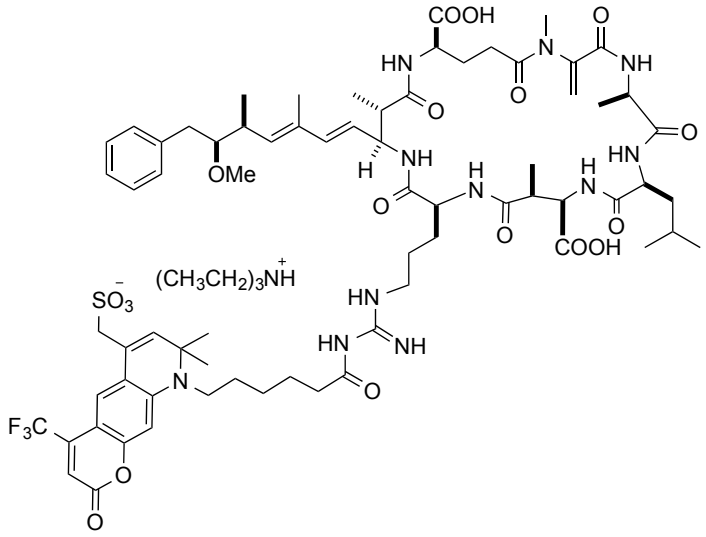

MC-LR-(Alexa-430), (3.2):

According to the general procedure compound **3.2** was synthesized starting from MC-LR (1.00 mg, 1.00 µmol). Barton's base (1.10 mg, 6.43 µmol) and Alexa 430 succinimidyl ester (0.78 mg, 1.11 µmol) were used. Direct purification by HPLC afforded **3.2** (1.36 mg, 0.92 µmol, 74 %) as a red solid. HPLC: t_R = 33.4 min; HRMS-ESI: calcd. for $C_{71}H_{95}N_{11}O_{18}F_3S^-$ $[M-H]^-$: 1478.6524; found: 1478.6527.

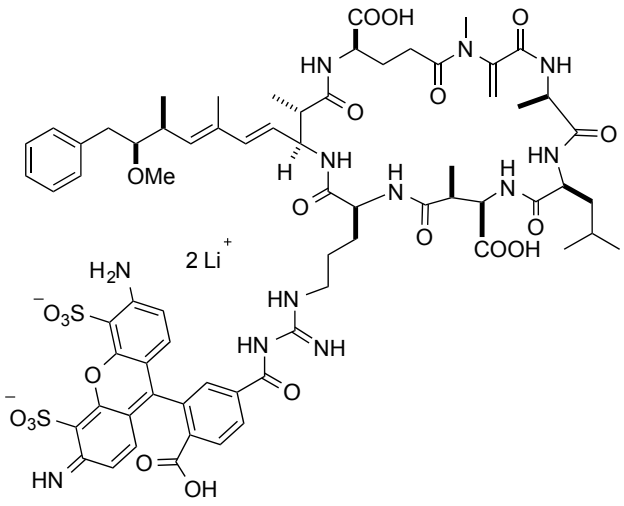

MC-LR-(Alexa-488), (3.3):

According to the general procedure compound **3.3** was synthesized starting from MC-LR (0.20 mg, 0.20 µmol). Barton's base (0.34 mg, 2.0 µmol) and Alexa 488 5-sulfodichlorphenol ester (0.25 mg, 0.30 µmol) were used. Direct purification by HPLC afforded **3.3** (0.17 mg, 0.11 µmol, 55 %) as a red solid. HPLC: t_R = 10.9 min; HRMS-ESI: calcd. for $C_{70}H_{84}N_{12}O_{22}S_2^{2-}$ $[M\text{-}H\text{-}H]^{2-}$: 754.2638; found: 754.2625.

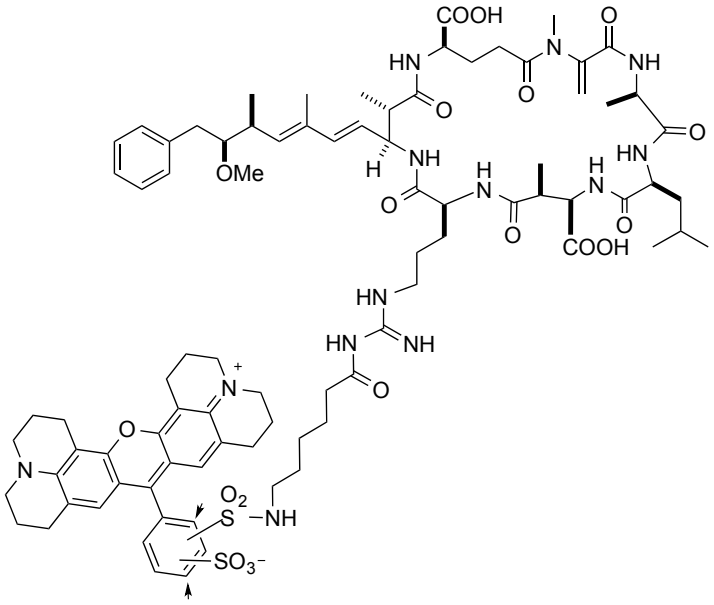

MC-LR-(Texas-Red), (3.4):

According to the general procedure compound **3.4** was synthesized starting from MC-LR (0.50 mg, 0.50 µmol). Barton's base (0.86 mg, 5.02 µmol) and Texas Red succinimidyl ester (0.50 mg, 0.61 µmol) were used. Direct purification by HPLC

afforded **3.4** (650 µg, 0.38 µmol, 76 %) as a red solid. HPLC: t_{R1} = 23.6 min; t_{R2} = 25.6 min; HRMS-ESI: calcd. for $C_{86}H_{114}N_{13}O_{19}S_2Na^{2+}$ $[M+H+Na]^{2+}$: 859.8841; found: 859.8852.

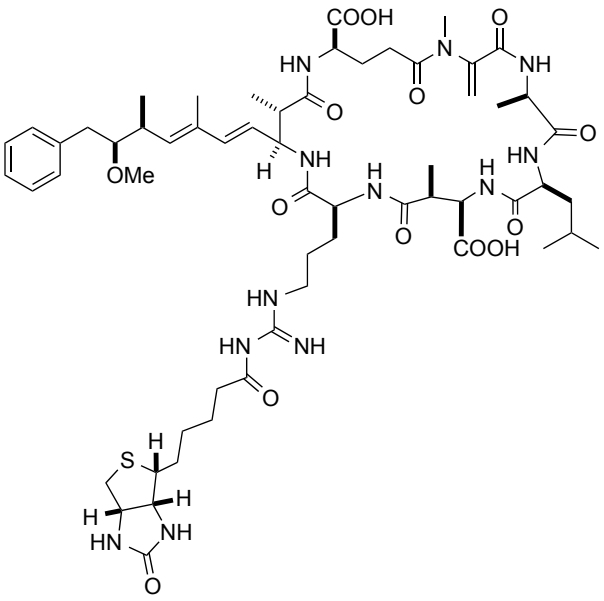

MC-LR-(Biotin), (3.5):

According to the general procedure compound **3.5** was synthesized starting from MC-LR (0.10 mg, 0.10 µmol). Barton's base (0.20 mg, 1.0 µmol) and *p*-nitrophenylester (40 µg, 0.11 µmol) were used. Direct purification by HPLC using first the gradient from the general procedure and for further purification 50 % CH_3CN in 0.1 % Formic acid/H_2O with isocratic conditions afforded **3.5** (46 µg, 0.038 µmol, 37 %) as a red solid. HPLC: t_R = 19.9 min (gradient); t_R = 8.5 min (isocratic); HRMS-ESI: calcd. for $C_{59}H_{89}N_{12}O_{14}S^+$ $[M+H]^+$: 1221.6336; found: 1221.6340.

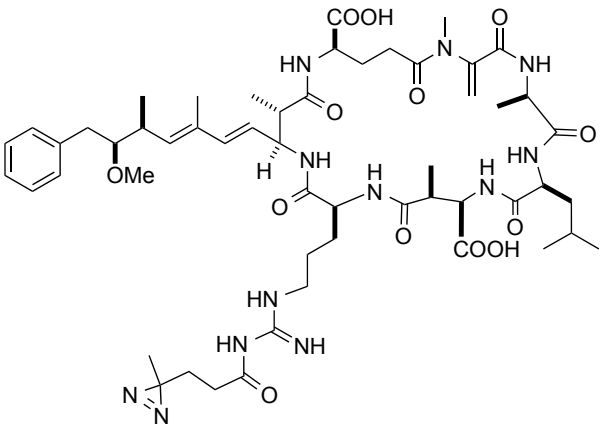

MC-LR-(DA), (3.6):

According to the general procedure compound **3.6** was synthesized starting from MC-LR (0.10 mg, 0.10 µmol). Barton's base (0.20 mg, 1.0 µmol) and succinimidyl-diazirine (90 µg, 0.40 µmol) were used. Direct purification by HPLC afforded **3.6** (39 µg, 0.035 µmol, 35 %) as a red solid. HPLC: t_R = 21.8 min; HRMS-ESI: calcd. for $C_{54}H_{81}N_{12}O_{13}^+$ $[M+H]^+$: 1105.6041; found: 1105.6039.

3.4.4 Phosphatase inhibition assays

The enzyme mixture was prepared as followed: 2 µl of the PP2A enzyme were dissolved in 650 µl EGTA (1 mM), 50 µl DTT (10 mM in 5 mM sodium acetate pH = 5.2), 200 µl $MnCl_2$ (6 mM) and 100 µl BSA (5 mg/mL). The reaction buffer was prepared out of 290 µl $MnCl_2$ (6 mM), 290 µl $MgCl_2$ (0.8 M) and 290 µl BSA (5 mg/mL). In a 200 µl well plate 25 µl of the enzyme mixture was used. To achieve a final concentration of 25 mU PP2A/200 µl, 30 µl Tris-HCl (50 mM, pH = 7.0) and 15 µl of the reaction buffer were added. The mixture was incubated for 10 minutes at 37 °C. Afterwards 10 µl of **3.1** and **3.2** were added in various concentrations (0.004 nM up to 40 nM). Only the fluorophores were used as control experiment to test possible interference with the experimental setup. Subsequent incubation at 37 °C for 10 minutes was followed. To start the measurement 120 µl of 6,8-difluoro-4-methylumbelliferyl phosphate (10 mM dissolved in 50 mM Tris-HCl pH = 7.0) solution were added. After a final incubation over 5 minutes at 37 °C the fluorescence measurement was started by taking a data point every 30 seconds for 45 minutes. To obtain the activity of the phosphatase, linear regression was used using Graph Pad Prism 4.1 for Windows.

3.4.5 RNA isolation, reverse transcription and quantitative (q)PCR for ER-stress response

Huh7 cells were plated at a density of 50000 cells per condition in 50 µl fractions in a 96-well plate with DMEM and GlutaMAX with 10 % FBS. After 24 h in a humidified incubator (5 % CO_2, 37 °C) different dilutions of compound **3.2** was added to the cells. After additional 24h the medium was removed and the RNA was isolated with Trizol reagent (LuBioScience) from the Huh7. Reverse transcription of the RNA was performed by the Moloney murine leukemia virus reverse transcriptase (Promega), random hexamers (Roche) and deoxynucleoside triphosphate. After incubation for 5 min at 70 °C, followed by an incubation over 1 h at 37 °C, the reaction was heated up to 95 °C for additional 5 min. qPCR was carried out with SYBR green (Roche) and with the primers for *BiP* (forward CGAGGAGGAGGACAAGAAGG; reverse CACCTTGAACGGCAAGAACT). The PCR cycle (BioRAD CFX 96 Real Time System) started with 95 °C for 5 min and continued with 40 cycles of 95 °C for 30 s and 60 °C for 60 s. Subsequently a melting curve was run. The cycle threshold value was determined by subtracting the value of the internal control *GAPDH* from the value of the target genes. The expression level of the mRNA was calculated afterwards according to the formula 2^(DCT untreated – DCT treated).

3.4.6 MTT assay for cytotoxicity

Huh7 cells were plated after growing in DMEM containing GlutaMAX (LuBioSciene) with 10 % FBS in a humidified incubator (5 % CO_2, 37 °C), in a 96-well plate at a density of 50000 cells per condition in 50 µl fractions. After 24 h of incubation, a series of diluted solution of compound **3.2** was added to the cells. After additional 24 h, the mixture was replaced with 200 µl fresh medium. Pictures of the uptake into the cells were taken with an Olympus CKX41 biological microscope with a 10x objective. Analysis of the pictures were performed with Cell B Version 3.2. Afterwards 20 µl of MTT (5mg/mL) was added, followed by an incubation over 2 h at 37 °C. Subsequently, the solution was removed and 200 µl DMSO was added and mixture was shaken for 15 min and cytotoxicity was measured.

3.4.7 Acute toxicity assay

To determine the acute toxicity of the modified MC-LR, compound **3.1** and **3.2** was utilized in an acute toxicity assay with *Thamnocephalus platyurus* in a multiwell plate using instar II-III larvae hatched from cysts during 24 hours. Compounds **3.1** and **3.2** were tested in various concentrations (0.5 to 100 µM) using 30 animals per condition. The LC_{50} value was calculated using the nonlinear regression Graph Pad Prism 4.1 for Windows was used.

3.4.8 Uptake studies in Daphnia galeata *and* Daphnia magna

Adult *Daphnia galeata* were exposed to 50 µM of compound **3.1** over 4 h at room temperature. In the next experiment *Daphnia magna* were placed in a 24-well-plate containing 1 mL of the labelled toxin. After 4 h the animals were rinsed with water and monitored with a Zeiss Axio Imager M1 microscope, equipped with a NIKON EOS 1000D camera. As contrast differential interference with an objective 10 x was used. Analysis of the images were performed with AxioVision 4.8.2.
Further uptake studies were performed in *Daphnia magna*. 48 h old *Daphnia magna* were exposed to 10 µM, 1 µM and 0.01 µM solution of compound **3.1** at 20 °C. 10 animals were placed in a 50 mL baker containing 15 mL of the test solution in M4 medium without food additions. The experiment was performed over 72 h, whereas after 3 h, 6 h, 24 h, 48 h and 72 h samples were taken. For this the *Daphnia* were rinsed with fresh medium and immobilized with 1 % agarose gel. The uptake of the fluorescent labelled compound **3.1** was followed on a Olympus Fluoview FV1000 confocal laser scanning biological microscope with a 4x objective. The excitation was performed at 488 nm with 15 % laser transmission. The analyses of the pictures was carried out with FV 10-ASW Version 03.00.02.00.

3.5 References

[1] L. Giannuzzi, D. Sedan, R. Echenique, D. Andrinolo, *Mar. Drugs* **2011**, *9*, 2164–2175.

[2] S. M. F. O. Azevedo, W. W. Carmichael, E. M. Jochimsen, K. L. Rinehart, S. Lau, G. R. Shaw, G. K. Eaglesham, *Toxicology* **2002**, *181*, 441–446.

[3] M. J. Pybus, D. P. Hobson, D. K. Onderka, **1986**, *22*, 449–450.

[4] H. W. Paerl, R. S. Fulton, P. H. Moisander, J. Dyble, *The Scientific World Journal* **2001**, *1*, 76–113.

[5] W. W. Carmichael, *J Appl Microbiol* **1992**, *72*, 445–459.

[6] Y. Ueno, S. Nagata, T. Tsutsumi, A. Hasegawa, M. F. Watanabe, H.-D. Park, G.-C. Chen, G. Chen, S.-Z. Yu, *Carcinogenesis* **1996**, *17*, 1317–1321.

[7] A. Ullah, *Anti-Cancer Agents in Med. Chem.* **2011**, *11*, 4–18.

[8] M. E. van Apeldoorn, H. P. van Egmond, G. J. A. Speijers, G. J. I. Bakker, *Mol. Nutr. Food Res.* **2007**, *51*, 7–60.

[9] I. Stewart, P. M. Webb, P. J. Schluter, G. R. Shaw, *Environ. Health* **2006**, *5*:6.

[10] P. Zeller, M. Clément, V. Fessard, *Toxicology* **2011**, *290*, 7–13.

[11] B. Mikalsen, G. Boison, O. M. Skulberg, J. Fastner, W. Davies, T. M. Gabrielsen, K. Rudi, K. S. Jakobsen, *J. Bact.* **2003**, *185,* 2774–2785.

[12] M. Welker, H. von Döhren, *FEMS Microbiol. Rev.* **2006**, *30*, 530–563.

[13] M. Namikoshi, K. L. Rinehart, R. Sakai, K. Sivonen, W. W. Carmichael, *J. Org. Chem.* **1990**, *55*, 6135–6139.

[14] M. F. Watanabe, S. Oishi, *Appl. Environ. Microbiol.* **1982**, *43*, 819–822.

[15] L. Pearson, T. Mihali, M. Moffitt, R. Kellmann, B. Neilan, *Mar. Drugs* **2010**, *8*, 1650–1680.

[16] E. Dittmann, B. A. Neilan, M. Erhard, H. von Döhren, T. Börner, *Mol. Microbiol.* **1997**, *26*, 779–787.

[17] T. Nishizawa, M. Asayama, K. Fujii, K. Harada, M. Shirai, *J. Biochem.* **1999**, *126*, 520–529.

[18] D. Tillett, E. Dittmann, M. Erhard, H. von Döhren, T. Börner, B. A. Neilan, *Chem. Biol.***2000**, *7*, 753–764.

[19] E. M. Rodríguez, J. L. Acero, L. Spoof, J. Meriluoto, *Water Res.* **2008**, *42*, 1744–1752.

[20] N. Gupta, S. C. Pant, R. Vijayaraghavan, P. V. L. Rao, *Toxicology* **2003**, *188*, 285–296.

[21] WHO Cyanobacterial toxins: Microcystin-LR in drinking water **2003**, 1–18.

[22] D. Barford, A. K. Das, M. P. Egloff, *Annu. Rev. Biophys. Biomol. Struct.* **1998**, *27*, 133–164.

[23] C. MacKintosh, K. A. Beattie, S. Klumpp, P. Cohen, G. A. Codd, *FEBS Lett.* **1990**, *264*, 187–192.

[24] W. W. Carmichael, *Sci. Am.* **1994**, *270*, 78–86.

[25] V. Christen, N. Meili, K. Fent, *Environ. Sci. Technol.* **2013**, *47*, 3378–3385.

[26] B. Žegura, I. Zajc, T. T. Lah, M. Filipič, *Toxicon* **2008**, *51*, 615–623.

[27] A. Campos, V. Vasconcelos, *Int. J. Mol. Sci.* **2010**, *11*, 268–287.

[28] A. Fischer, S. J. Hoeger, K. Stemmer, D. J. Feurstein, D. Knobeloch, A. Nussler, D. R. Dietrich, *Toxicol. Appl. Pharmacol.* **2010**, *245*, 9–20.

[29] V. F. Magalhães, M. M. Marinho, P. Domingos, A. C. Oliveira, S. M. Costa, L. O. Azevedo, S. M. F. O. Azevedo, *Toxicon* **2003**, *42*, 289–295.

[30] M. Lürling, *Limnology and Oceanography* **2003**, *48*, 2214–2220.

[31] T. S. Dao, L.-C. Do-Hong, C. Wiegand, *Toxicon* **2010**, *55*, 1244–1254.

[32] R. Ortiz-Rodríguez, T. S. Dao, C. Wiegand, *J. Exp. Biol.* **2012**, *215*, 2795–2805.

[33] J. Cazenave, D. A. Wunderlin, M. de Los Angeles Bistoni, M. V. Amé, E. Krause, S. Pflugmacher, C. Wiegand, *Aquat. Toxicol.* **2005**, *75*, 178–190.

[34] J. Goldberg, H. B. Huang, Y. G. Kwon, P. Greengard, A. C. Nairn, J. Kuriyan, *Nature* **1995**, *376*, 745–753.

[35] K. R. Shreder, Y. Liu, T. Nomanhboy, S. R. Fuller, M. S. Wong, W. Z. Gai, J. Wu, P. S. Leventhal, J. R. Lill, S. Corral, *Bioconjug. Chem.* **2004**, *15*, 790–798.

[36] M. Liu, H. Zhao, S. Chen, H. Yu, X. Quan, *Environ. Sci. Technol.* **2012**, *46*, 12567–12574.

[37] K. Harada, K. Tsuji, M. F. Watanabe, F. Kondo, *Phycologia* **1996**, *35***,** 83–88.

[38] M- D'Este, D. Eglin, M. Alini, *Carbohydr. Polym.* **2014**, *108*, 239–246.

[39] J. F. Blom, F. Jüttner, *Toxicon* **2005**, *46***,** 465–470.

[40] S. R. Pereira, V. M. Vasconcelos, A. Antunes, *FEBS J.* **2013**, *280*, 674–680.

[41] R. W. MacKintosh, K. N. Dalby, D. G. Campbell, P. T. Cohen, P. Cohen, C. MacKintosh, *FEBS Lett.* **1995**, *371*, 236–240.

[42] W. J. Fischer, S. Altheimer, V. Cattori, P. J. Meier, D. R. Dietrich, B. Hagenbuch, *Toxicol. Appl. Pharmacol.* **2005**, *203*, 257–263.

[43] M. Agrawal, S. Yadav, C. Patel, *Euro. J. Exp. Bio.* **2012**, *2*, 321–336.

[44] G. Nałęcz Jawecki, L. Szczęsny, D. S. J. Solecka, *Int. J. Environ. Sci. Tech.* **2011**, *8*, 687–694.

[45] F. Jüttner, J. Leonhardt, S. Möhren, *J. Gen. Microbiol.* **1983**, *129*, 407–412.

4

Structure Elucidation of Aeruginosin 828A

4.1 Introduction

Cyanobacteria produce various toxins with a great diversity for the different compound classes, whereby the majority are peptides or contain a peptide-like structure. Every year, new compounds are isolated and new biological activities are discovered. Some of the most potent toxins produced by cyanobacteria are the microcystins, which is one reason for the high attention for microcystin-producing organisms and therefore toxic cyanobacteria. The common genetic background of these species is the *myc* gene cluster, which is responsible for the toxin production.[1] The main purpose of the production of various microcystins is not clear yet, whereas an evolutionary protection against grazers and so also a biological advantage against non microcystin-producing cyanobacteria is likely. However, it was found, that *Planktothrix* with inactive *myc* gene cluster shows no disadvantages of growth in contrast to microcystin-producing strains. Another possibility is yet unknown peptides or group of peptides replacing microcystin in its biological role.[2]

In this regard, our cooperation partner (Esther Kohler, University of Zurich) examined, with HPLC-guided fractionation, the activity of six different *Planktothrix* strains against *Thamnocephalus platyurus* and detected an unknown chlorinated and sulphated toxic peptide. This toxin appeared to be from the aeruginosin family, as judged from its retention time, spectral properties and the preliminary MS-experiments.

Aeruginosins are produced by the cyanobacterial genus *Microcystis* and *Planktothrix*.[3] Aeruginosins show a great structural variety due to their synthesis through the NRPS pathway, as post-translational modification with sugar moieties, chlorine or sulphate substituents is also possible.[3,4] At the moment, more than 40 variants of this compound class are known, with the characteristic core structure containing the unusual amino acid 2-carboxy-6-hydroxyoctahydroindole (Choi) and hydroxyphenyllactic acid (Hpla) or lactic acid (Pla). In addition, the aeruginosins contain a variable hydrophobic amino acid (Leu, Ile, Phe, or Tyr) and an arginine derivative (**Figure 4.1**).[5]

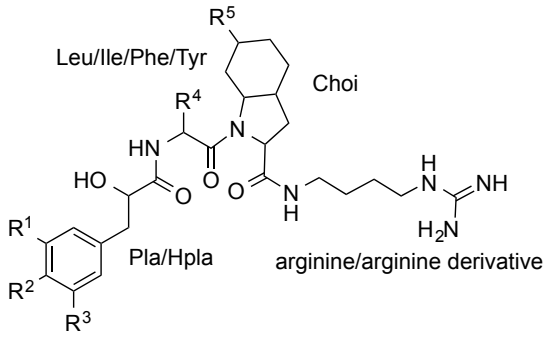

Figure 4.1. General structure of Aeruginosin

Characteristic for this class is its ability to inhibit trypsin-like serine proteases, especially trypsin and thrombin.[6-8] This is due to its high affinity for the catalytic pocket of the protease. Since thrombin participates in the blood coagulation cascade, aeruginosins might be used for treatment of thrombotic disorders.[9] Furthermore, certain compounds from that group show inhibitory activity against other proteases like papain.[9] Additionally, compounds with new biological activity are constantly isolated, like aerguniosin-865. This compound, containing for the first time an uronic acid and a fatty acid moiety, shows anti inflammatory activity through inhibition of the translocation of NF-κB to the cell nucleus.[10] Despite of this inhibition ability, no toxicity is so far linked to this compound class. This work discusses the structure elucidation of a newly isolated unknown chlorine and sulphate-containing aeruginosin.

4.2 Results and discussion

Our cooperation partner, Esther Kohler (University of Zurich), analysed the toxicity of six *Plankthothrix* strains. For that purpose, methanolic extractions of the cyanobacterial biomass followed by HPLC-guided fractionation was performed. The toxicity of these fractions was evaluated with acute toxicity assays against the crustacean *Thamnocephalus platyurus*. Further fractionation and toxicity screening lowered the number of highly toxic fractions down to twelve. Final investigations revealed the presence of three already known microcystins, seven unknown sulphated cyanopepotlins and ten sulphate and chlorine-containing aeruginosins. Interestingly, the last compound class associated with high toxicity, could only be found in four non- microcystin-producing cyanobacteria strains. With regard to that, a so far unknown member of the aeruginosin family, aeruginosin 828A, has been isolated from the *Plankthothrix rubescens* strain 91/1. In order to elucidate its structure, we obtained it in a pure form. HRMS experiments showed the putative molecular ions of *m/z* = 851.3019 $[M+Na]^+$ and *m/z* = 853.3003 $[M+Na]^+$, which correspond to a molecular formula of $C_{36}H_{53}{}^{35}ClN_6O_{12}SNa^+$ or $C_{36}H_{53}{}^{37}ClN_6O_{12}SNa^+$ respectively. The 749-fragment indicated the presence of a sulphate group. The characteristic isotopic pattern showed that the molecule was chlorinated (**Figure 4.2**).

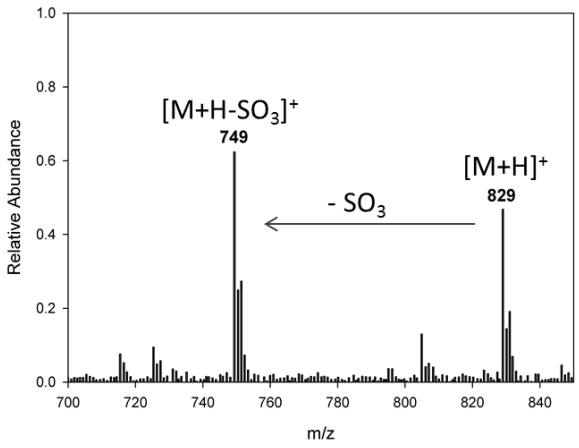

Figure 4.2. ESI mass spectrum of aeruginosin 828A (**4.1**)

Acid hydrolysis tests with aeruginosin 828A from *Plankthothrix rubescens* strain 91/1 showed that it contains a derivatized leucyl residue and no arginine. To investigate the C-H-network of the unknown toxin, a series of NMR experiments were carried out. The ^{1}H–NMR spectrum of aeruginosin 828A (**4.1**) revealed two sets of characteristic resonances for a peptide structure (amide protons in the range of 7.0 – 8.0 ppm and α-protons in the range 4.0 – 5.0 ppm) (**Spectrum 10**). The constitution of each peptide-component was assigned using COSY, HSQC, HMBC and NOESY experiments. The measured chemical shifts are reported in **Table 4.1**. 2D-NMR experiments and comparison with the literature data led to the identification of the following building blocks: phenyllactic acid (Pla); chloroleucine (Cleu); a 2-carboxy-6-(4'-sulfo-xylosyl)-octahydroindole moiety (Choi) and a 3-aminoethyl-1-*N*-amidino-Δ^3-pyrroline moiety (Aeap). All this classified the compound as a member of the aeruginosin family (**Figure 4.3**).

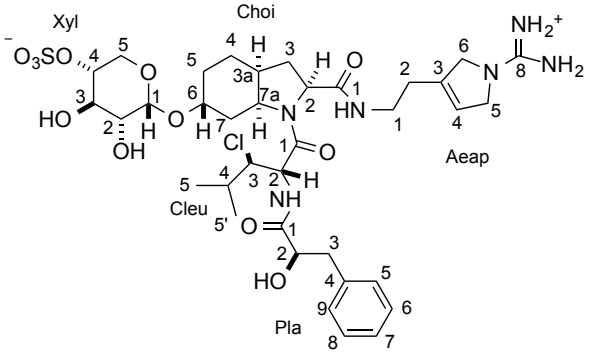

Figure 4.3. NMR assignments of aeruginosin 828A (**4.1**)

The position of the chlorine atom in Cleu was determined based on the characteristic chemical shift of the corresponding Cβ atom of the Leu moiety (δ_c = 68.6 ppm).[11] The presence of a xylose residue was suggested by the low-field shifted carbon atoms ($\delta_c \approx 70$ ppm), which indicated the presence of oxygen substituents.

Table 4.1. ^{1}H and ^{13}C chemical shifts of aeruginosin 828A in DMSO (700MHz, DMSO-d6, 298K)

Unit	C/H no.	δ_H (*J* in Hz)	δ_C	HMBC[a]	NOE
Xyl	1eq	4.94 d (3.8)	95.0	Xyl 2,3,5, Choi 6	Choi 6, Xyl 2,4',7,7'
	2ax	3.28 m	71.8	Xyl 3,5	Xyl 1,4
	3ax	3.57 ddd (2.6, 9.0, 9.1)	71.4	Xyl 2,4,5	Xyl 4,5ax, 3-OH
	4ax	3.93 ddd (5.8, 9.1, 10.6)	74.7	Xyl 3,5	Xyl 1,2,5ax,5eq,3-OH
	5ax	3.36 dd (10.6, 10.7)	59.3	Xyl 1,3,4	Xyl 4,5eq
	5eq	3.67 dd (5.8, 10.7)		Xyl 1,3,4	Xyl 4,5ax
	2-	4.41 (7.3)	-	Xyl 1,2	-
	3-	4.96 (2.6)	-	Xyl 2,3,5	Xyl 3,4
Choi	1	-	171.	-	-
	2	4.18 dd (9.4, 8.2)	59.5	Choi 1,3	Aeap NH, Choi 3,3',3a,7
	3	2.01 ddd (12.6, 7.3, 7.3)	30.5	Choi 3a,7a	Choi 2,3a,3',4',6,7',7a
	3'	1.81 ddd (12.6, 12.6, 9.7)	-	Choi 1,2,3a	Choi 2,3,3a,4',5',7
	3a	2.25 m	35.6	Choi 3,4,5,7,7a	Choi 2,3',4',7
	4	2.14 m	19.1	Choi 3,3a,5	Choi 3a,4',5,5'
	4'	1.48 m	-	Choi 5,6,7a	Choi 3a,4,5',6
	5	1.49 m	24.4	Choi 6,7a	Choi 6,Cleu 2
	5'	1.54 m	-	-	Choi 3a,4,5,6,7'
	6	3.83 m	68.4	-	Choi 5,5',7,7', Xyl 5ax
	7	1.58 dd (11.9, 12.9)	28.4	Choi 7a	Cleu 2, Choi 6,7'
	7'	2.25 m	-	Choi 5,7a	Choi 2,6,7',7a, Cleu 2
	7a	4.32 ddd (11.9, 6.4, 6.4)	54.1	Choi 2,3,3a,7, Cleu	Choi 4,4',7,7', Cleu 2,5
Pla	1	-	172.	-	-
	2	4.18 (br)	71.5	-	Pla 3, 3'
	3	2.79 dd (14.0, 7.6)	39.7	Pla 1,2,4,5,9	Pla 2,3'
	3'	2.96 dd (14.0, 3.7)	-	Pla 1,2,4,5,9	Pla 2,3
	4	-	137.	-	-
	5,9	7.23 m	129.	Pla 3,5,7,9	Pla 3,3',7
	6,8	7.26 m	127.	Pla 4,6,8	Pla 5,7,9
	7	7.18 m	125.	Pla 5,9	-
	2-	-	-	-	-
Cleu	1	-	167.	-	-
	2	4.93 dd (10.7,8.7)	50.9	Cleu 1,3, Pla 1	Cleu 3,4,5, Choi 7a,7,7'
	3	4.00 dd (10.7, 1.8)	68.6	Cleu 1,2,4,5,5'	Cleu 2,4,5'
	4	1.71 dsept. (6.6, 1.8)	27.3	Cleu 5,5'	Cleu 2,3,5
	5	0.87 3H, d (6.6)	15.3	Cleu 3,4,5'	Cleu 2,3,4 Choi 7',7a
	5'	0.86 3H, d (6.6)	20.6	Cleu 3,4,5	
	NH	7.68 d (8.7)	-	-	Cleu 3
Aeap	1	3.16 dddd (13.0, 6.5, 6.5,	36.3	Aeap 2,3, Choi 1	Aeap 2,4,5,6,NH, Choi 2
	1'	3.23 dddd (13.0, 6.5, 6.5,	-	Aeap 2,3, Choi 1	
	2	2.25 2H, m	28.1	Aeap 1,3,4,6	Aeap 1,1',4,5,6,NH
	3	-	136.	-	-
	4	5.61 t (1.6)	119.	Aeap 2,3,5,6	Aeap 1,1',2,5,6,NH
	5	4.07 2H, d (1.6)	53.6	Aeap 3,4	Aeap 1,1',2,4
	6	4.07 2H, s	54.9	Aeap 3,4	
	NH	8.00 dd (5.7, 5.7)	-	Aeap 1, Choi 1	Aeap 1,1',2,4,5,6, Choi
	8	-	154.	-	-

[a]HMBC correlations are given from proton(s) stated to the indicated carbon atom

The position of the sulphate group was established by the typical chemical shift of Xyl C-4 (δ_c = 74.7 ppm)[12], as well as by the COSY correlations between H-2 (δ_H = 3.28 ppm) and Xyl OH-2 (δ_H = 4.41 ppm), and Xyl H-3 (δ_H = 3.57 ppm) and Xyl OH-3 (δ_H = 4.96 ppm) (**Figure 4.4**). The relative configuration of the carbohydrate moiety was assigned by the NOESY spectrum and *J*-coupling constants (**Figure 4.4**).

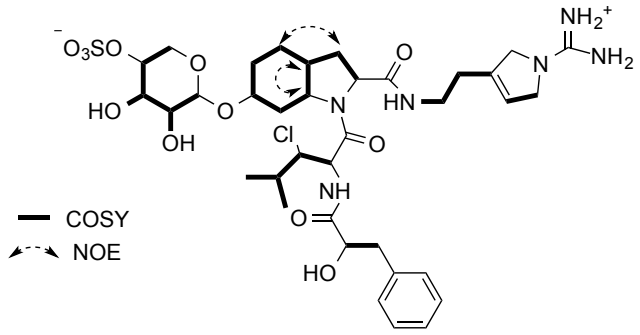

Figure 4.4. Key COSY and NOE correlations in aeruginosin 828A (**4.1**)

The α-anomer of the sugar moiety was identified by its small coupling constant (*J* = 3.8 Hz), which results from the (+)-*sc* arrangement between Xyl H-1 to Xyl H-2 (**Figure 4.5**).

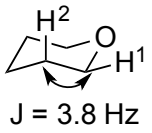

Figure 4.5. J coupling between Xyl H-1 to Xyl H-2

The configuration of the Choi moiety was determined using the relevant NOE correlations between Choi H-3' (δ_H = 1.81 ppm) and Choi H-4' (δ_H = 1.48 ppm), as well as Choi H-4 (δ_H = 2.14 ppm) and Choi H-3a (δ_H = 2.25 ppm), Choi H-3 (δ_H = 2.01, 1.81 ppm) to Choi H-3a (δ_H = 2.25 ppm) and, additionally, to Choi H-6 (δ_H = 3.83 ppm) and Choi H-7' (δ_H = 2.25 ppm) (**Table 4.1**). The configuration of the C-6 stereogenic center of Choi was assigned on the basis of the line width of its signal (total ~ 16 Hz), which implies that no trans-diaxial relationship of the Choi H-6 to its coupling partners is present (**Figure 4.6, A**).

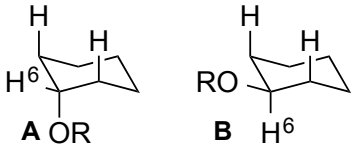

Figure 4.6. Possible configurations of Choi C-6
A: no trans-diaxial relationship of H-6
B: trans-diaxial relationship of H-6

Due to the lack of commercially available, authentic standards for the Cleu and Choi residues, we did not perform hydrolysis and subsequent analysis on chiral stationary phases. Nevertheless, the syntheses of these entities are currently being carried out in our laboratory, which would allow us to confirm the hypothesized configuration. The observed NOE between Choi H-3a and Choi H-7a supports the relative *cis*-configuration, which is further substantiated by numerous literature examples of identical configurations (**Figure 4.7**).

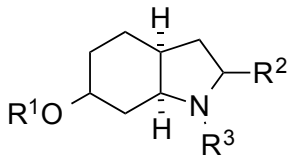

Figure 4.7. *Cis*-configuration of Choi

The tentatively assigned relative configuration of aeruginosin 828A (**4.1**) is further corroborated by comparison with data reported for the structurally similar aeruginosin 205B (**Table 4.2**).

Table 4.2. ^{1}H and ^{13}C chemical shifts of aeruginosin 828A in DMSO (700MHz, DMSO-d6, 298K) in comparison to ^{1}H and ^{13}C chemical shifts of aeruginosin 205B as described by Hanessian et al.[13]

Aeruginosin 828A				Natural aeruginosin 205B	
Unit	C/H no.	δ_H	δ_C	δ_H	δ_C
Xyl	1eq	4.94	95.0	4.93	95.2
	2ax	3.28	71.8	3.28	72.1
	3ax	3.57	71.4	3.58	71.7
	4ax	3.93	74.7	3.93	74.9
	5ax	3.36	59.3	3.37	59.6
	5eq	3.67		3.67	
	2-OH	4.41	-		
	3-OH	4.96	-		
Choi	1	-	171.1		
	2	4.18	59.5	4.19	59.8
	3	2.01	30.5	2.02	30.8
	3'	1.81	-	1.84	
	3a	2.25	35.6	2.24	35.8
	4	2.14	19.1	2.13	19.4
	4'	1.48	-	1.48	
	5	1.49	-	1.54	24.7
	5'	1.54	24.4	1.54	
	6	3.83	68.4	3.83	68.7
	7	1.58	28.4	1.59	28.7
	7'	2.25	-	2.23	
	7a	4.32	54.1	4.23	54.2
Pla	1	-	172.5		172.4
	2	4.18	71.5	4.19	71.9
	3	2.79	39.7	2.78	40.0
	3'	2.96	-	2.93	
	4	-	137.9	-	137.9
	5,9	7.23	129.5	7.23	129.6
	6,8	7.26	127.7	7.25	127.9
	7	7.18	125.8	7.18	126.0
	2-OH	-	-	-	-
Cleu	1	-	167.4	-	167.3
	2	4.93	50.9	4.9	51.1
	3	4.00	68.6	3.98	68.9
	4	1.71	27.3	1.69	27.5
	5	0.87	15.3	0.88	15.4
	5'	0.86	20.6	0.85	20.8
	NH	7.68	-	7.62	
Aeap	1	3.16	36.3		
	1'	3.23	-		
	2	2.25	28.1		
	3	-	136.1		
	4	5.61	119.0		
	5	4.07	53.6		
	6	4.07	54.9		
	NH	8.00	-		
	8	-	154.9		

The difference between aeruginosin 828A and aeruginosin 205B is the presence of an agmatine moiety instead of the Aeap residue and shows almost identical ^{1}H and ^{13}C shifts (maximal shift 0.3 ppm in the ^{1}H-NMR and 0.4 ppm in the ^{13}C-NMR spectra). An (*R*)-configuration for the C-2 of Pla and C-3 of Cleu building blocks, as well as the (*S*)-configuration for the C-2 of Cleu was tentatively assigned. We are aware that its final structure elucidation will require the use of total chemical synthesis. To validate such preliminary assignments, the synthesized aeruginosin 828A with the known configuration will be used for direct comparison to the natural product.

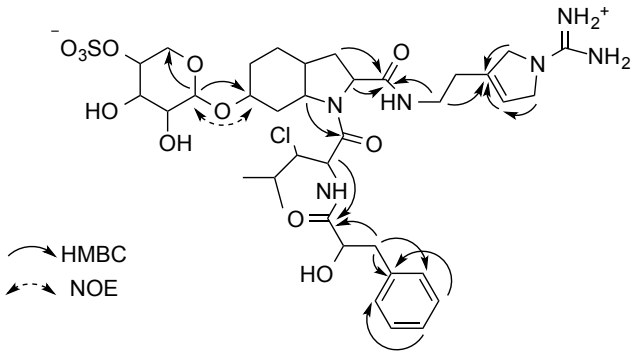

Figure 4.8. Key HMBC and NOE correlations in aeruginosin 828A (**4.1**)

The assembly of the different fragments was established by HMBC and NOESY experiments (**Figure 4.8**). The linkage between central Choi and the Cleu was suggested by the HMBC correlation between Choi H-7α (δ_H = 4.32 ppm) and Cleu C-1 (δ_c = 167.4 ppm). In a similar fashion, the connection between the Choi and the Aeap residues was determined by the coupling between Aeap H-1 and H-1' (δ_H = 3.16 ppm and 3.23 ppm) and Choi C-1 (δ_c = 171.1 ppm). The HMBC correlation from Cleu H-2 (δ_H = 4.93 ppm) to Pla C-1 (δ_c = 172.5 ppm) demonstrated the connection of these moieties. In addition, the connection of the Xylose unit with the Choi moiety was elucidated by the NOE correlation of the Xyl H-1 (δ_H = 4.94 ppm) to Choi H-6 (δ_H = 3.83 ppm) as well as an HMBC correlation.

Interestingly, our cooperation partner described for aeruginosin 828A not only thrombin (IC_{50} = 21.8 nM) and trypsin (IC_{50} = 112 nM) inhibition ability, as it exhibits activity towards *Thamnocephalus platyurus* (LC_{50} = 22.4 µM). This is the first time such activity was observed within this compound class. Additional toxicity tests were carried out with aeruginosins containing only sulphate or neither sulphate, nor

chlorine moiety. These tests showed, that aeruginosins shows toxicity against aquatic organisms only if a sulphate group and a chlorine are present. Intriguingly, this toxic sulphate and chlorine-containing compound class was only found in microcystin-deficient strains. These interesting findings indicate, that these molecules can be a substitute for microcystins.

4.3 Conclusion

The structure of aeruginosin 828A isolated from *P. rubescens* strain 91/1 was elucidated. The presence of phenyllactic acid (Pla), chloroleucine (Cleu), 2-carboxy-6-(4'-sulfo-xylosyl)-octahydroindole residue (Choi) and a 3-aminoethyl-1-*N*-amidino-Δ^3-pyrroline moiety (Aeap) was confirmed by 2D-NMR experiments. These supports that the compound as a member of the aeruginosin family. It exhibits trypsin and thrombin inhibitory activity in low nanomolar concentrations and shows toxicity against *Thamnocephalus platyurus* comparable to that of microcystins. This compound was found only in microcystin-deficient cyanobacterial strains, which makes us believe it has a similar function to compensate the lack of microcystins.

4.4 Methods

^{1}H-NMR spectra were recorded on a Bruker Avance III Ultrashield 600MHz with a 5mm BBFO+ plus SP probe or a Bruker Avance III Ascend 700MHz with a 5mm TCI (H-C/N-D) cryo probe spectrometers at room temperature. Chemical shifts (δ-values) are reported in ppm, spectra were calibrated related to solvent`s residual proton chemical shift (DMSO, δ = 2.50). Multiplicity is reported as follows: s = singlet, bs = broad singlet, d = doublet, dd = doublet of doublet, t = triplet, m = multiplet. The coupling constant *J* is specified in Hz. HRMS spectra were obtained on a Bruker maXis 4G with ESI in positive mode.

4.5 References

[1] T. Nishizawa, A. Ueda, M. Asayama, K. Fujii, K. Harada, K. Ochi & M. Shirai, *J Biochem.* **2000**, *127*, 779–789.

[2] V. Ostermaier, R. Kurmayer, *Microb Ecol* **2009**, *58*, 323–333.

[3] K. Ishida, M. Welker, G. Christiansen, S. Cadel-Six, C. Bouchier, E. Dittmann, C. Hertweck, N. Tandeau de Marsac, *Appl. Environ. Microbiol.* **2009**, *75*, 2017–2026.

[4] K. Ishida, G. Christiansen, W. Y. Yoshida, R. Kurmayer, M. Welker, N. Valls, J. Bonjoch, C. Hertweck, T. Börner, T. Hemscheidt, *et al.*, *Chemistry & Biology* **2007**, *14*, 565–576.

[5] S. Elkobi-Peer, R. K. Singh, T. M. Mohapatra, S. P. Tiwari, S. Carmeli, *J. Nat. Prod.* **2013**, *76*, 1187–1190.

[6] K. Ersmark, J. R. Del Valle, S. Hanessian, *Angew. Chem. Int. Ed.* **2008**, *47*, 1202–1223.

[7] M. Murakami, K. Ishida, T. Okino, Y. Okita, H. Matsuda, *Tetrahedron Lett.* **1995**, *36*, 2785–2788.

[8] H. J. Shin, H. Matsuda, M. Murakami, K. Yamaguchi, *J. Org. Chem.* **1997**, *62*, 1810–1813.

[9] K. Ersmark, J. R. Del Valle, S. Hanessian, *Angew. Chem. Int. Ed.* **2008**, *47*, 1202–1223.

[10] A.Kapuścik, P.Hrouzek, M. Kuzma, S. Bártová, P. Novák, J. Jokela, M. Pflüger, A. Eger, H. Hundsberger, J.Kopecký, *ChemBioChem* **2013**, *14*, 2329–2337.

[11] N. Valls, M. Borregán, J. Bonjoch, *Tetrahedron Lett.* **2006**, *47*, 3701–3705.

[12] A. Rahman (**2003**). Studies in Natural Products Chemistry. Elsevier Science B. V., Amsterdam.

[13] S. Hanessian, X. T. Wang, K. Ersmark, J. R. Del Valle, E. Klegraf, *Org. Lett.* **2009**, *11*, 4232–4235.

5

Chemical Modification of Cyanopeptolin 1020

5.1 Introduction

Cyanopeptolins (CP) are an abundant, but not very well studied group of cyclic depsipeptides deriving from cyanobacteria. They are mainly isolated from the genus *Anabaena*, *Microcystis* and *Planktothrix*, as not all strains from the same family are able to produce these toxins.[1] There are also cyanobacterial strains, which are able to synthesize more than one variant of this compound class. This is the case for *Microcystis* HUB08B03, where 13 different cyanopeptolins variants were found within the same strain.[2] Usually other toxic molecules, mainly microcystins, are also produced along with these toxins.[3] As microcystins, cyanopeptolins are synthesized *via* the non-ribosomal pathway and show, due to this, a great structural variety.[4] Their core structure contains seven amino acids, six of them constitute a cyclic system.[4] Positions R^1 and R^2 show high structural variability of the proteinogenic amino acids (e.g. Arg, Lys, Phe). In contrast, position R^3 is restricted to Ile or Val (**Figure 5.1**).[4]

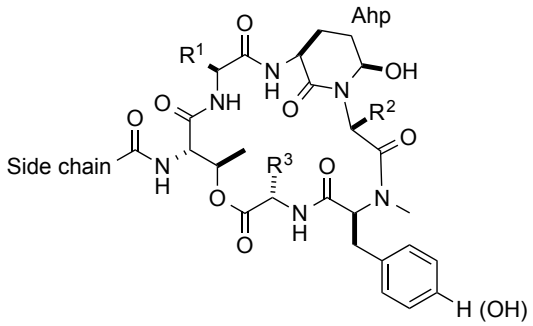

Figure 5.1. General structure of cyanopeptolin

The main structural diversity is observed in the side-chain, where different amino acids or non-amino acid constituents (e.g. fatty acid) can be incorporated.[5] The common structural elements that cyanopeptolin variants share are the unusual amino acid 3-amino-6-hydroxy-2-piperidone (Ahp) and an ester connectivity between the β-OH group of Thr and the C-terminal amino acid.[3,4] Concerning biological activity, cyanopeptolins are protease-inhibitors, active on serine or threonine-proteases, such as chymotrypsin or trypsin.[6,7] One member of this compound class is cyanopeptolin 1020 (CP1020), which has been isolated in our group in 2010 from a *Microcystis* strain (**Figure 5.2**).[8]

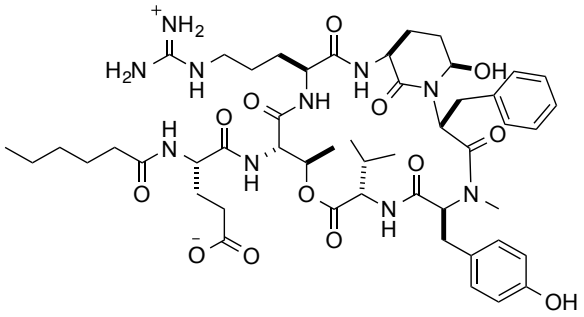

Figure 5.2. Structure of cyanopeptolin 1020

This highly potent toxin inhibits trypsin with an inhibitory concentration in the picomolar range, and human kallikrein and factor Xia with an inhibitory concentration in the nanomolar range.[8] Furthermore, it shows toxic activity against the freshwater crustacean *Thamnocephalus playturus* with an LC_{50} value of 8.8 µM, which is in the same range as the microcystins. Recent studies on global transcriptome analysis in *Danio rerio* embryos showed that CP1020 acts on DNA-damage recognition and repair, circadian rhythm, and response behaviour to light. [9] These findings showed, that CP1020 causes DNA-damage and has neurotoxic properties.[9] This peptide consists of eight residues: Glu, Thr, Arg, Ahp, Phe, *N*-Me-Tyr, Val, and hexanoic acid, as the Glu residue is not involved in enzyme binding as showed by a model structure.[8] As CPs and particularly CP1020 have not been investigated in detail, the goal of this study was to develop a labelling procedure for the carboxylic acid moiety of CP1020.

5.2 Results and discussion

5.2.1 Synthesis of modified CP1020

Cyanopeptolin1020, isolated from *Microcystis aeruginosa* UV-006, was used for the reactions. The limited amount of the toxin presented a major challenge to its modification. Also the unknown extinction coefficient of the toxin, which is especially required for yield determination, posed a problem. Our strategy was to find an efficient protocol for labelling the Glu function *via* amide bond formation. Another obstacle was the sensitivity of the toxin as for example, the ester function on the threonine-residue easily eliminates to form a double bond and the free carboxylic acid (**Figure 5.3**).

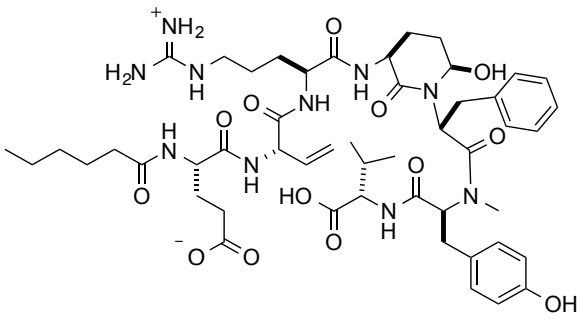

Figure 5.3. Undesired degradation product of CP1020

A careful screen identified DMSO as the best solvent for CP1020. The toxin, however, was not stable in that solvent when stored at -20 °C, which necessitated to work with small freshly prepared aliquots (50 µg). We first treated CP1020 with 10 % pyridine in DMF, DCC (1.1 eq.), 1-hydroxybenzotriazole (1.5 eq.) and 5-((2-aminoethyl)amino)naphthalene-1-sulfonic acid (1.5 eq.) for eight hours, however, no product formation was observed. The use of a catalytic amount of DMAP did not improve the reactivity. Then, another standard peptide coupling procedure was attempted: 5-((2-aminoethyl)amino)naphthalene-1-sulfonic acid (1.5 eq.), NEt_3 and TBTU (1.2 eq.). However, these conditions gave a complex reaction mixture. These results could be due to the instability of the fluorophore. For this reason, Alexa 488 cadaverine sodium salt was used, known for its higher stability. A first attempt using Alexa 488 cadaverine sodium salt (1.1 eq.), NEt_3 (2 eq.) and TBTU (1.1 eq.) was undertaken. To follow this reaction, a sample was taken after one hour and analysed by LC-MS. It was observed that the starting material

was fully converted, but no peak with the desired product mass could be detected. The change of the coupling reagent to HATU (1.1 eq.) did not influence the reactivity. Also with pyridine (2 eq.), HATU (1.1 eq.) and Alexa 488 cadaverine sodium salt (1.1 eq.) no desired product mass could be detected. One problem was supposed to be the size of the fluorophore that might be unable to access the Glu position in CP1020. Furthermore, an intermolecular reaction between the arginine and the activated carboxylic acid is possible. To exclude these hypotheses, a small and highly nucleophilic amine was chosen. In this context, benzylamine, HATU and pyridine were used in excess. After one hour, no starting material could be observed, neither desired product formation. A change to NEt_3 did not lead to better results. These observations suggested, that CP1020 might be sensitive towards NEt_3. CP1020 treated with excess of NEt_3 showed absence of the starting material, but rather the presence of another species of m/z 467 which Portmann previously identified this fragment by MS-MS studies as Hex-Glu-didehydrobutyrate-Arg.[10] This fragment is formed by an elimination reaction at the threonine function and cleavage of the peptide bond at Arg. We believe that the use of a base together with CP1020 enhances this undesired side-reaction. In this context, the use of a bulkier base was expected to overcome the problem. Two test reactions with Hünig's base (*N,N*-diisopropylethylamine) or DBU identified the former as a good candidate for the coupling reaction. Attempts with Hünig's base, benzylamine and HATU or TBTU did not yield the desired product. However, a combination of Hünig's base, benzylamine and EDC resulted in formation of a species with the desired mass. A coumarin-derivative of the toxin was also synthesized using the same protocol (**Figure 5.4**).

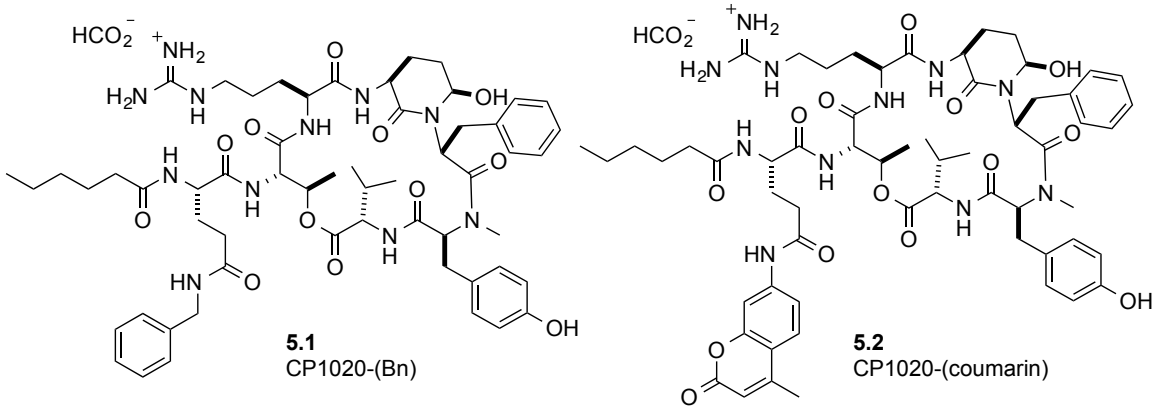

Figure 5.4. Derivatization of CP1020

Unfortunately, the obtained products were rather unstable, as decomposition was observed directly after purification. The coumarin derivative **5.2** was particularly unstable and its identity was only supported by MS.

5.5 Conclusion

Derivatization of CP1020 by a variety of conditions proved to be difficult and inefficient, mainly due to the instability of the toxin. Partial success was achieved with Hünig's base and EDC. The resulting species, however, were quite labile and no further biological tests could be performed. A more detailed screening of coupling conditions, tag moieties, and purification strategies is required for an increased stability of the products.

5.4 Methods

5.4.1 General

All chemicals were purchased from Sigma-Aldrich Co., were of analytical grade and freshly distilled before use. HPLC purifications of the functionalized CP1020 were performed on a Dionex P-680 HPLC System with a Phenomenex Gemini C18 5µ (250 mm x 4.6 mm) column or a Phenomenex Gemini C18 5µ (150 mm x 4.6 mm) column using a linear gradient: 5 % to 100 % CH_3CN in 0.1 % Formic acid/H_2O over 40 minutes at a flow rate of 1 mL/min. As ionization method electrospray ionization was used. HRMS spectra were obtained on a Bruker maXis 4G with ESI in positive mode. MS-MS experiments were obtained on a Bruker Esquire 3000 with ESI in positive mode.

5.4.2 Cell culturing, extraction and isolation

Microcystis aeruginosa UV-006 was cultivated in 500mL Falcon tubes in 200 mL mineral medium at 25 °C with 12 h light and night cycle.[11] The resulting biomass was harvested every three months with a 6K15 centrifuge (Sigma), freezed and stored at -20 °C. To obtain pure CP1020 without methylated product, the cyanobacteria were suspended in 20 mL of 60% acetonitrile per 1 g biomass and sonicated for 10 min (Branson 2510). The resulting homogenous mixture was centrifuged for 15 min at 25000 x g and the supernatants were combined and evaporated in a rotarory evaporator (Büchi, Switzerland). The residue was dissolved in 60 % acetonitrile and prepurified on a C_{18} SPE cartridge (10 g, Supelco). The crude mixture was eluted with 80 % acetonitrile (500 mg biomass afforded 15 mg crude extract), concentrated and applied on a Dionex P-680 HPLC System with a Phenomenex Gemini-NX C18 5 µ (75 mm x 21.2 mm) column using a linear gradient: 5 % to 100 % CH_3CN in 0.1 % Formic acid/H_2O over 40 minutes at a flow rate of 5 mL/min for further purification. For removal of the formic acid a final purification step was performed on a C_{18} SPE cartridge (500 mg, Supelco) starting with a first washing step with water to remove the acid and a final elution step with 80 % acetonitrile. After removal of all volatiles and lyophilisation pure CP1020 (900 µg from 15 mg crude extract) was afforded as a white solid. HPLC: t_R = 14.4 min; MS (ESI): *m/z* = 1021.5 $[M+H]^+$

5.4.3 Synthesis of modified CP1020

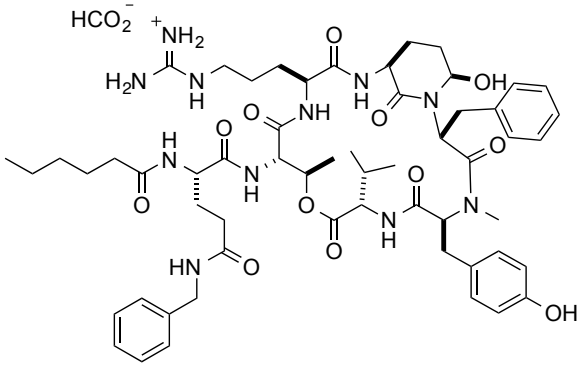

CP1020-(Bn), (5.1): Compound **5.1** was synthesized starting from CP1020 dissolved in DMSO (50 µg, 0.05 µmol). Hünig's base, EDC and benzylamine were added in excess. The mixture was stirred for 1.5 h at room temperature. Purification by HPLC afforded **5.1** as a white solid. (Due to the missing extinction coefficient no yield can be reported) HPLC: t_R = 17.9 min; HRMS-ESI: calcd. for $C_{57}H_{80}N_{11}O_{12}^{+}$ $[M+H]^{+}$: 1110.5982; found: 1110.5982.

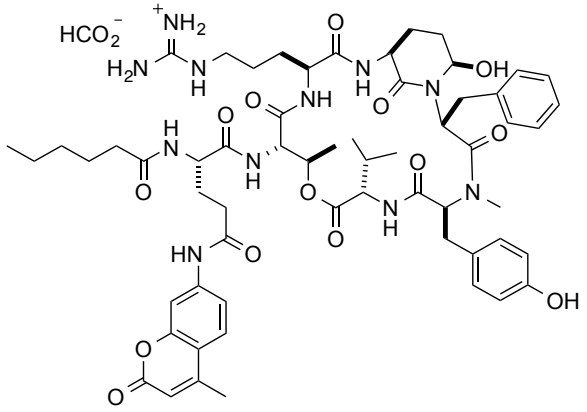

CP1020-(coumarin), (5.2): Compound **5.2** was synthesized starting from CP1020 dissolved in DMSO (50 µg, 0.05 µmol). Hünig's base, EDC and 7-amino-4-methylcoumarin were added in excess. The mixture was stirred for 1.5 h at room temperature. Purification by HPLC afforded **5.2** as a white solid. (Due to the missing extinction coefficient no yield can be reported) HPLC: t_R = 11.8 min; MS-ESI: calcd. for $C_{60}H_{81}N_{11}O_{14}^{2+}$ $[M+H+H]^{2+}$:589.2; found: 589.2. (Due to the high instability of the compound no HRMS could be recorded)

5.5 References

[1] M. Welker, H. Döhren, *FEMS Microbiol. Rev.* **2006**, *30*, 530–563.

[2] O. Czarnecki, M. Henning, I. Lippert, M. Welker, *Environ. Microbiol.* **2006**, *8*, 77–87.

[3] C. Martin, L. Oberer, T. Ino, W. A. König, M. Busch, J. Weckesser, *J. Antibiot.* **1993**, *46*, 1550–1556.

[4] T. B. Rounge, T. Rohrlack, A. Tooming-Klunderud, T. Kristensen, K. S. Jakobsen, *Appl. Environ. Microbiol.* **2007**, *73*, 7322–7330.

[5] J. Weckesser, C. Martin, C. Jakobi, *System. Appl. Microbiol.* **1996**, *19*, 133–138.

[6] J. F. Blom, H. I. Baumann, G. A. Codd, F. Jüttner, 2006, *Arch. Hydrobiol.* **2006**, *167*, 547–559.

[7] B. Bister, S. Keller, H. I. Baumann, G. Nicholson, S. Weist, G. Jung, R. D. Süssmuth, F. Jüttner, *J. Nat. Prod.* **2004**, *67*, 1755–1757.

[8] K. Gademann, C. Portmann, J. F. Blom, M. Zeder, F. Jüttner, *J. Nat. Prod.* **2010**, *73*, 980–984.

[9] S. Faltermann, S. Zucchi, E. Kohler, J. F. Blom, J. Pernthaler, K. Fent, *Aquat. Toxicol.* **2014**, *149*, 33–39.

[10] C. Portmann (2010). Biologically active secondary metabolites from cyanobacteria. Ph.D. Thesis. École Polytechnique Fédérale de Lausanne.

[11] F. Jüttner, J. Leonhardt, S. Möhren, *J. Gen. Microbiol.* **1983**, *129*, 407–412.

6

Conclusion

6. Conclusion

The present work addresses important questions concerning the structure, modification and biological activity of a group of secondary metabolites, produced by cyanobacteria. The detailed investigation of the chemistry and toxicity of MC-LR and CP1020 (isolated from *Microcystis aeruginosa* UV-006) and the structure elucidation of an unknown toxin isolated from *Plankthothrix rubescens* are key elements of this work.

As only limited amounts of microcystin-LR were available for testing, a method for efficient labelling of the arginine-containing peptides was developed. Various peptides were prepared and applied to different syntheses strategies. An established method was finally tested with several substrates in order to detect limitations. Future work will concentrate on elaborating the method for peptides containing as well cysteine-residues.

The new method, initially tested on model peptides, was applied to modification of microcystin-LR. Fluorescent, biotin and diazirine derivatives were synthesized and tested to assess whether the biological activity of the parent compound had been retained. Enzyme phosphatase 2A inhibition assays, acute toxicity assays and cell viability assays showed maintained activity of the derivatives. Further tests in *Danio rerio* and *Daphnia magna* will be performed with fluorescent microcystin-LR by our cooperation partner (Susanne Faltermann, University of Applied Sciences and Arts Northwestern Switzerland) to answer open questions regarding uptake, distribution, accumulation and excretion of microcystin-LR.

The structure of a newly isolated toxin [aeruginosin 828A] from the *Plankthothrix rubescens* strain 91/1 was elucidated using NMR studies and MS-characterization. This compound is a member of the aeruginosin family, it contains phenyllactic acid (Pla), chloroleucine (Cleu), a 2-carboxy-6-(4'-sulfo-xylosyl)-octahydroindole moiety (Choi) and a 3-aminoethyl-1-*N*-amidino-Δ^3-pyrroline moiety (Aeap). Toxicity towards the aquatic organism, *Thamnocephalus platyurus*, was proven in a biological study

for the first time. In the future, further *in vivo* studies in *Daphnia magna* will be conducted to investigate the mode of action.

A new approach towards the modification of the toxin cyanopeptolin 1020 was achieved and a benzylamine and a fluorescent derivative were synthesized. Although the target modified species were detected by MS-techniques and isolated, further studies were not possible, due to the instability of the modification products. Additional tests in that direction would bring us one step closer to complete understanding of the function of the fascinating compound class. In the future, a more detailed screening of coupling conditions, tag moieties, and purification strategies will be performed.

7

Appendix

7.1 Chromatograms

Chromatogram 1. HPLC trace of Bz-Arg(Dansyl)-OMe (**2.1)**

Chromatogram 2. HPLC trace of Bz-Arg(*N*-succinimid)-OEt (**2.2**)

Chromatogram 3. HPLC trace of Boc-Arg(*N*-succinimid)-OH (**2.3**)

Chromatogram 4. HPLC trace of *N*-Ac-Arg(Alexa488)-OH (**2.4**)

Chromatogram 5. HPLC trace of *N*-Ac-Arg(6-FAM)-OH (**2.5**)

Chromatogram 6. HPLC trace of *N*-Ac-Arg(coumarin)-OH (**2.6**)

Chromatogram 7. HPLC trace of *N*-Ac-Gly-Val-Phe-Arg-Gly-OH (**2.7**)

Chromatogram 8. HPLC trace of *N*-Ac-Gly-Val-Glu-Phe-Arg-Gly-OH (**2.8**)

Chromatogram 9. HPLC trace of *N*-Ac-Gly-Lys-Phe-Arg-Gly-OH (**2.9**)

Chromatogram 10. HPLC trace of *N*-Ac-Gly-Phe-Arg-Arg-Gly-OH (**2.10**)

Chromatogram 11. HPLC trace of *N*-Ac-Gly-Phe-Val-Arg-Gly-Val-Gly-OH (**2.11**)

Chromatogram 12. HPLC trace of *N*-Ac-Gly-Val-Arg-Phe-Ser-Gly-OH (**2.12**)

Chromatogram 13. HPLC trace of *N*-Ac-Gly-Val-Cys-Arg-Phe-Gly-OH (**2.13**)

Chromatogram 14. HPLC trace of *N*-Ac-Gly-Phe-His-Ala-Arg-Gly-OH (**2.14**)

Chromatogram 15. HPLC trace of *N*-Ac-Gly-Val-Dha-Arg-Phe-Gly-OH (**2.15**)

Chromatogram 16. HPLC trace of *N*-Ac-Gly-Val-Phe-Arg(6-FAM)-Gly-OH (**2.16**)

Chromatogram 17. HPLC trace of *N*-Ac-Gly-Val-Glu-Phe-Arg(6-FAM)-Gly-OH (**2.17**)

Chromatogram 18. HPLC trace of *N*-Ac-Gly-Val-Arg(6-FAM)-Phe-Ser-Gly-OH (**2.18**)

Chromatogram 19. HPLC trace of *N*-Ac-Gly-Phe-His-Ala-Arg(6-FAM)-Gly-OH (**2.19**)

Chromatogram 20. HPLC trace of *N*-Ac-Gly-Phe-Arg(6-FAM)-Arg(6-FAM)-Gly-OH (**2.20**)

Chromatogram 21. HPLC trace of *N*-Ac-Gly-Phe-Val-Arg(6-FAM)-Gly-Val-Gly-OH (**2.21**)

Chromatogram 22. HPLC trace of *N*-Ac-Gly-Val-Dha-Arg(6-FAM)-Phe-Gly-OH (**2.22**)

Chromatogram 23. HPLC trace of *N*-Ac-Gly-Val-Cys(6-FAM)-Arg-Phe-Gly-OH (**2.23**)

Chromatogram 24. HPLC trace of *N*-Ac-Gly-Lys(6-FAM)-Phe-Arg-Gly-OH (**2.24**)

Chromatogram 25. HPLC trace of *N*-Ac-Gly-Phe-Val-Arg(Biotin)-Gly-Val-Gly-OH (**2.25**)

Chromatogram 26. HPLC trace of *N*-Ac-Gly-Val-Glu-Phe-Arg(Biotin)-Gly-OH (**2.26**)

Chromatogram 27. HPLC trace of *N*-Ac-Gly-Phe-Val-Arg(DA)-Gly-Val-Gly-OH (**2.27**)

Chromatogram 28. HPLC trace of *N*-Ac-Gly-Val-Glu-Phe-Arg(DA)-Gly-OH (**2.28**)

Chromatogram 29. HPLC trace of Pyr-His-Trp-Ser-Tyr-D-Leu-Leu-Arg(6-FAM)-Pro-NHEt (**2.30**)

Chromatogram 30. HPLC trace of *N*-Ac-Gly-Lys(Boc)-Phe-Arg-Gly-OH (**2.31**)

Chromatogram 31. HPLC trace of *N*-Ac-Gly-Lys(Boc)-Phe-Arg(6-FAM)-Gly-OH (**2.32**)

Chromatogram 32. HPLC trace of *N*-Ac-Gly-Lys-Phe-Arg(6-FAM)-Gly-OH (**2.33**)

Chromatogram 33. HPLC trace of MC-LR

Chromatogram 34. HPLC trace of MC-LR-(6-FAM) (**3.1**)

Chromatogram 35. HPLC trace of MC-LR-(Alexa-430) (**3.2**)

Chromatogram 36. HPLC trace of MC-LR-(Alexa-488) (**3.3**)

Chromatogram 37. HPLC trace of MC-LR-(Texas-Red) (**3.4**)

Chromatogram 38. HPLC trace of MC-LR-(Biotin) (**3.5**)

Chromatogram 39. HPLC trace of MC-LR-(DA) (**3.6**)

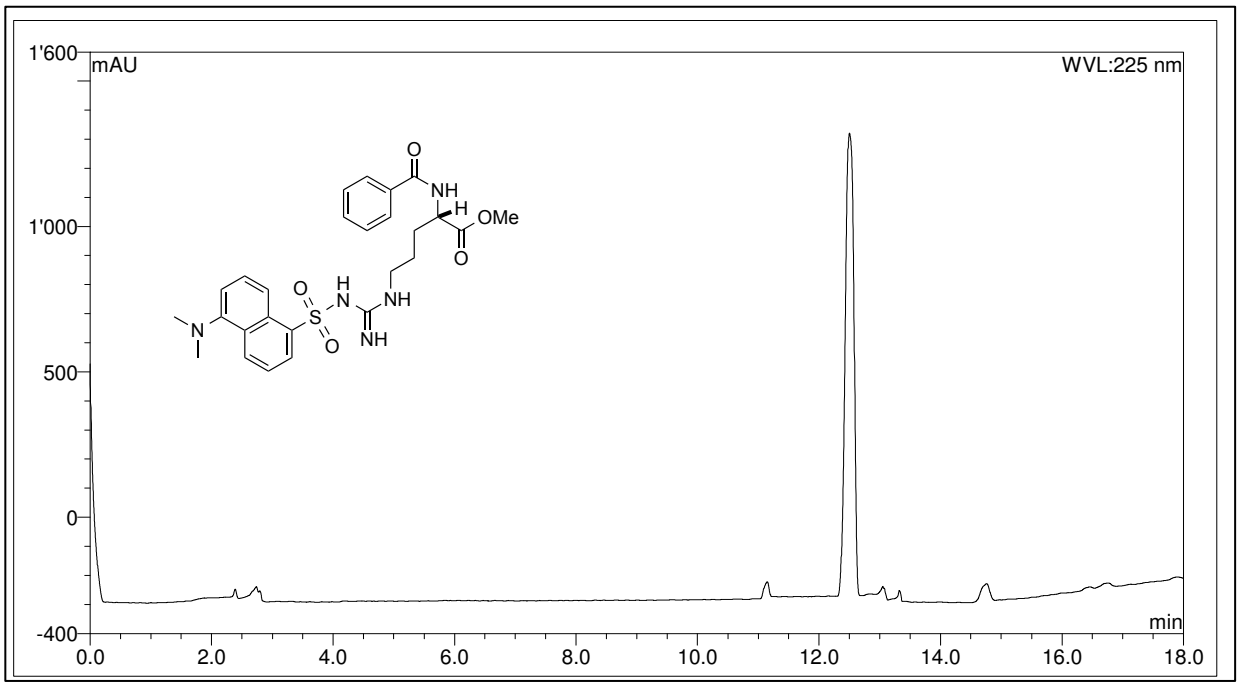

Chromatogram 1. HPLC trace of Bz-Arg(Dansyl)-OMe (**2.1)**

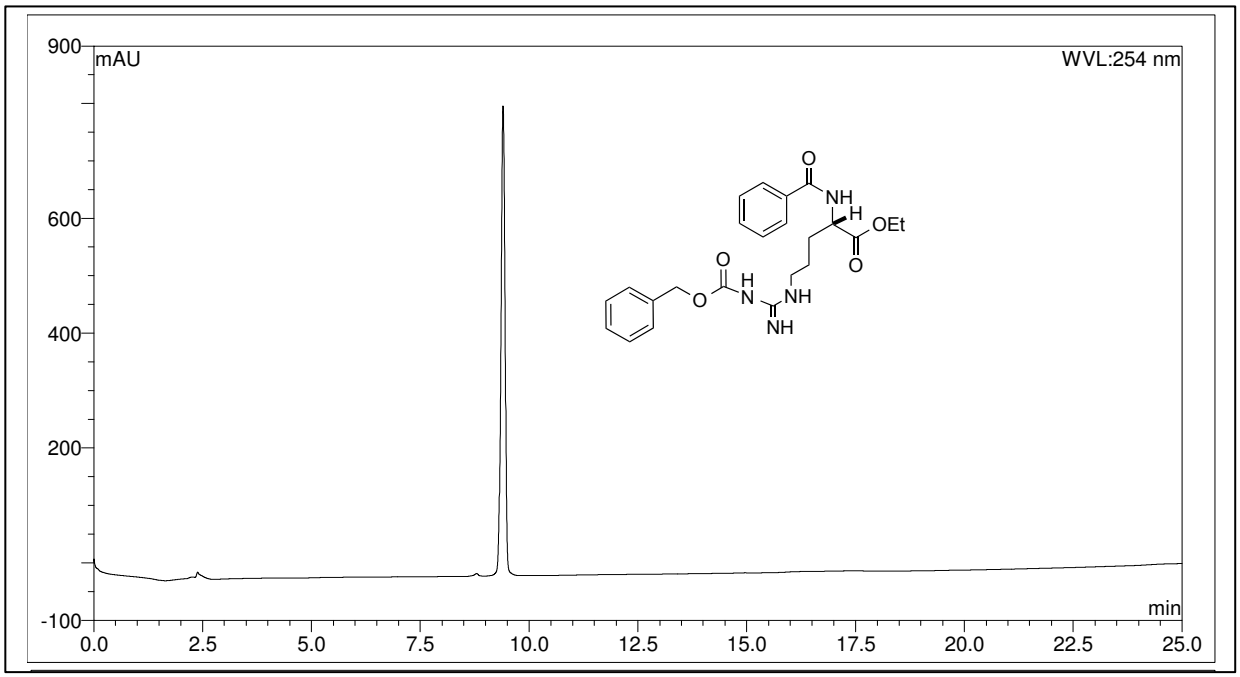

Chromatogram 2. HPLC trace of Bz-Arg(*N*-succinimid)-OEt (**2.2**)

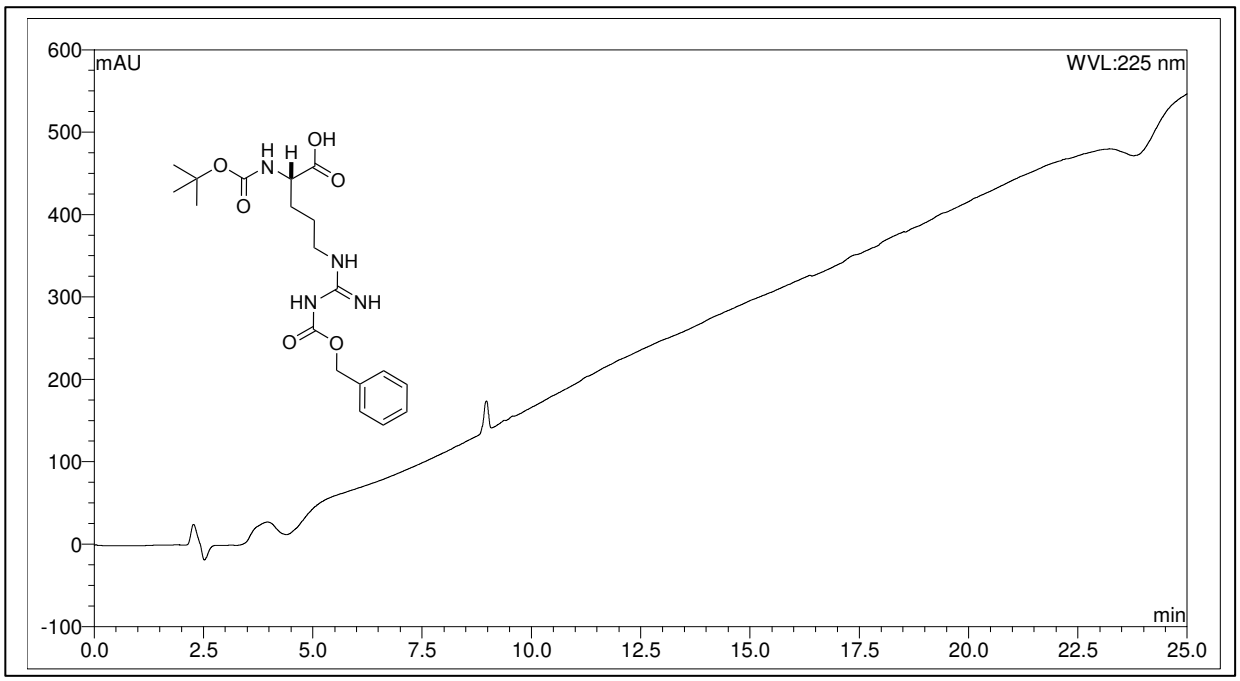

Chromatogram 3. HPLC trace of Boc-Arg(*N*-succinimid)-OH (**2.3**)

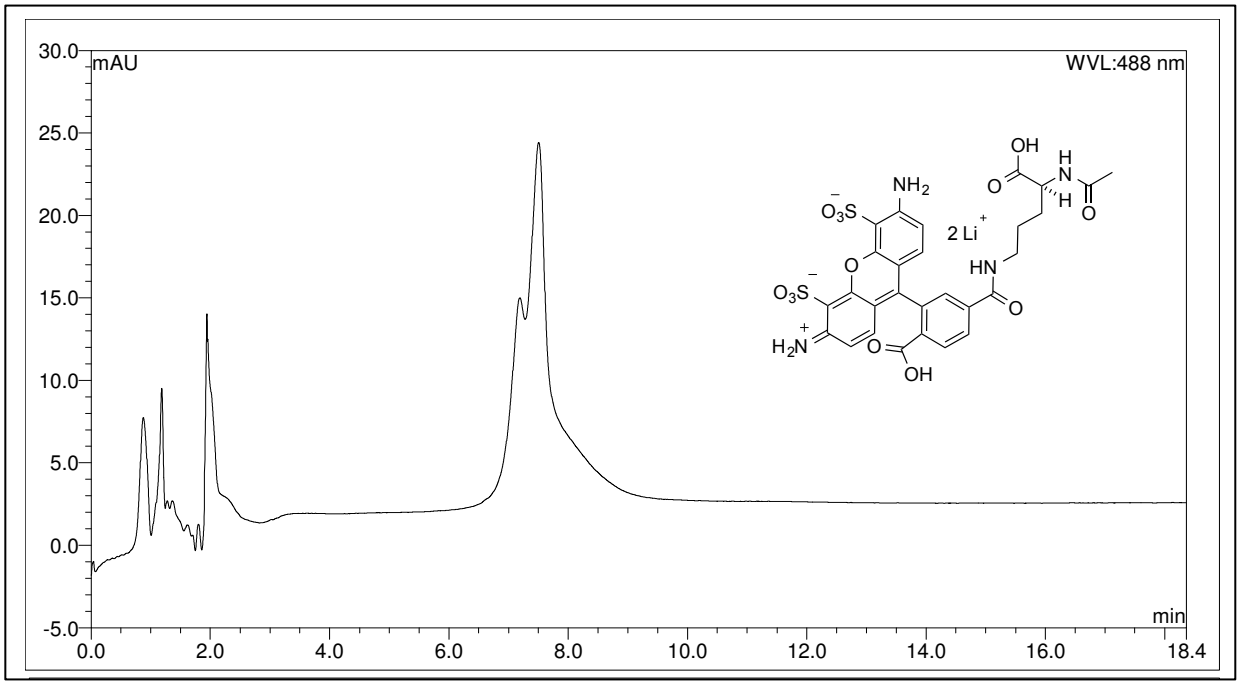

Chromatogram 4. HPLC trace of *N*-Ac-Arg(Alexa488)-OH (**2.4**)

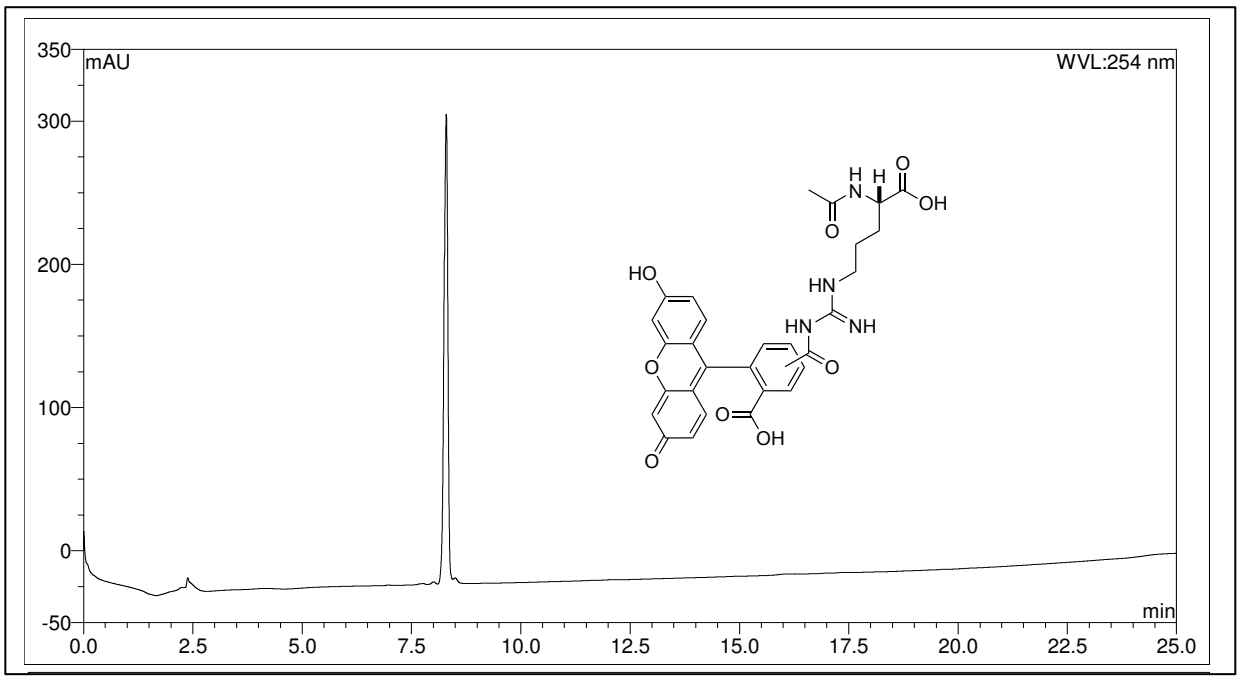

Chromatogram 5. HPLC trace of *N*-Ac-Arg(6-FAM)-OH (**2.5**)

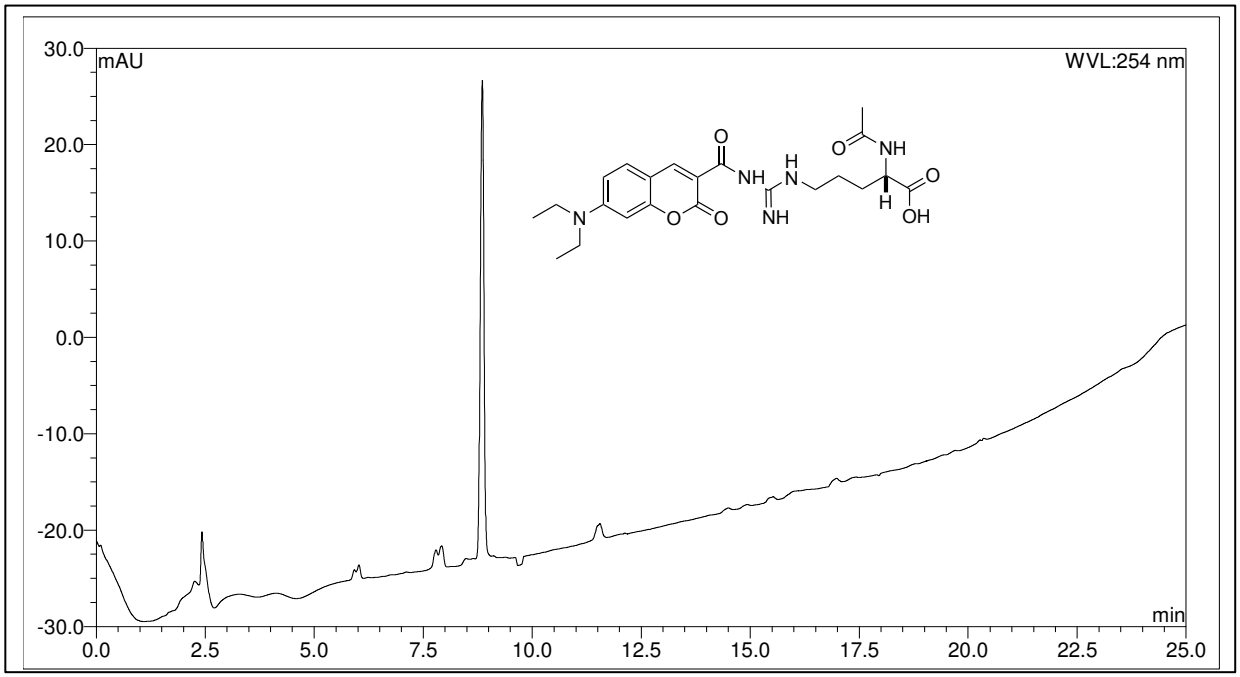

Chromatogram 6. HPLC trace of *N*-Ac-Arg(coumarin)-OH (**2.6**)

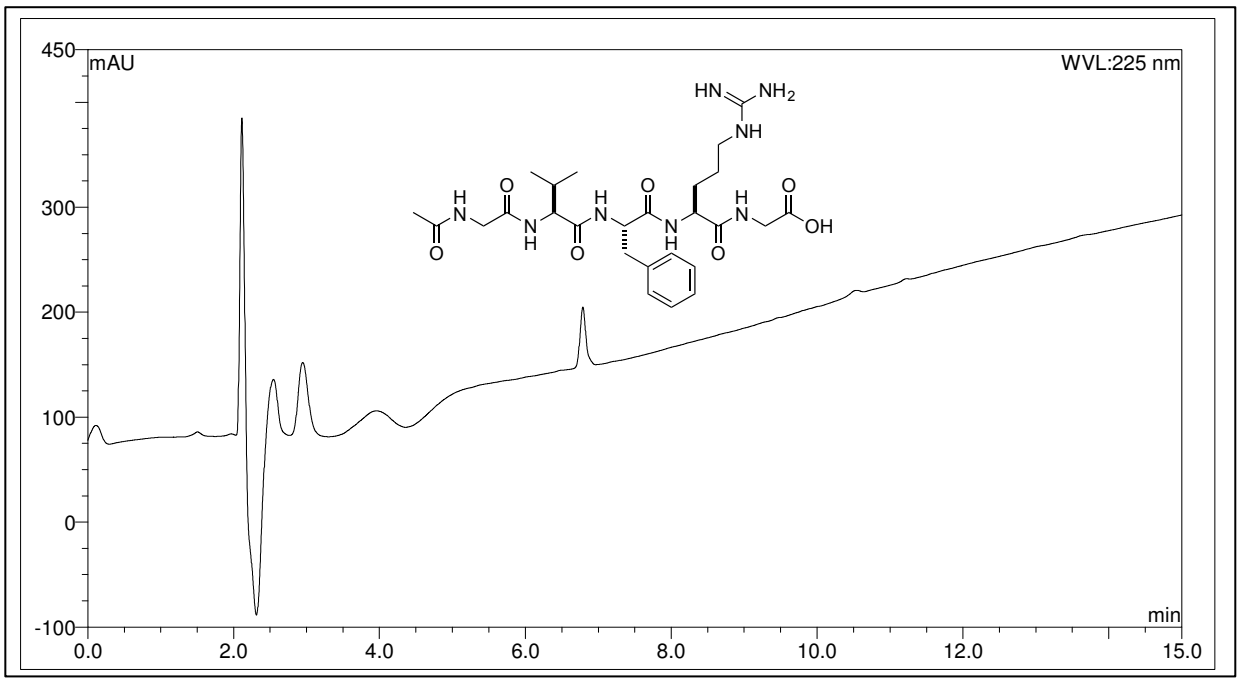

Chromatogram 7. HPLC trace of *N*-Ac-Gly-Val-Phe-Arg-Gly-OH (**2.7**)

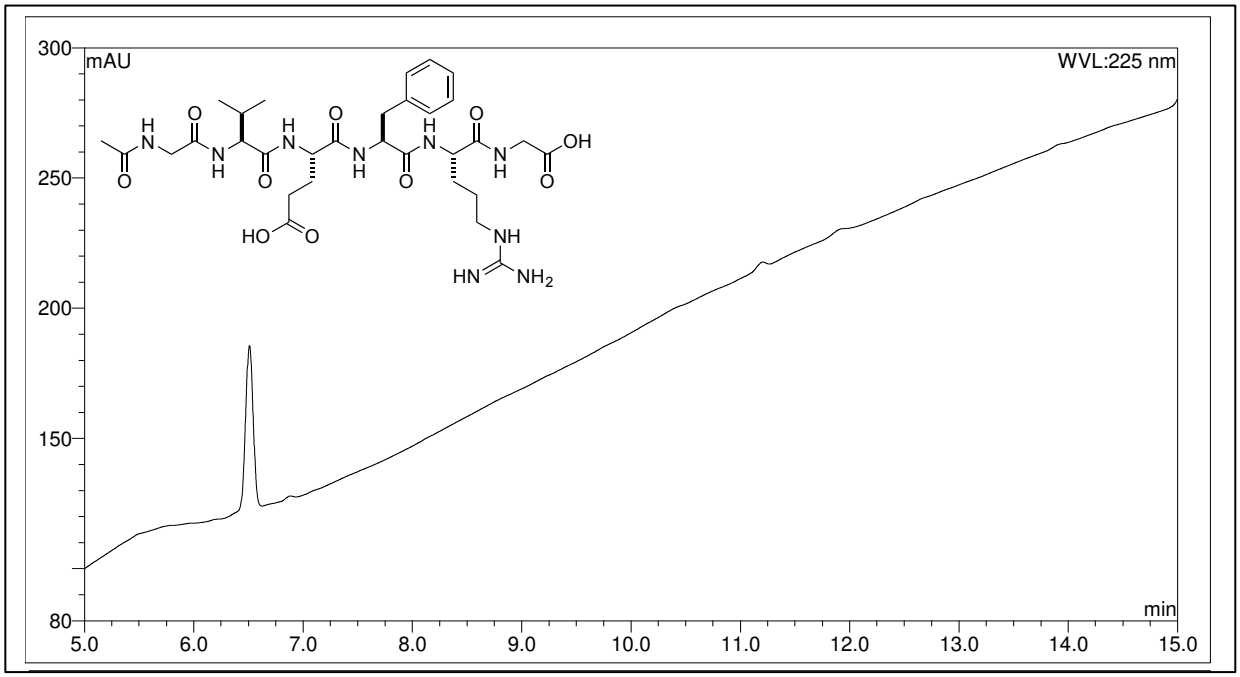

Chromatogram 8. HPLC trace of *N*-Ac-Gly-Val-Glu-Phe-Arg-Gly-OH (**2.8**)

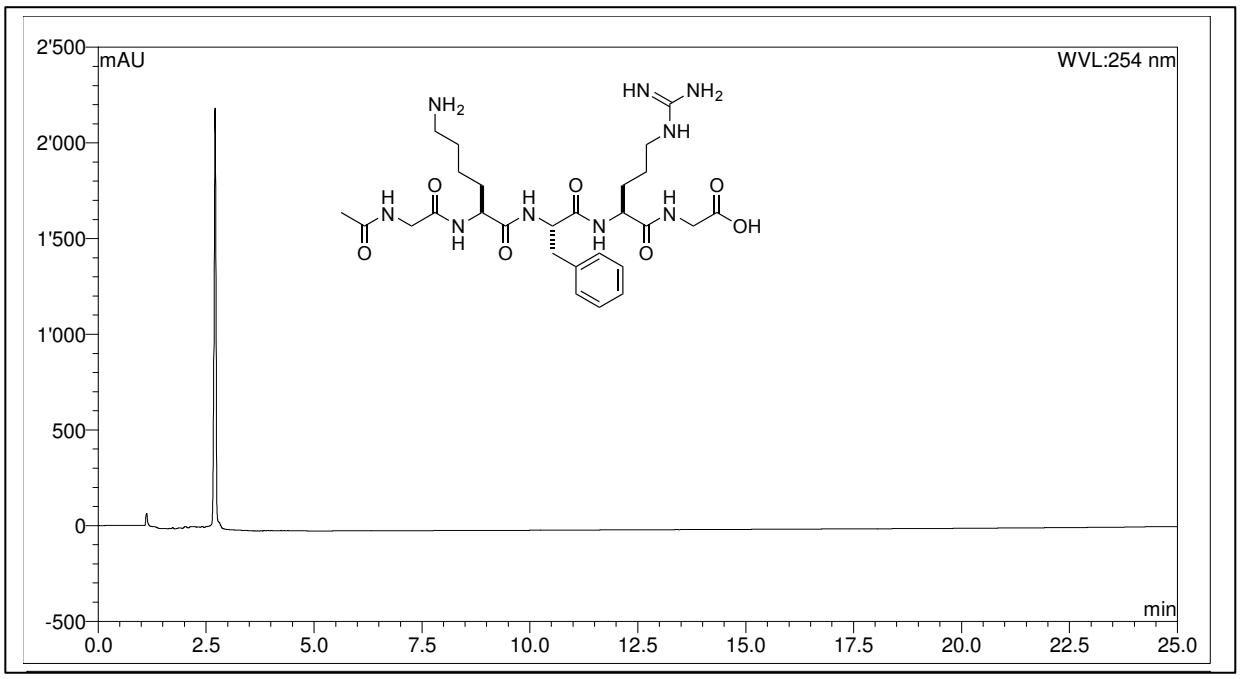

Chromatogram 9. HPLC trace of *N*-Ac-Gly-Lys-Phe-Arg-Gly-OH (**2.9**)

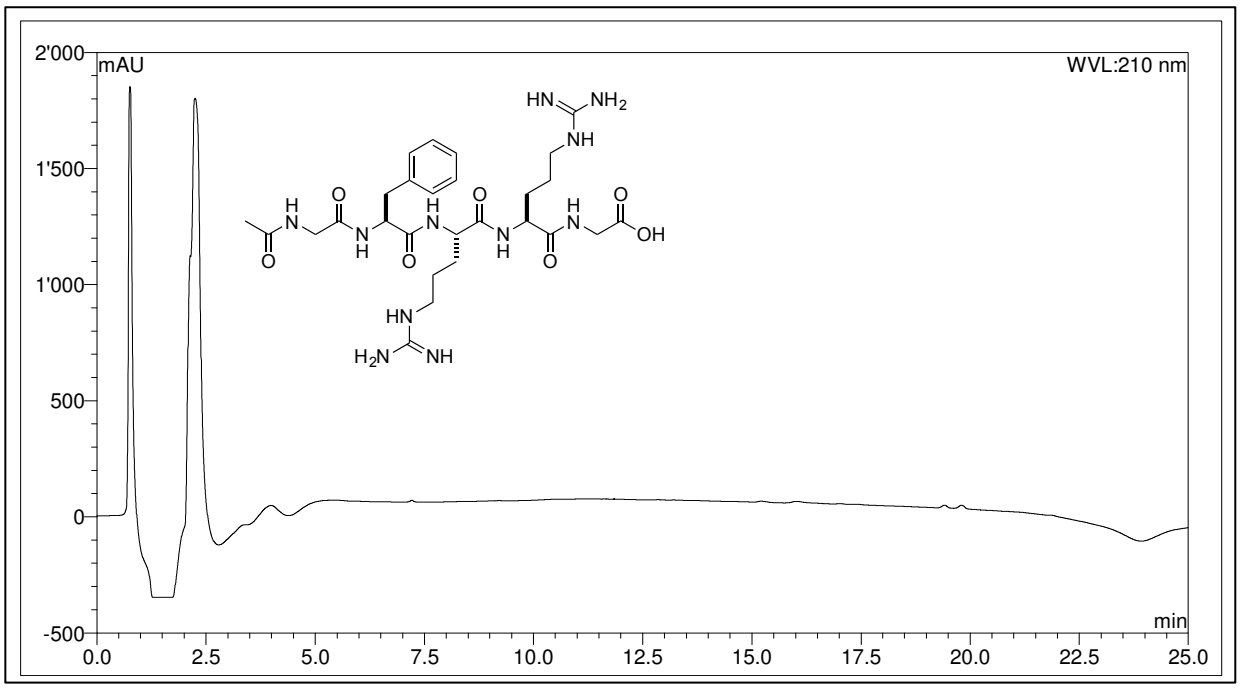

Chromatogram 10. HPLC trace of *N*-Ac-Gly-Phe-Arg-Arg-Gly-OH (**2.10**)

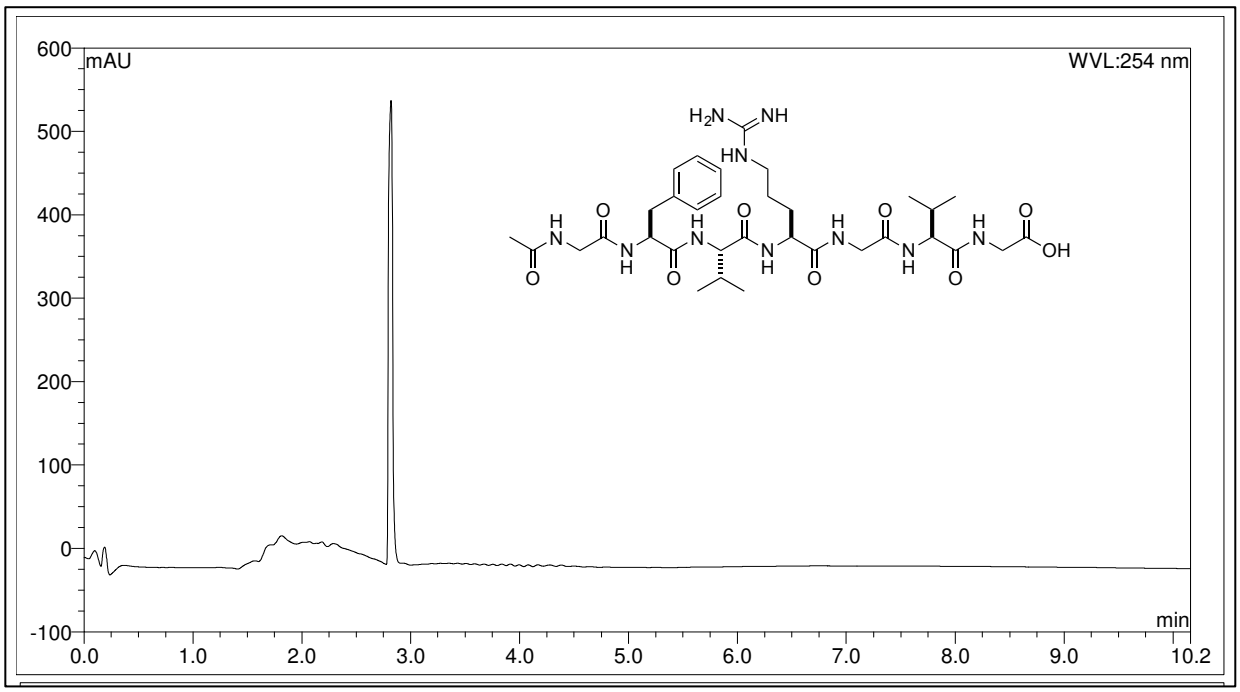

Chromatogram 11. HPLC trace of *N*-Ac-Gly-Phe-Val-Arg-Gly-Val-Gly-OH (**2.11**)

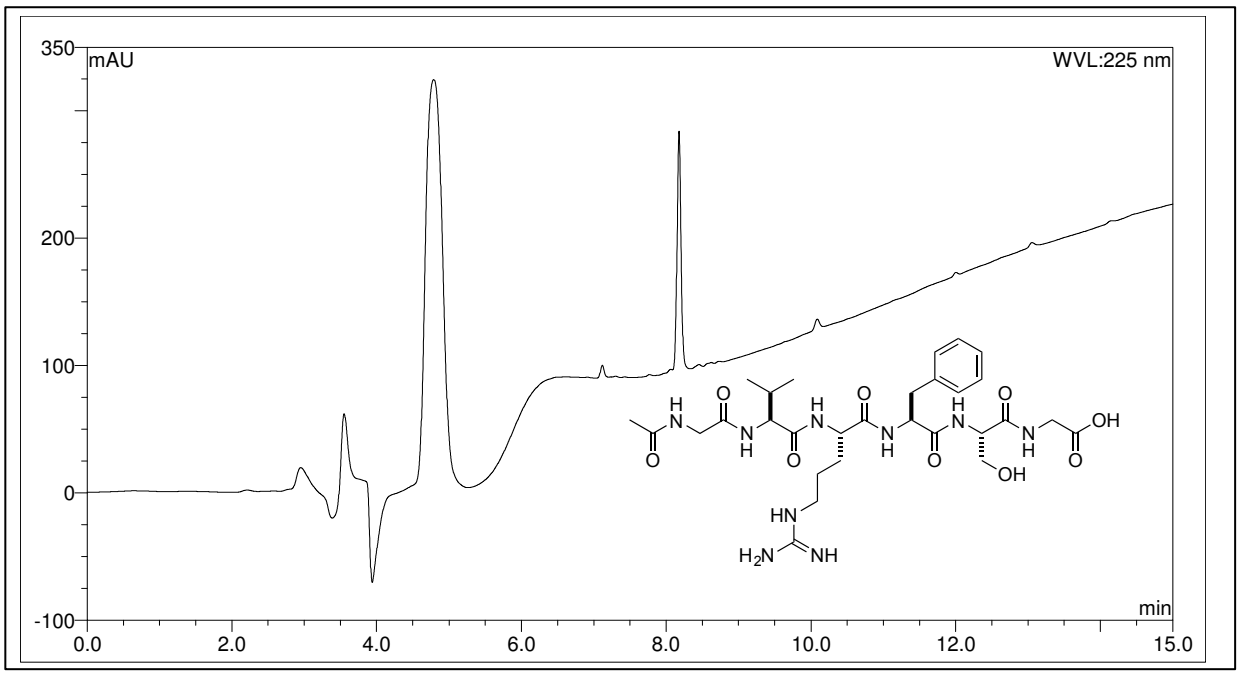

Chromatogram 12. HPLC trace of *N*-Ac-Gly-Val-Arg-Phe-Ser-Gly-OH (**2.12**)

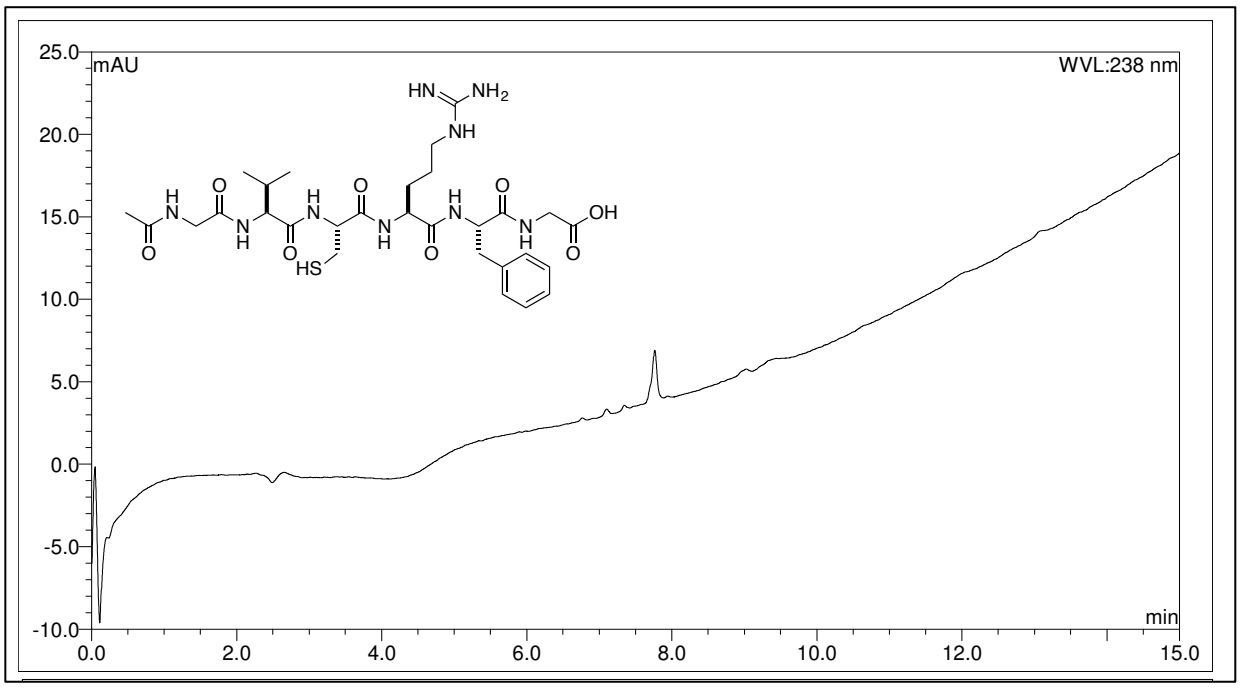

Chromatogram 13. HPLC trace of *N*-Ac-Gly-Val-Cys-Arg-Phe-Gly-OH (**2.13**)

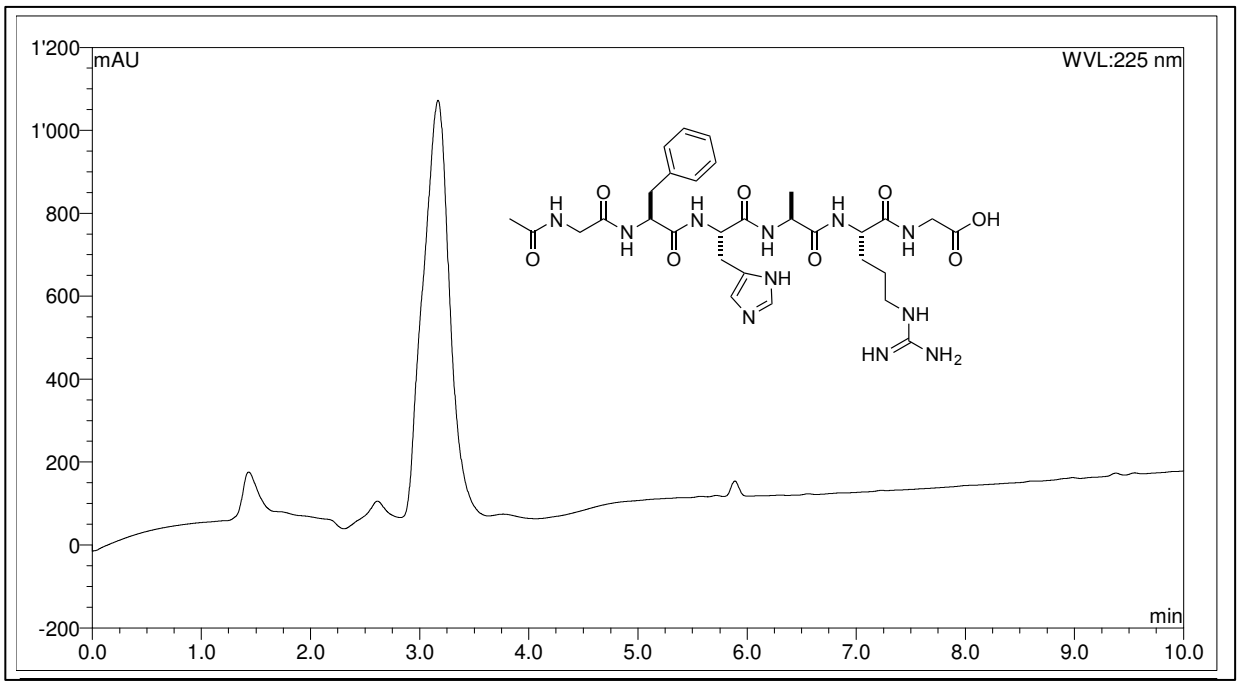

Chromatogram 14. HPLC trace of *N*-Ac-Gly-Phe-His-Ala-Arg-Gly-OH (**2.14**)

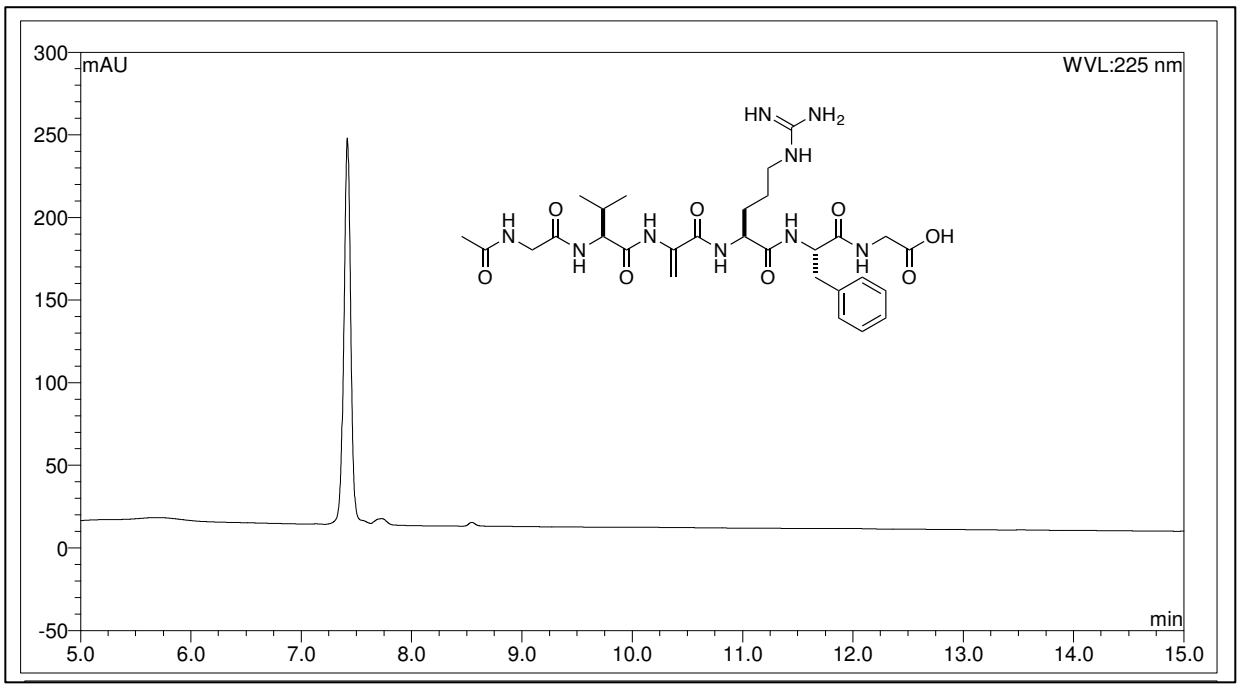

Chromatogram 15. HPLC trace of *N*-Ac-Gly-Val-Dha-Arg-Phe-Gly-OH (**2.15**)

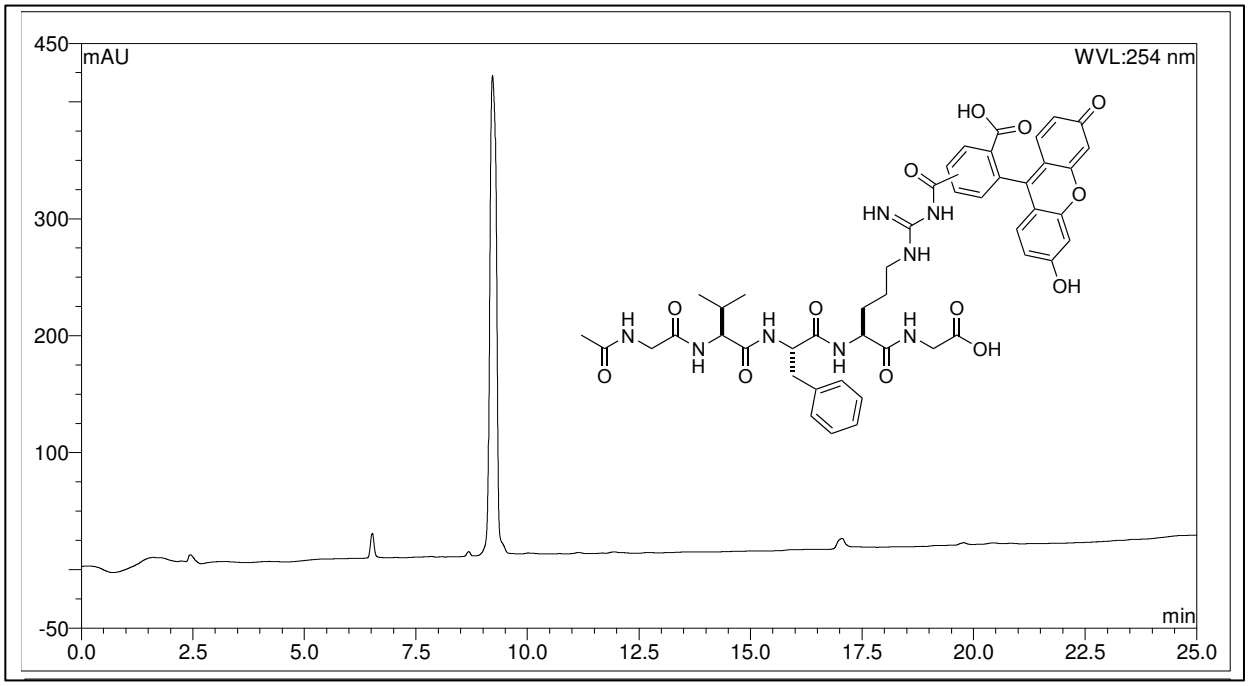

Chromatogram 16. HPLC trace of *N*-Ac-Gly-Val-Phe-Arg(6-FAM)-Gly-OH (**2.16**)

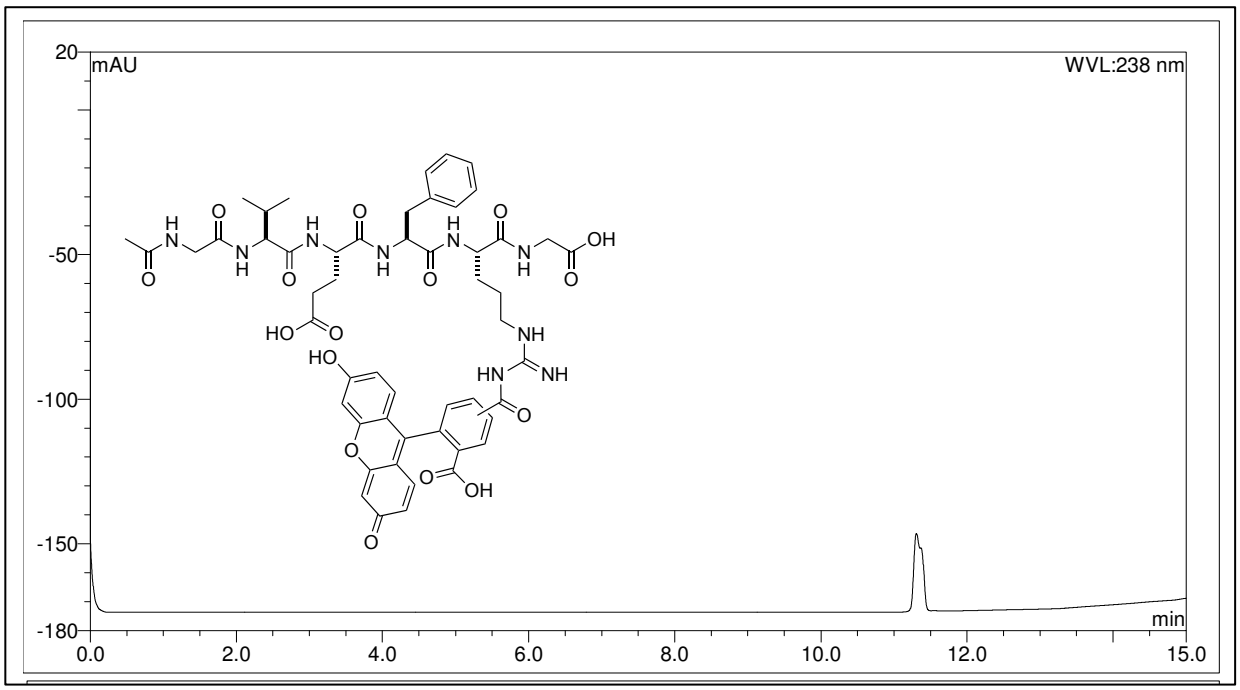

Chromatogram 17. HPLC trace of *N*-Ac-Gly-Val-Glu-Phe-Arg(6-FAM)-Gly-OH (**2.17**)

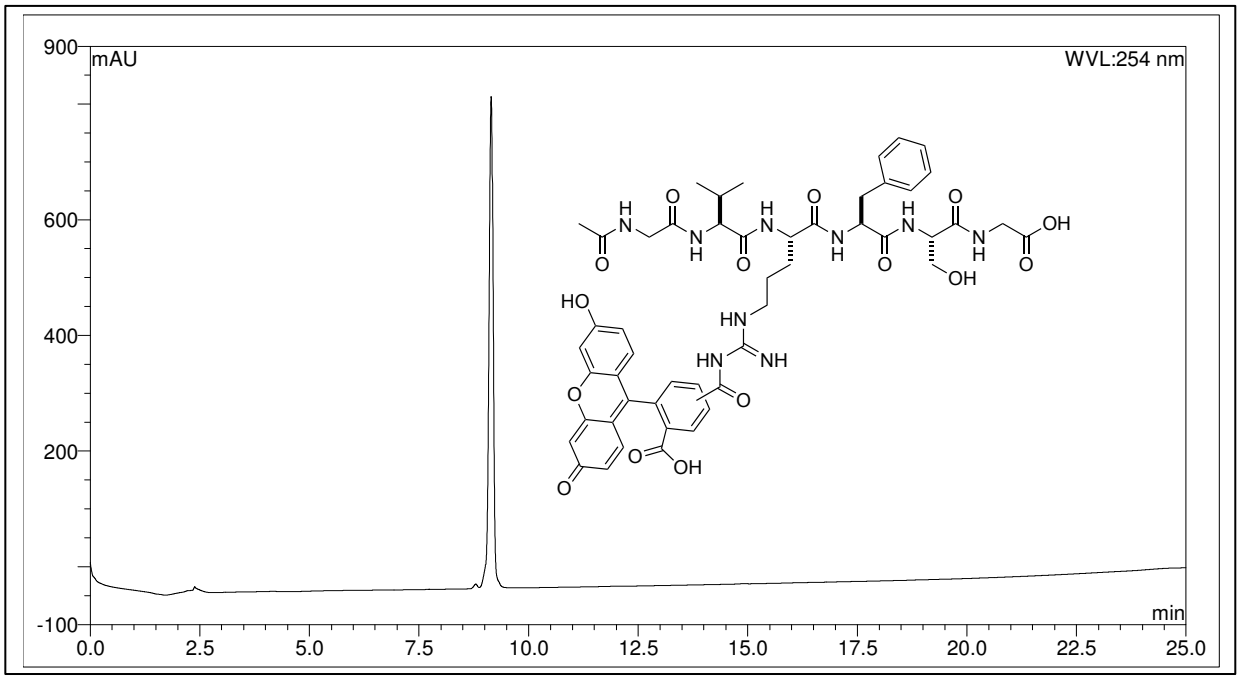

Chromatogram 18. HPLC trace of *N*-Ac-Gly-Val-Arg(6-FAM)-Phe-Ser-Gly-OH (**2.18**)

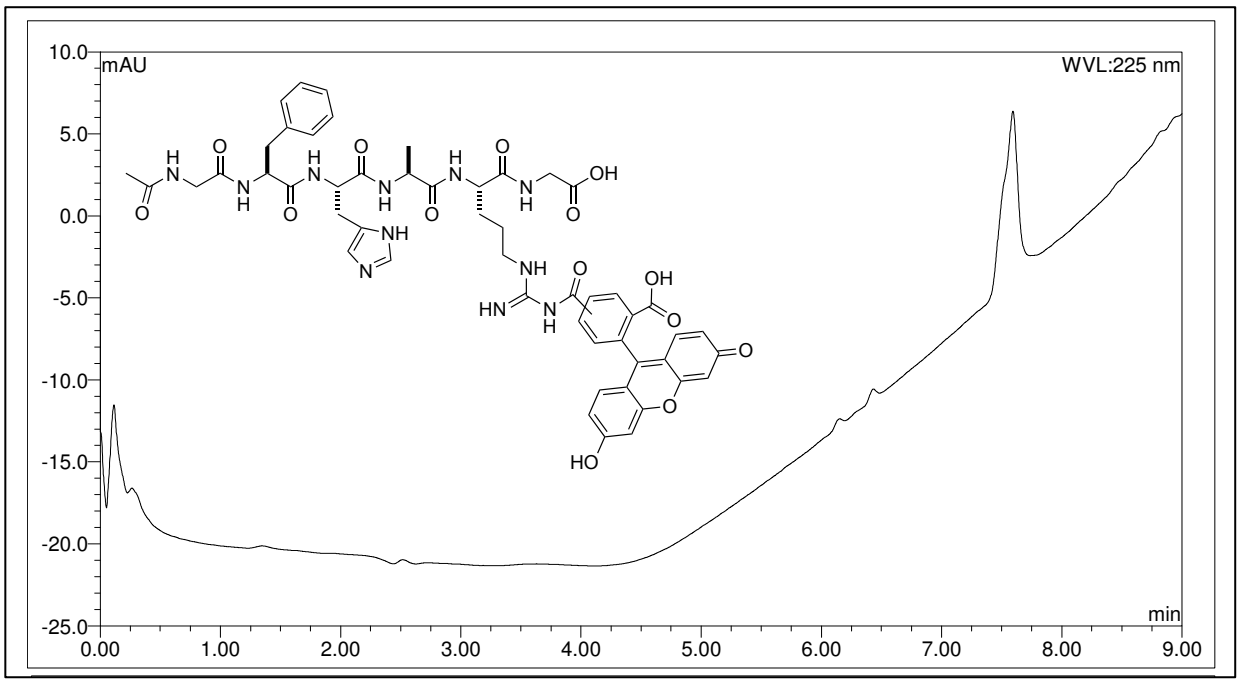

Chromatogram 19. HPLC trace of *N*-Ac-Gly-Phe-His-Ala-Arg(6-FAM)-Gly-OH (**2.19**)

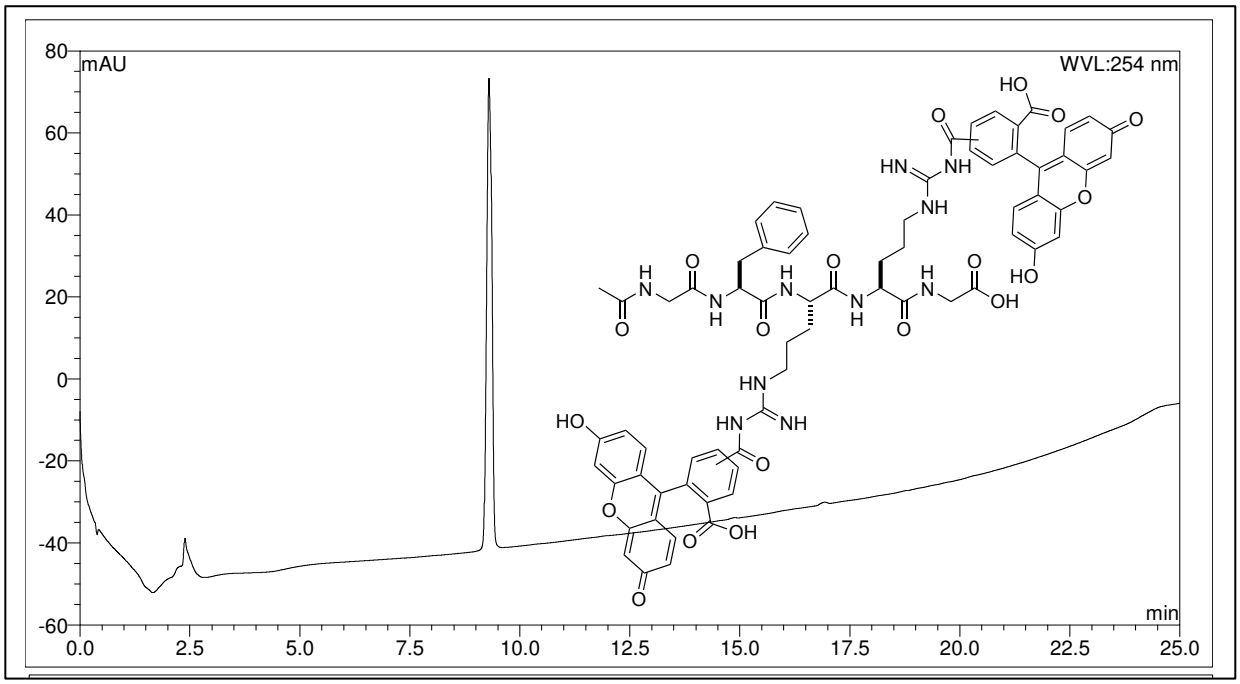

Chromatogram 20. HPLC trace of *N*-Ac-Gly-Phe-Arg(6-FAM)-Arg(6-FAM)-Gly-OH (**2.20**)

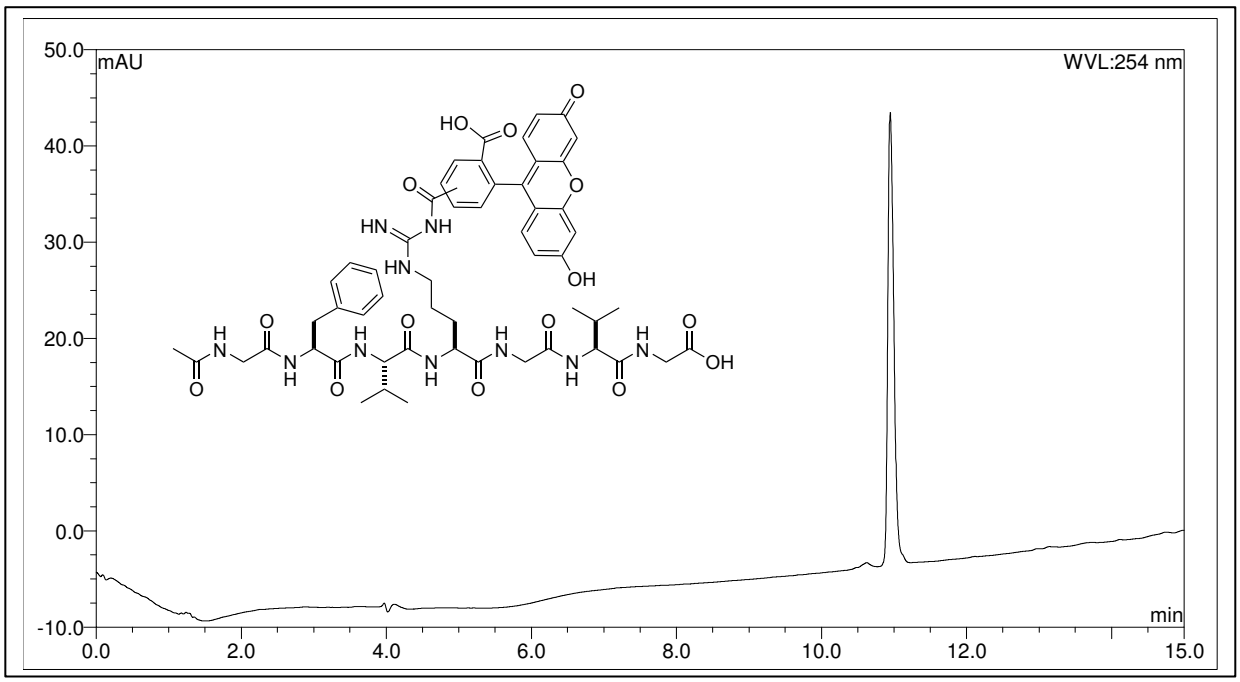

Chromatogram 21. HPLC trace of *N*-Ac-Gly-Phe-Val-Arg(6-FAM)-Gly-Val-Gly-OH (**2.21**)

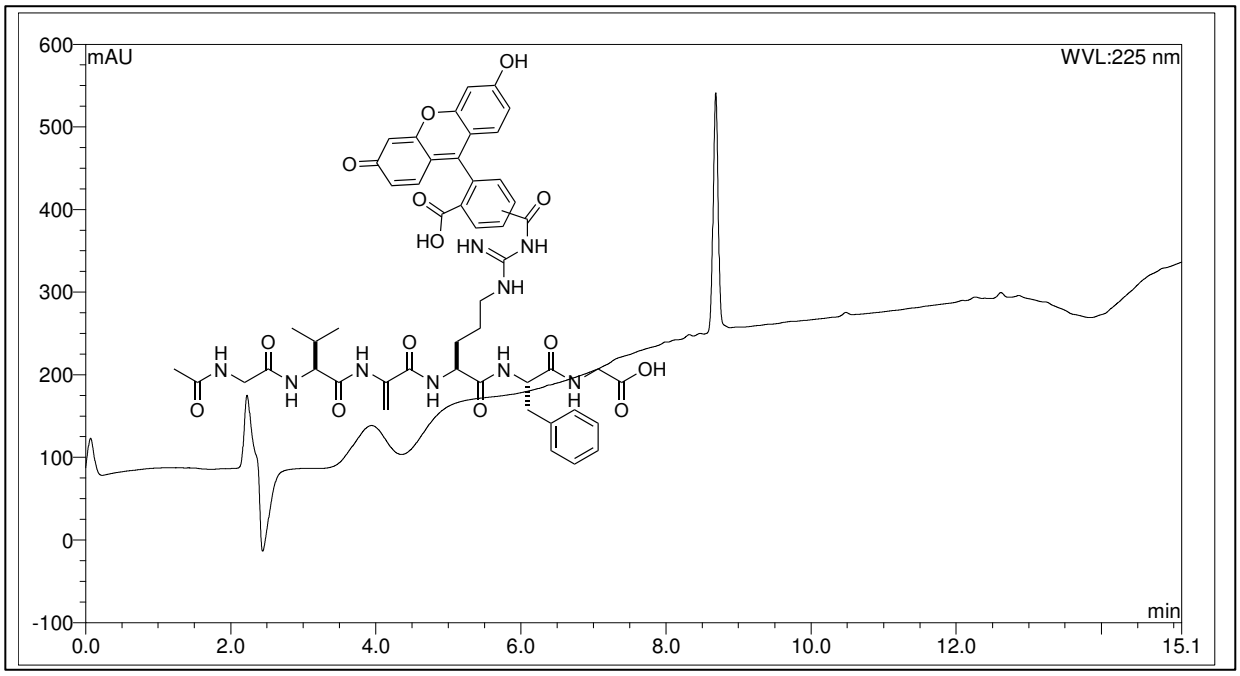

Chromatogram 22. HPLC trace of *N*-Ac-Gly-Val-Dha-Arg(6-FAM)-Phe-Gly-OH (**2.22**)

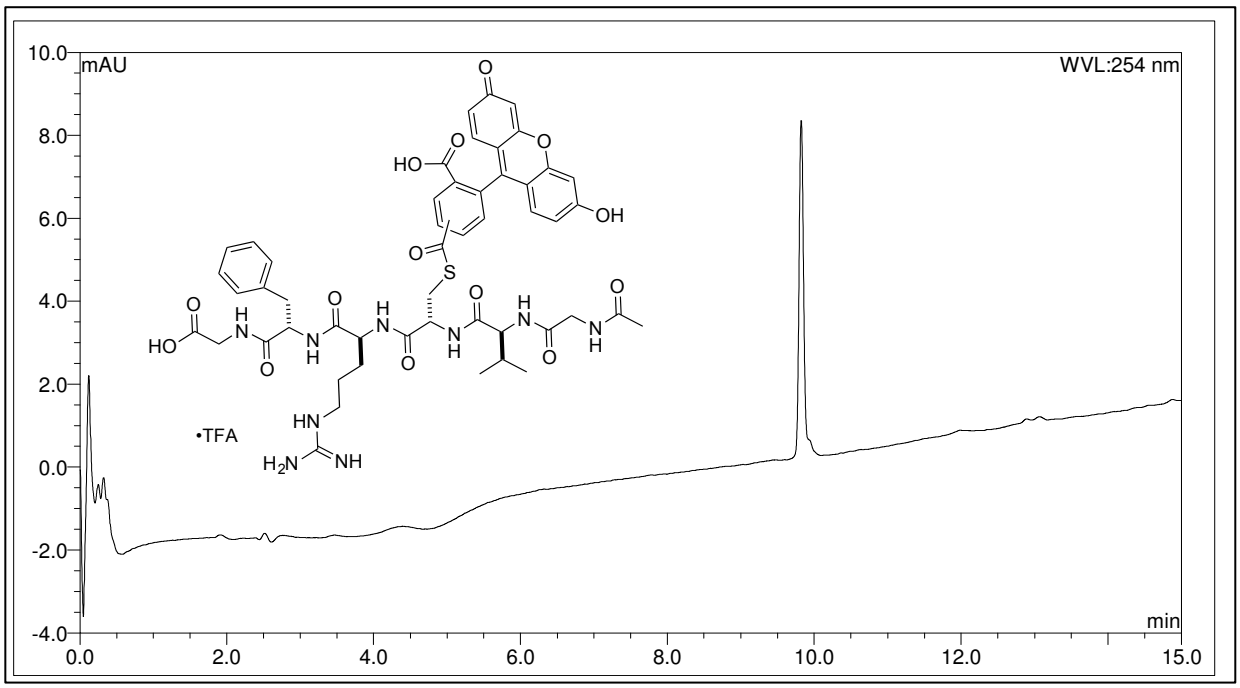

Chromatogram 23. HPLC trace of *N*-Ac-Gly-Val-Cys(6-FAM)-Arg-Phe-Gly-OH (**2.23**)

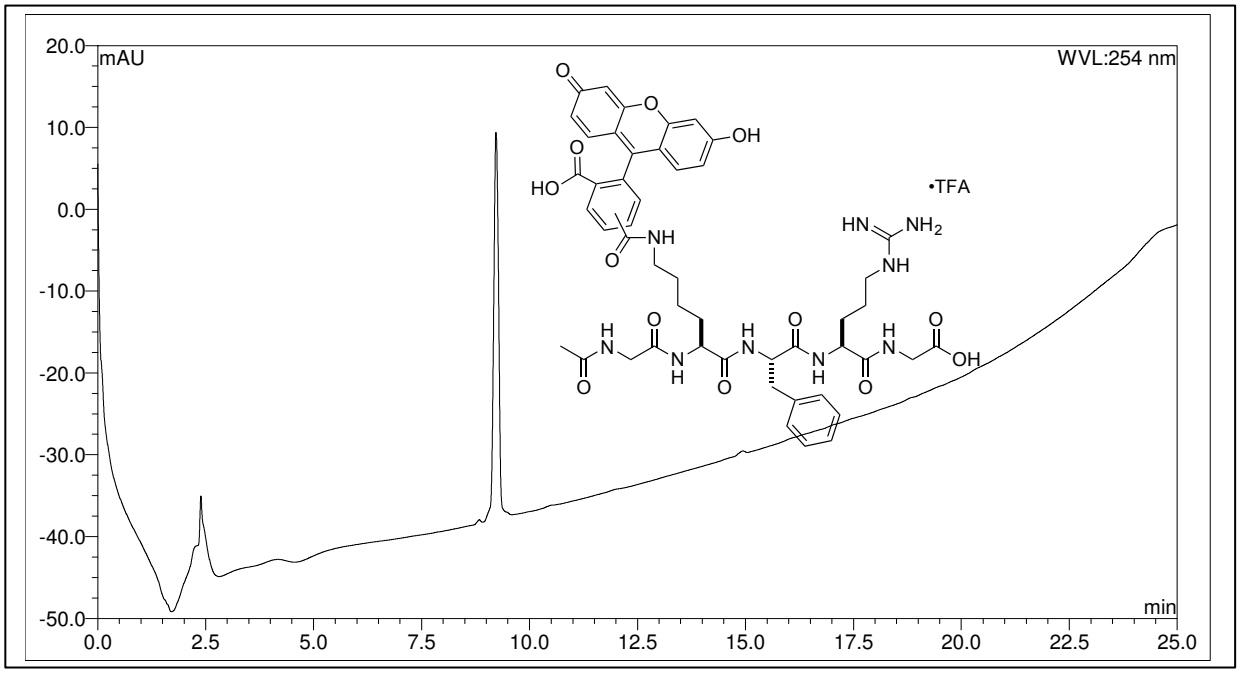

Chromatogram 24. HPLC trace of *N*-Ac-Gly-Lys(6-FAM)-Phe-Arg-Gly-OH (**2.24**)

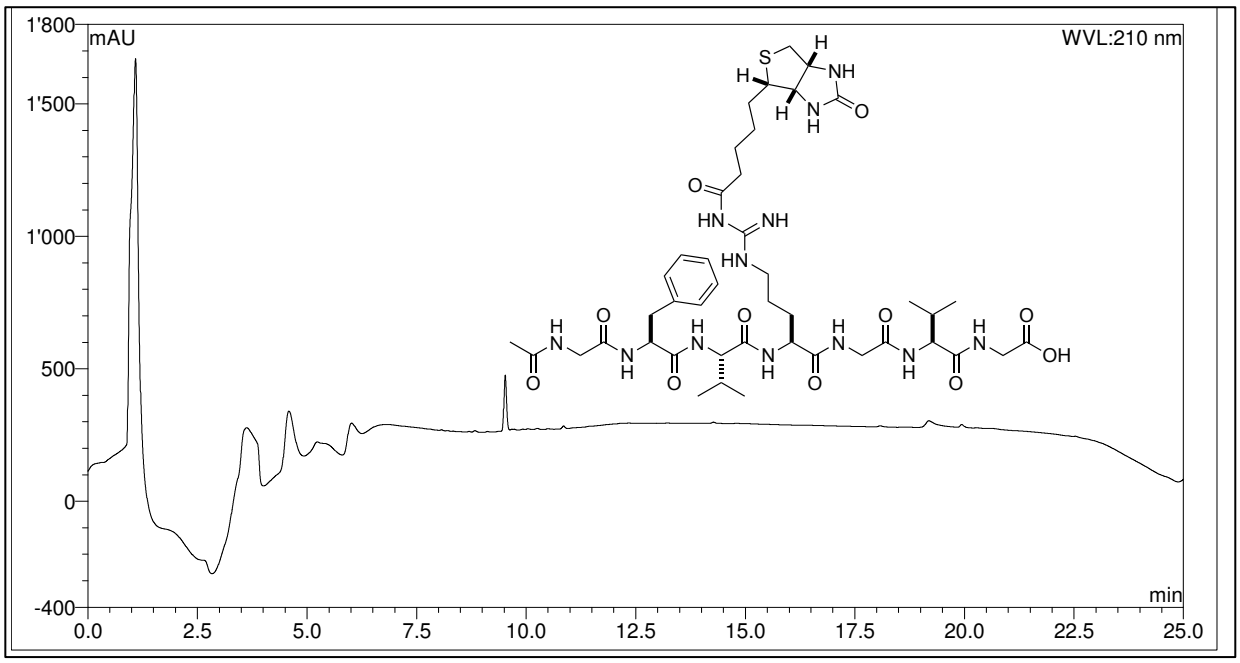

Chromatogram 25. HPLC trace of *N*-Ac-Gly-Phe-Val-Arg(Biotin)-Gly-Val-Gly-OH (**2.25**)

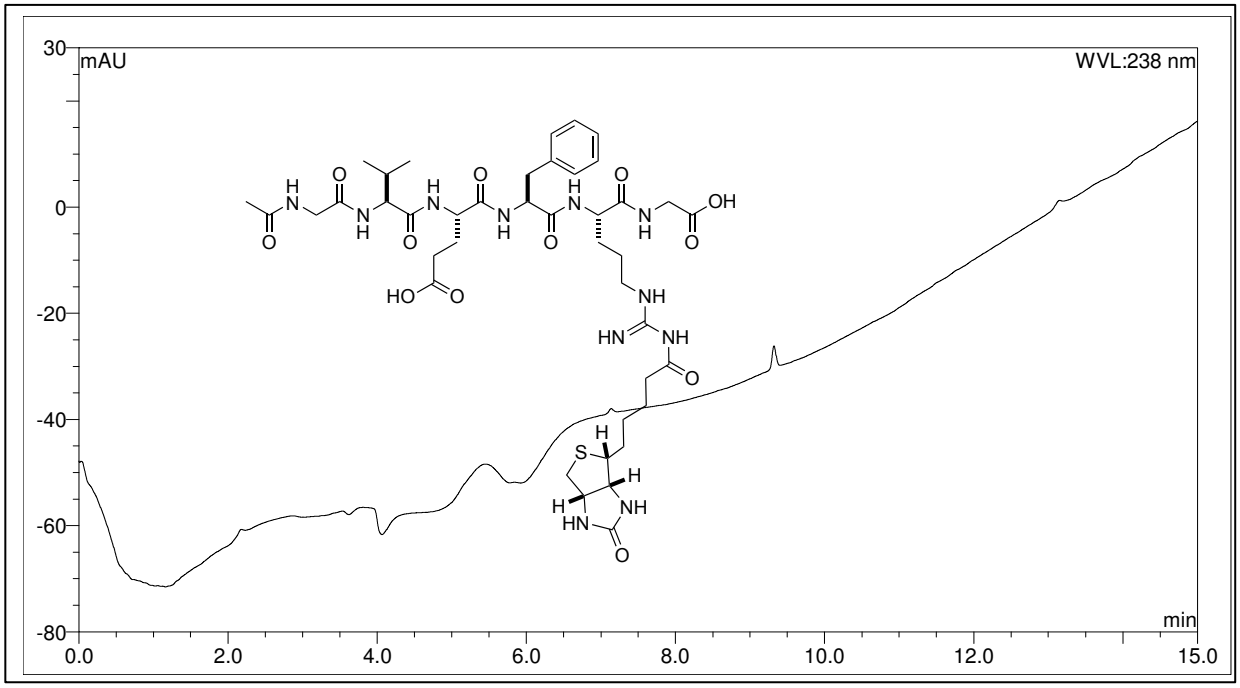

Chromatogram 26. HPLC trace of *N*-Ac-Gly-Val-Glu-Phe-Arg(Biotin)-Gly-OH (**2.26**)

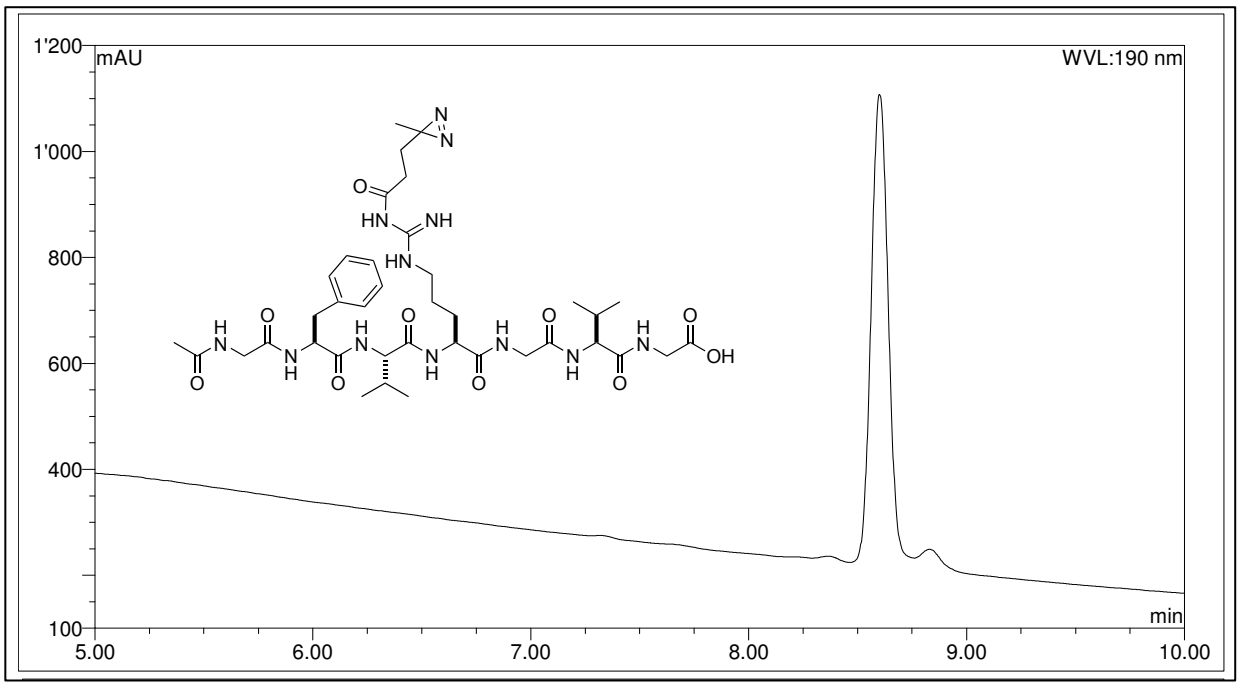

Chromatogram 27. HPLC trace of *N*-Ac-Gly-Phe-Val-Arg(DA)-Gly-Val-Gly-OH (**2.27**)

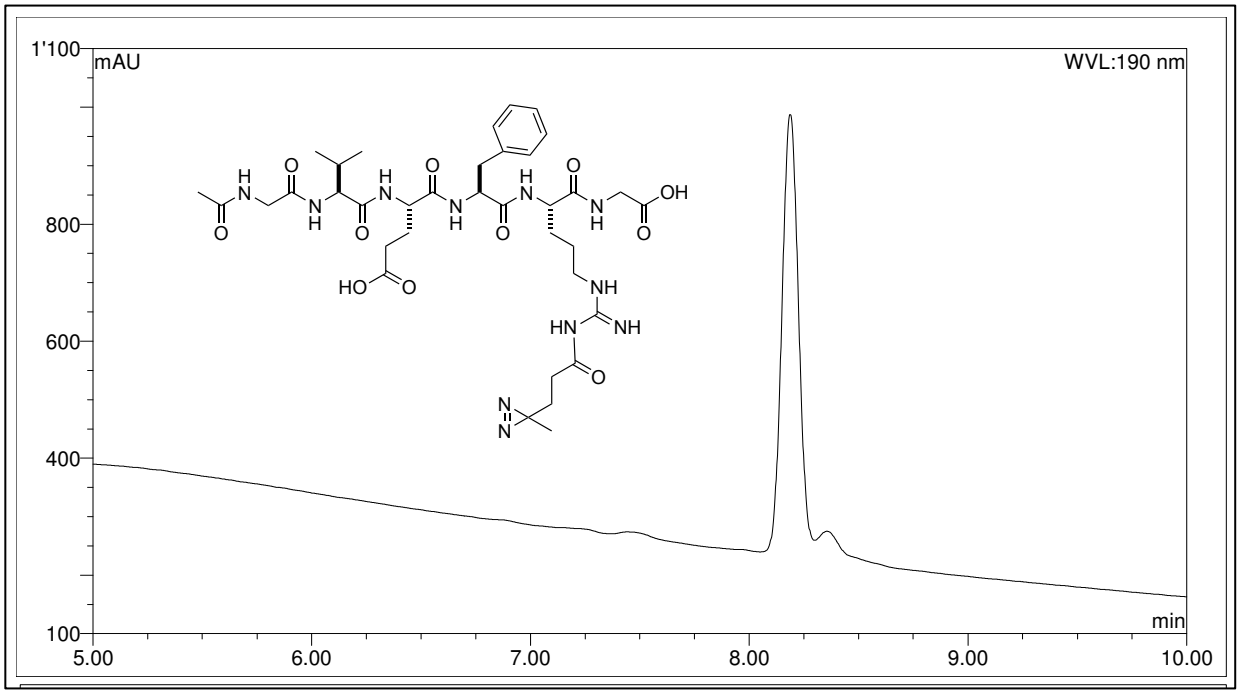

Chromatogram 28. HPLC trace of *N*-Ac-Gly-Val-Glu-Phe-Arg(DA)-Gly-OH (**2.28**)

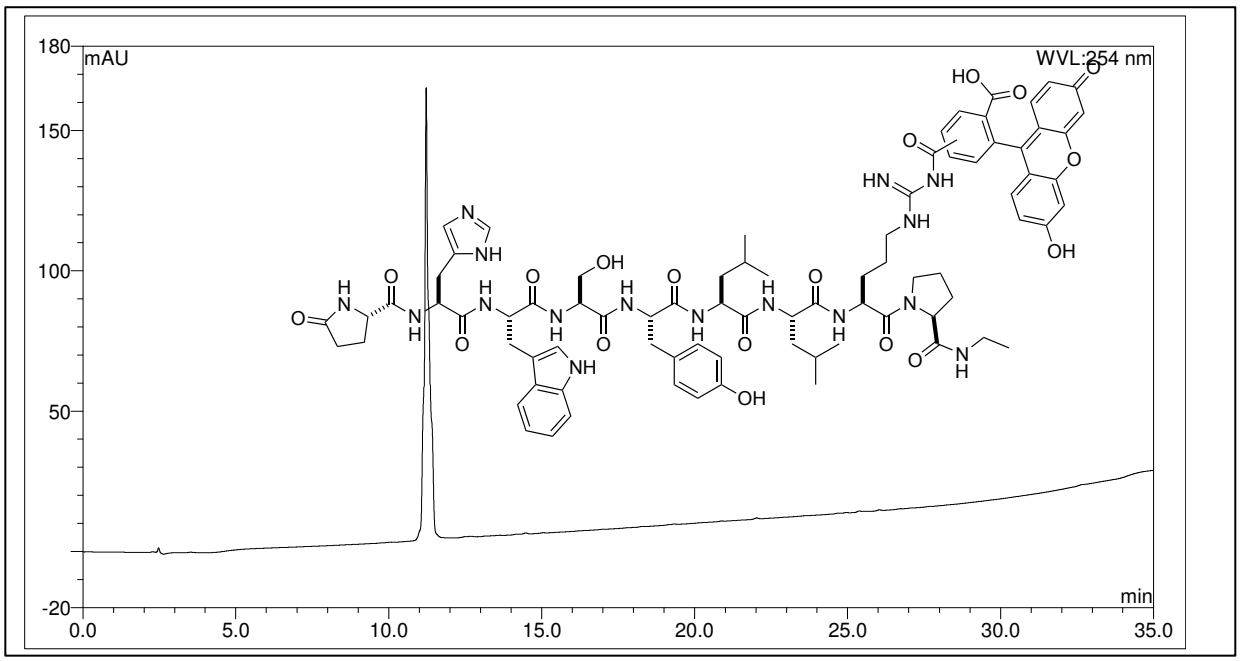

Chromatogram 29. HPLC trace of Pyr-His-Trp-Ser-Tyr-D-Leu-Leu-Arg(6-FAM)-Pro-NHEt (**2.30**)

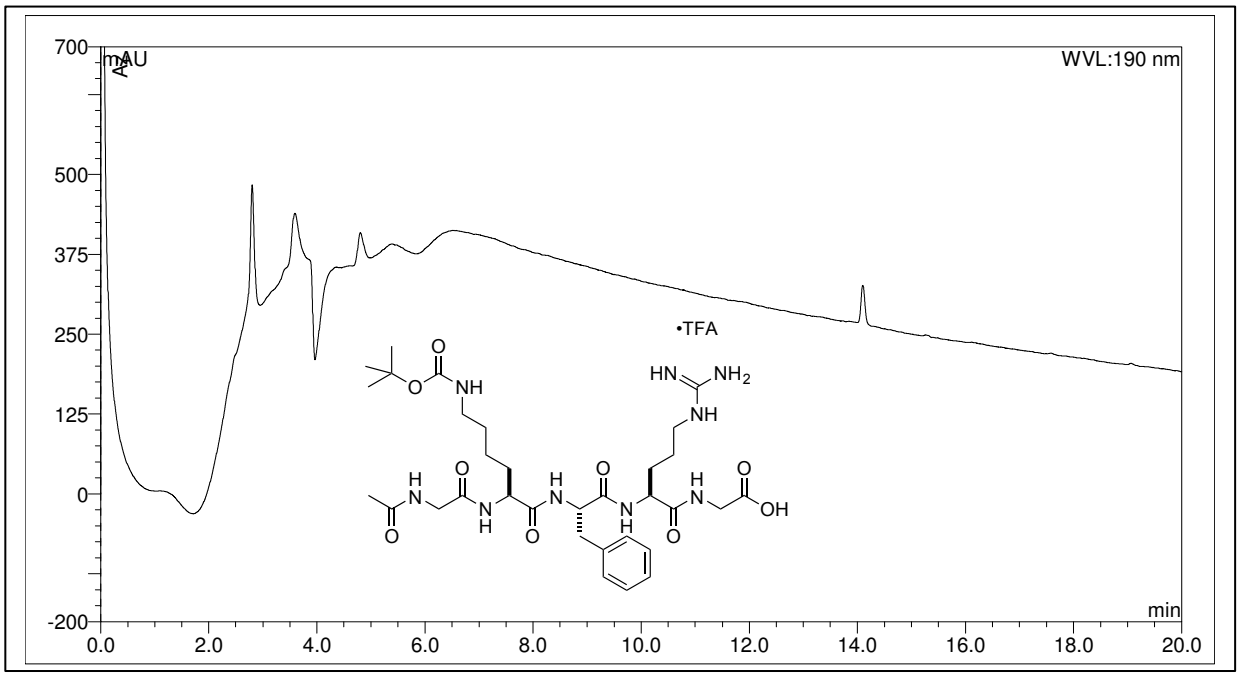

Chromatogram 30. HPLC trace of *N*-Ac-Gly-Lys(Boc)-Phe-Arg-Gly-OH (**2.31**)

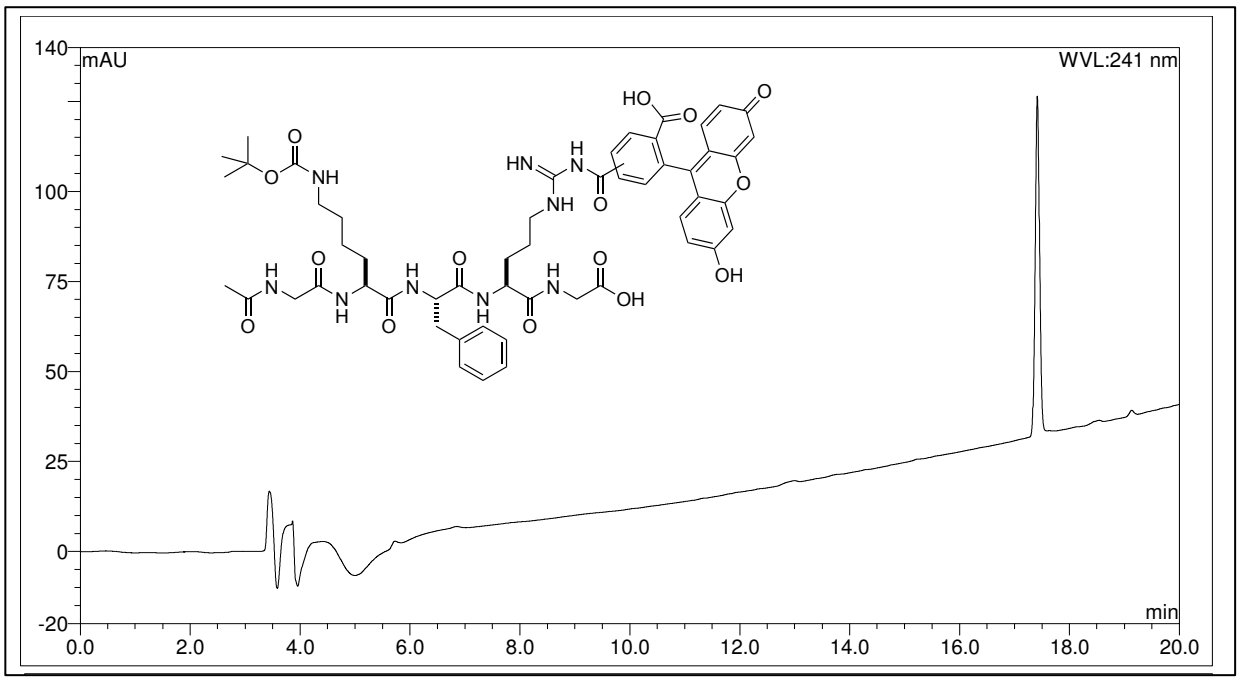

Chromatogram 31. HPLC trace of *N*-Ac-Gly-Lys(Boc)-Phe-Arg(6-FAM)-Gly-OH (**2.32**)

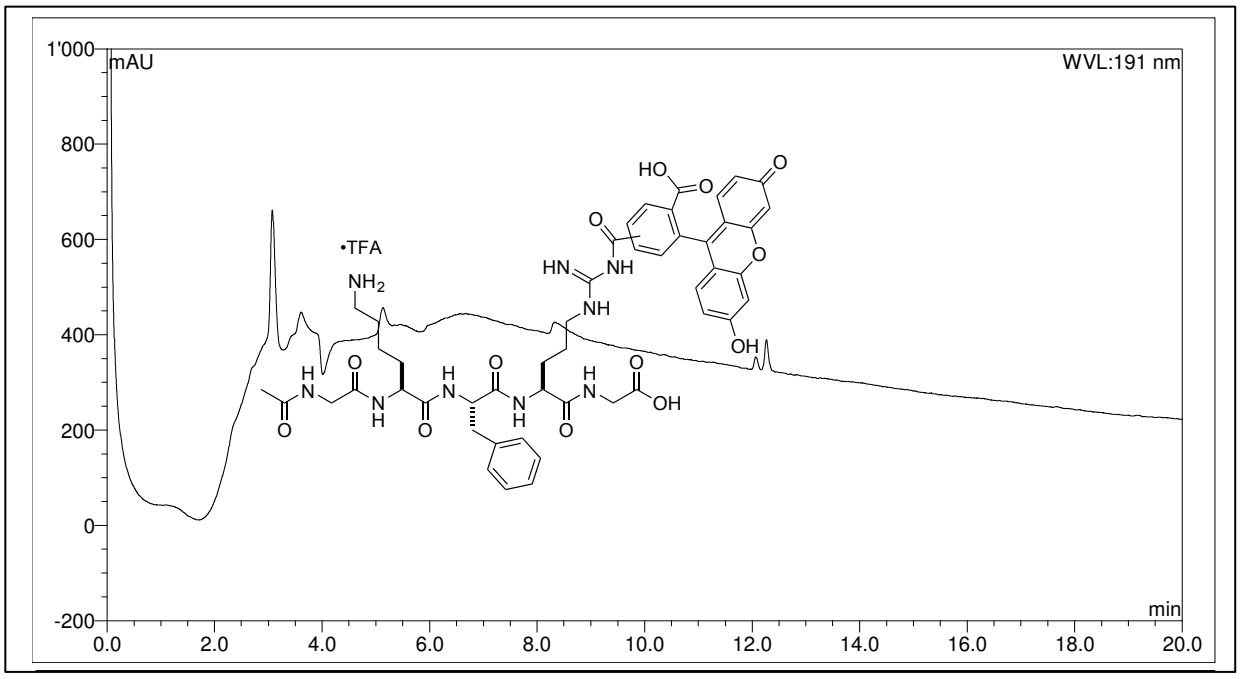

Chromatogram 32. HPLC trace of *N*-Ac-Gly-Lys-Phe-Arg(6-FAM)-Gly-OH (**2.33**)

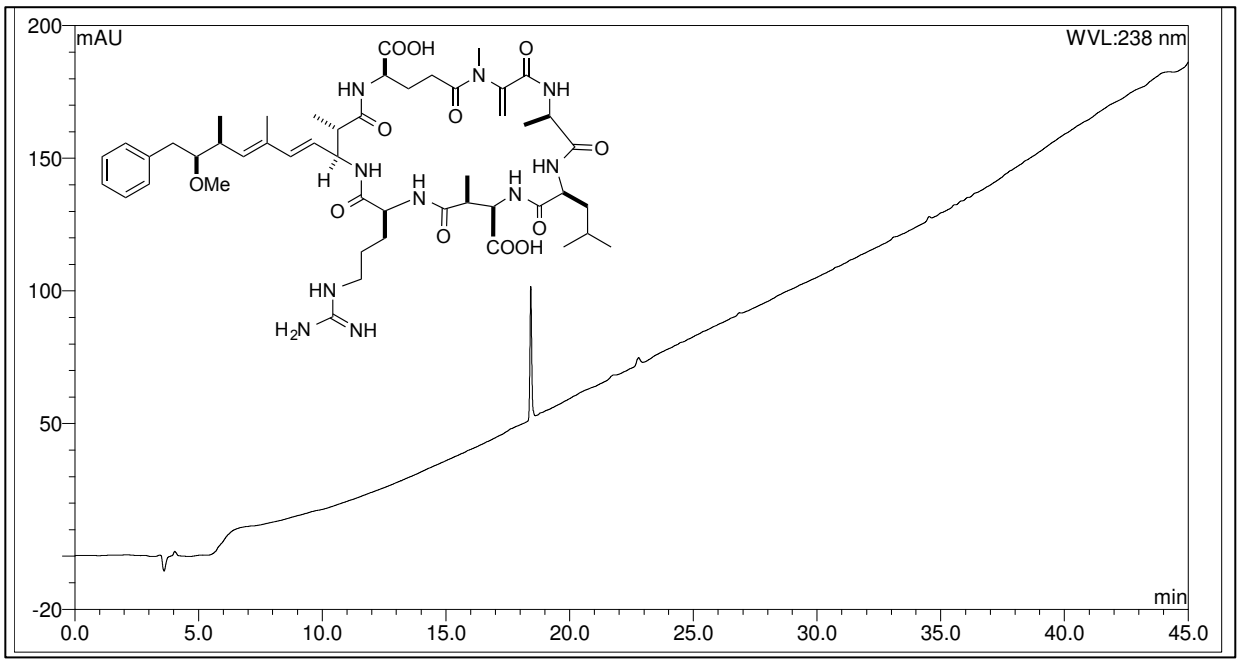

Chromatogram 33. HPLC trace of MC-LR

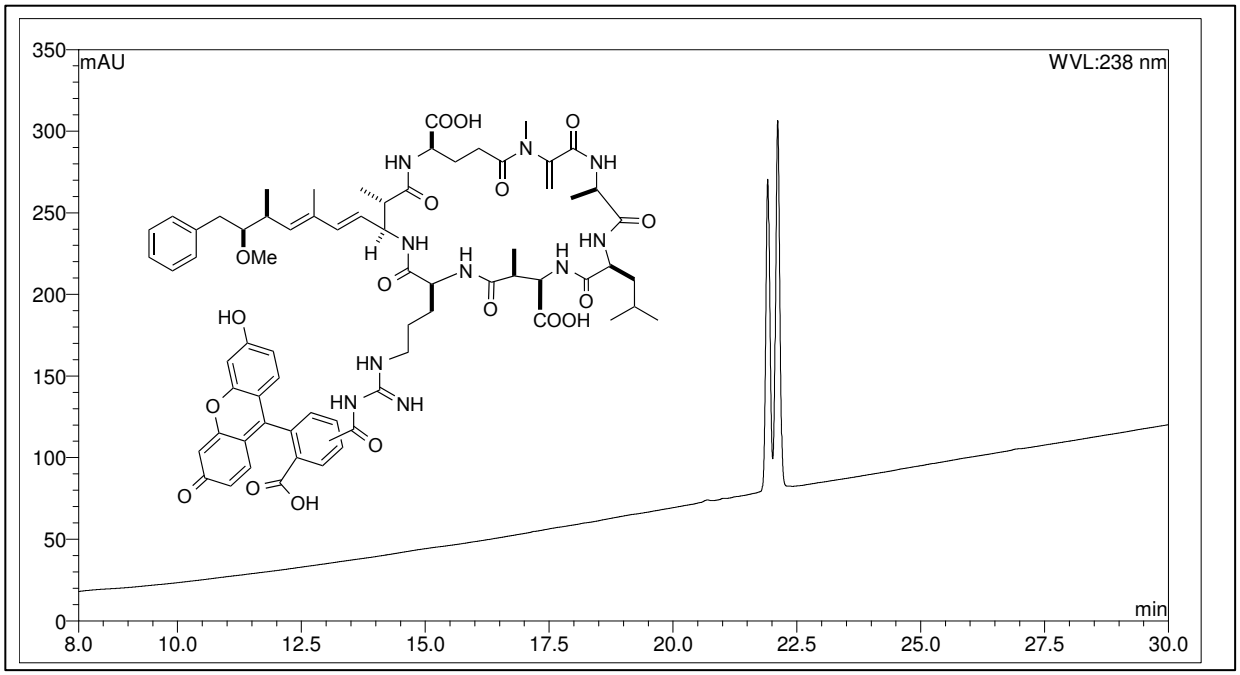

Chromatogram 34. HPLC trace of MC-LR-(6-FAM) (**3.1**)

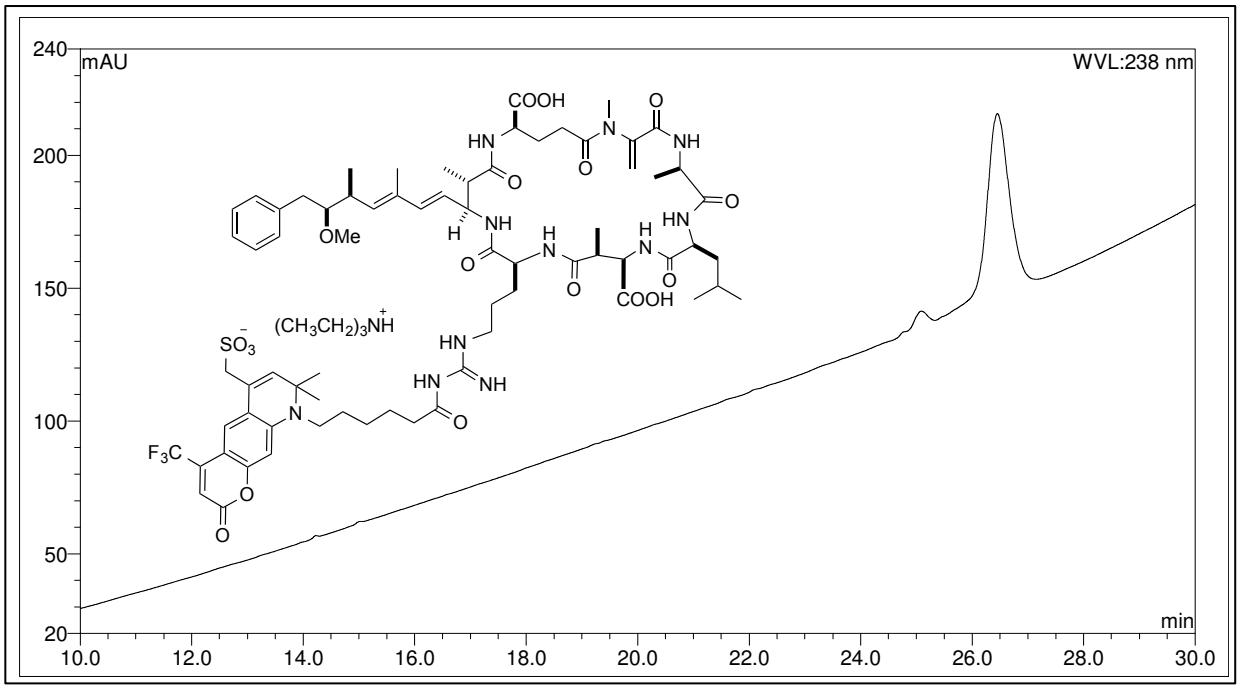

Chromatogram 35. HPLC trace of MC-LR-(Alexa-430) (**3.2**)

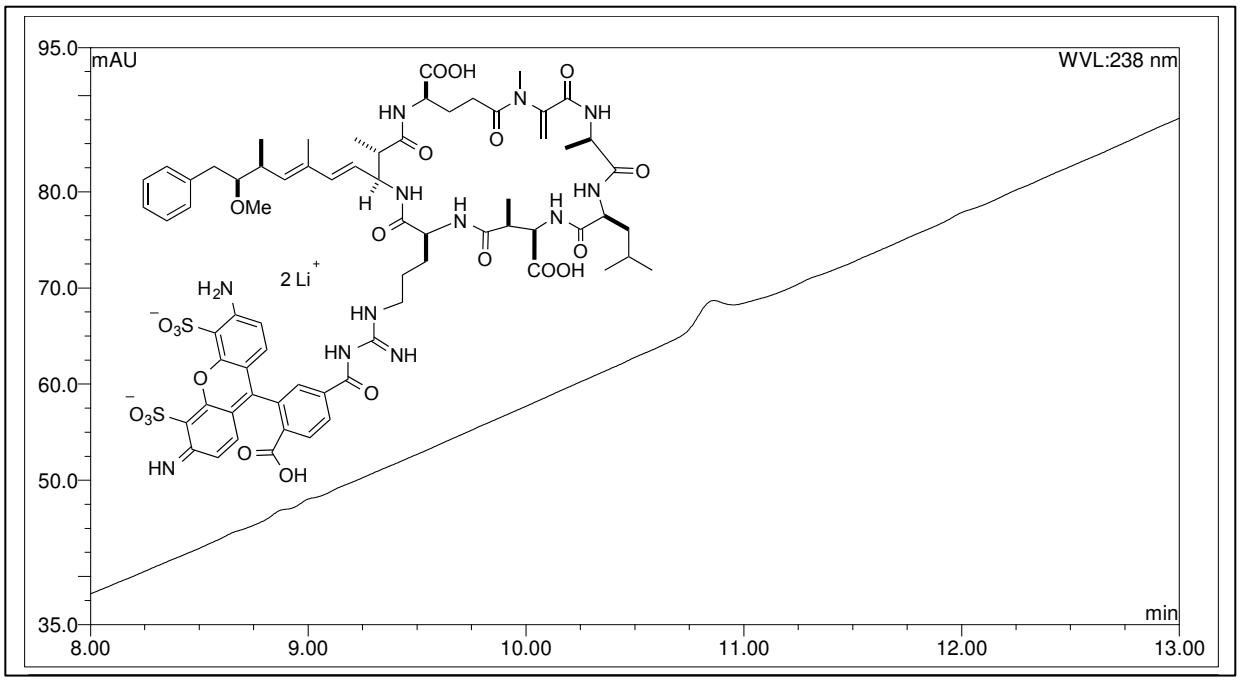

Chromatogram 36. HPLC trace of MC-LR-(Alexa-488) (**3.3**)

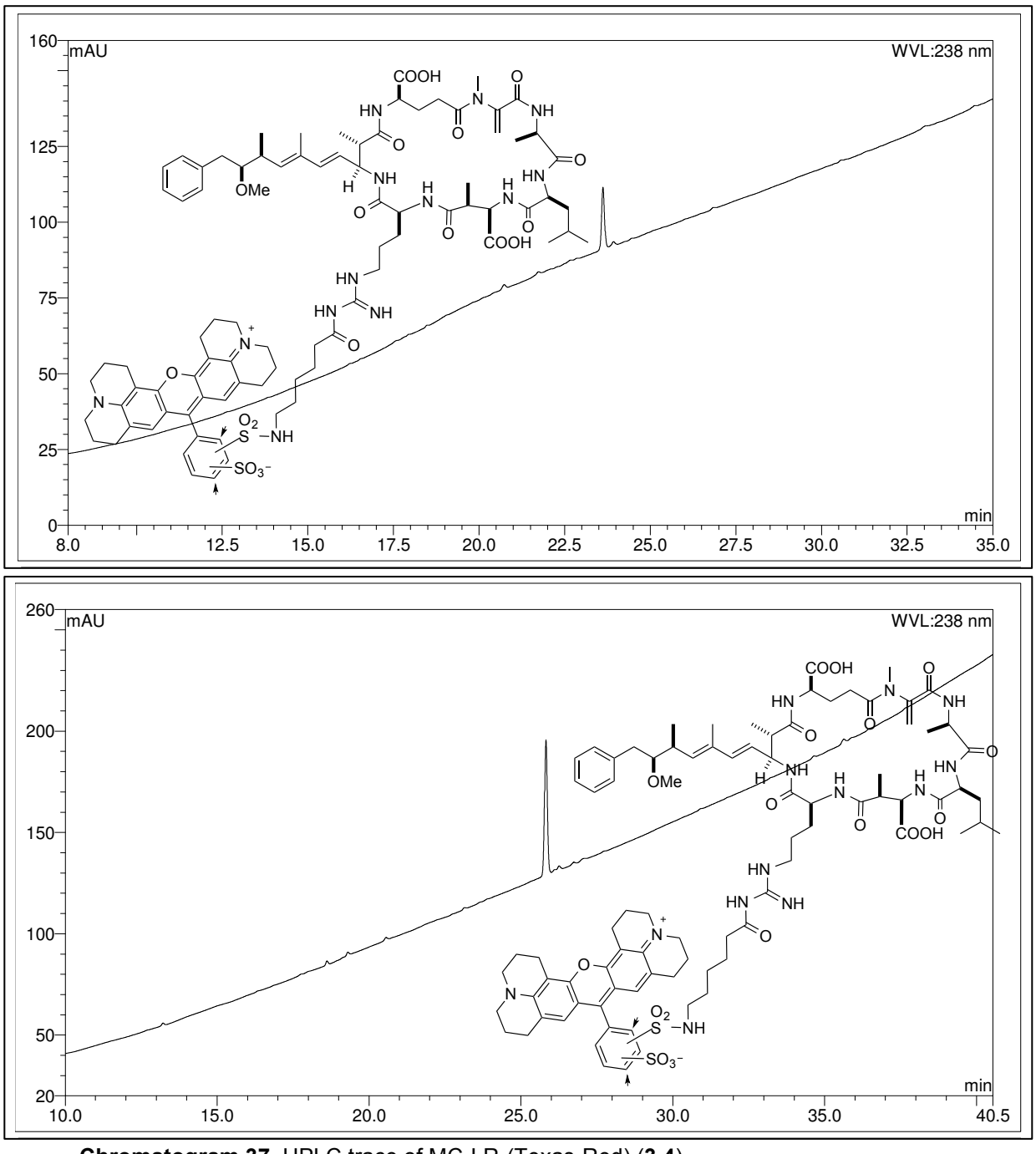

Chromatogram 37. HPLC trace of MC-LR-(Texas-Red) (**3.4**)

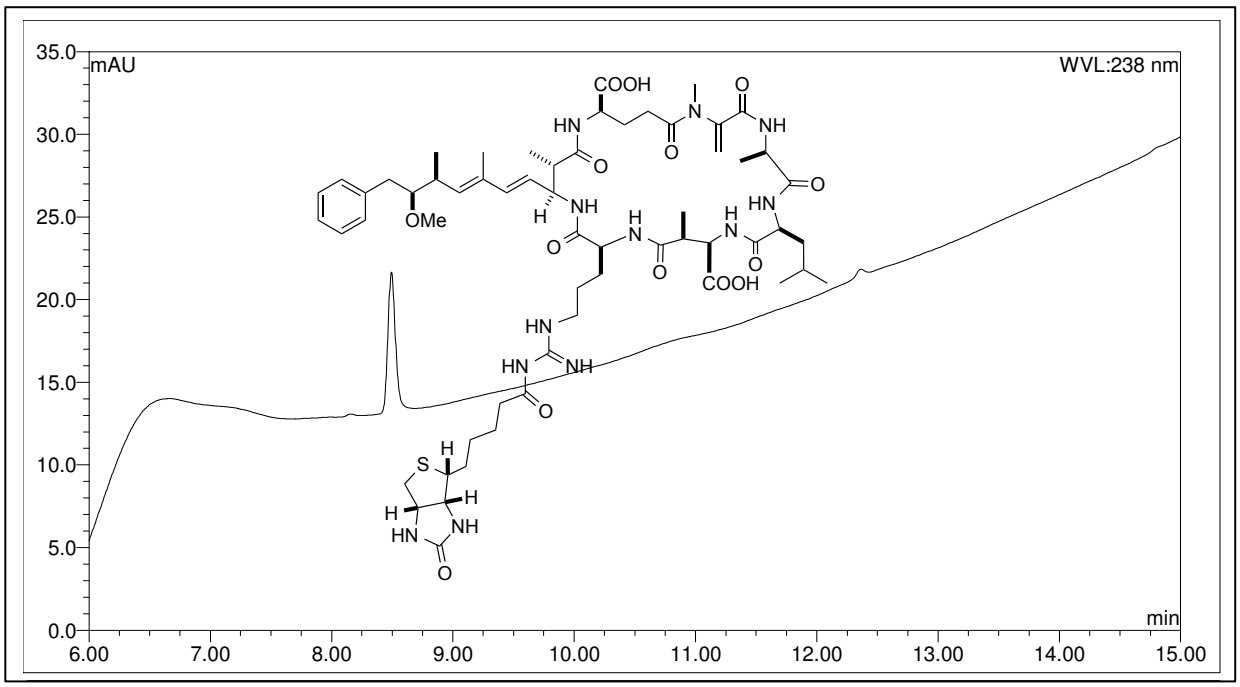

Chromatogram 38. HPLC trace of MC-LR-(Biotin) (**3.5**)

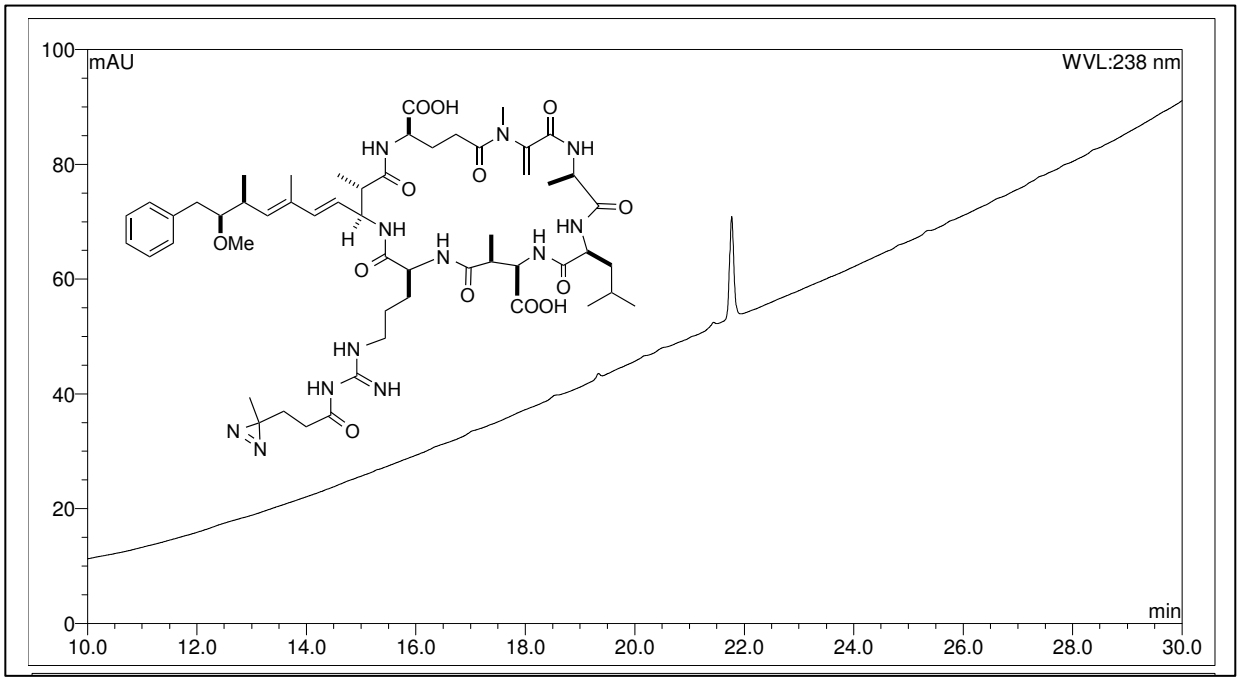

Chromatogram 39. HPLC trace of MC-LR-(DA) (**3.6**)

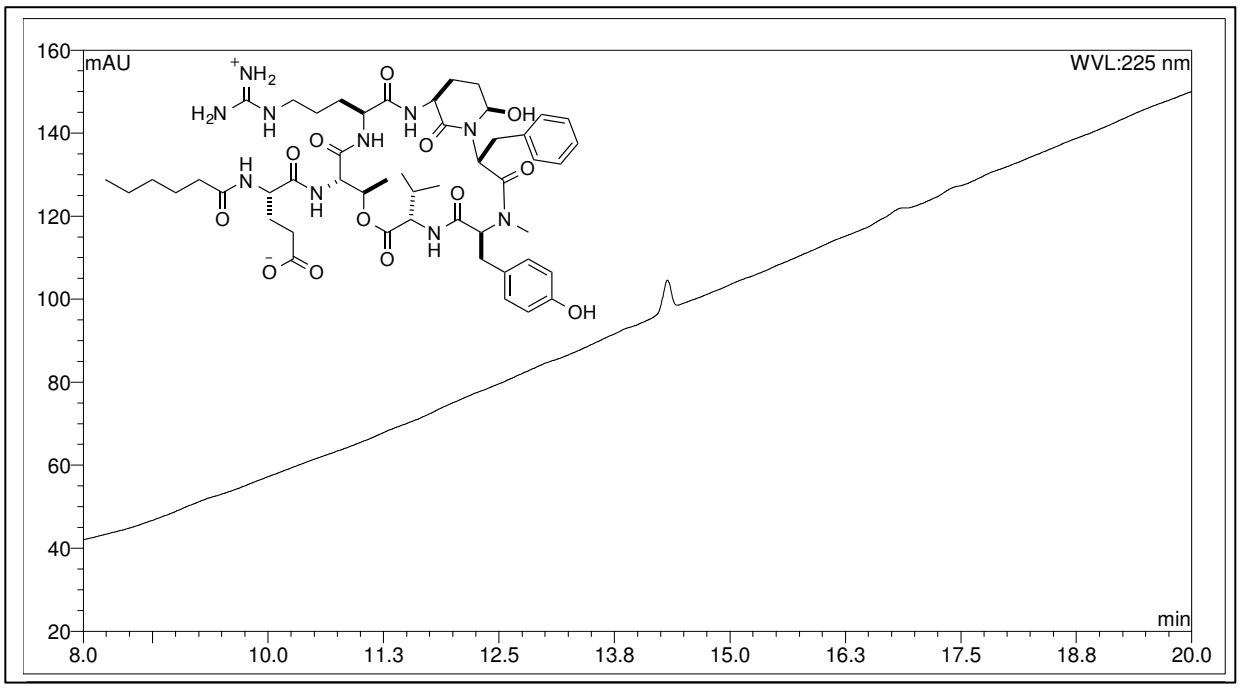

Chromatogram 40. HPLC trace of CP1020

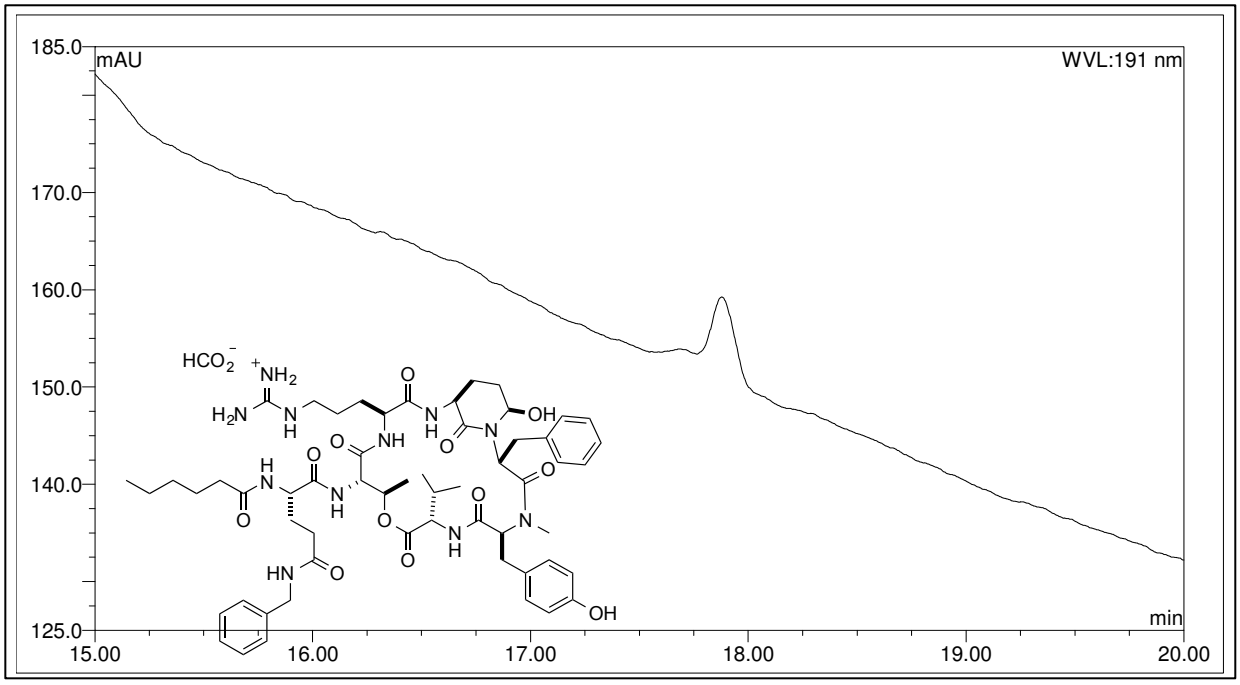

Chromatogram 41. HPLC trace of CP1020(Benzylamin) (**5.1**)

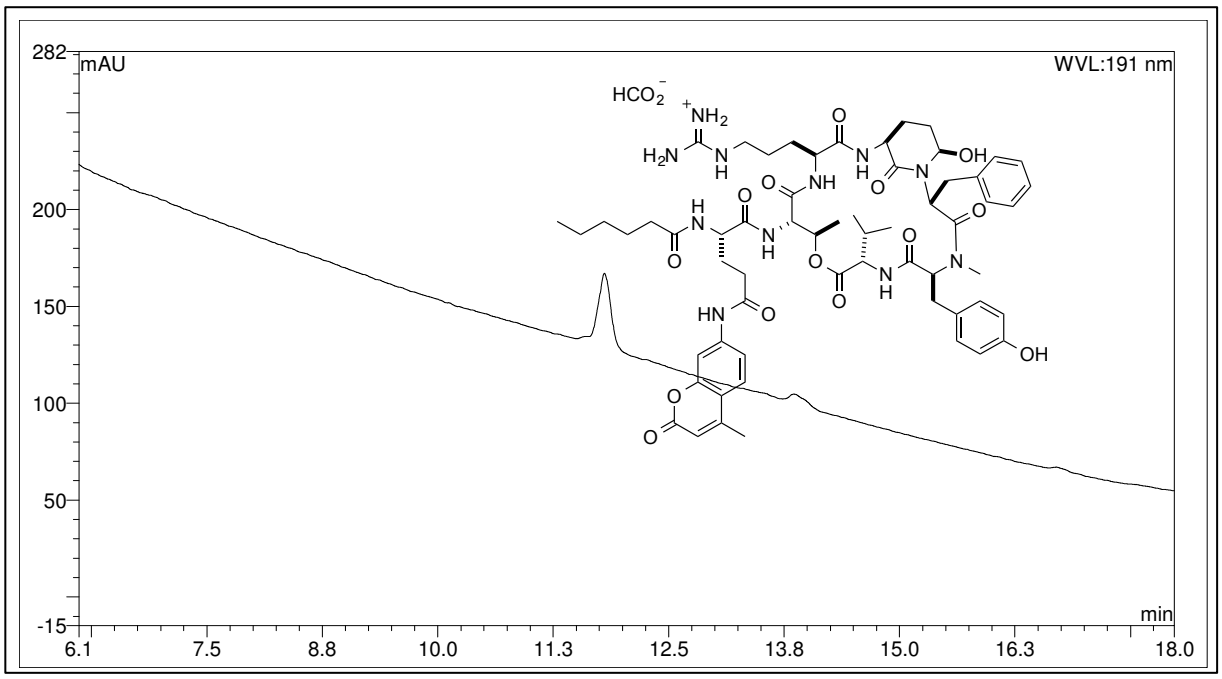

Chromatogram 42. HPLC trace of CP1020(Coumarin) (**5.2**)

7.2 NMR-Spectra

NMR spectrum 1. ^{1}H NMR spectrum of *N*-Ac-Gly-Val-Phe-Arg-Gly-OH (**2.7**) in DMSO-d_6 (400MHz)
NMR spectrum 2. ^{1}H NMR spectrum of *N*-Ac-Gly-Val-Glu-Phe-Arg-Gly-OH (**2.8**) in DMSO-d_6 (400MHz)
NMR spectrum 3. ^{1}H NMR spectrum of *N*-Ac-Gly-Lys-Phe-Arg-Gly-OH (**2.9**) in DMSO-d_6 (400MHz)
NMR spectrum 4. ^{1}H NMR spectrum of *N*-Ac-Gly-Phe-Arg-Arg-Gly-OH (**2.10**) in DMSO-d_6 (400MHz)
NMR spectrum 5. ^{1}H NMR spectrum of *N*-Ac-Gly-Phe-Val-Arg-Gly-Val-Gly-OH (**2.11**) in DMSO-d_6 (400MHz)
NMR spectrum 6. ^{1}H NMR spectrum of *N*-Ac-Gly-Val-Arg-Phe-Ser-Gly-OH (**2.12**) in DMSO-d_6 (400MHz)
NMR spectrum 7. ^{1}H NMR spectrum of *N*-Ac-Gly-Val-Cys-Arg-Phe-Gly-OH (**2.13**) in DMSO-d_6 (400MHz)
NMR spectrum 8. ^{1}H NMR spectrum of *N*-Ac-Gly-Phe-His-Ala-Arg-Gly-OH (**2.14**) in DMSO-d_6 (400MHz)
NMR spectrum 9. ^{1}H NMR spectrum of *N*-Ac-Gly-Val-Dha-Arg-Phe-Gly-OH (**2.15**) in DMSO-d_6 (400MHz)
NMR spectrum 10. ^{1}H NMR spectrum of MC-LR-(6-FAM) (**3.1**) in DMSO-d_6 (700MHz)
NMR spectrum 11. ^{1}H NMR spectrum of aeruginosin 828A in DMSO-d_6 (700MHz)
NMR spectrum 12. HMBC NMR spectrum of aeruginosin 828A in DMSO-d_6 (700MHz)
NRM spectrum 13. NOESY NMR spectrum of aeruginosin 828A in DMSO-d_6 (700MHz)
NMR spectrum 14. COSY NMR spectrum of aeruginosin 828A in DMSO-d_6 (700MHz)
NMR spectrum 15. HMQC NMR spectrum of aeruginosin 828A in DMSO-d_6 (700MHz)

NMR spectrum 1. ^{1}H NMR spectrum of *N*-Ac-Gly-Val-Phe-Arg-Gly-OH (**2.7**) in DMSO-d_6 (400MHz)

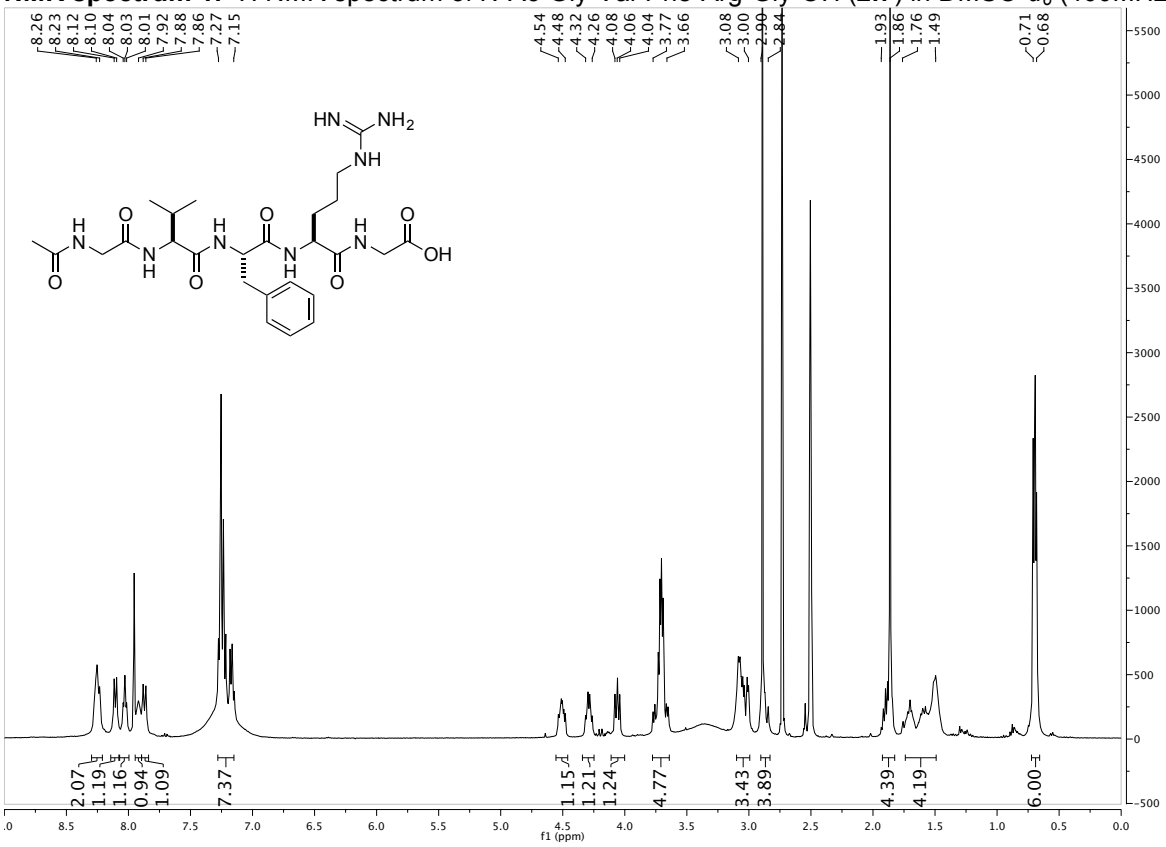

NMR spectrum 2. ^{1}H NMR spectrum of *N*-Ac-Gly-Val-Glu-Phe-Arg-Gly-OH (**2.8**) in DMSO-d_6 (400MHz)

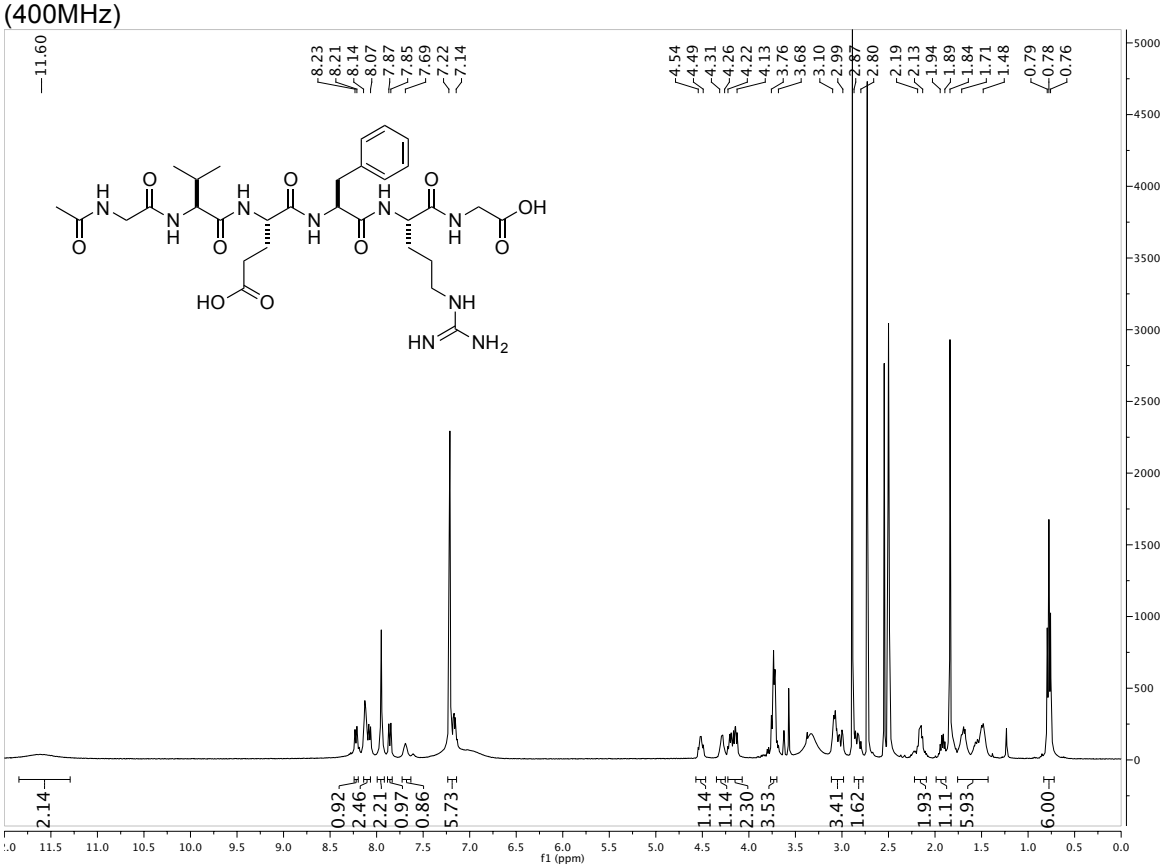

NMR spectrum 3. ^{1}H NMR spectrum of *N*-Ac-Gly-Lys-Phe-Arg-Gly-OH (**2.9**) in DMSO-d_6 (400MHz)

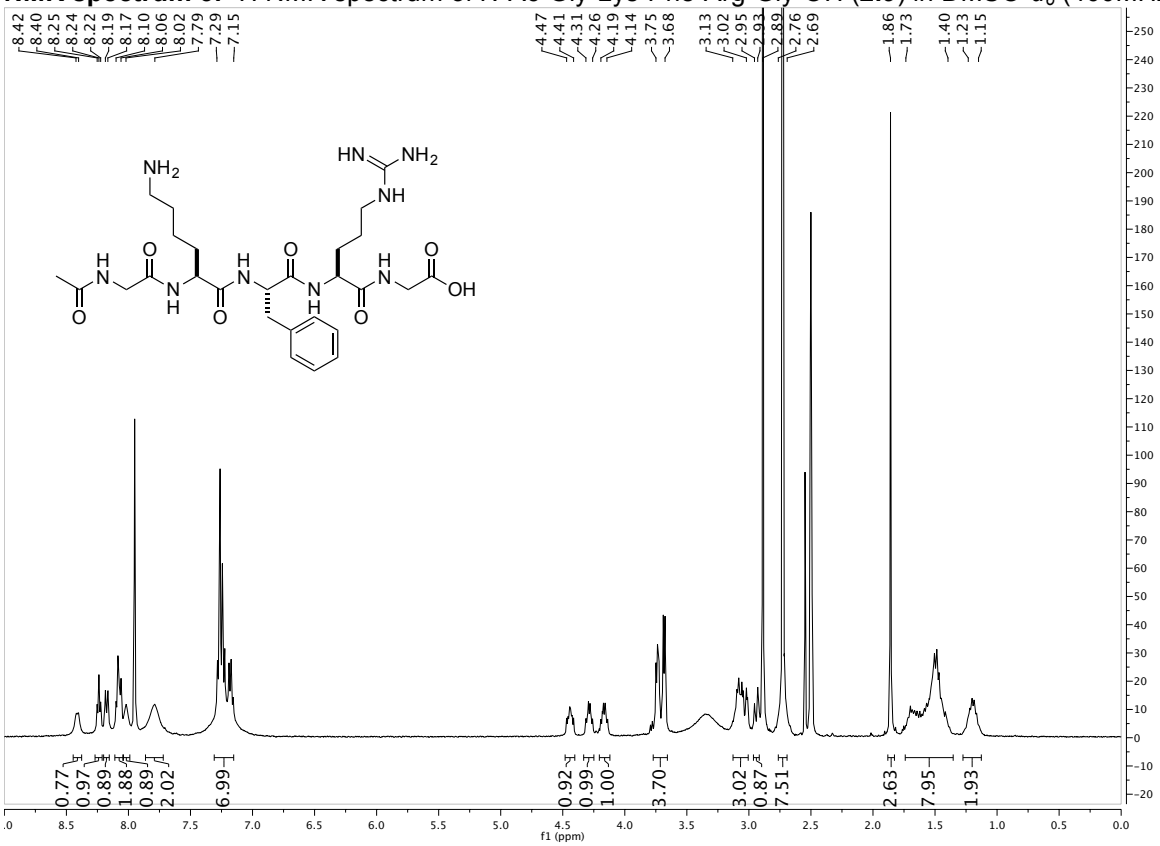

NMR spectrum 4. ^{1}H NMR spectrum of *N*-Ac-Gly-Phe-Arg-Arg-Gly-OH (**2.10**) in DMSO-d_6 (400MHz)

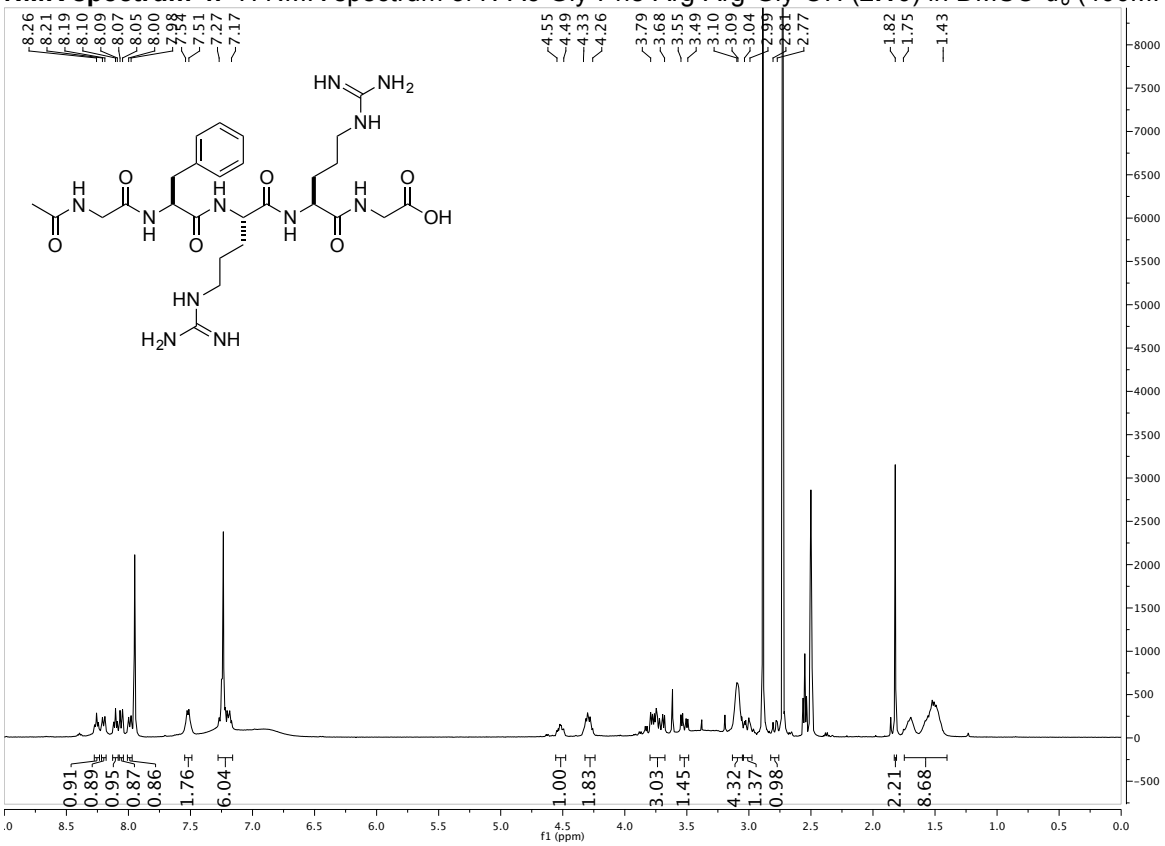

NMR spectrum 5. ^{1}H NMR spectrum of *N*-Ac-Gly-Phe-Val-Arg-Gly-Val-Gly-OH (**2.11**) in DMSO-d_6 (400MHz)

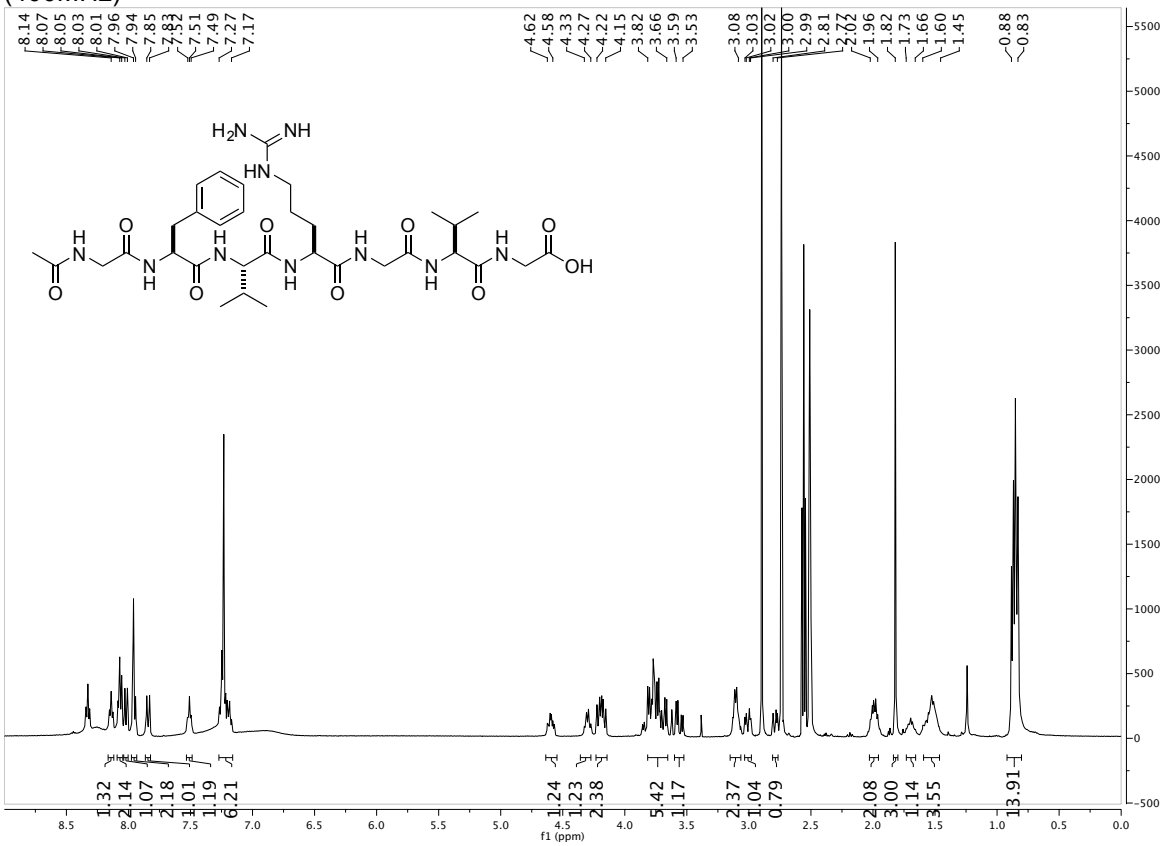

NMR spectrum 6. ^{1}H NMR spectrum of *N*-Ac-Gly-Val-Arg-Phe-Ser-Gly-OH (**2.12**) in DMSO-d_6 (400MHz)

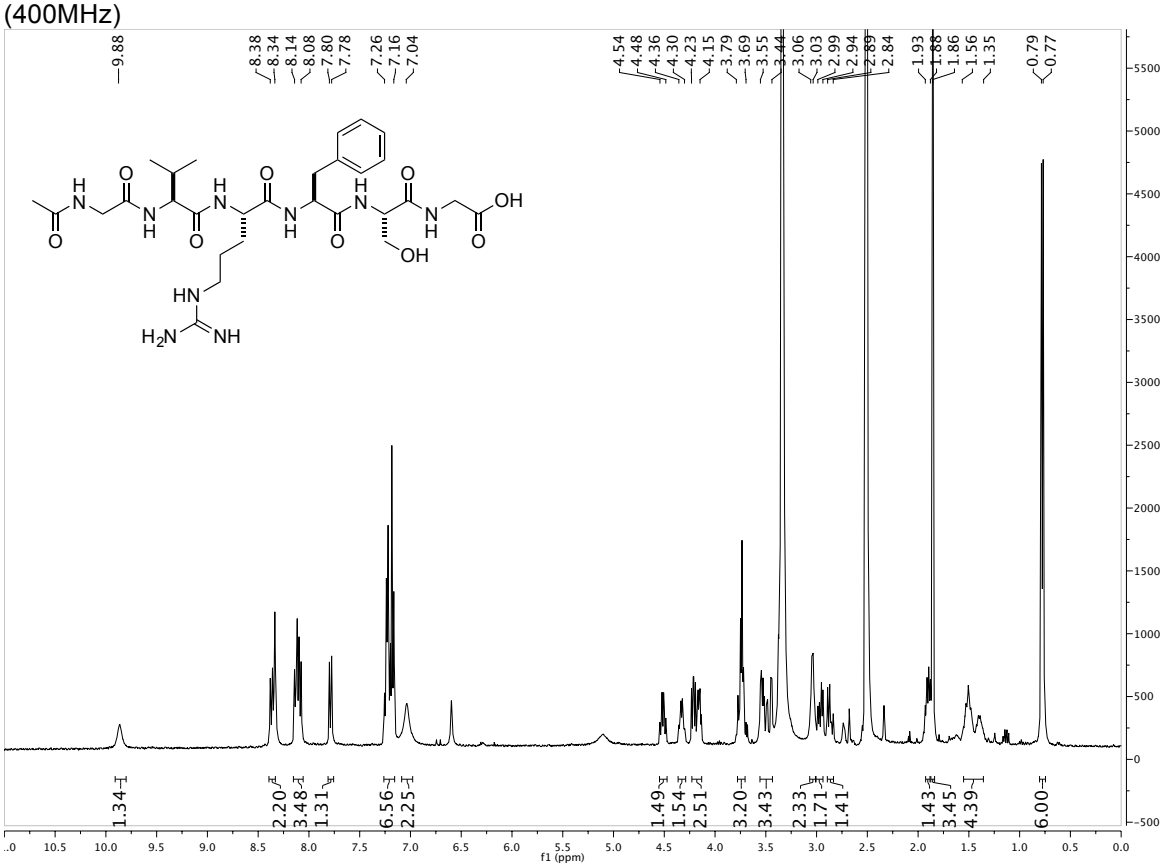

NMR spectrum 7. ^{1}H NMR spectrum of *N*-Ac-Gly-Val-Cys-Arg-Phe-Gly-OH (**2.13**) in DMSO-d_6 (400MHz)

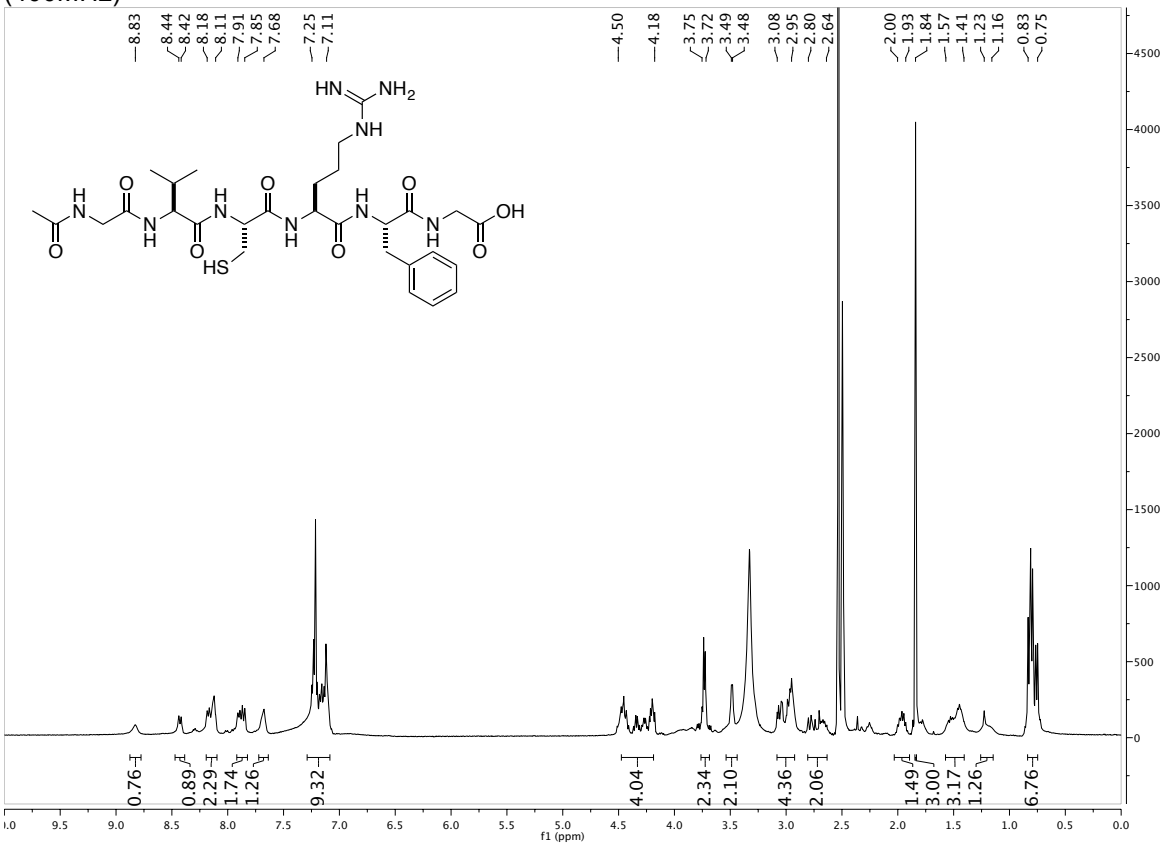

NMR spectrum 8. ^{1}H NMR spectrum of *N*-Ac-Gly-Phe-His-Ala-Arg-Gly-OH (**2.14**) in DMSO-d_6 (400MHz)

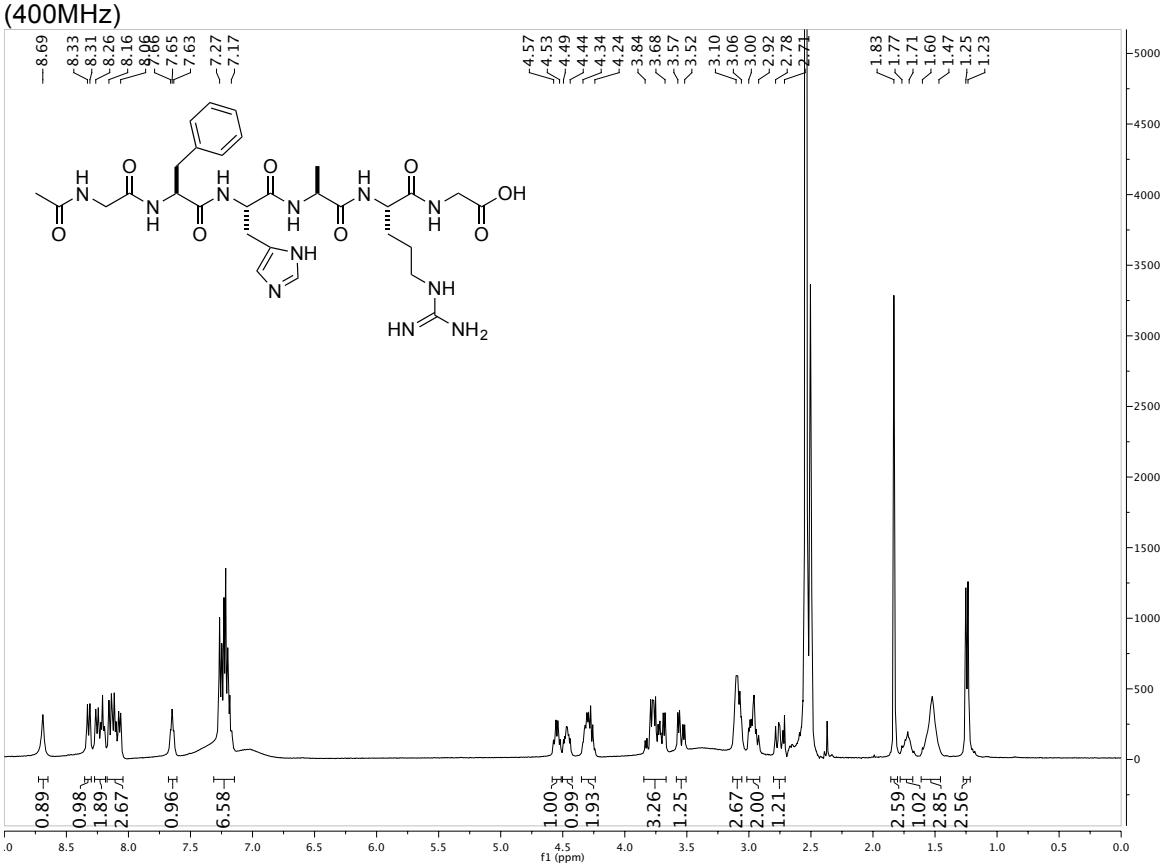

NMR spectrum 9. ^{1}H NMR spectrum of *N*-Ac-Gly-Val-Dha-Arg-Phe-Gly-OH (**2.15**) in DMSO-d_6 (400MHz)

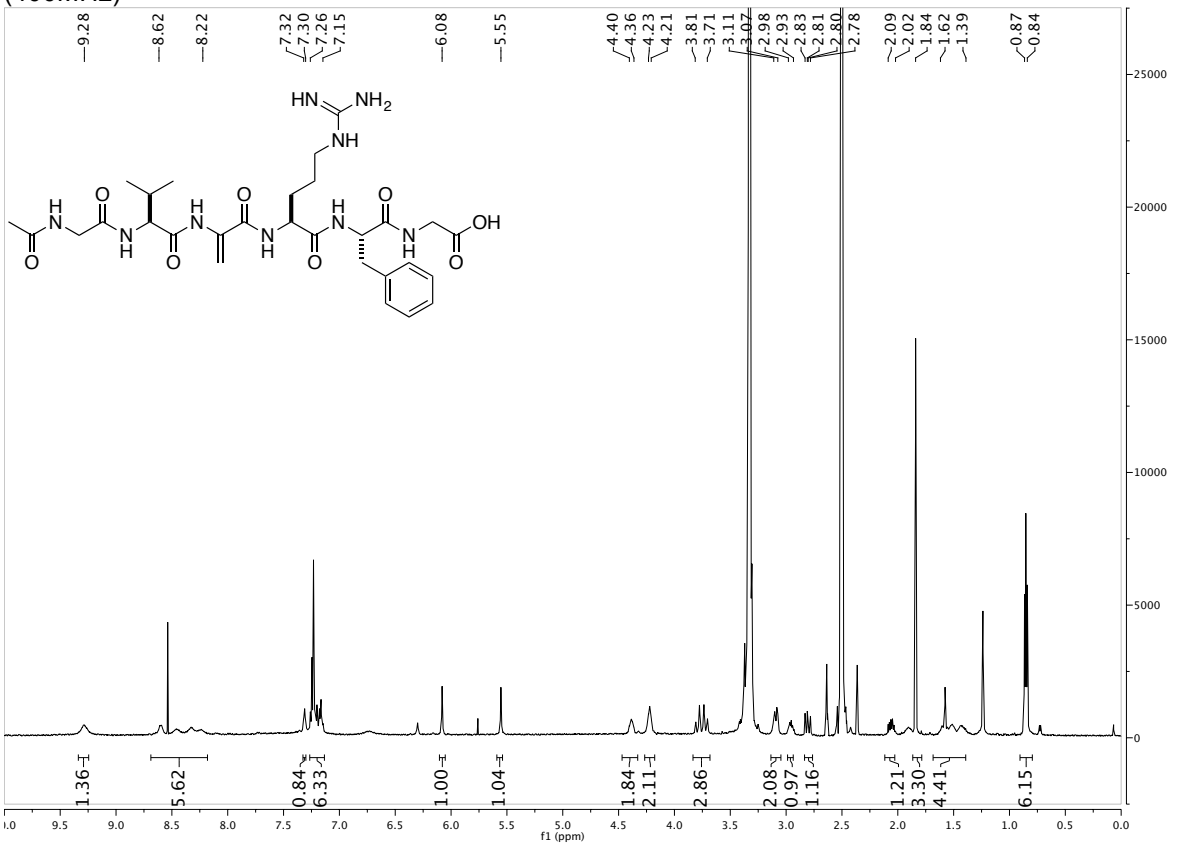

NMR spectrum 10. ^{1}H NMR spectrum of MC-LR-(6-FAM) (**3.1**) in DMSO-d_6 (700MHz)

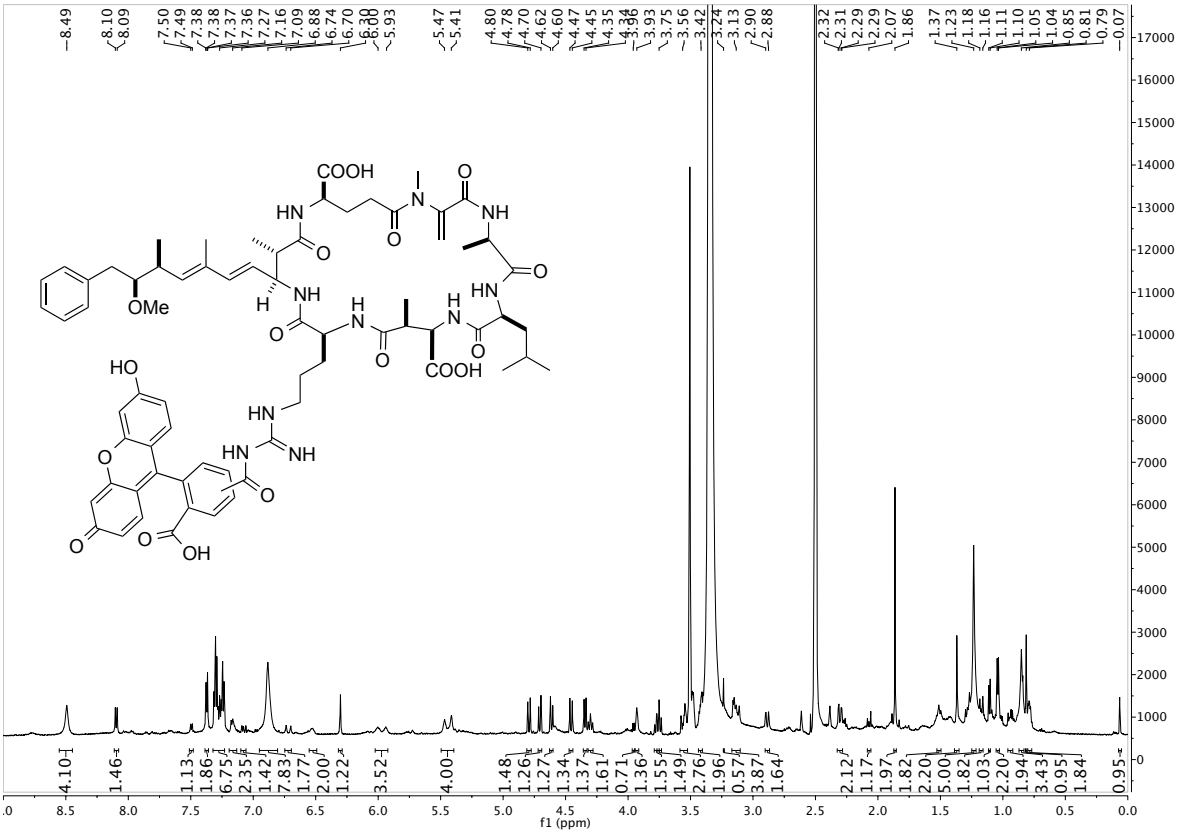

NMR spectrum 11. ^{1}H NMR spectrum of aeruginosin 828A in DMSO-d_6 (700MHz)

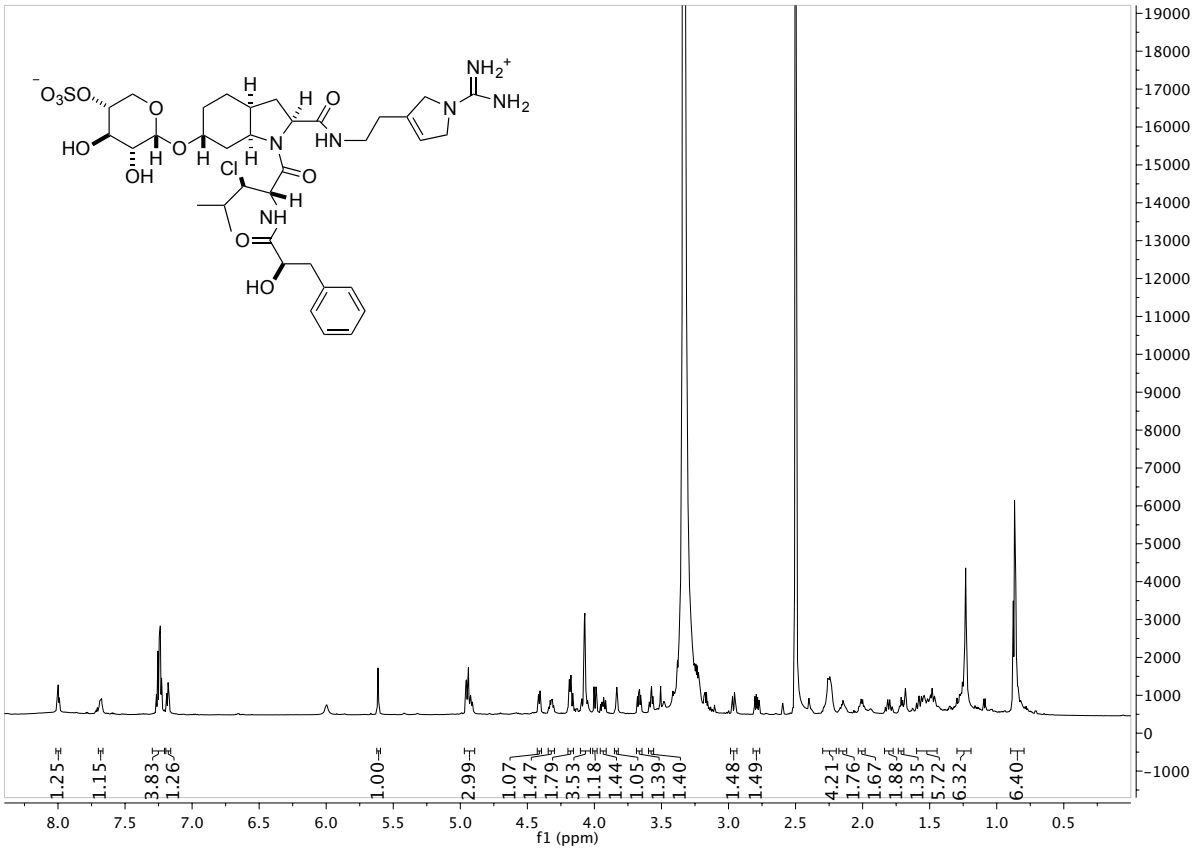

NMR spectrum 12. HMBC NMR spectrum of aeruginosin 828A in DMSO-d_6 (700MHz)

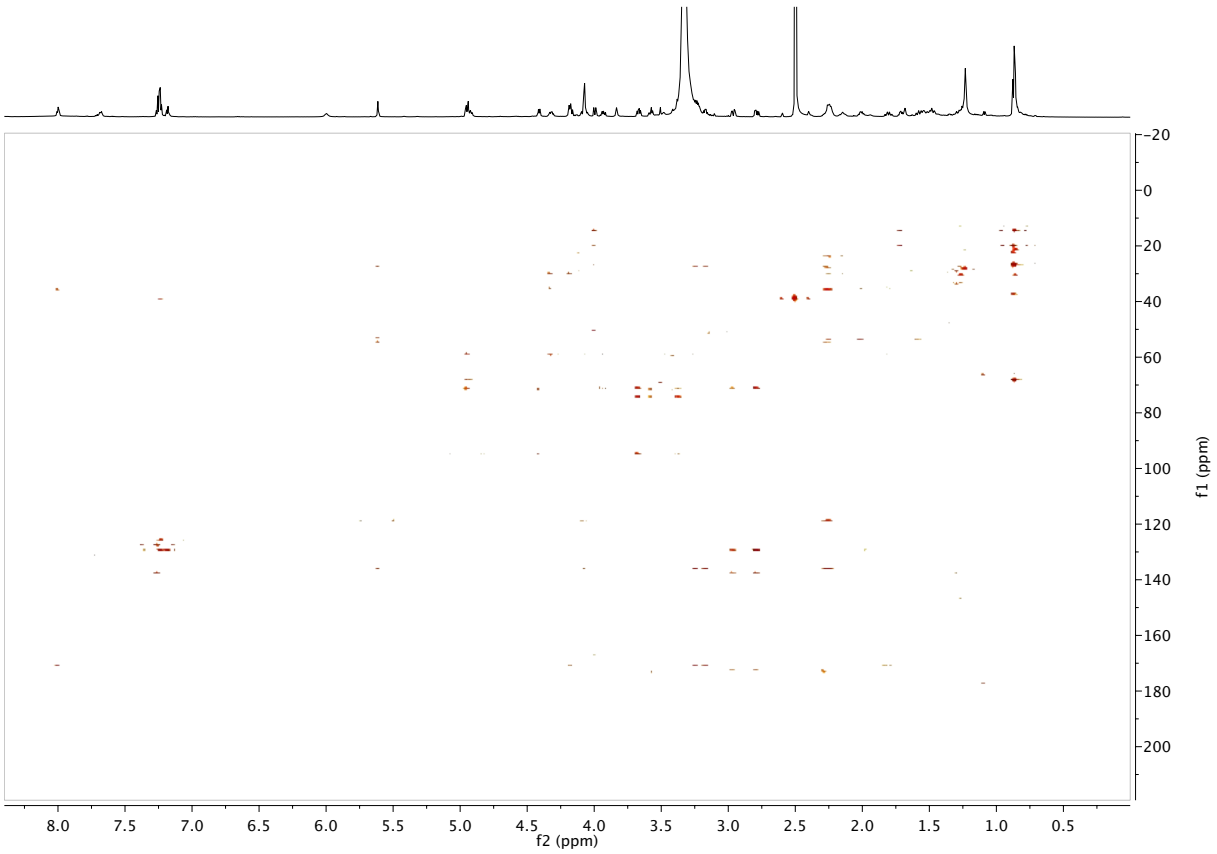

NRM spectrum 13. NOESY NMR spectrum of aeruginosin 828A in DMSO-d_6 (700MHz)

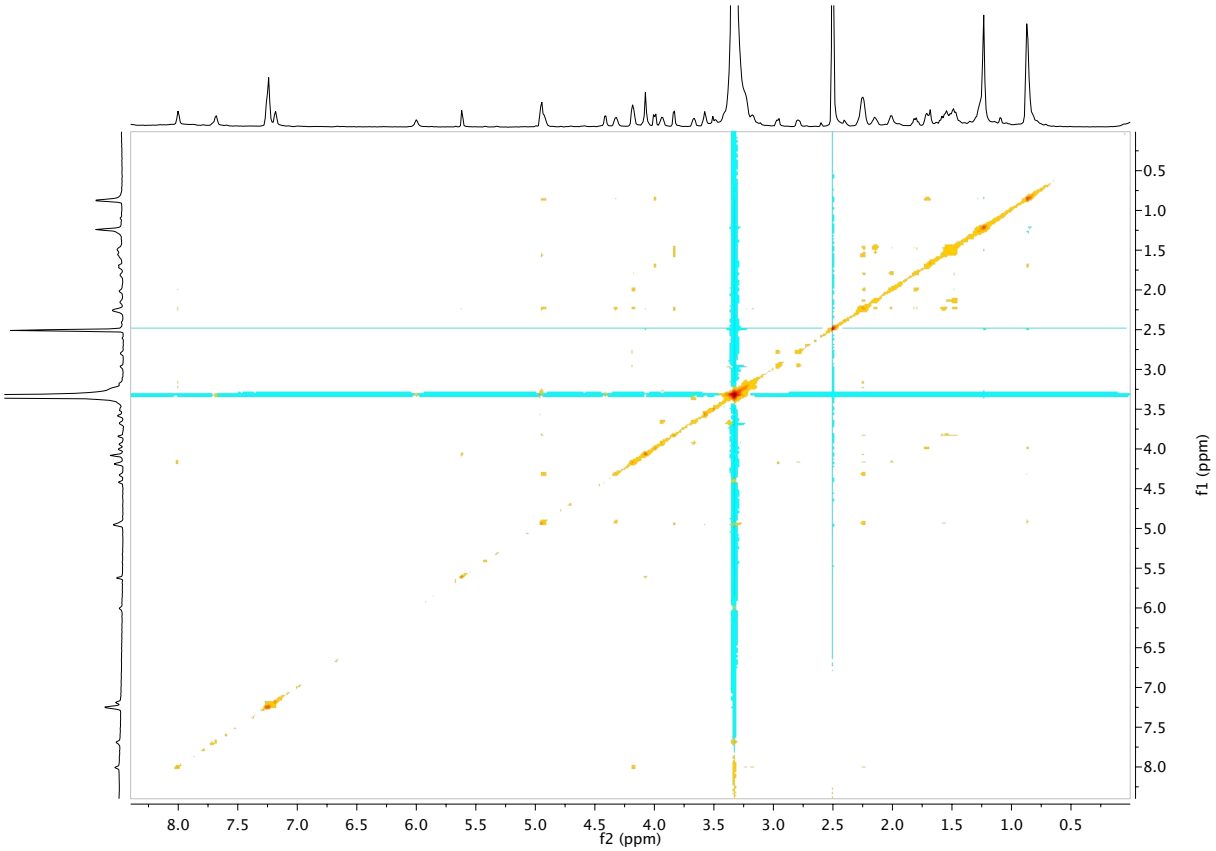

NMR spectrum 14. COSY NMR spectrum of aeruginosin 828A in DMSO-d_6 (700MHz)

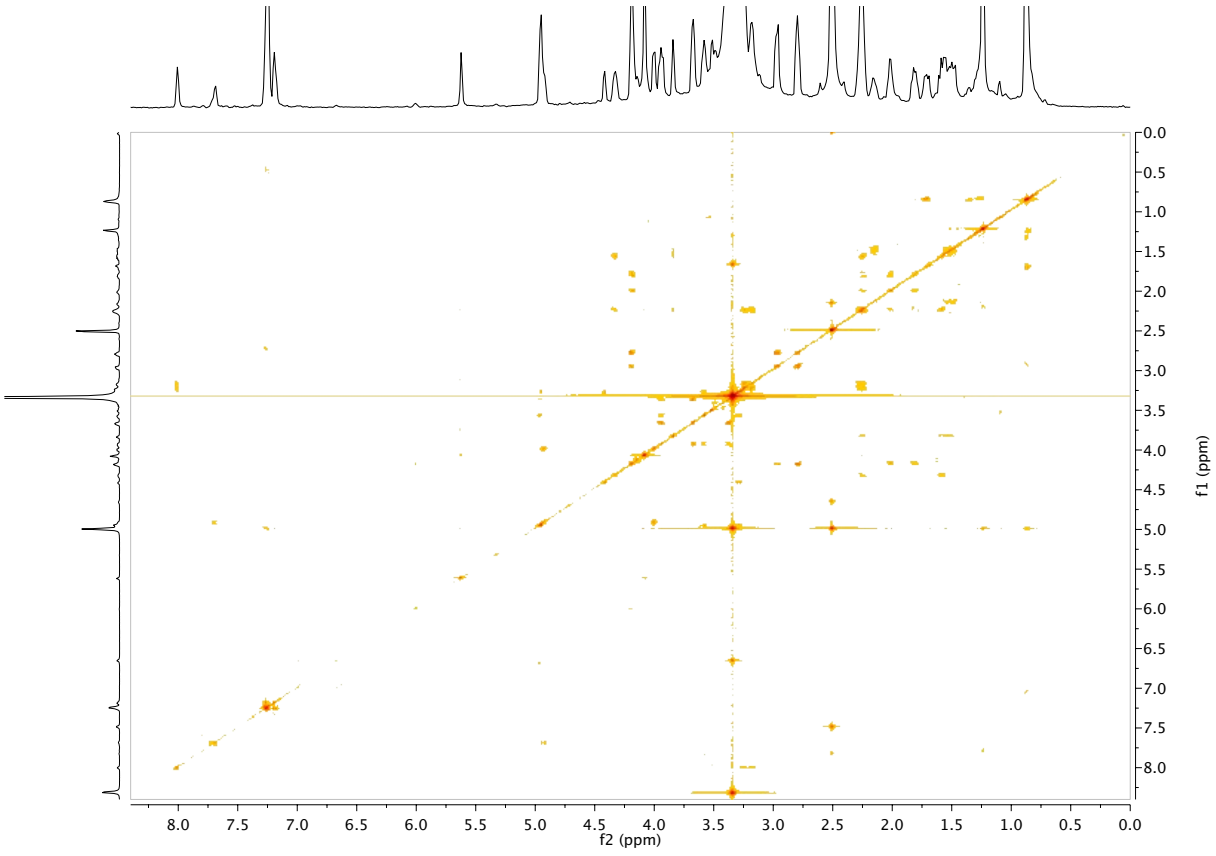

NMR spectrum 15. HMQC NMR spectrum of aeruginosin 828A in DMSO-d_6 (700MHz)

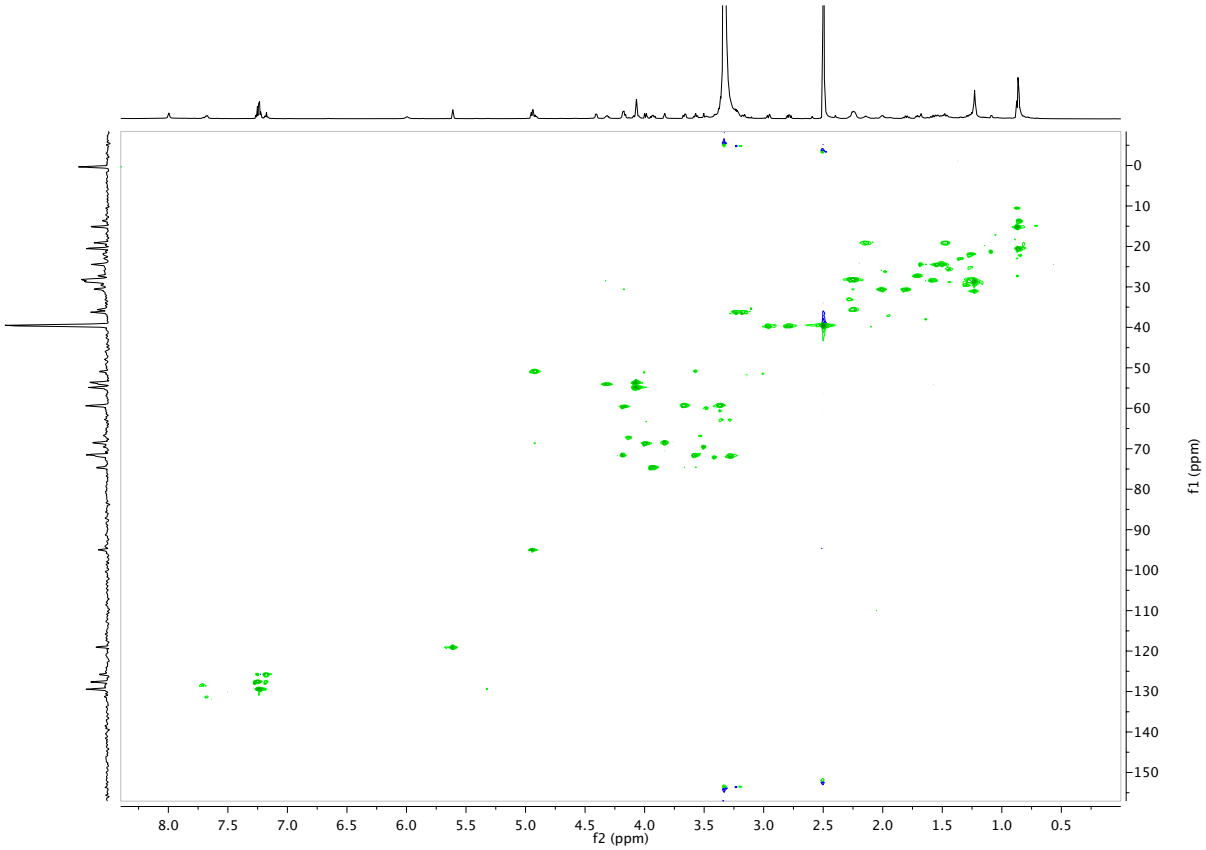
f2 (ppm)
f1 (ppm)

7.3 HRMS/MS-Spectra

HRMS spectrum 1. Positive ionisation of Bz-Arg(Dansyl)-OMe (**2.1**)
HRMS spectrum 2. Positive ionisation of Bz-Arg(*N*-succinimid)-OEt (**2.2**)
HRMS spectrum 3. Positive ionisation of Boc-Arg(*N*-succinimid)-OH (**2.3**)
HRMS spectrum 4. Negative ionisation of *N*-Ac-Arg(Alexa488)-OH (**2.4**)
HRMS spectrum 5. Positive ionisation of N-Ac-Arg(6-FAM)-OH (**2.5**)
HRMS spectrum 6. Positive ionisation of *N*-Ac-Arg(coumarin)-OH (**2.6**)
HRMS spectrum 7. Positive ionisation of *N*-Ac-Gly-Val-Phe-Arg-Gly-OH (**2.7**)
HRMS spectrum 8. Positive ionisation of *N*-Ac-Gly-Val-Glu-Phe-Arg-Gly-OH (**2.8**)
HRMS spectrum 9. Positive ionisation of *N*-Ac-Gly-Lys-Phe-Arg-Gly-OH (**2.9**)
HRMS spectrum 10. Positive ionisation of *N*-Ac-Gly-Phe-Arg-Arg-Gly-OH (**2.10**)
HRMS spectrum 11. Positive ionisation of *N*-Ac-Gly-Phe-Val-Arg-Gly-Val-Gly-OH (**2.11**)
HRMS spectrum 12. Positive ionisation of *N*-Ac-Gly-Val-Arg-Phe-Ser-Gly-OH (**2.12**)
HRMS spectrum 13. Positive ionisation of *N*-Ac-Gly-Val-Cys-Arg-Phe-Gly-OH (**2.13**)
HRMS spectrum 14. Positive ionisation of *N*-Ac-Gly-Phe-His-Ala-Arg-Gly-OH (**2.14**)
HRMS spectrum 15. Positive ionisation of *N*-Ac-Gly-Val-Dha-Arg-Phe-Gly-OH (**2.15**)
HRMS spectrum 16. Positive ionisation of *N*-Ac-Gly-Val-Phe-Arg(6-FAM)-Gly-OH (**2.16**)
HRMS spectrum 17. Negative ionisation of *N*-Ac-Gly-Val-Glu-Phe-Arg(6-FAM)-Gly-OH (**2.17**)
HRMS spectrum 18. Negative ionisation of *N*-Ac-Gly-Val-Arg(6-FAM)-Phe-Ser-Gly-OH (**2.18**)
HRMS spectrum 19. Positive ionisation of *N*-Ac-Gly-Phe-His-Ala-Arg(6-FAM)-Gly-OH (**2.19**)
HRMS spectrum 20. Positive ionisation of *N*-Ac-Gly-Phe-Arg(6-FAM)-Arg(6-FAM)-Gly-OH (**2.20**)
HRMS spectrum 21. Positive ionisation of *N*-Ac-Gly-Phe-Val-Arg(6-FAM)-Gly-Val-Gly-OH (**2.21**)
HRMS spectrum 22. Positive ionisation of *N*-Ac-Gly-Val-Dha-Arg(6-FAM)-Phe-Gly-OH (**2.22**)
HRMS spectrum 23. Positive ionisation of *N*-Ac-Gly-Val-Cys(6-FAM)-Arg-Phe-Gly-OH (**2.23**)
HRMS spectrum 24. Positive ionisation of *N*-Ac-Gly-Lys(6-FAM)-Phe-Arg-Gly-OH (**2.24**)
HRMS spectrum 25. Positive ionisation of *N*-Ac-Gly-Phe-Val-Arg(Biotin)-Gly-Val-Gly-OH (**2.25**)
HRMS spectrum 26. Positive ionisation of *N*-Ac-Gly-Val-Glu-Phe-Arg(Biotin)-Gly-OH (**2.26**)
HRMS spectrum 27. Positive ionisation of *N*-Ac-Gly-Phe-Val-Arg(DA)-Gly-Val-Gly-OH (**2.27**)
HRMS spectrum 28. Positive ionisation of *N*-Ac-Gly-Val-Glu-Phe-Arg(DA)-Gly-OH (**2.28**)
HRMS spectrum 29. Positive ionisation of Pyr-His-Trp-Ser-Tyr-D-Leu-Leu-Arg(6-FAM)-Pro-NHEt (**2.30**)
HRMS spectrum 30. Positive ionisation of *N*-Ac-Gly-Lys(Boc)-Phe-Arg-Gly-OH (**2.31**)
HRMS spectrum 31. Positive ionisation of *N*-Ac-Gly-Lys(Boc)-Phe-Arg(6-FAM)-Gly-OH (**2.32**)
HRMS spectrum 32. Positive ionisation of *N*-Ac-Gly-Lys-Phe-Arg(6-FAM)-Gly-OH (**2.33**)
HRMS spectrum 33. Positive ionisation of MC-LR-(6-FAM) (**3.1**)
HRMS spectrum 34. Negative ionisation of MC-LR-(Alexa-430) (**3.2**)
HRMS spectrum 35. Negative ionisation of MC-LR-(Alexa-488) (**3.3**)
HRMS spectrum 36. Positive ionisation of MC-LR-(Texas-Red) (**3.4**)
HRMS spectrum 37. Positive ionisation of MC-LR-(Biotin) (**3.5**)
HRMS spectrum 38. Positive ionisation of MC-LR-(DA) (**3.6**)

HRMS spectrum 39. Positive ionisation of CP1020(Benzylamin) (**5.1**)

MS spectrum 40. Positive ionisation of CP1020(Coumarin) (**5.2**)

HRMS spectrum 1. Positive ionisation of Bz-Arg(Dansyl)-OMe (**2.1**)

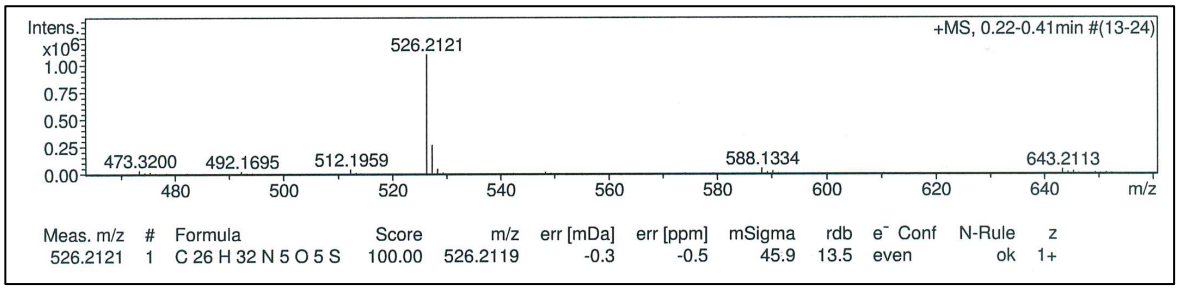

Meas. m/z	#	Formula	Score	m/z	err [mDa]	err [ppm]	mSigma	rdb	e⁻ Conf	N-Rule	z
526.2121	1	C 26 H 32 N 5 O 5 S	100.00	526.2119	-0.3	-0.5	45.9	13.5	even	ok	1+

HRMS spectrum 2. Positive ionisation of Bz-Arg(*N*-succinimid)-OEt (**2.2**)

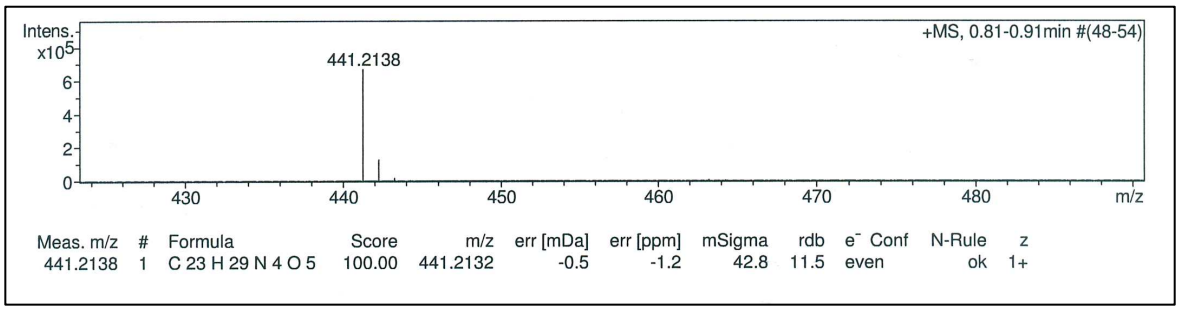

Meas. m/z	#	Formula	Score	m/z	err [mDa]	err [ppm]	mSigma	rdb	e⁻ Conf	N-Rule	z
441.2138	1	C 23 H 29 N 4 O 5	100.00	441.2132	-0.5	-1.2	42.8	11.5	even	ok	1+

HRMS spectrum 3. Positive ionisation of Boc-Arg(*N*-succinimid)-OH (**2.3**)

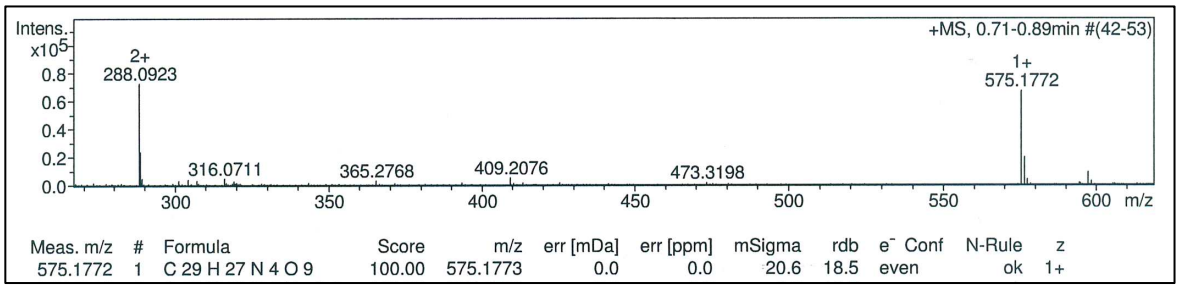

Meas. m/z	#	Formula	Score	m/z	err [mDa]	err [ppm]	mSigma	rdb	e⁻ Conf	N-Rule	z
575.1772	1	C 29 H 27 N 4 O 9	100.00	575.1773	0.0	0.0	20.6	18.5	even	ok	1+

HRMS spectrum 4. Negative ionisation of *N*-Ac-Arg(Alexa488)-OH (**2.4**)

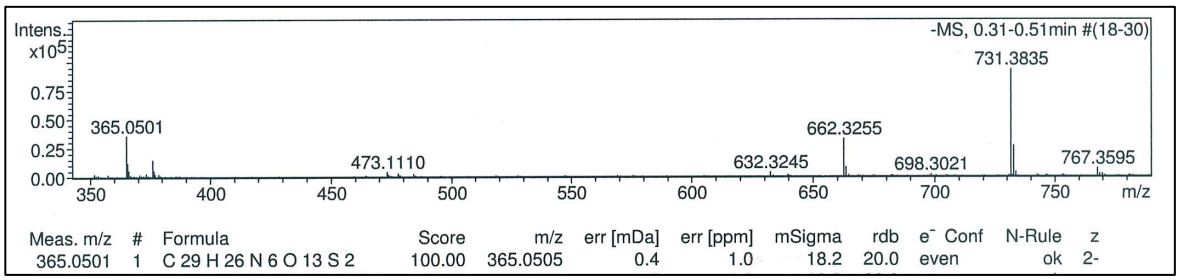

Meas. m/z	#	Formula	Score	m/z	err [mDa]	err [ppm]	mSigma	rdb	e⁻ Conf	N-Rule	z
365.0501	1	C 29 H 26 N 6 O 13 S 2	100.00	365.0505	0.4	1.0	18.2	20.0	even	ok	2-

HRMS spectrum 5. Positive ionisation of N-Ac-Arg(6-FAM)-OH (**2.5**)

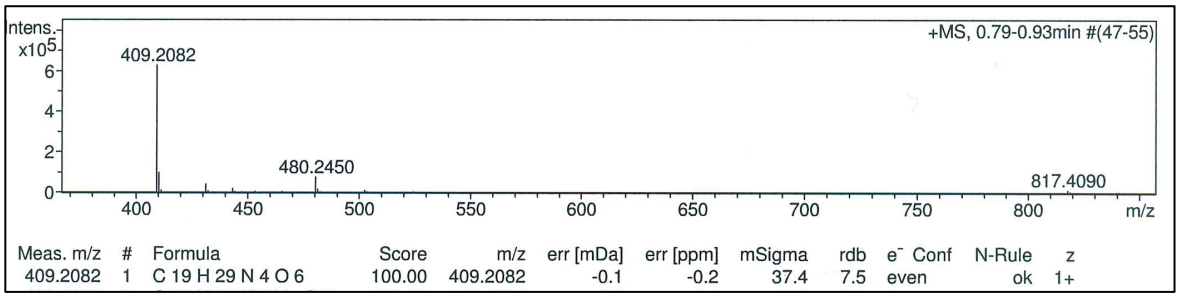

Meas. m/z	#	Formula	Score	m/z	err [mDa]	err [ppm]	mSigma	rdb	e⁻ Conf	N-Rule	z
409.2082	1	C 19 H 29 N 4 O 6	100.00	409.2082	-0.1	-0.2	37.4	7.5	even	ok	1+

HRMS spectrum 6. Positive ionisation of *N*-Ac-Arg(coumarin)-OH (**2.6**)

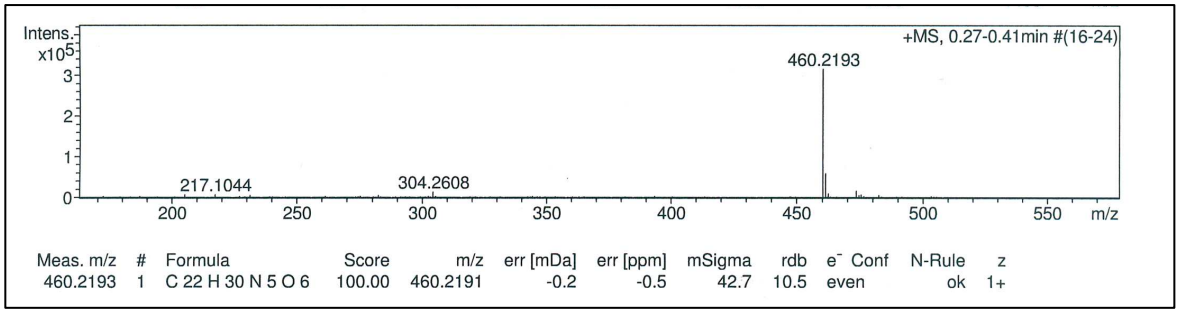

Meas. m/z	#	Formula	Score	m/z	err [mDa]	err [ppm]	mSigma	rdb	e⁻ Conf	N-Rule	z
460.2193	1	C 22 H 30 N 5 O 6	100.00	460.2191	-0.2	-0.5	42.7	10.5	even	ok	1+

HRMS spectrum 7. Positive ionisation of *N*-Ac-Gly-Val-Phe-Arg-Gly-OH (**2.7**)

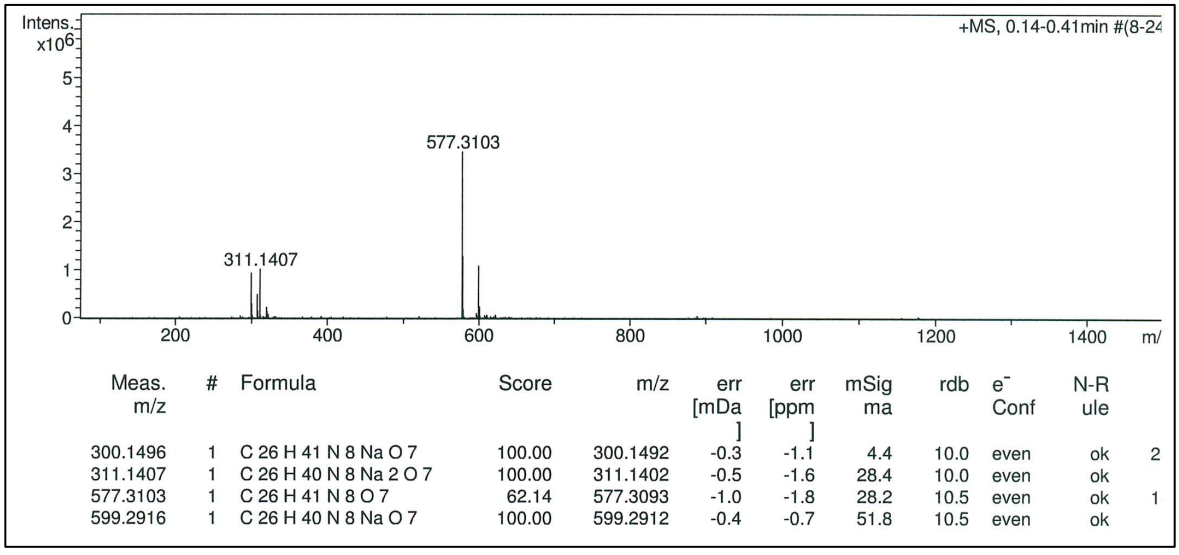

Meas. m/z	#	Formula	Score	m/z	err [mDa]	err [ppm]	mSigma	rdb	e⁻ Conf	N-Rule	
300.1496	1	C 26 H 41 N 8 Na O 7	100.00	300.1492	-0.3	-1.1	4.4	10.0	even	ok	2
311.1407	1	C 26 H 40 N 8 Na 2 O 7	100.00	311.1402	-0.5	-1.6	28.4	10.0	even	ok	
577.3103	1	C 26 H 41 N 8 O 7	62.14	577.3093	-1.0	-1.8	28.2	10.5	even	ok	1
599.2916	1	C 26 H 40 N 8 Na O 7	100.00	599.2912	-0.4	-0.7	51.8	10.5	even	ok	

HRMS spectrum 8. Positive ionisation of *N*-Ac-Gly-Val-Glu-Phe-Arg-Gly-OH (**2.8**)

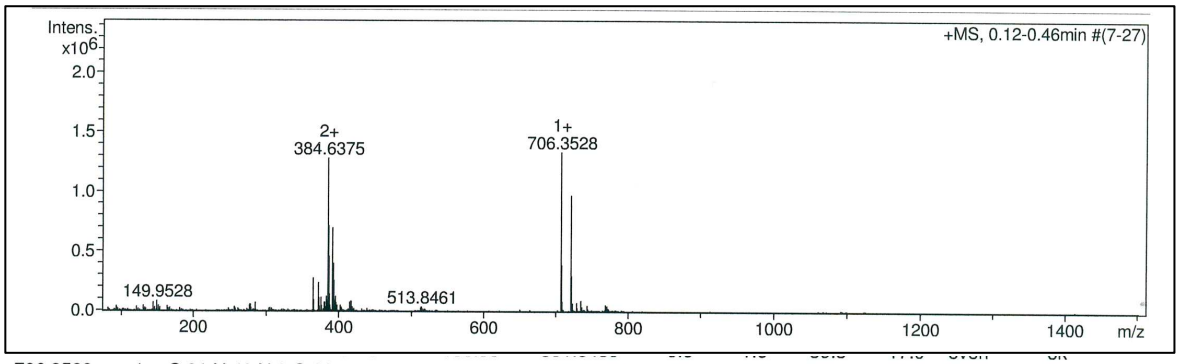

706.3528	1	C 31 H 48 N 9 O 10	100.00	706.3519	-0.9	-1.3	47.2	12.5	even	ok	1+

HRMS spectrum 9. Positive ionisation of *N*-Ac-Gly-Lys-Phe-Arg-Gly-OH (**2.9**)

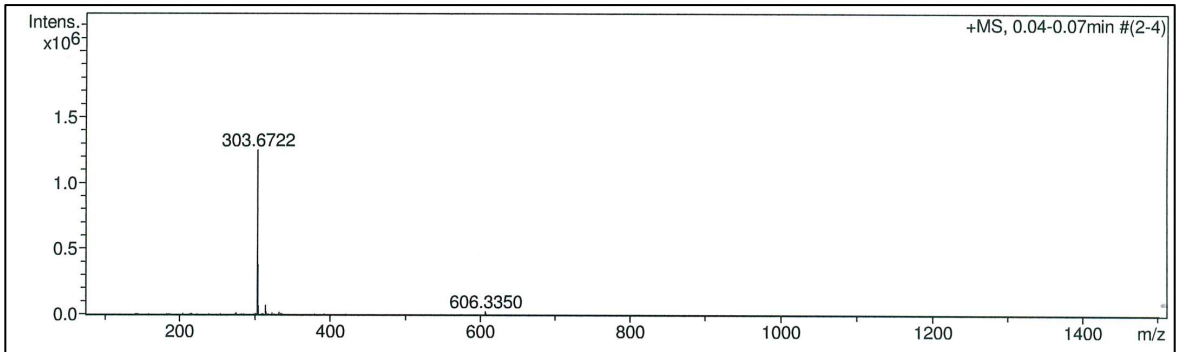

Meas. m/z	#	Formula	Score	m/z	err [mDa]	err [ppm]	mSigma	rdb	e⁻ Conf	N-Rule	z
303.6722	1	C 27 H 45 N 9 O 7	100.00	303.6715	-0.6	-2.0	15.8	10.0	even	ok	2+
314.6626	1	C 27 H 44 N 9 Na O 7	100.00	314.6625	-0.1	-0.3	3.3	10.0	even	ok	
606.3350	1	C 27 H 44 N 9 O 7	100.00	606.3358	0.8	1.3	8.2	10.5	even	ok	1+

HRMS spectrum 10. Positive ionisation of *N*-Ac-Gly-Phe-Arg-Arg-Gly-OH (**2.10**)

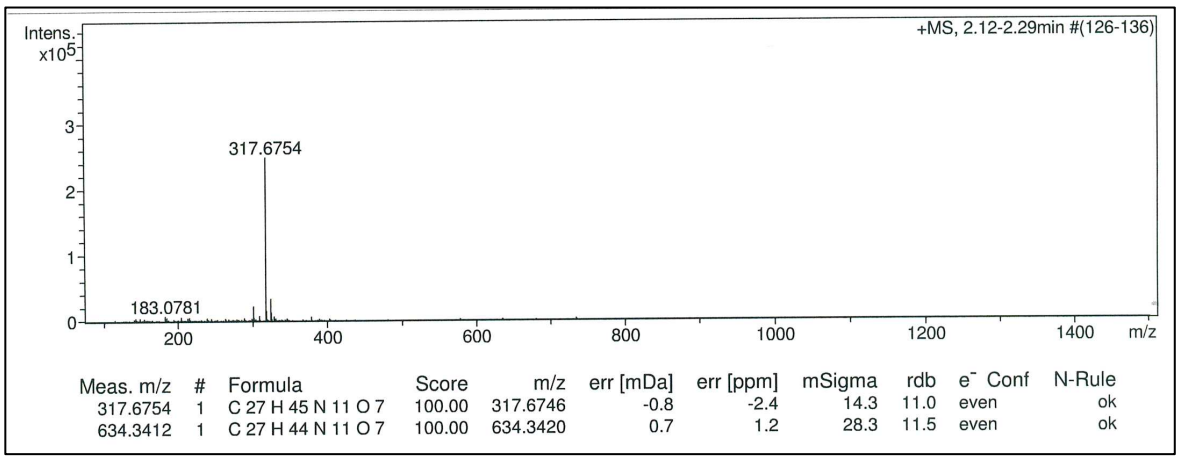

Meas. m/z	#	Formula	Score	m/z	err [mDa]	err [ppm]	mSigma	rdb	e⁻ Conf	N-Rule
317.6754	1	C 27 H 45 N 11 O 7	100.00	317.6746	-0.8	-2.4	14.3	11.0	even	ok
634.3412	1	C 27 H 44 N 11 O 7	100.00	634.3420	0.7	1.2	28.3	11.5	even	ok

HRMS spectrum 11. Positive ionisation of *N*-Ac-Gly-Phe-Val-Arg-Gly-Val-Gly-OH (**2.11**)

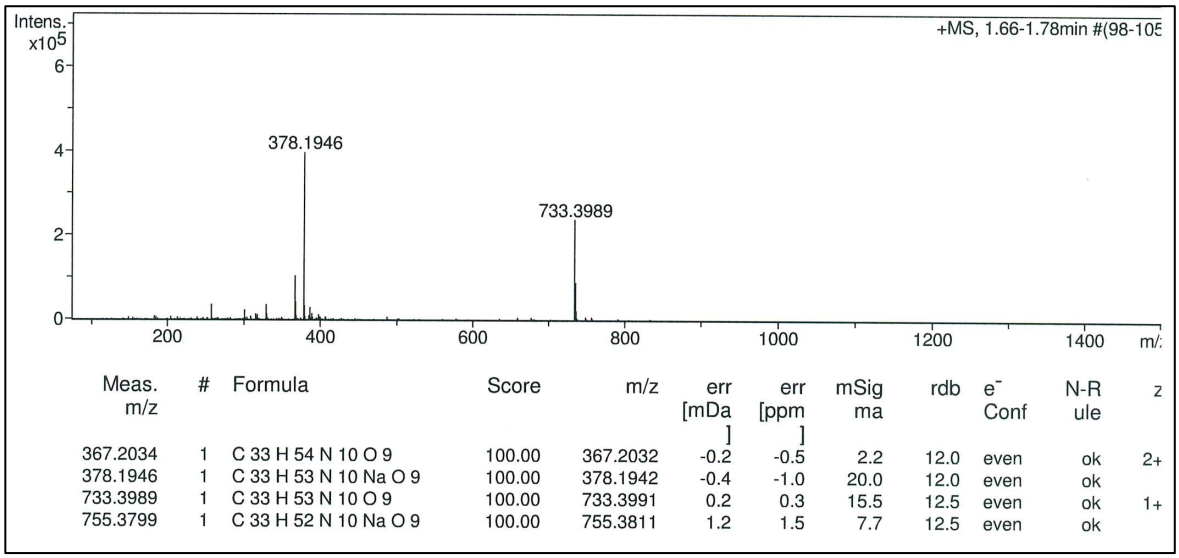

Meas. m/z	#	Formula	Score	m/z	err [mDa]	err [ppm]	mSigma	rdb	e⁻ Conf	N-Rule	z
367.2034	1	C 33 H 54 N 10 O 9	100.00	367.2032	-0.2	-0.5	2.2	12.0	even	ok	2+
378.1946	1	C 33 H 53 N 10 Na O 9	100.00	378.1942	-0.4	-1.0	20.0	12.0	even	ok	
733.3989	1	C 33 H 53 N 10 O 9	100.00	733.3991	0.2	0.3	15.5	12.5	even	ok	1+
755.3799	1	C 33 H 52 N 10 Na O 9	100.00	755.3811	1.2	1.5	7.7	12.5	even	ok	

HRMS spectrum 12. Positive ionisation of *N*-Ac-Gly-Val-Arg-Phe-Ser-Gly-OH (**2.12**)

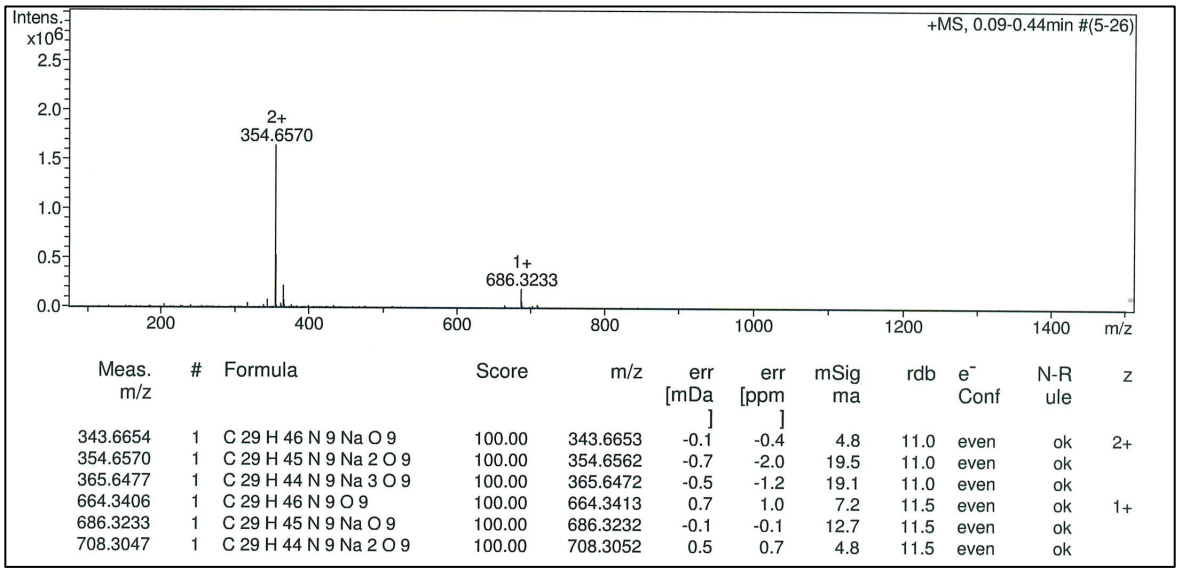

Meas. m/z	#	Formula	Score	m/z	err [mDa]	err [ppm]	mSigma	rdb	e⁻ Conf	N-Rule	z
343.6654	1	C 29 H 46 N 9 Na O 9	100.00	343.6653	-0.1	-0.4	4.8	11.0	even	ok	2+
354.6570	1	C 29 H 45 N 9 Na 2 O 9	100.00	354.6562	-0.7	-2.0	19.5	11.0	even	ok	
365.6477	1	C 29 H 44 N 9 Na 3 O 9	100.00	365.6472	-0.5	-1.2	19.1	11.0	even	ok	
664.3406	1	C 29 H 46 N 9 O 9	100.00	664.3413	0.7	1.0	7.2	11.5	even	ok	1+
686.3233	1	C 29 H 45 N 9 Na O 9	100.00	686.3232	-0.1	-0.1	12.7	11.5	even	ok	
708.3047	1	C 29 H 44 N 9 Na 2 O 9	100.00	708.3052	0.5	0.7	4.8	11.5	even	ok	

HRMS spectrum 13. Positive ionisation of *N*-Ac-Gly-Val-Cys-Arg-Phe-Gly-OH (**2.13**)

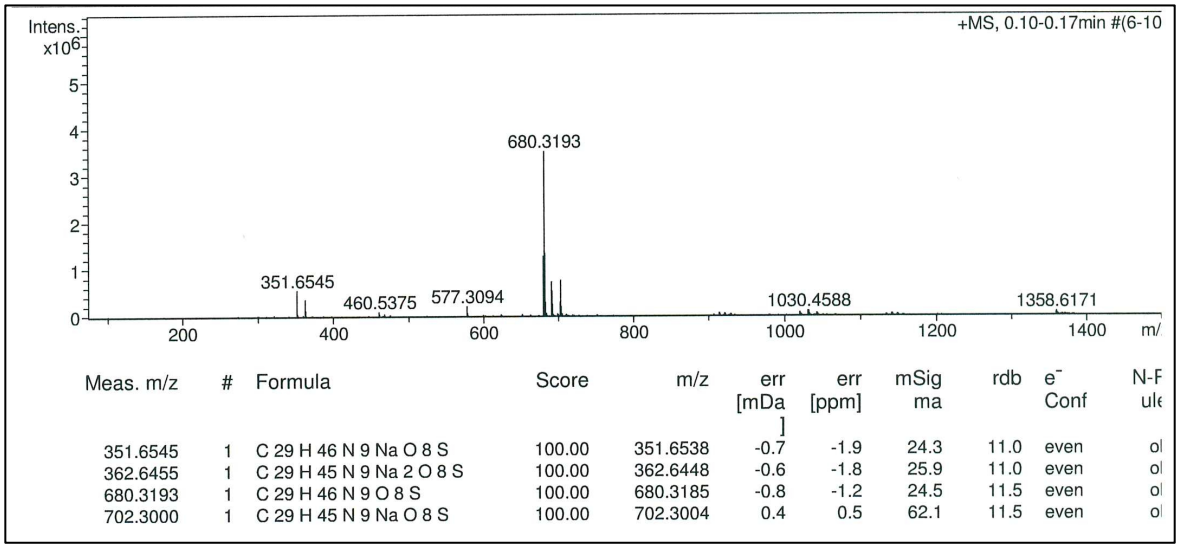

Meas. m/z	#	Formula	Score	m/z	err [mDa]	err [ppm]	mSigma	rdb	e⁻ Conf	N-Rule
351.6545	1	C 29 H 46 N 9 Na O 8 S	100.00	351.6538	-0.7	-1.9	24.3	11.0	even	ok
362.6455	1	C 29 H 45 N 9 Na 2 O 8 S	100.00	362.6448	-0.6	-1.8	25.9	11.0	even	ok
680.3193	1	C 29 H 46 N 9 O 8 S	100.00	680.3185	-0.8	-1.2	24.5	11.5	even	ok
702.3000	1	C 29 H 45 N 9 Na O 8 S	100.00	702.3004	0.4	0.5	62.1	11.5	even	ok

HRMS spectrum 14. Positive ionisation of *N*-Ac-Gly-Phe-His-Ala-Arg-Gly-OH (**2.14**)

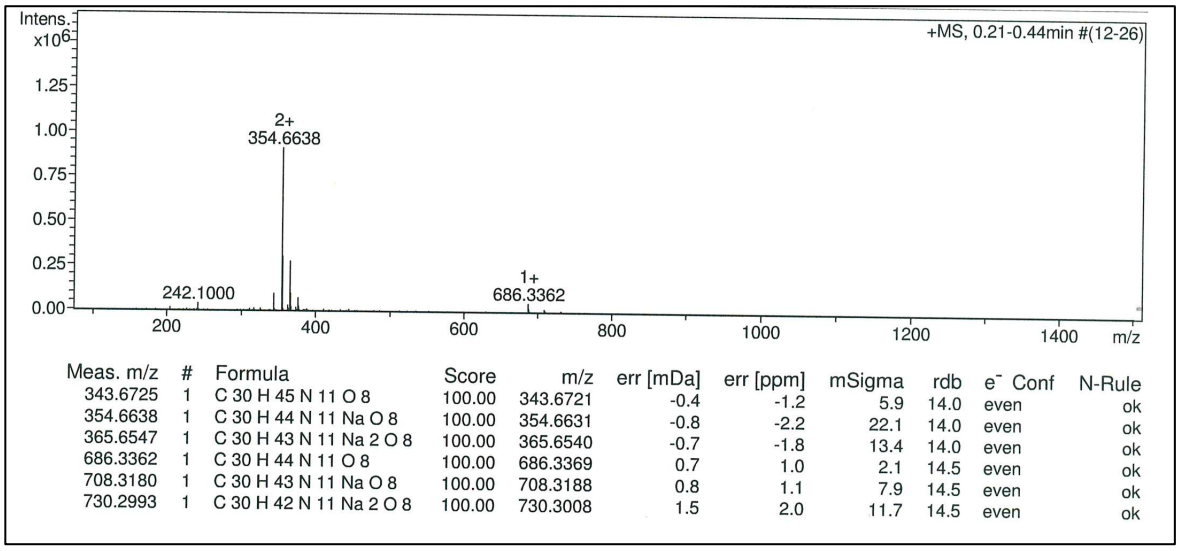

Meas. m/z	#	Formula	Score	m/z	err [mDa]	err [ppm]	mSigma	rdb	e⁻ Conf	N-Rule
343.6725	1	C 30 H 45 N 11 O 8	100.00	343.6721	-0.4	-1.2	5.9	14.0	even	ok
354.6638	1	C 30 H 44 N 11 Na O 8	100.00	354.6631	-0.8	-2.2	22.1	14.0	even	ok
365.6547	1	C 30 H 43 N 11 Na 2 O 8	100.00	365.6540	-0.7	-1.8	13.4	14.0	even	ok
686.3362	1	C 30 H 44 N 11 O 8	100.00	686.3369	0.7	1.0	2.1	14.5	even	ok
708.3180	1	C 30 H 43 N 11 Na O 8	100.00	708.3188	0.8	1.1	7.9	14.5	even	ok
730.2993	1	C 30 H 42 N 11 Na 2 O 8	100.00	730.3008	1.5	2.0	11.7	14.5	even	ok

HRMS spectrum 15. Positive ionisation of *N*-Ac-Gly-Val-Dha-Arg-Phe-Gly-OH (**2.15**)

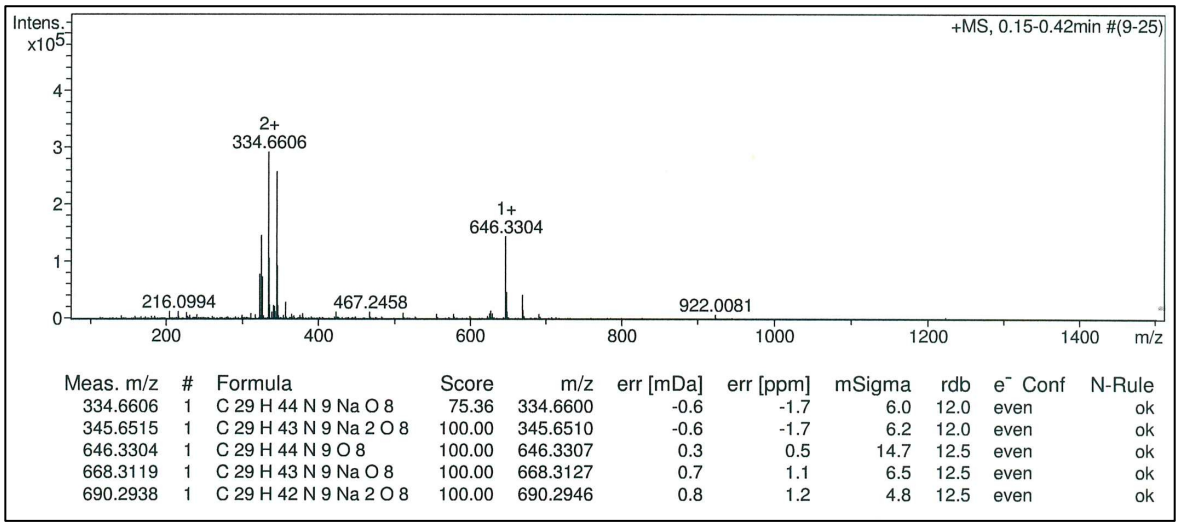

Meas. m/z	#	Formula	Score	m/z	err [mDa]	err [ppm]	mSigma	rdb	e⁻ Conf	N-Rule
334.6606	1	C 29 H 44 N 9 Na O 8	75.36	334.6600	-0.6	-1.7	6.0	12.0	even	ok
345.6515	1	C 29 H 43 N 9 Na 2 O 8	100.00	345.6510	-0.6	-1.7	6.2	12.0	even	ok
646.3304	1	C 29 H 44 N 9 O 8	100.00	646.3307	0.3	0.5	14.7	12.5	even	ok
668.3119	1	C 29 H 43 N 9 Na O 8	100.00	668.3127	0.7	1.1	6.5	12.5	even	ok
690.2938	1	C 29 H 42 N 9 Na 2 O 8	100.00	690.2946	0.8	1.2	4.8	12.5	even	ok

HRMS spectrum 16. Positive ionisation of *N*-Ac-Gly-Val-Phe-Arg(6-FAM)-Gly-OH (**2.16**)

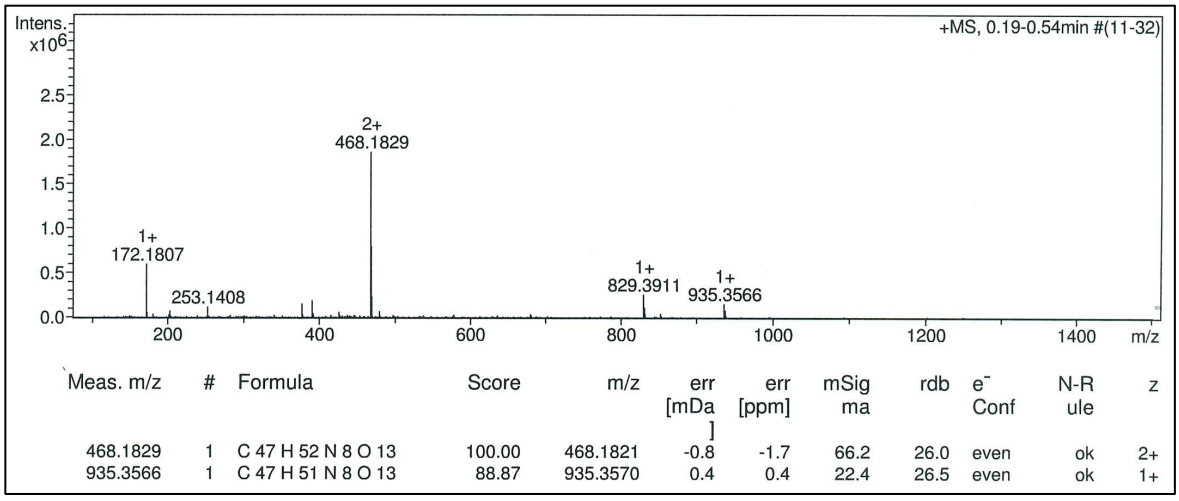

Meas. m/z	#	Formula	Score	m/z	err [mDa]	err [ppm]	mSigma	rdb	e⁻ Conf	N-Rule	z
468.1829	1	C 47 H 52 N 8 O 13	100.00	468.1821	-0.8	-1.7	66.2	26.0	even	ok	2+
935.3566	1	C 47 H 51 N 8 O 13	88.87	935.3570	0.4	0.4	22.4	26.5	even	ok	1+

HRMS spectrum 17. Negative ionisation of *N*-Ac-Gly-Val-Glu-Phe-Arg(6-FAM)-Gly-OH (**2.17**)

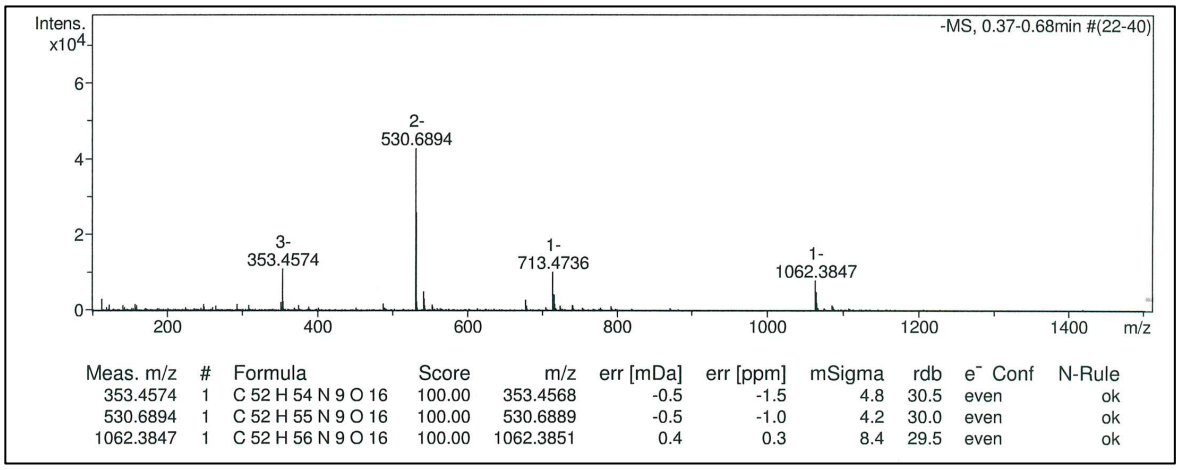

Meas. m/z	#	Formula	Score	m/z	err [mDa]	err [ppm]	mSigma	rdb	e⁻ Conf	N-Rule
353.4574	1	C 52 H 54 N 9 O 16	100.00	353.4568	-0.5	-1.5	4.8	30.5	even	ok
530.6894	1	C 52 H 55 N 9 O 16	100.00	530.6889	-0.5	-1.0	4.2	30.0	even	ok
1062.3847	1	C 52 H 56 N 9 O 16	100.00	1062.3851	0.4	0.3	8.4	29.5	even	ok

HRMS spectrum 18. Negative ionisation of *N*-Ac-Gly-Val-Arg(6-FAM)-Phe-Ser-Gly-OH (**2.18**)

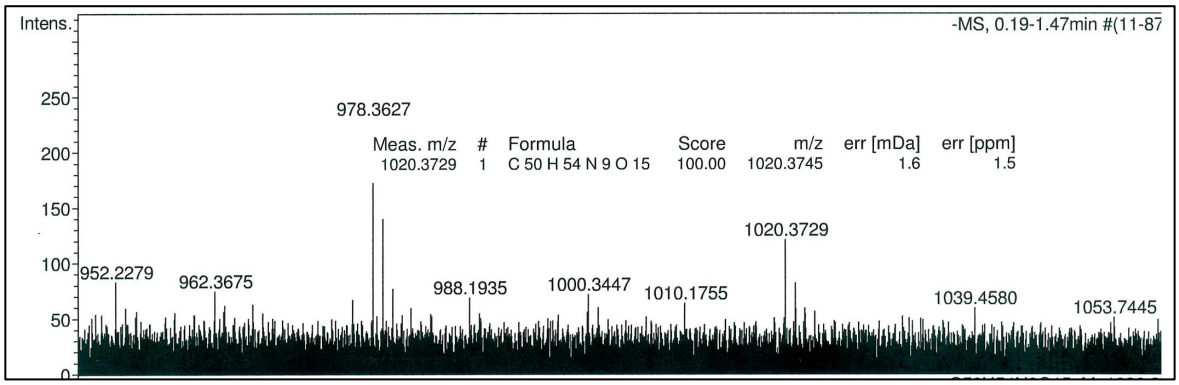

HRMS spectrum 19. Positive ionisation of *N*-Ac-Gly-Phe-His-Ala-Arg(6-FAM)-Gly-OH (**2.19**)

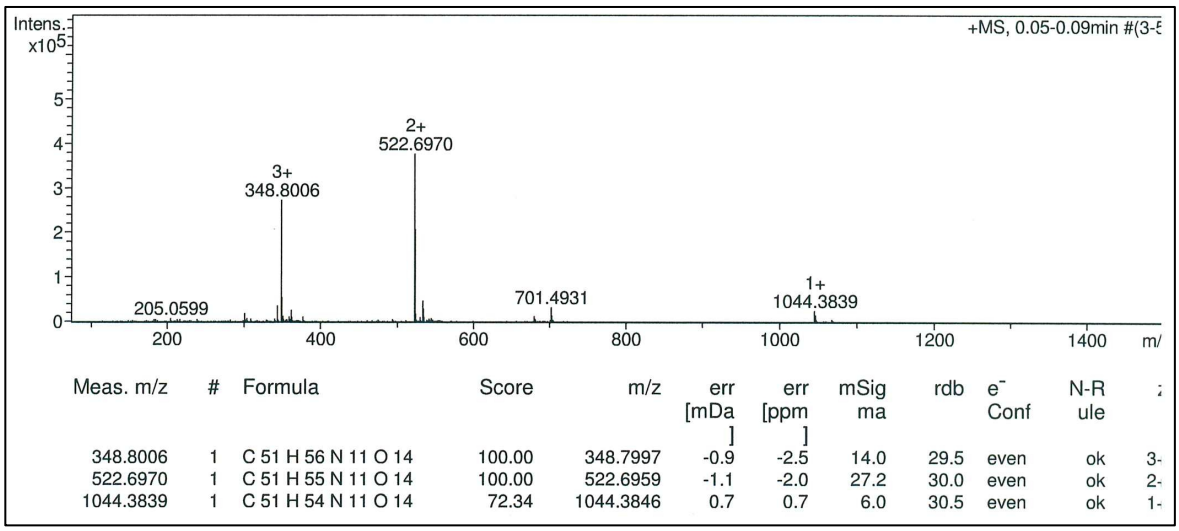

Meas. m/z	#	Formula	Score	m/z	err [mDa]	err [ppm]	mSigma	rdb	e⁻ Conf	N-Rule	
348.8006	1	C 51 H 56 N 11 O 14	100.00	348.7997	-0.9	-2.5	14.0	29.5	even	ok	3-
522.6970	1	C 51 H 55 N 11 O 14	100.00	522.6959	-1.1	-2.0	27.2	30.0	even	ok	2-
1044.3839	1	C 51 H 54 N 11 O 14	72.34	1044.3846	0.7	0.7	6.0	30.5	even	ok	1-

HRMS spectrum 20. Positive ionisation of *N*-Ac-Gly-Phe-Arg(6-FAM)-Arg(6-FAM)-Gly-OH (**2.20**)

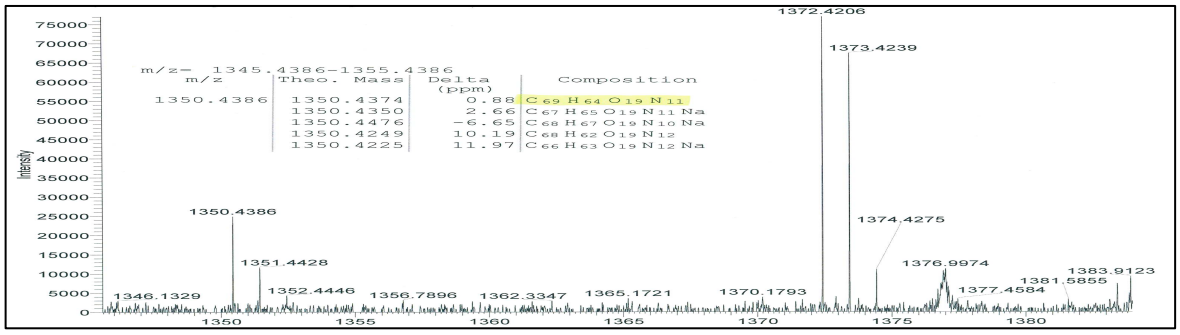

HRMS spectrum 21. Positive ionisation of *N*-Ac-Gly-Phe-Val-Arg(6-FAM)-Gly-Val-Gly-OH (**2.21**)

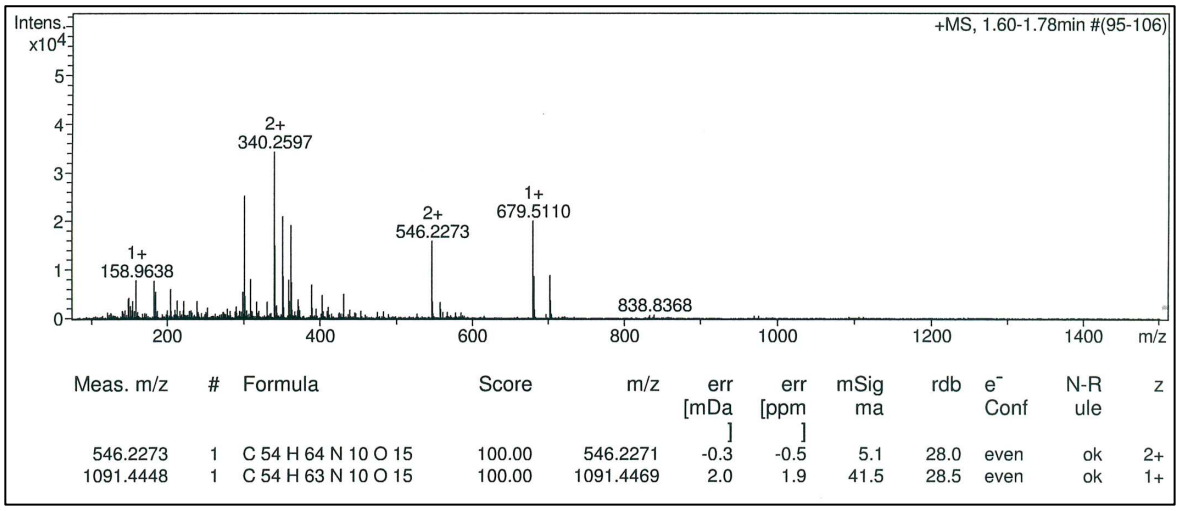

Meas. m/z	#	Formula	Score	m/z	err [mDa]	err [ppm]	mSigma	rdb	e⁻ Conf	N-Rule	z
546.2273	1	C 54 H 64 N 10 O 15	100.00	546.2271	-0.3	-0.5	5.1	28.0	even	ok	2+
1091.4448	1	C 54 H 63 N 10 O 15	100.00	1091.4469	2.0	1.9	41.5	28.5	even	ok	1+

HRMS spectrum 22. Positive ionisation of *N*-Ac-Gly-Val-Dha-Arg(6-FAM)-Phe-Gly-OH (**2.22**)

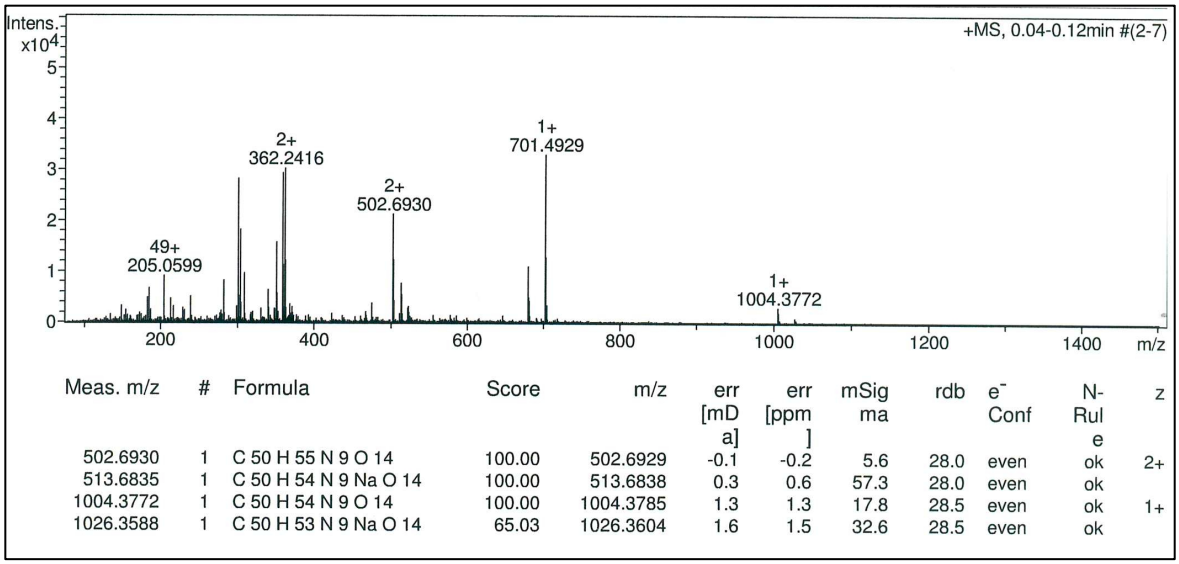

Meas. m/z	#	Formula	Score	m/z	err [mDa]	err [ppm]	mSigma	rdb	e⁻ Conf	N-Rule	z
502.6930	1	C 50 H 55 N 9 O 14	100.00	502.6929	-0.1	-0.2	5.6	28.0	even	ok	2+
513.6835	1	C 50 H 54 N 9 Na O 14	100.00	513.6838	0.3	0.6	57.3	28.0	even	ok	
1004.3772	1	C 50 H 54 N 9 O 14	100.00	1004.3785	1.3	1.3	17.8	28.5	even	ok	1+
1026.3588	1	C 50 H 53 N 9 Na O 14	65.03	1026.3604	1.6	1.5	32.6	28.5	even	ok	

HRMS spectrum 23. Positive ionisation of *N*-Ac-Gly-Val-Cys(6-FAM)-Arg-Phe-Gly-OH (**2.23**)

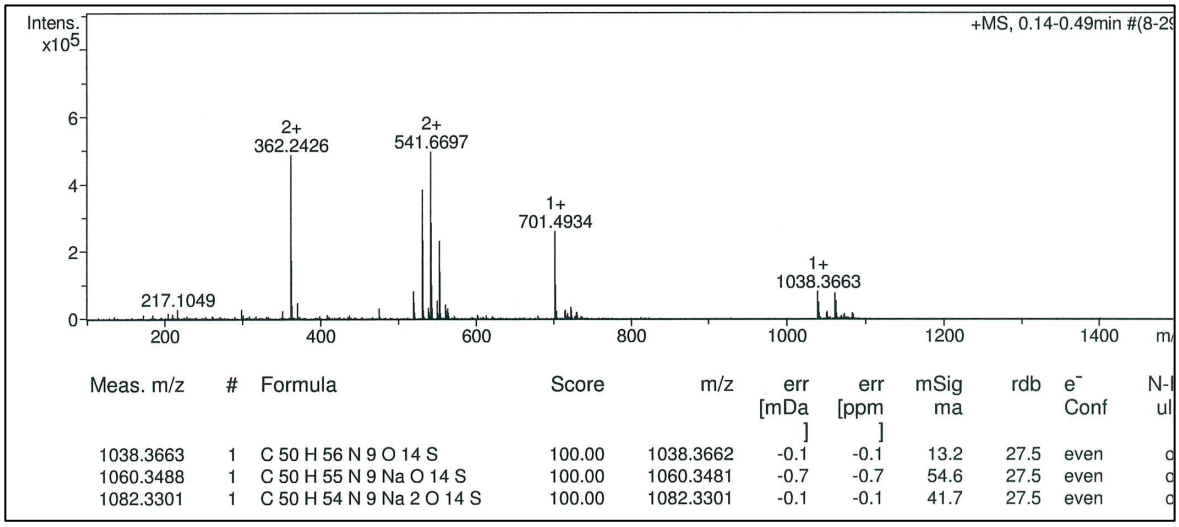

Meas. m/z	#	Formula	Score	m/z	err [mDa]	err [ppm]	mSigma	rdb	e⁻ Conf	N-Rule
1038.3663	1	C 50 H 56 N 9 O 14 S	100.00	1038.3662	-0.1	-0.1	13.2	27.5	even	o
1060.3488	1	C 50 H 55 N 9 Na O 14 S	100.00	1060.3481	-0.7	-0.7	54.6	27.5	even	o
1082.3301	1	C 50 H 54 N 9 Na 2 O 14 S	100.00	1082.3301	-0.1	-0.1	41.7	27.5	even	o

HRMS spectrum 24. Positive ionisation of *N*-Ac-Gly-Lys(6-FAM)-Phe-Arg-Gly-OH (**2.24**)

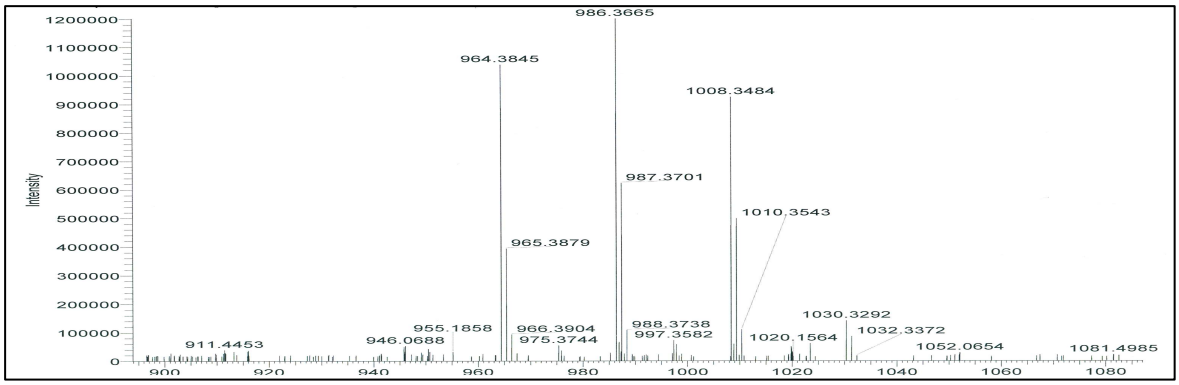

Elemental composition search on mass 964.3845

m/z= 959.3845-969.3845

m/z	Theo. Mass	Delta (ppm)	Composition
964.3845	964.3836	0.93	$C_{48}H_{54}O_{13}N_9$
	964.3812	3.43	$C_{46}H_{55}O_{13}N_9Na$
	964.3937	-9.61	$C_{47}H_{57}O_{13}N_8Na$
	964.3961	-12.11	$C_{49}H_{56}O_{13}N_8$
	964.3726	12.30	$C_{50}H_{53}O_{11}N_8Na$
	964.3964	-12.39	$C_{50}H_{55}O_{10}N_9Na$

HRMS spectrum 25. Positive ionisation of *N*-Ac-Gly-Phe-Val-Arg(Biotin)-Gly-Val-Gly-OH (**2.25**)

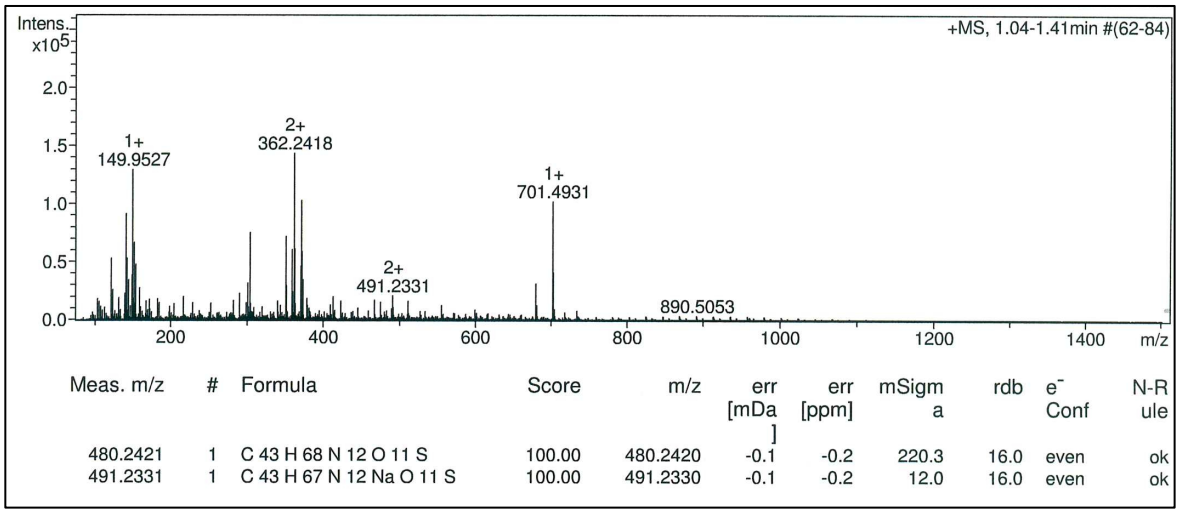

Meas. m/z	#	Formula	Score	m/z	err [mDa]	err [ppm]	mSigma	rdb	e⁻ Conf	N-Rule
480.2421	1	C 43 H 68 N 12 O 11 S	100.00	480.2420	-0.1	-0.2	220.3	16.0	even	ok
491.2331	1	C 43 H 67 N 12 Na O 11 S	100.00	491.2330	-0.1	-0.2	12.0	16.0	even	ok

HRMS spectrum 26. Positive ionisation of *N*-Ac-Gly-Val-Glu-Phe-Arg(Biotin)-Gly-OH (**2.26**)

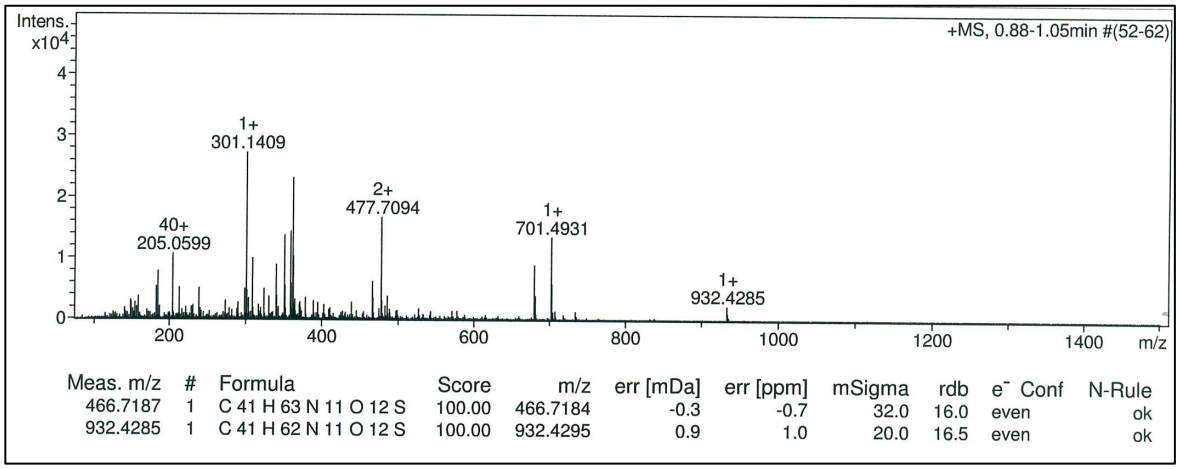

Meas. m/z	#	Formula	Score	m/z	err [mDa]	err [ppm]	mSigma	rdb	e⁻ Conf	N-Rule
466.7187	1	C 41 H 63 N 11 O 12 S	100.00	466.7184	-0.3	-0.7	32.0	16.0	even	ok
932.4285	1	C 41 H 62 N 11 O 12 S	100.00	932.4295	0.9	1.0	20.0	16.5	even	ok

HRMS spectrum 27. Positive ionisation of *N*-Ac-Gly-Phe-Val-Arg(DA)-Gly-Val-Gly-OH (**2.27**)

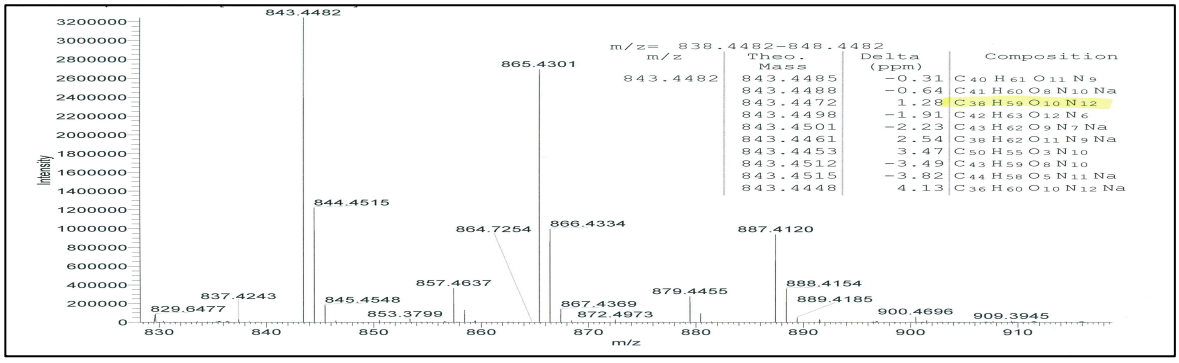

m/z= 838.4482-848.4482

m/z	Theo. Mass	Delta (ppm)	Composition
843.4482	843.4485	-0.31	$C_{40}H_{61}O_{11}N_9$
	843.4488	-0.64	$C_{41}H_{60}O_8N_{10}Na$
	843.4472	1.28	$C_{38}H_{59}O_{10}N_{12}$
	843.4498	-1.91	$C_{42}H_{63}O_{12}N_6$
	843.4501	-2.23	$C_{43}H_{62}O_9N_7Na$
	843.4461	2.54	$C_{38}H_{62}O_{11}N_9Na$
	843.4453	3.47	$C_{50}H_{55}O_3N_{10}$
	843.4512	-3.49	$C_{43}H_{59}O_8N_{10}$
	843.4515	-3.82	$C_{44}H_{58}O_5N_{11}Na$
	843.4448	4.13	$C_{36}H_{60}O_{10}N_{12}Na$

HRMS spectrum 28. Positive ionisation of *N*-Ac-Gly-Val-Glu-Phe-Arg(DA)-Gly-OH (**2.28**)

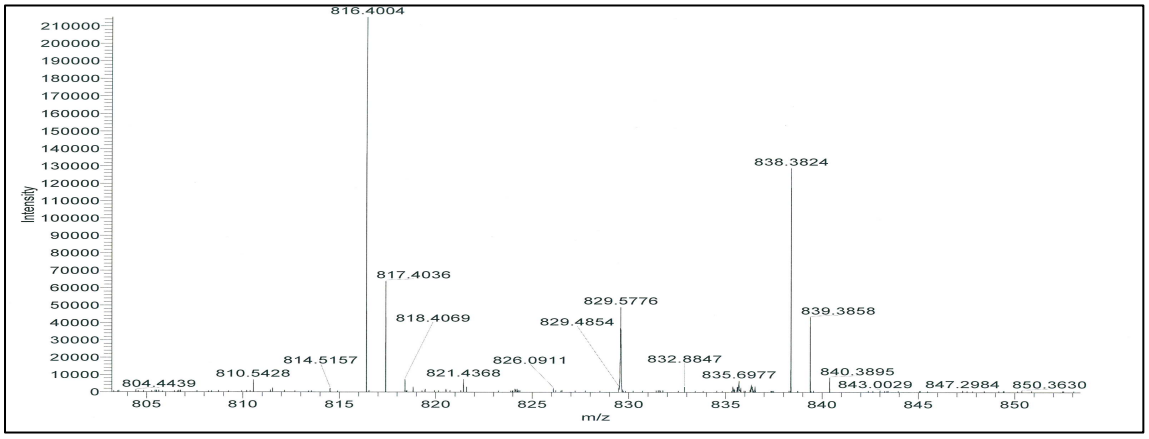

m/z= 811.4004-821.4004

m/z	Theo. Mass	Delta (ppm)	Composition
816.4004	816.4002	0.30	$C_{38}H_{59}O_{13}N_5Na$
	816.3999	0.64	$C_{36}H_{54}O_{11}N_{11}$
	816.4012	-1.00	$C_{38}H_{56}O_{12}N_8$
	816.3994	1.26	$C_{50}H_{52}O_5N_6$
	816.4015	-1.34	$C_{39}H_{55}O_9N_9Na$
	816.3988	1.94	$C_{36}H_{57}O_{12}N_8Na$
	816.3983	2.56	$C_{50}H_{55}O_6N_3Na$
	816.3983	2.57	$C_{49}H_{49}ON_{10}Na$
	816.4026	-2.65	$C_{40}H_{58}O_{13}N_5$
	816.3980	2.90	$C_{49}H_{56}O_9N_2$

HRMS spectrum 29. Positive ionisation of Pyr-His-Trp-Ser-Tyr-D-Leu-Leu-Arg(6-FAM)-Pro-NHEt (**2.30**)

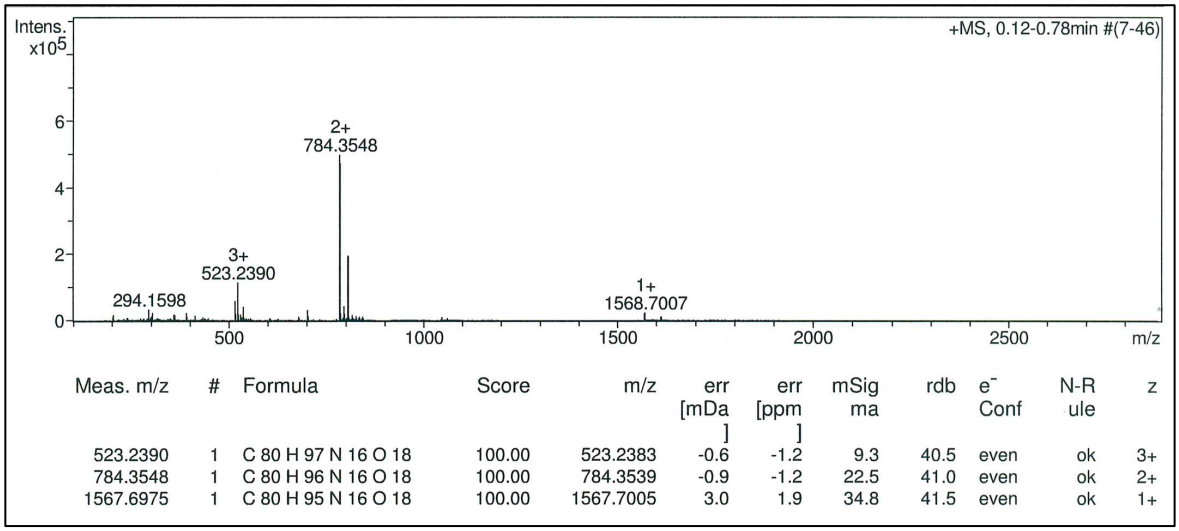

Meas. m/z	#	Formula	Score	m/z	err [mDa]	err [ppm]	mSigma	rdb	e⁻ Conf	N-Rule	z
523.2390	1	C 80 H 97 N 16 O 18	100.00	523.2383	-0.6	-1.2	9.3	40.5	even	ok	3+
784.3548	1	C 80 H 96 N 16 O 18	100.00	784.3539	-0.9	-1.2	22.5	41.0	even	ok	2+
1567.6975	1	C 80 H 95 N 16 O 18	100.00	1567.7005	3.0	1.9	34.8	41.5	even	ok	1+

HRMS spectrum 30. Positive ionisation of *N*-Ac-Gly-Lys(Boc)-Phe-Arg-Gly-OH (**2.31**)

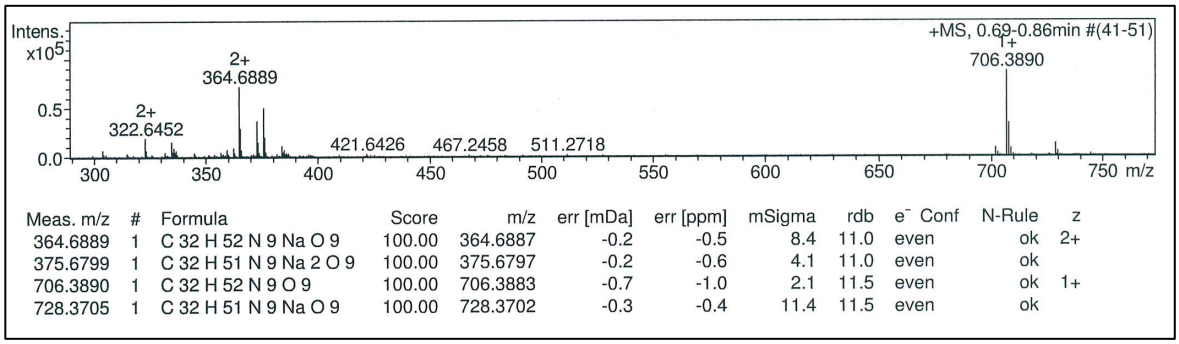

Meas. m/z	#	Formula	Score	m/z	err [mDa]	err [ppm]	mSigma	rdb	e⁻ Conf	N-Rule	z
364.6889	1	C 32 H 52 N 9 Na O 9	100.00	364.6887	-0.2	-0.5	8.4	11.0	even	ok	2+
375.6799	1	C 32 H 51 N 9 Na 2 O 9	100.00	375.6797	-0.2	-0.6	4.1	11.0	even	ok	
706.3890	1	C 32 H 52 N 9 O 9	100.00	706.3883	-0.7	-1.0	2.1	11.5	even	ok	1+
728.3705	1	C 32 H 51 N 9 Na O 9	100.00	728.3702	-0.3	-0.4	11.4	11.5	even	ok	

HRMS spectrum 31. Positive ionisation of *N*-Ac-Gly-Lys(Boc)-Phe-Arg(6-FAM)-Gly-OH (**2.32**)

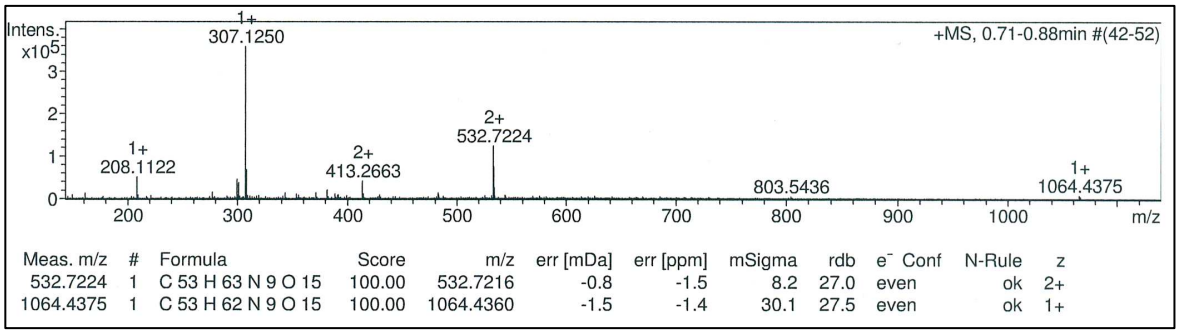

Meas. m/z	#	Formula	Score	m/z	err [mDa]	err [ppm]	mSigma	rdb	e⁻ Conf	N-Rule	z
532.7224	1	C 53 H 63 N 9 O 15	100.00	532.7216	-0.8	-1.5	8.2	27.0	even	ok	2+
1064.4375	1	C 53 H 62 N 9 O 15	100.00	1064.4360	-1.5	-1.4	30.1	27.5	even	ok	1+

HRMS spectrum 32. Positive ionisation of *N*-Ac-Gly-Lys-Phe-Arg(6-FAM)-Gly-OH (**2.33**)

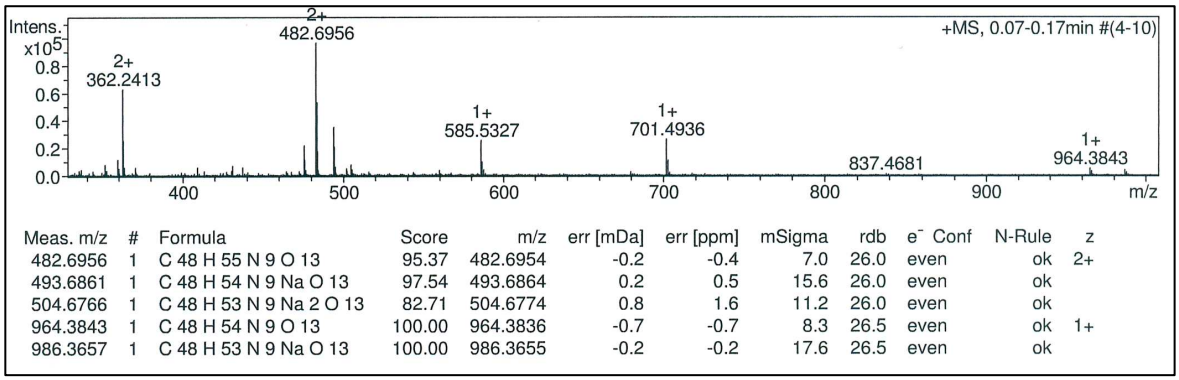

Meas. m/z	#	Formula	Score	m/z	err [mDa]	err [ppm]	mSigma	rdb	e⁻ Conf	N-Rule	z
482.6956	1	C 48 H 55 N 9 O 13	95.37	482.6954	-0.2	-0.4	7.0	26.0	even	ok	2+
493.6861	1	C 48 H 54 N 9 Na O 13	97.54	493.6864	0.2	0.5	15.6	26.0	even	ok	
504.6766	1	C 48 H 53 N 9 Na 2 O 13	82.71	504.6774	0.8	1.6	11.2	26.0	even	ok	
964.3843	1	C 48 H 54 N 9 O 13	100.00	964.3836	-0.7	-0.7	8.3	26.5	even	ok	1+
986.3657	1	C 48 H 53 N 9 Na O 13	100.00	986.3655	-0.2	-0.2	17.6	26.5	even	ok	

HRMS spectrum 33. Positive ionisation of MC-LR-(6-FAM) (**3.1**)

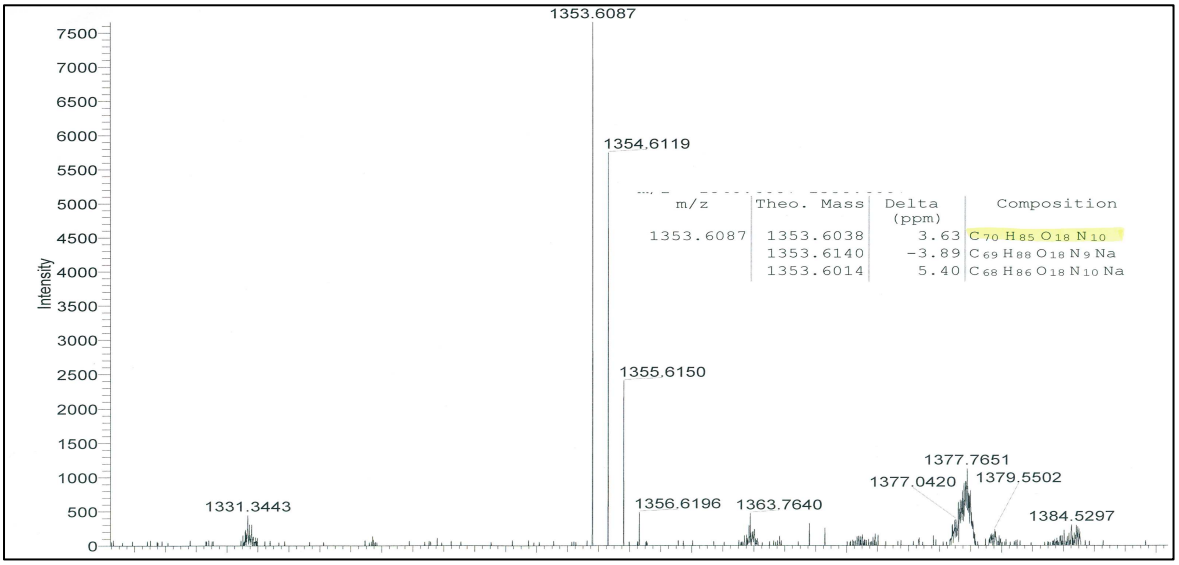

HRMS spectrum 34. Negative ionisation of MC-LR-(Alexa-430) (**3.2**)

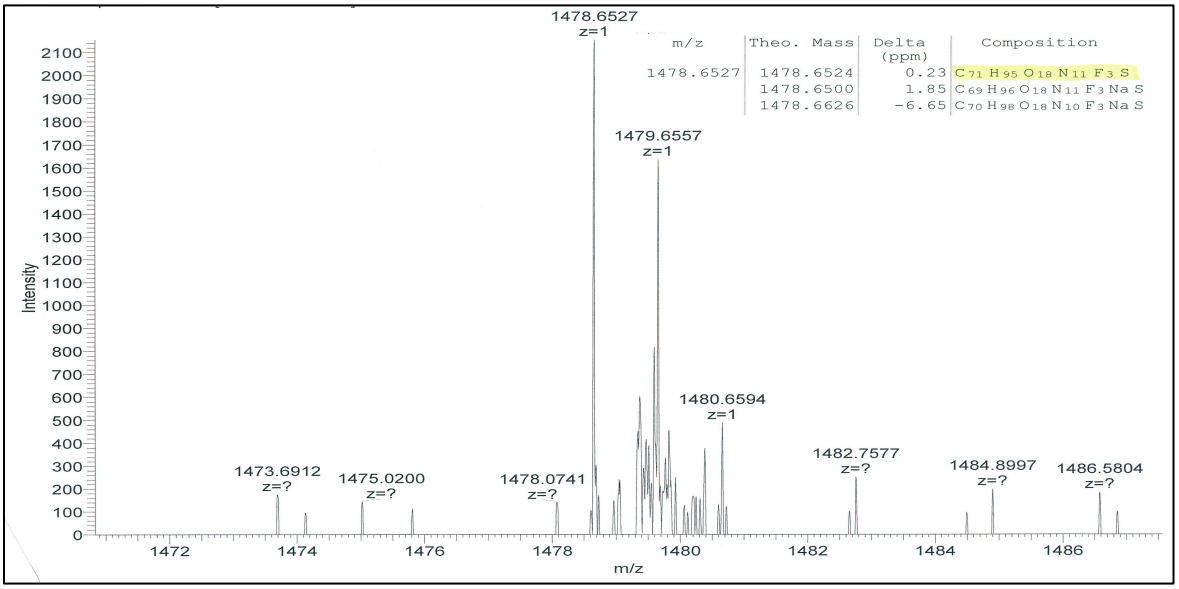

HRMS spectrum 35. Negative ionisation of MC-LR-(Alexa-488) (**3.3**)

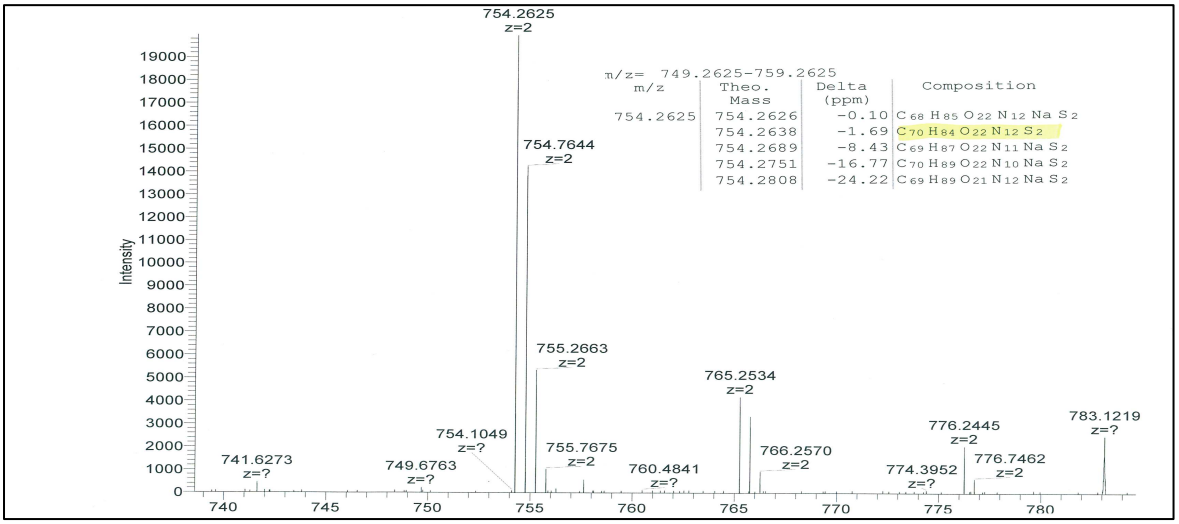

HRMS spectrum 36. Positive ionisation of MC-LR-(Texas-Red) (**3.4**)

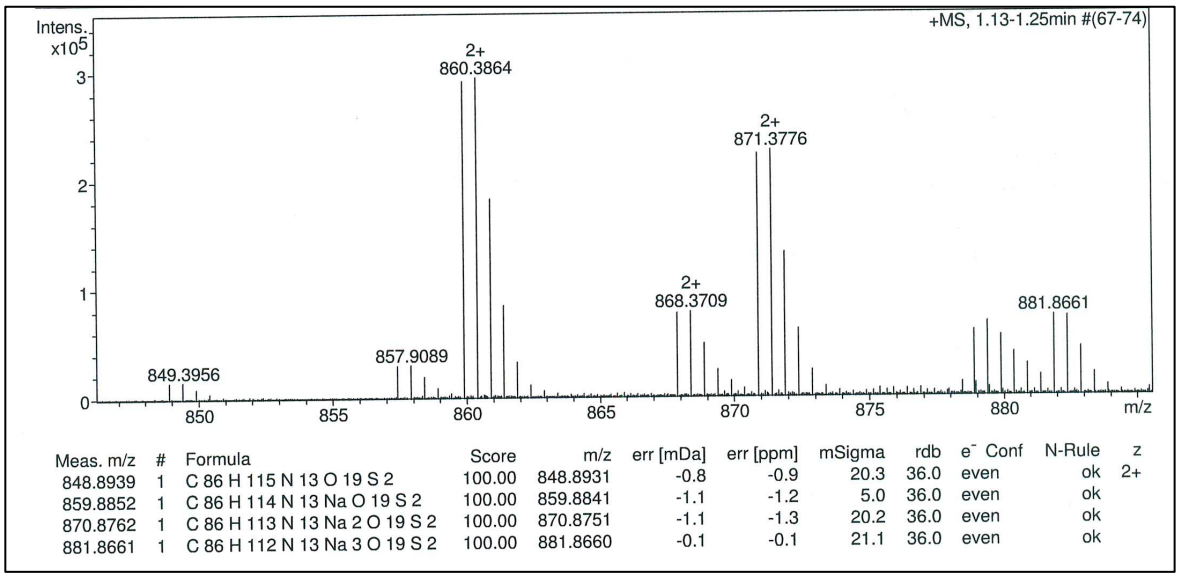

Meas. m/z	#	Formula	Score	m/z	err [mDa]	err [ppm]	mSigma	rdb	e⁻ Conf	N-Rule	z
848.8939	1	C 86 H 115 N 13 O 19 S 2	100.00	848.8931	-0.8	-0.9	20.3	36.0	even	ok	2+
859.8852	1	C 86 H 114 N 13 Na O 19 S 2	100.00	859.8841	-1.1	-1.2	5.0	36.0	even	ok	
870.8762	1	C 86 H 113 N 13 Na 2 O 19 S 2	100.00	870.8751	-1.1	-1.3	20.2	36.0	even	ok	
881.8661	1	C 86 H 112 N 13 Na 3 O 19 S 2	100.00	881.8660	-0.1	-0.1	21.1	36.0	even	ok	

HRMS spectrum 37. Positive ionisation of MC-LR-(Biotin) (**3.5**)

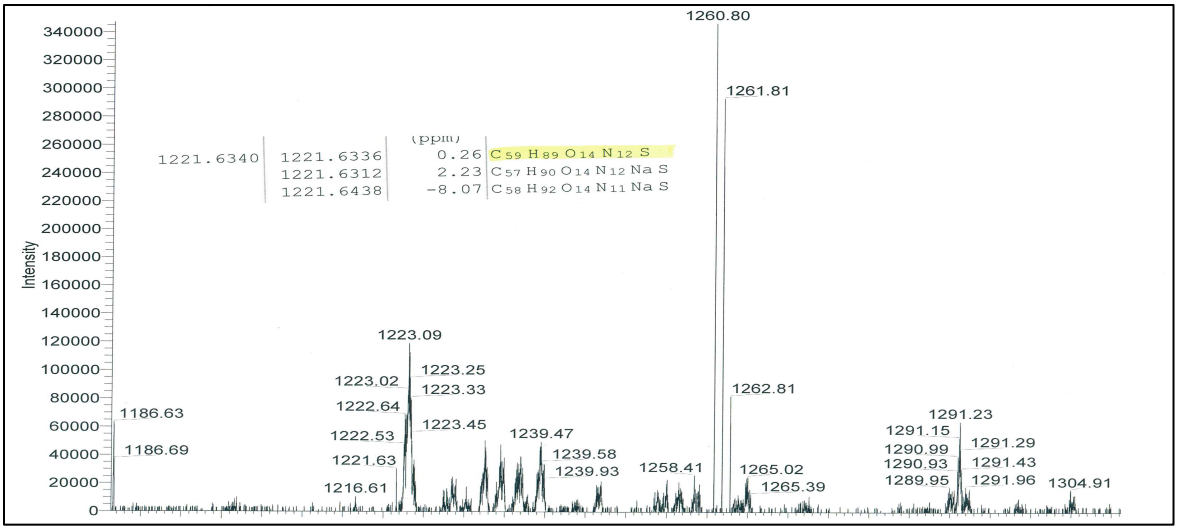

HRMS spectrum 38. Positive ionisation of MC-LR-(DA) (**3.6**)

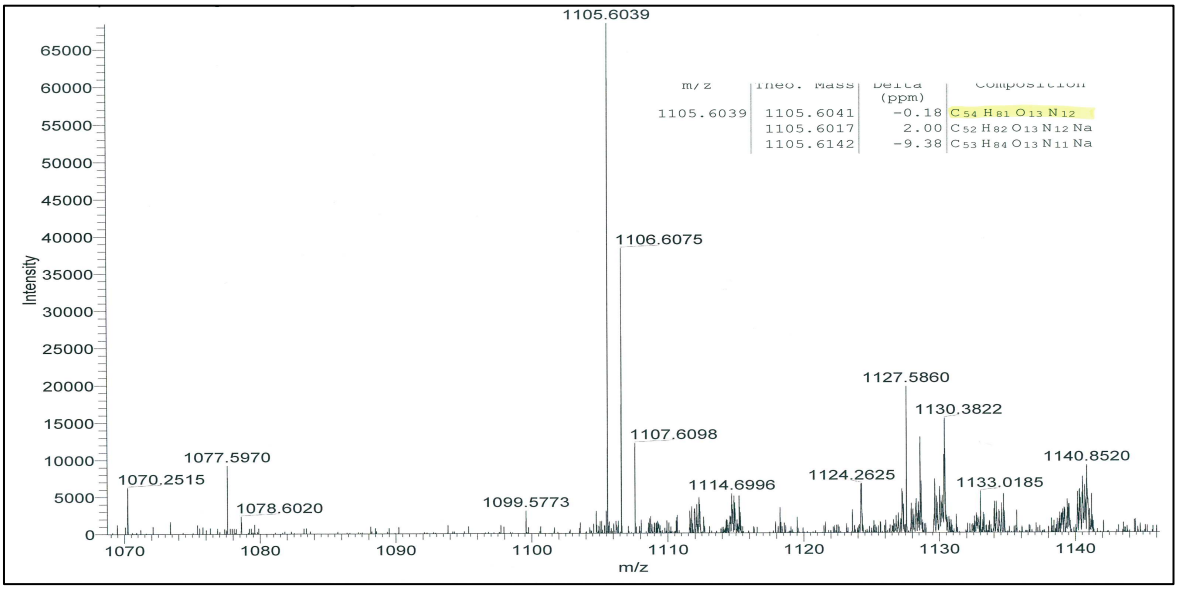

HRMS spectrum 39. Positive ionisation of CP1020(Benzylamin) (**5.1**)

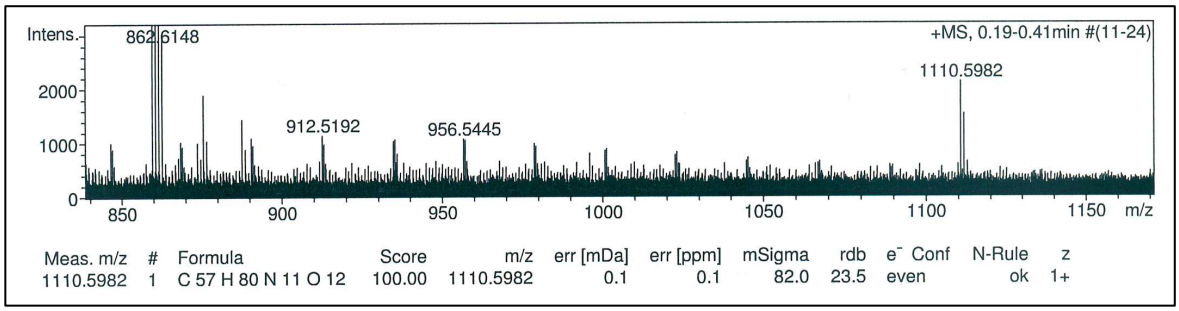

Meas. m/z	#	Formula	Score	m/z	err [mDa]	err [ppm]	mSigma	rdb	e⁻ Conf	N-Rule	z
1110.5982	1	C 57 H 80 N 11 O 12	100.00	1110.5982	0.1	0.1	82.0	23.5	even	ok	1+

MS spectrum 40. Positive ionisation of CP1020(Coumarin) (**5.2**)

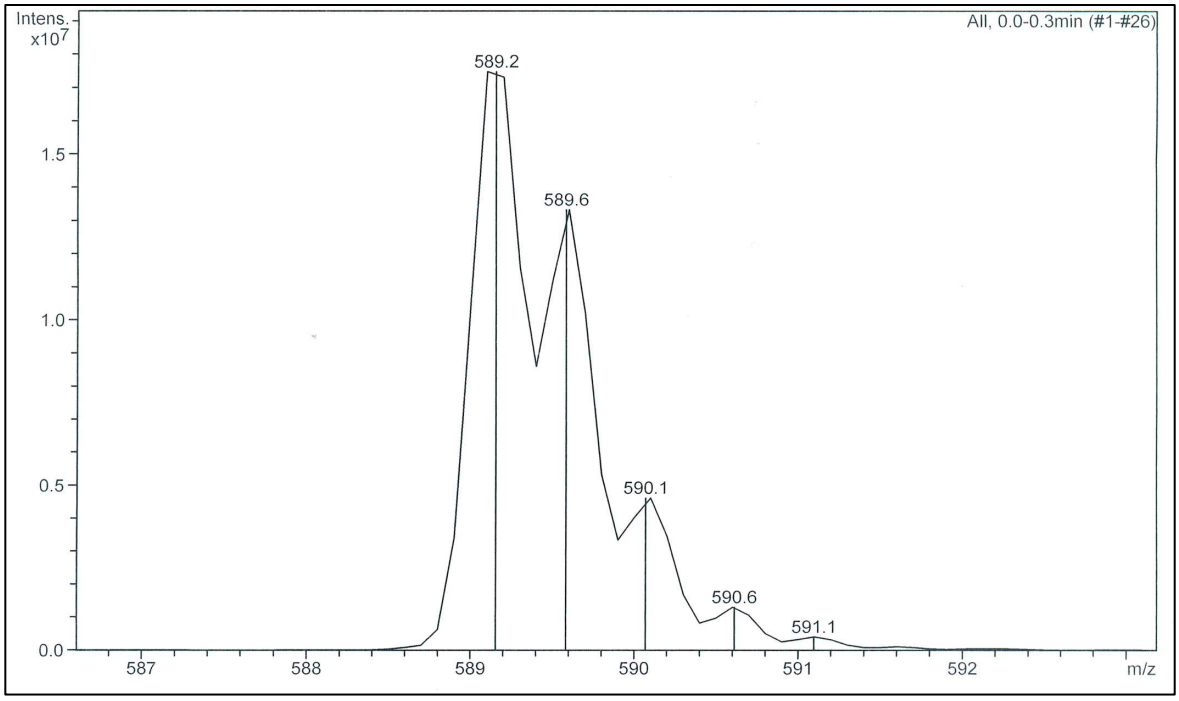

7.4 MS-MS-Spectra

MS-MS spectrum 1. Positive fragmentation of *N*-Ac-Gly-Val-Glu-Phe-Arg(6-FAM)-Gly-OH (**2.17**)

MS-MS spectrum 2. Positive fragmentation of *N*-Ac-Gly-Val-Arg(6-FAM)-Phe-Ser-Gly-OH (**2.18**)

MS-MS spectrum 3. Positive fragmentation of *N*-Ac-Gly-Phe-His-Ala-Arg(6-FAM)-Gly-OH (**2.19**)

MS-MS spectrum 4. Positive fragmentation of *N*-Ac-Gly-Val-Cys(6-FAM)-Arg-Phe-Gly-OH (**2.23**)

MS-MS spectrum 5. Positive fragmentation of *N*-Ac-Gly-Lys(6-FAM)-Phe-Arg-Gly-OH (**2.24**)

MS-MS spectrum 6. Positive fragmentation of Pyr-His-Trp-Ser-Tyr-D-Leu-Leu-Arg(6-FAM)-Pro-NHEt (**2.30**)

MS-MS spectrum 7. Positive fragmentation of *N*-Ac-Gly-Lys-Phe-Arg(6-FAM)-Gly-OH (**2.33**)

MS-MS spectrum 8. Negative fragmentation of MC-LR-(6-FAM) (**3.1**)

MS-MS spectrum 9. Negative fragmentation of MC-LR-(Alexa-430) (**3.2**)

MS-MS spectrum 10. Positive fragmentation of MC-LR-(Texas-Red) (**3.4**)

MS-MS spectrum 11. Positive fragmentation of CP1020(Benzylamin) (**5.1**)

MS-MS spectrum 1. Positive fragmentation of *N*-Ac-Gly-Val-Glu-Phe-Arg(6-FAM)-Gly-OH (**2.17**)

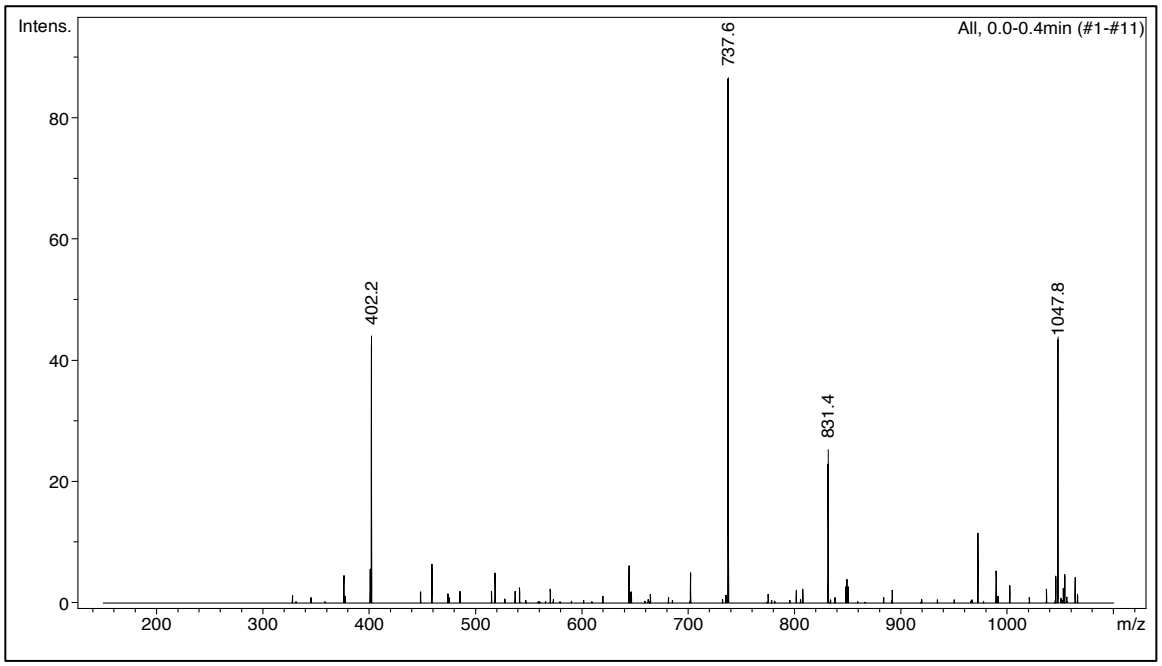

Mass	Fragment
737.6	$^{+}H_3N$-Phe-Arg(6-FAM)-Gly-OH

The ion at *m*/*z* = 737.6 supports the assignment of the labelled Arg residue.

MS-MS spectrum 2. Positive fragmentation of *N*-Ac-Gly-Val-Arg(6-FAM)-Phe-Ser-Gly-OH (**2.18**)

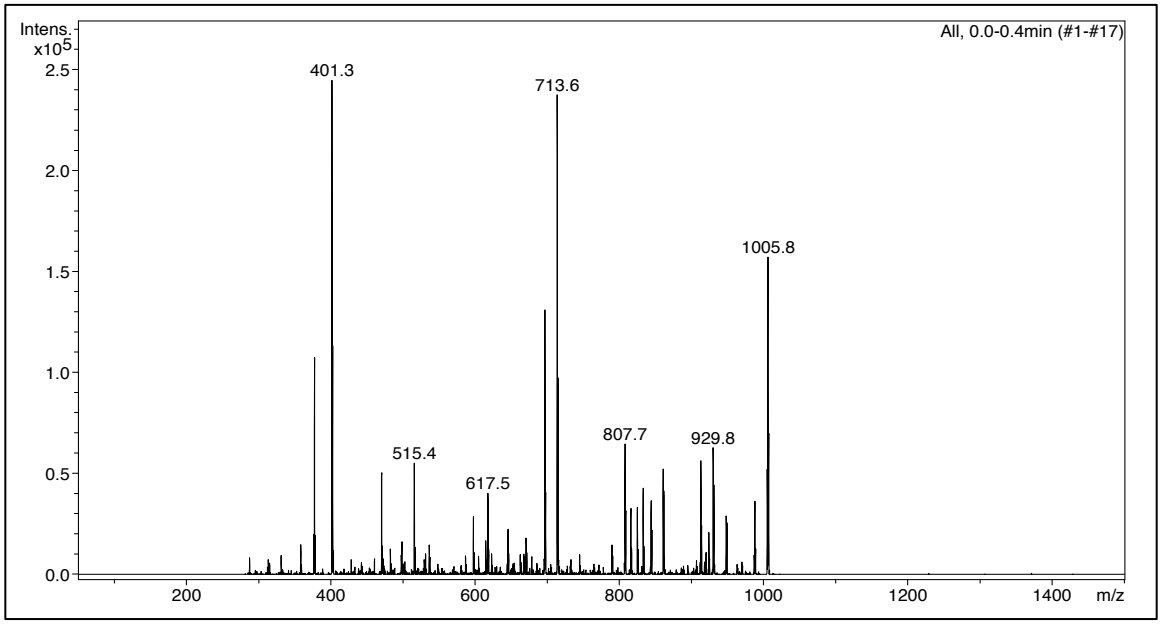

Mass	Fragment
713.6	*N*-Ac-Gly-Val-Arg(6-FAM)- O^{+}
1005.8	*N*-Ac-Gly-Val-Arg(6-FAM)-Phe-Ser-Gly-O^{+}

The ion at *m*/*z* = 713.6 supports the assignment of the labelled Arg residue.

MS-MS spectrum 3. Positive fragmentation of *N*-Ac-Gly-Phe-His-Ala-Arg(6-FAM)-Gly-OH (**2.19**)

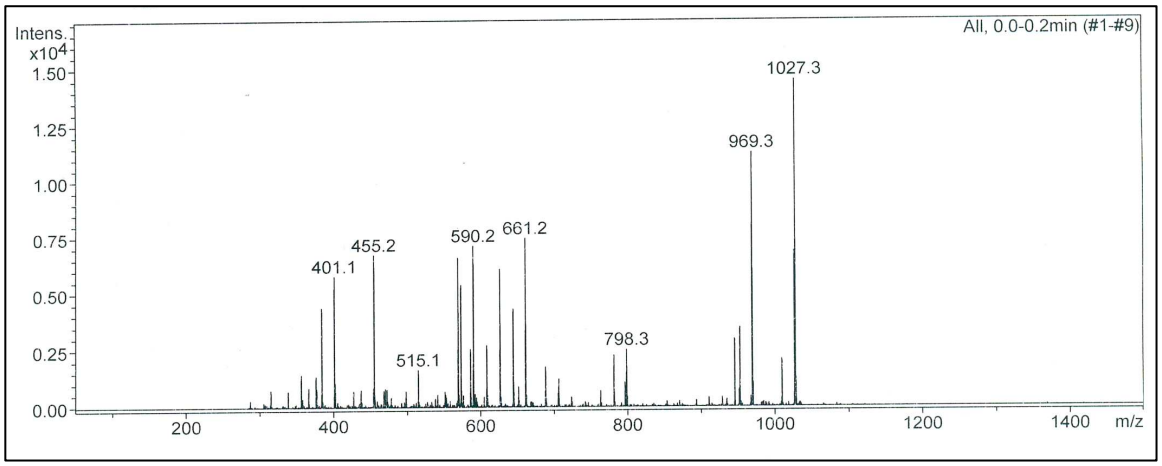

Mass	Fragment
401.1	*N*-Ac-Gly-Phe-His-NH_3^+
455.2	*N*-Ac-Gly-Phe-His-Ala-O^+
590.2	^+H_3N-Arg(6-FAM)-Gly-OH
661.2	^+H_3N-Ala-Arg(6-FAM)-Gly-OH
798.3	^+H_3N -His-Ala-Arg(6-FAM)-Gly-OH
969.3	*N*-Ac-Gly-Phe-His-Ala-Arg(6-FAM)-O^+
1027.3	*N*-Ac-Gly-Phe-His-Ala-Arg(6-FAM)-Gly-O^+

The ion at *m*/*z* = 590.2 supports the assignment of the labelled Arg residue.

MS-MS spectrum 4. Positive fragmentation of *N*-Ac-Gly-Val-Cys(6-FAM)-Arg-Phe-Gly-OH (**2.23**)

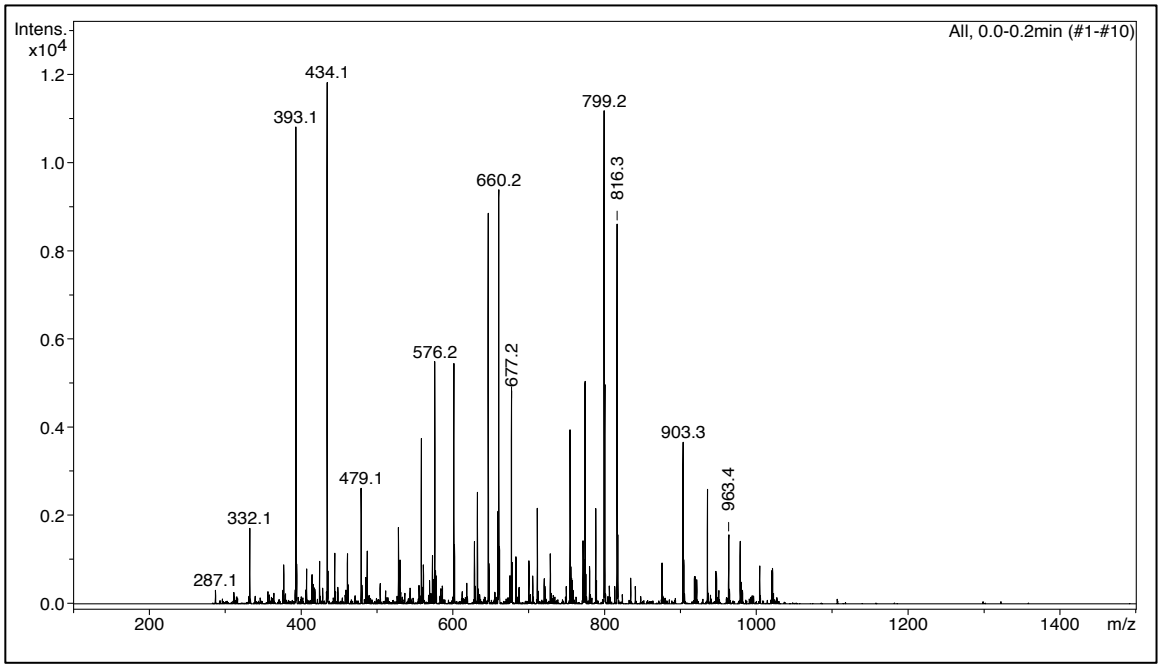

Mass	Fragment
660.2	*N*-Ac-Gly-Val-Cys(6-FAM)-O^+
677.2	*N*-Ac-Gly-Val-Cys(6-FAM)-NH_3^+
816.3	*N*-Ac-Gly-Val-Cys(6-FAM)-Arg-O^+
963.4	*N*-Ac-Gly-Val-Cys(6-FAM)-Arg-Phe-O^+

The ion at *m*/*z* = 963.4 supports the assignment of the labelling of the unfavoured Cys residue.

MS-MS spectrum 5. Positive fragmentation of *N*-Ac-Gly-Lys(6-FAM)-Phe-Arg-Gly-OH (**2.24**)

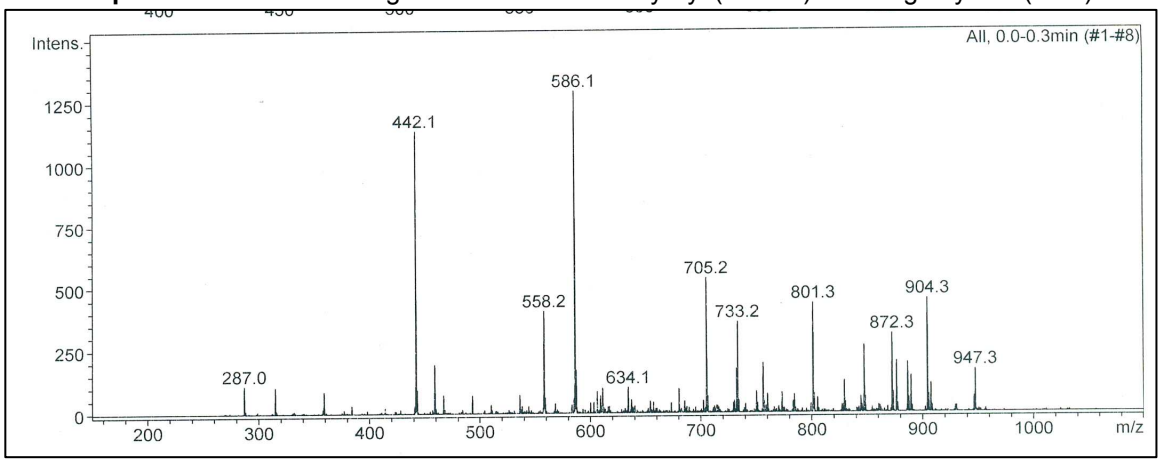

Mass	Fragment
586.1	*N*-Ac-Gly-Lys(6-FAM)-O^+
733.2	*N*-Ac-Gly-Lys(6-FAM)-Phe-O^+

The ion at *m*/*z* = 586.1 and 733.2 supports the assignment of the labelling of the unfavoured Lys residue.

MS-MS spectrum 6. Positive fragmentation of Pyr-His-Trp-Ser-Tyr-D-Leu-Leu-Arg(6-FAM)-Pro-NHEt (**2.30**)

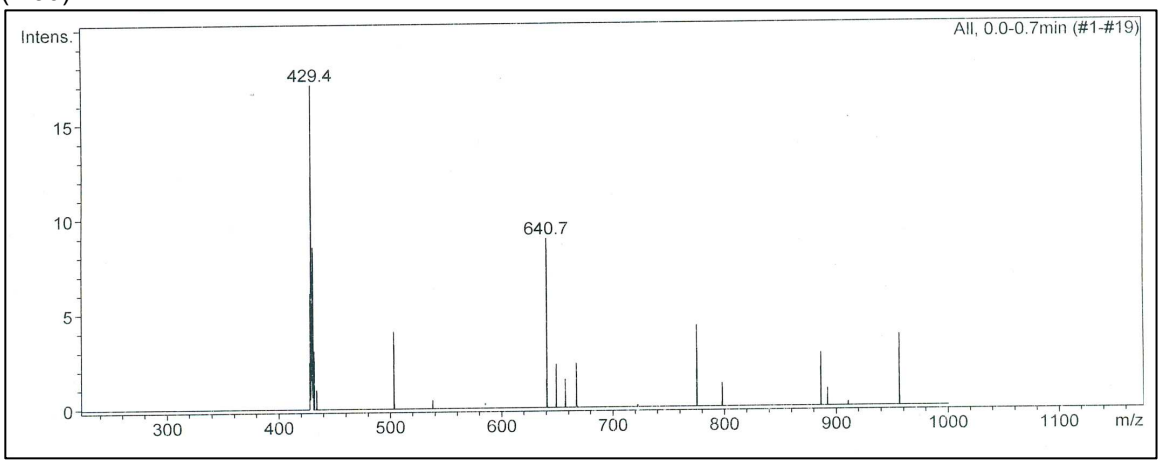

Mass	Fragment
640.7	$^+$Arg(6-FAM)-Pro-NHEt

The ion at *m*/*z* = 640.7 supports the assignment of the labelled Arg residue.

MS-MS spectrum 7. Positive fragmentation of *N*-Ac-Gly-Lys-Phe-Arg(6-FAM)-Gly-OH (**2.33**)

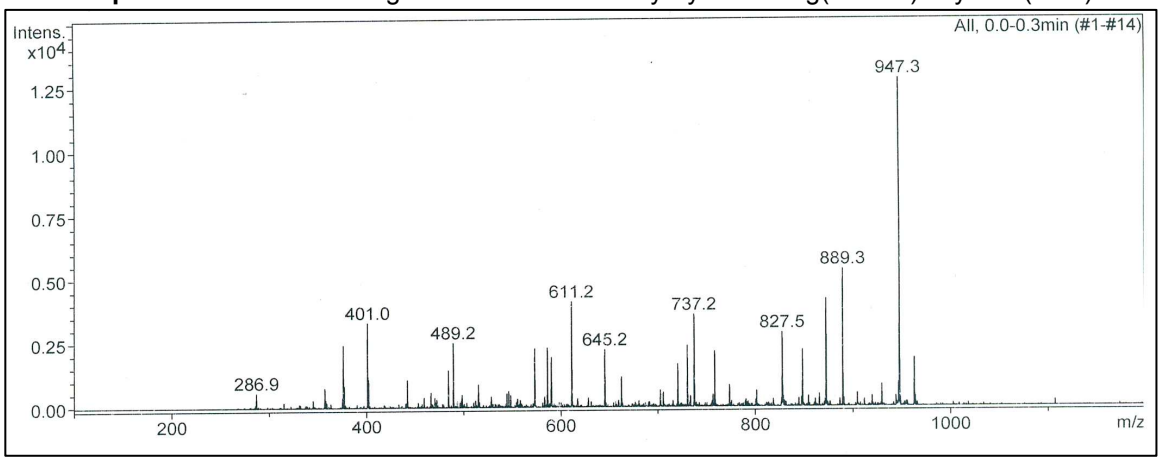

Mass	Fragment
737.2	$^{+}NH_3$-Phe.Arg(6-FAM)-Gly-OH
889.3	*N*-Ac-Gly-Lys-Phe-Arg(6-FAM)-O^{+}

The ion at *m*/*z* = 737.2 supports the assignment of the labelled Arg residue.

The ions with 135 mass units less, result from the cleavage of the Adda side chain, between the methylester and the methyl group.[1]

MS-MS spectrum 8. Negative fragmentation of MC-LR-(6-FAM) (**3.1**)

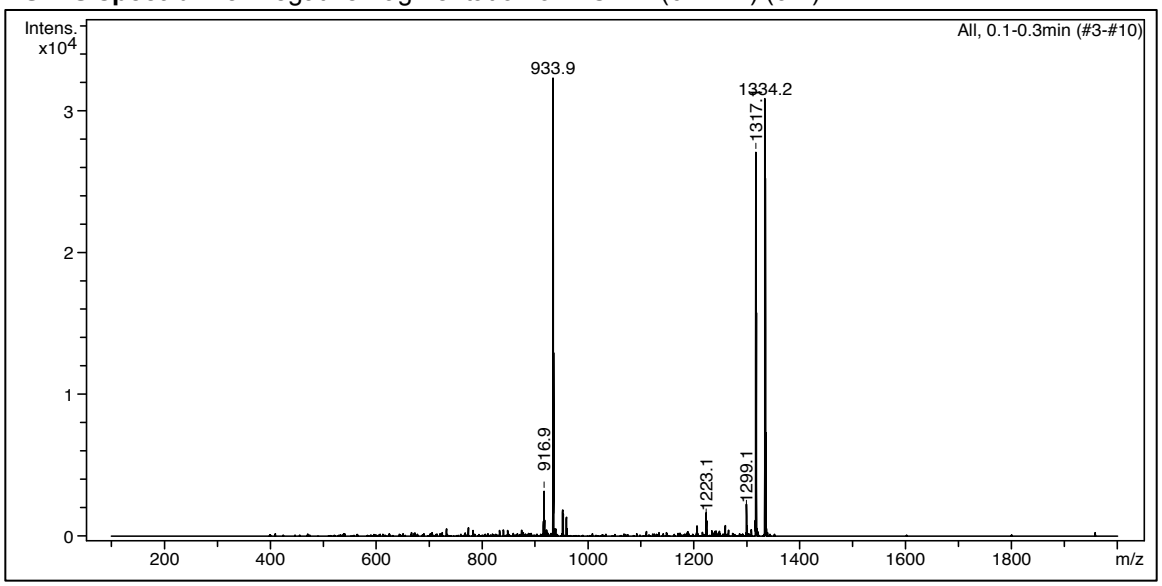

Mass	Fragment
1334.2	- H_2O
1317.1	- H_2O, NH_3
1299.1	- Dha
1223.1	- Leu,H_2O
933.9	MeAsp-Arg-(6-FAM)-Glu-(-135,-H_2O)
916.8	MeAsp-Arg-(6-FAM)-Glu-(-135,-H_2O,-NH_3)

Unfortunately no fragment can entirely exclude the attachment of the fluorophore to the Glu or MeAsp side chain.

MS-MS spectrum 9. Negative fragmentation of MC-LR-(Alexa-430) (**3.2**)

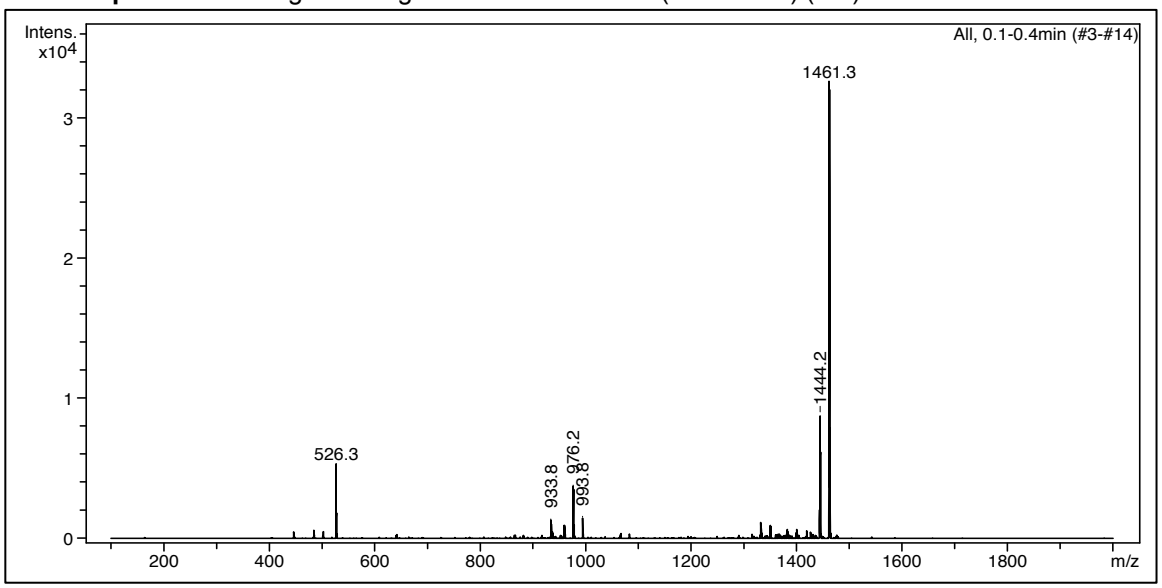

Mass	Fragment
1461.3	- H_2O
1444.2	- H_2O, NH_3
993.8	Adda-Arg-(Alexa-430)-MeAsp-(-135)
976.2	Adda-Arg-(Alexa-430)-MeAsp-(-135,-NH_3)
933.8	Arg-(Alexa-430)-Glu-(-135,-NH_3)
526.3	MeAsp-Leu-Ala-Mdha-Glu

The ion at *m*/*z* = 526.3 supports the assignment of the labelled Arg residue.

MS-MS spectrum 10. Positive fragmentation of MC-LR-(Texas-Red) (**3.4**)

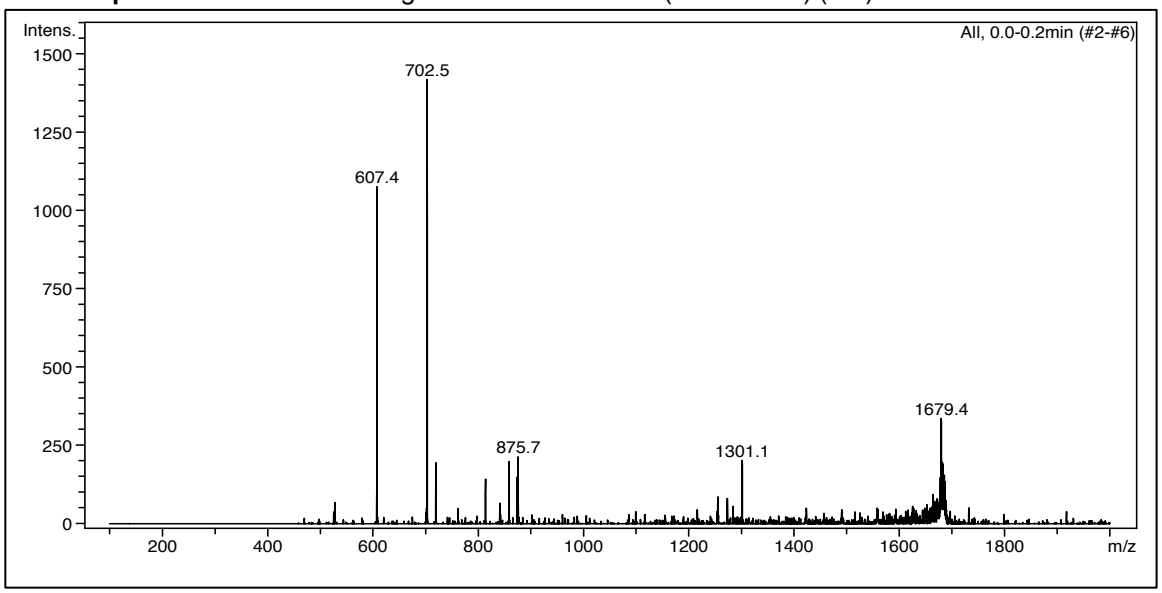

Mass	Fragment
1679.5	- H_2O
1301.1	Adda-Arg-(Texas-Red)-Glu-O^+
875.7	Arg-(Texas-Red)-NH_3^+
702.5	Adda-Glu-Mdha-Ala-Leu-MeAsp(-135,-NH_3)
607.4	Adda-Glu-Mdha-Ala-Leu-CH_3^+(-135)

The ion at *m*/*z* = 875.7 and 702.5 supports the assignment of the labelled Arg residue.

MS-MS spectrum 11. Positive fragmentation of CP1020(Benzylamin) (**5.1**)

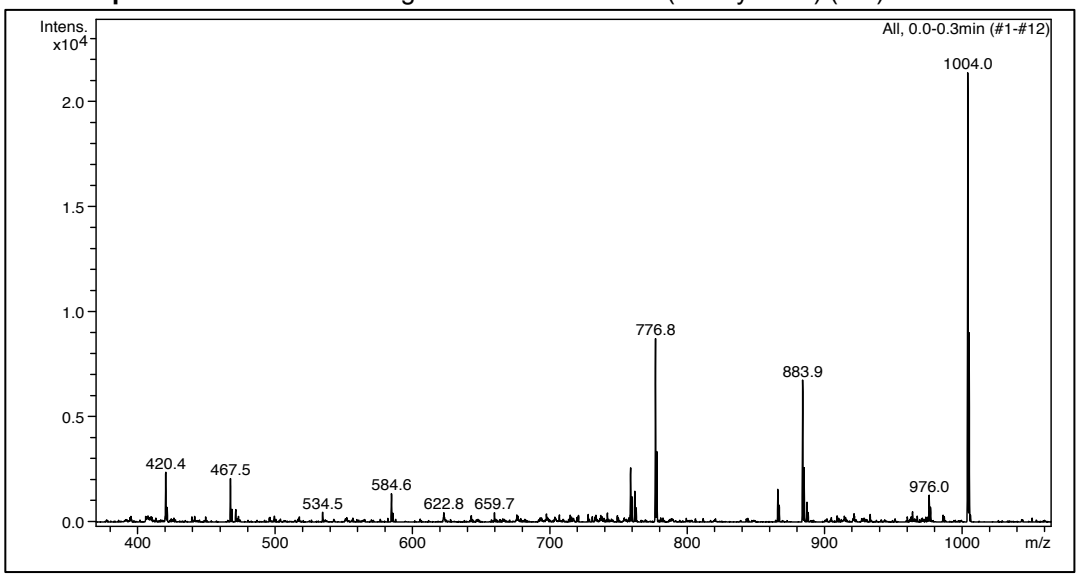

Mass	Fragment
1004.0	- Bn
776.8	-AhpBn
467.5	Hex-Glu-Didehydrobutyrate-Arg$^+$
420.4	Phe-Tyr-Val-OH$^+$

The ion at *m*/*z* = 1004 supports the attachment of the amine at the carboxylic acid.

7.5 References

[1] T. Mayumi, H. Kato, S. Imanishi, Y. Kawasaki, M. Hasegawa, K.Harada, *J. Antibiot* **2006**, *59*, 710–719.

Acknowledgements

After three and a half years it is time to close this chapter of my life and move on to the next one. I had very good and some bad moments in the past years. But nevertheless, retrospectively, I would walk this way again. So what is left is getting sentimental and saying *Thank you*.

I would like to start with my doctor father *Prof. Dr. Karl Gademann*. Thank you very much for giving me the chance to be in the *ProDoc* program, I had a great time there. Further thanks, for supporting my work, for financial resources, all the freedom I enjoyed and your continual interest in my research. I learned many valuable things from you.

Of course I would like to thank my thesis committee and referees *Prof. Dr. Michael Arand* and *Prof. Dr. Rik Eggen*, for their continuous helpful suggestions and open ears for my concerns during my whole thesis. Thank you very much. Further thanks to *Prof. Dr. Dennis Gillingham* for hosting my defence.

I would like to thank the *ProDoc* program and *Xerr* for a really great time I had. All the meetings, excursions, seminars and conferences enriched, knowledge and fun wise, my last years. Special thanks to *Dr. Timo Buetler* for all the organization. And of course to all the *CanDocs* I had an awesome time with you.

Further thanks to our project and cooperation partners, *Prof. Dr. Jakob Pernthaler*, *Dr. Judith Blom*, *Esther Kohler*, *Prof. Dr. Karl Fent* and *Susanne Faltermann* for their hospitality, financial resources, knowledge and fun during the last years. A special thanks to *Esther Kohler* for accommodate me in Zurich so many times and all the great moments we shared.

PD Dr. Daniel Häussinger, thanks a million for all your endless time and help with the NMR measurements. Without you I would have been lost, gell.

I also would like to thank the good souls *Johanna Zalewski*, *Marina Mambelli Johnson*, and *Brigitte Howald* for all their help with everything.

Nothing would have worked or everything would have gone down the drain if the always nice and helpful people of the Werkstatt would have not been there. Thanks to *Mr. Ast*, *Mr. Cabrera*, and *Mr. Hermida*. Thanks to *Dr. Heinz Nadig* for all the HRMS measurements and discussions. And of course *Markus Hauri* and *Roy Lips* for their help, and the supply of not only chemicals. Thank you very much.

Thanks to *Dr. Malika Makhlouf*, *Srba Vujovic* and *Dr. Luc Eberhardt* for welcoming me in Basel and being nice to me. You made my start a lot easier. Thanks to *Robin Wehlauch* for all the fruitful discussions, the laughter and the fun we had, you made my days. My dear *Patrick Burch*, it was not always easy in our group but with you for sure funnier. *Elias Kaufmann*, thank you for your help with the IT stuff and your eternal friendliness. Thanks to *Samuel Bader* for teaching me many many things in the lab. Thanks to *Robin Scheil* for being my hardworking student. *Heiko Gsellinger*, thank you for cheering me up all the time and for all the pleasant conversations in the measurement room and elsewhere. Thanks to *Gero Harzmann* for all the nice chit-chats on the floor and in the lab. Thanks to *Luca Schweighauser* for being always a nice and funny conversation partner. Thanks to *Laëtitia da Silva* for introducing me in the first mysteries of the HPLC. *Matthias Knop*, thank you very much for helping me in the beginning with all the peptide related questions. Thanks to *Cathrin Ertl* for taking your time to measure the whole day with me all these photochemical thingies.

Thanks to our post-docs *Dr. Malika Makhlouf*, *Dr. Luc Eberhardt*, *Dr. Hideki Miyatake Ondozabal*, *Dr. Suman De Sarkar*, *Dr. Regina Berg* and *Dr. Erika Crane*. You always helped me gladly and a lot.

My dear lab 102, thank you very much dearies, I had a great time with you guys. Best lab ever. *Fabian*, jesus, you are a very special person, but whenever it got complicated I could count on you. *Simon*, I had great times with you where we laughed a lot. *Hidak*, you are a great mate, you made me laugh so much and thanks for all your help during the past years. *Robin*, I think you are one of the only persons, who truly understood me, I had so many great talks and laughs with you, thank you.

Thanks to my group and all the people, which made my life easier and more fun in these past years at the University of Basel.

A big, mega thank you to *Christophe Thommen*, *Dr. Christof Sparr* and *Kiril Tishinov* for proof reading my thesis. Without you …. Oiski! Poiski! or well, you know. *Dr. Regina Berg*, million thanks for correcting everything else of importance with such great accuracy, you are a great person.

Of course I would like to thank all my friends, which stick with me over the years, cheered me up, laughed with me, supported me and just simply were there for me. Special thanks to: *Flora*, merci beaucoup pour avoir partagé de beaux moments avec moi, pour ta cuisine, tes leçons et ton soutien. *Kiril*, you are a great person, don't change, you were always there when I needed you. Благодаря-ви. *Annalisa* grazie mille for being there for me, laugh with me, getting angry with me, cheering me up and just having good times together. *Susanne*, vielen Dank für all dein Wissen, deine Zeit und die schönen Momente. Geteiltes Leid ist halbes Leid. *Alexander*, vielen Dank für all die Unterstützung und Beistand durch mein ganzes Studium hindurch. Mein lieber *Ferdi* danke, dass du nie deinen Humor und die Sicht auf die normale Welt verloren hast. *Kristina*, zusammen haben wir es durch diese verrückte Zeit geschafft, vielen Dank. *Julia* und *Eva*, ihr seid meine besten und wahrsten Freunde, ich bin sehr dankbar, euch an meiner Seite zu wissen.

Christophe, mon amour, mon cœur. Merci pour ton amour, ton soutien, ta patience et ton encouragement. Tu as enduré mes caprices. Tu es la meilleure chose qui me soit jamais arrivée, tu es mon futur, ma source, ma vie. Je t'aime.

Meine liebe, liebe Familie, meine liebe Mama, mein lieber Papa und meine liebe Schwester; der Weg war das Ziel und ohne Euch hätte ich es nicht erreicht. Ich denke es gibt keine Worte, die ausdrücken können, wie dankbar ich bin, dass ich Euch habe. Ihr seid die beste Familie, die man sich wünschen kann. All die Liebe, die seelisch und moralische Unterstützung und den Beistand über die Jahre, was kann man sich mehr wünschen. Danke für Alles. Ihr seid meine Stütze, mein Halt, mein Zuhause.

Curriculum Vitae

EDUCATION

2011– 2014	**PhD** in Organic Chemistry *Probing the Mode of Action of Cyanobacterial Toxins by Chemical Biology Approaches* Supervisor: Prof. Dr. K. Gademann, University of Basel, Switzerland
2005 –2010	**Chemistry Diploma** University of Würzburg, Germany **Diploma Thesis** *Role of Bax1 in the Nucleotide Excision Repair Mechanism Expression, Purification and Crystallization of IGHMBP2* Supervisor: Prof. Dr. C. Kisker, Rudolf-Virchow-Center for Experimental Biomedicine, University of Würzburg, Germany
1995 – 2005	**Abitur** Armin-Knab-Gymnasium, Kitzingen, Germany

ADVANCED TRAINING

2011 – present	**Training Courses in Toxicology**, German Society for Experimental and Clinical Pharmacology and Toxicology Five courses successfully completed: • Food Toxicology • Molecular Cell Toxicology • Organ Toxicology and Pathology • Xenobiotic Metabolism/Toxicokinetics • Ecotoxicology
2011 – 2013	**Member of the ProDoc program *Predictive Toxicology***, Center for Xenobiotic Risk Research (XeRR), Zurich, Switzerland

EXPERIENCE

Conferences	*International conference on toxic cyanobacteria*, South Africa, 2013 (presentation) *Eurotox*, Switzerland, 2013 (poster)
Publication	H. M. Roth, J. Römer, V. Grundler, B. Van Houten, C. Kisker, I. Tessmer, *DNA Repair* **2012**, *11*, 286-293.